# THE REGIOSELECTIVE HYDROGENATION OF ACRYLIC ACIDS USING RHODIUM-MIXED ANHYDRIDE CATALYST PRECURSORS

Neil Robert Fairfax

A Thesis Submitted for the Degree of PhD
at the
University of St Andrews

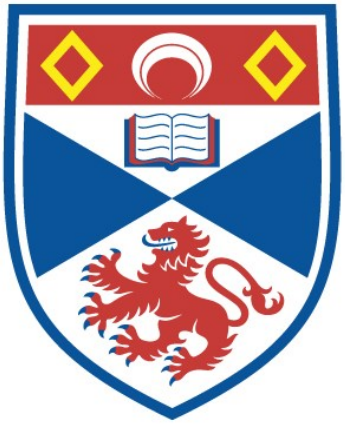

1993

# THE REGIOSELECTIVE HYDROGENATION OF ACRYLIC ACIDS USING RHODIUM-MIXED ANHYDRIDE CATALYST PRECURSORS

A thesis presented by

NEIL ROBERT FAIRFAX

to the

University of St Andrews

in application for

the Degree of Doctor of Philosophy

St Andrews

September 1992

Declaration for the Degree of Ph.D.

I Neil R Fairfax hereby certify that this thesis has been composed by myself, that it is a record of my own work, and that it has not been accepted in partial or complete fulfilment of any other degree of professional qualification.

Signed ..... ..... Date .....

I was admitted to the Faculty of Science of the University of St Andrews under Ordinance General No 12 on ..... and as a candidate for the degree of Ph.D. on .....

Signed ..... ..... Date .....

I hereby certify that the candidate has fulfilled the conditions of the Resolution and Regulations appropriate to the Degree of Ph.D.

Signature of Supervisor Date 9th November 1992

## Copyright

TO MUM AND DAD

WITH THANKS FOR THEIR SUPPORT.

INDEX

ACKNOWLEDGEMENTS

I would like to thank Professor David Cole-Hamilton for his encouragement, advice and friendship throughout the duration of my postgraduate studies.

I would also like to express my gratitude to The Royal Society of Chemistry for the funds they have provided and for the good work that they regularly perform.

Many thanks to:-

All my friends in St Andrews, past and present, who helped make my years there the most enjoyable of my life so far, especially Doug Foster and Lachlan Arblaster who helped make it home from home.

Ahmed Iraqi for his help and advice in the laboratory.

Katrina Bennett and Colette McFarlane for their hours of patient word processing "after hours". Thanks also to William M Mercer Fraser Limited, Edinburgh for the use of their facilities.

## ABSTRACT

Complexes of general composition $[RhCl(PPh_3)_n(Ph_2PO_2CCR=CR'R'')]$ (n=2, R=H, R'=R''=Me; R=R'=H, R''=CH=CHMe; R=Me, R'=H, R''=Ph; n=1, R=R'=H, R''=Me or CH=CHMe) have been used as precursors for the catalytic hydrogenation of various substituted acrylic acids, $[HO_2CCR=CR'R'']$.

The reactions of $[RhCl(PPh_3)(Ph_2PO_2CCH=CHMe)]$ and $^-[O_2CCH=CHMe]$ and $[RhCl(PPh_3)_2(Ph_2PO_2CCMe=CHPh)]$ and $^-[O_2CCMe=CHPh]$ give $[Rh(O_2CCH=CHMe)(PPh_3)(Ph_2PO_2CCH=CHMe)]$ and $[Rh(O_2CCMe=CHPh)(PPh_3)(Ph_2PO_2CCMe=CHPh)]$ accordingly and these complexes are the respective active species in the catalytic hydrogenation of but-2-enoic acid and 2-methyl-3-phenylpropenoic acid.

The crossed reactions between $[RhCl(PPh_3)(Ph_2PO_2CCH=CHMe)]$ and $^-[O_2CCMe=CHPh]$, $[RhCl(PPh_3)_2(Ph_2PO_2CCMe=CHPh)]$ and $^-[O_2CCH=CHMe]$, $[RhCl(PPh_3)(Ph_2PO_2CCH=CHMe)]$ and $^-[O_2CCH=CMe_2]$ and $[RhCl(PPh_3)_2(Ph_2PO_2CCH=CMe_2)]$ and $^-[O_2CCH=CHMe]$ predominantly yield products in which the chelate mixed anhydride ligand is but-2-enoic acid derived, on account of its lesser substituted carbon-carbon double bond.

Attempts at isolating hydride intermediates in the catalytic cycle have proved unsuccessful. However, investigations of the step by which the product carboxylic

acid anion is released from the metal complex (transesterification reaction) have involved the synthesis of $[RhCl(PPh_3)_2(Ph_2PO_2CCH_2CH_2Me)]$ (2 isomers) from $[RhCl(PPh_3)_3]$ and $[Ph_2PO_2CCH_2CH_2Me]$ and $[Rh(PPh_3)_2(Ph_2PO_2CCH_2CH_2Me)]^+$ from $[RhCl(PPh_3)_2(Ph_2PO_2CCH_2CH_2Me)]$ and $TlPF_6$. The reactions of both these products with $^-[O_2CCH=CHMe]$ yield the active species $[Rh(O_2CCH=CHMe)(PPh_3)(Ph_2PO_2CCH=CHMe)]$.

Prior to transesterification the most likely intermediate in the catalytic cycle is $[Rh(O_2CCH_2CH_2Me)(PPh_3)_n(Ph_2PO_2CCH_2CH_2Me)]$ (n=1 or 2) in which both the mixed anhydride and the coordinated anion have been hydrogenated. The reaction of $[RhCl(PPh_3)_2(Ph_2PO_2CCH_2CH_2CH_3)]$ with $K[O_2CCH_2CH_2CH_3)]$ affords the fluxional, square-planar species, $[Rh(O_2CCH_2CH_2CH_3)(PPh_3)_2(Ph_2PO_2CCH_2CH_2CH_3)]$.

The hydrogenation of hexa-2,4-dienoic acid, $[HO_2CCH=CHCH=CHMe]$, using rhodium-mixed anhydride complexes yields both hexanoic and hex-4-enoic acids via two concurrent mechanisms, since the active species, $[Rh(O_2CCH=CHCH=CHMe)(PPh_3)(Ph_2PO_2CCH=CHCH=CHMe)]$ exists in two forms; one containing a chelate mixed anhydride, the other a chelate hexa-2,4-dieonate ligand. The production of hexanoic acid is brought about by the active involvement of the chelate hexa-2,4-dienoate ligand in the catalytic cycle. Attempts to prevent this involvement have centred around the replacement of the chloride ligand in the catalyst precursor with non-labile fluoride and trifluoromethyl anions.

$[RhF(PPh_3)_3]$ reacts with mixed anhydride ligands to give 5-coordinate species, $[RhF(PPh_3)_2(Ph_2PO_2CCR=CR'R'')]$, in which the mixed anhydride is bound via phosphorus and carbonyl oxygen, however these precursors show no increased regioselectivity. The reaction of $[RhCl(PPh_3)_3]$ with $[Hg(CF_3)_2]$ does not yield $[RhCF_3(PPh_3)_3]$ but $[RhCl(PF_3)(PPh_3)_2]$, and in the presence of excess $PPh_3$ yields $[RhCl(CF_3)_2(PPh_3)_2]$. Other attempts to prevent the involvement of the bidentate hexa-2,4-dienoate ligand in the catalytic cycle have involved the addition of $PPh_3$ or $CH_3CO_2H$ to the catalytic solution, and to a certain degree increased regioselectivity towards the production of hex-4-enoic acid has been achieved.

NOTE:

All $^{31}P$ NMR spectra presented, have their chemical shifts quoted relative to $H_3PO_4$, whilst all $^{19}F$ NMR shifts are relative to $CCl_3F$.

# CHAPTER 1

# REGIOSELECTIVE HYDROGENATION OF POLYENES VIA HOMOGENEOUS CATALYSIS

## 1.1 Introduction.

A catalyst is a substance that causes a reaction to proceed more rapidly to equilibrium. It does not change the value of the equilibrium constant and it does not itself undergo any net change, therefore it can be used in small amounts. In terms of the absolute reaction rate theory, the role of a catalyst is to lower the free energy of activation, $\Delta G^{*}$, of the rate determining steps. It achieves this by the formation of one or more intermediates or transition states in which it is temporarily bound. With regards to the coordination chemistry aspects of catalysis, it is necessary to look more closely at what is meant by the term "catalyst" in relation to homogeneous catalysis. Homogeneous catalytic reactions in solution are generally very complex and proceed via linked chemical reactions in a closed cycle, the catalytic cycle involving different metal species. The idea of one particular species being "the catalyst", even if it is the one added to initiate or accelerate the reaction, has no sound basis. It would be better termed the "catalyst precursor".

Many catalytic cycles can be studied mechanistically and spectroscopically, and in certain cases intermediates in the reaction cycles, isolated or otherwise, can be characterised. The principles upon which these reactions are based are mainly coordinative unsaturation, oxidative-addition, insertion, $\beta$-H abstraction and

reductive elimination reactions and attacks on coordinated ligands by electrophiles or nucleophiles. These are considered further in Section 1.2.

The uncatalysed addition of $H_2$ to an alkenic double bond, although thermodynamically favourable, is symmetry forbidden in the ground state via a concerted cis addition, as shown in Figure 1.1.1. Electrons are unable to flow from $H_2$ to the empty $\pi^*$-orbital because there is no net orbital overlap. The d-orbitals of a transition metal however, have the correct symmetry to react directly with $H_2$. Electron flow both from the filled d-orbitals into the empty $\sigma^*$-orbital of $H_2$ and from the bonding orbital of $H_2$ into a vacant metal orbital dissociates the H-H bond and forms two metal-hydride bonds.

Without doubt, one role of the catalyst is to overcome symmetry restrictions, although the mechanism of simultaneous transfer of two H atoms to a non-coordinated substrate has not been observed.

Figure 1.1.1

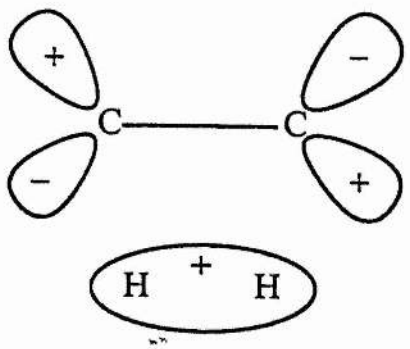

The catalysed hydrogenation of unsaturated carbon-carbon double bonds inevitably involves the formation of intermediate metal hydrides and this is discussed in Section 1.2.

## 1.2 Activation of Hydrogen and Hydridometal Catalysts.

A frequently demonstrated mode of $H_2$ activation is by oxidative addition. Equation 1.2.1 shows this process in basic terms, whereby there is a cleavage of a hydrogen-hydrogen bond and an increase of two in the formal oxidation state of the metal.

Equation 1.2.1

$$L_yM^n + H_2 \rightleftharpoons L_yM^{n+2}H_2$$

Despite the H-H bond energy (450kJ $mol^{-1}$), oxidative addition can occur with great ease. The mechanism of addition has been the subject of a lengthy discussion. [1,2] It is now deemed likely that a molecular hydrogen complex is initially formed, whereby the $H_2$ $\sigma$ bond acts as an electron donor into an empty $d_\sigma$ orbital on the metal. The $\sigma^*$ orbital of $H_2$, however, accepts metal $d_\pi$ electrons. Both processes are illustrated in Figure 1.2.1(a). The $H_2(\sigma)$ donor component leads to the formation of a molecular orbital which is bonding with respect to all three atoms, as shown in Figure 1.2.1(b). The $H_2(\sigma)$ donor component of the bonding only weakens but does not break the H-H bond because the two electons that used to hold the $H_2$ together are now bonding over all three atoms. The $\pi$ back donation

from a filled M($d_\pi$) orbital goes into a $\sigma^*$ orbital, which is antibonding with respect to $H_2$ and has a node between the two H's, so the effect of filling the orbital is to break the H-H bond, as illustrated in Figure 1.2.1(c)

Figure 1.2.1 (a) (b) (c)

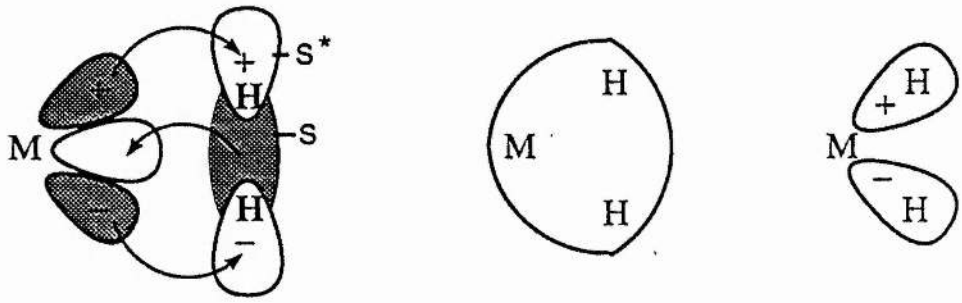


At normal temperature and hydrogen pressure this process is often reversible and the reverse reaction is termed "reductive-elimination". The forward reaction is generally promoted by a low initial oxidation state, high metal $\pi$-basicity and unsaturation in the cooordination sphere. [3] The first two factors are indicative of complexes with greater electron density undergoing reactions which decrease such density. The loss of electrons by oxidation is countered by the gain of electrons through an increased coordination number. Thus, the early transition metals ($d^1$ to $d^4$) tend to form complexes of higher coordination number than those of $d^7$ - $d^{10}$ systems, and as a result of steric requirements show less tendency to undergo oxidative-addition, although such a constraint should not be so acute for oxidative-addition of hydrogen. The non-reactivity of trans-[$RhCl(CO)(PPh_3)_2$] towards $H_2$ at ambient conditions, in contrast to trans-[$IrCl(CO)(PPh_3)_2$] and [$RhCl(PPh_3)_3$], is attributed to the weaker basicity of Rh compared with Ir and the introduction of the $\pi$-acid CO ligand respectively.[4] The addition of hydrogen to [$RhCl(PPh_3)_3$]

produces the dihydride $[RhH_2Cl(PPh_3)_3]$ and as a result the rhodium metal centre removes electron density by going from an oxidation state of +1 to +3. In the case of $[RhCl(CO)(PPh_3)_2]$, addition of hydrogen affords $[RhH_2Cl(CO)(PPh_3)_2]$ which is less stable than $[RhH_2Cl(PPh_3)_3]$ because of the decreased availability of electron density for the $\pi$-acceptor CO ligand.

The complexes of $d^8$ electron configuration, which are of special interest for use as homogeneous catalysts, favour a square planar (4-coordinate) geometry with 16 electrons in the outer shell. Oxidative addition of hydrogen produces an 18-electron, 6-coordinate system; a $d^8 \rightarrow d^6$ process. This is the case for the complex $[RhCl(PPh_3)_3]$, now known as Wilkinson's catalyst, as shown in Equation 1.2.2.

Equation 1.2.2

$$[Rh^{I}Cl(PPh_3)_3] + H_2 \rightleftharpoons [Rh^{III}H_2Cl(PPh_3)_3]^{5}$$

In some cases dihydride formation is accompanied by the loss of one ligand and this is especially prevalent for complexes that already have 18 electrons. An example of this is shown in Equation 1.2.3 where a triphenylphosphine ligand is dissociated prior to hydrogen addition.

Equation 1.2.3

$$[Ru^{0}(CO)_2(PPh_3)_3] + H_2 \rightleftharpoons Ru^{II}H_2(CO)_2(PPh_3)_2] + PPh_3^{6}$$

Certain dihydrides formed from mononuclear complexes are catalytically inactive

at least under mild conditions, probably due to the thermodynamic or kinetic stability of the metal-hydride bonds. An example of this is shown in Equation 1.2.4.

Equation 1.2.4

$$[Ir^{I}Cl(PPh_3)_3] + H_2 \rightleftharpoons [Ir^{III}H_2Cl(PPh_3)_3]$$ [7]

Alternatively the Ir-P bond may not be labile enough, and as a result a vacant site needed for alkene coordination is not available.

A $d^7$ metal complex can attain the $d^6$ octahedral configuration via a net $H_2$ addition to two metal centres, a classic case being that of pentacyanocobaltate(II) which is shown in Equation 1.2.5.

Equation 1.2.5

$$2[Co^{II}(CN)_5]^{3-} \text{ or } [Co_2{}^{II}(CN)_{10}]^{6-} + H_2 \rightleftharpoons 2[Co^{III}H(CN)_5]^{3-}$$ [8]

Oxidative addition of $H_2$ to a dimer resulting in a dimeric product with one hydrogen atom bound to each metal is exemplified in Equation 1.2.6. [9] The Ir(II) $d^7$ atoms in the product maintain an 18-electron-rule configuration by formation of a metal-metal bond. In contrast to this the chlorine-bridged $d^8$ complex $[[RhCl(PPh_3)_2]_2]$ adds $H_2$ at only one metal to give the mixed-valence product $[(Ph_3P)_2Rh(\mu\text{-}Cl)_2RhH_2(PPh_3)_2]$. [10]

Equation 1.2.6

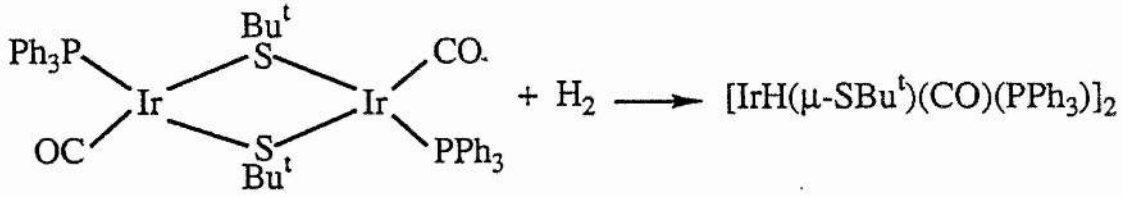


It should be noted that the term "homolytic splitting" of $H_2$ is not exactly the same as oxidative addition. Homolytic splitting of $H_2$ formally becomes an oxidative addition only when electrons are transferred from the metal to the hydrogen atoms. This is shown in Figure 1.2.2, where for a divalent complex homolytic splitting of $H_2$ can give three products that differ only in the position of the electron originally associated with the hydrogen atom.

Figure 1.2.2

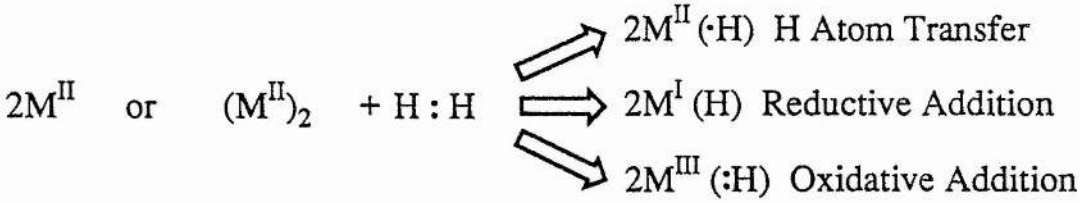


There are many cases where a metal hydride is formed via a net heterolytic splitting of $H_2$ and this is generalised for a divalent metal complex in Equation 1.2.7. The formal oxidation state of the metal remains unchanged with the reaction basically being one of substitution whereby hydride usually replaces an initially coordinated ligand X, which is usually anionic. The released proton is often stabilised by a base, which may be the ligand X, the solvent or an externally added base.

Equation 1.2.7

$$M^{II}X + H_2 \rightleftharpoons M^{II}H + H^+ + X^-$$

This mode of hydrogen activation is common for ruthenium(II) complexes. An example is shown in Equation 1.2.8. [11]

Equation 1.2.8

$$[Ru^{II}Cl_2(PPh_3)(\eta\text{-}C_6Me_6)] + H_2 \rightleftharpoons [Ru^{II}HCl(PPh_3)(\eta C_6Me_6)] + H^+ + Cl^-$$

Examples of a coordinated ligand (X) stabilising the released proton came from early studies on Cu(II) salts and Ag(I) amine complexes. Correlations between rates of hydrogen activation and ligand basicity were demonstrated and plausible transition states, as shown in Figure 1.2.3, were involved. [12] Similar figures involving a polarized $H_2$ molecule can be written, with X=solvent or added base.

Figure 1.2.3

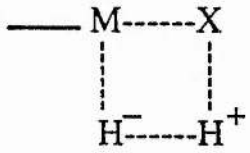


The reversible nature of Equation 1.2.7 has been demonstrated for only a few hydride systems. One example is the protonation of $[RuHCl(PPh_3)_3]$ to give $[RuCl_2(PPh_3)_3]$ and $H_2$. [13]

A net heterolytic $H_2$ cleavage can also result via oxidative addition of $H_2$, followed by reductive elimination of HX which again may be base assisted. An example of this is shown in Equation 1.2.9. [14] It is difficult in some cases to distinguish between the two-stage process and a real heterolytic cleavage via a transition state such as that shown in Figure 1.2.3.

Equation 1.2.9

$$\text{trans-}[IrCl(CO)(PPh_3)_2] + H_2 \rightleftharpoons [IrH_2Cl(CO)(PPh_3)_2]$$

$$[IrH_2Cl(CO)(PPh_3)_2] \xrightarrow{\text{base}} \text{trans-}[IrH(CO)(PPh_3)_2]$$

Kinetic data has shown that oxidative addition of $H_2$, to give isolable dihydrides, generally proceeds with $\Delta H^{\ddagger}$ values of up to $60kJmol^{-1}$.[15] Activation parameters determined in, or close to, these ranges for a net heterolytic $H_2$ cleavage can offer indirect support for the two-stage process shown in Equation 1.2.9. Genuinely heterolytic processes such as in Cu(II), Cu(I), Ag(I), Ru(III) and Rh(III) systems have $\Delta H^{\ddagger}$ values considerably above the value of $60kJmol^{-1}$.

## 1.3 Activation of the Unsaturated Organic Substrate and Hydrogen Transfer.

In instances where the hydridometal complex has been preformed, activation of the unsaturated organic substrate generally involves its simple coordination. Catalytic cycles operating via such initial steps have been termed the "hydride" route. In

contrast, binding of the unsaturated organic substate followed by activation of $H_2$ as the initial steps in the catalysis has been labelled an "unsaturate" route. [16]

In almost all cases reported, the addition of $H_2$ to carbon-carbon double bonds appear to be cis. This was first demonstrated for a homogeneous catalyst with the $D_2$ addition experiments to a chlororuthenate(II) system using maleic and fumaric acids as substrates. [17]

Monohydride Catalysts

Scheme 1.3.1 summarizes the proposed mechanistic pathways for monohydride catalysts. [18] Step (A) defines the hydride route and step (B) the unsaturate route.

An important alkyl intermediate (4) is usually assumed to be formed via hydride migration (alkene insertion) within the hydridoalkene complex (3). Despite the fact that alkene insertion and the reverse process ($\beta$-hydride extraction) are well documented, there has never been an example in a catalytic hydrogenation system where step (C) has been observed directly. The hydride migration is a facile process and is therefore never rate determining. Overall the equilibrium for steps A and C must favour high M-H + alkene concentrations with only very small concentrations of both (3) and (4).

Scheme 1.3.1 Mechanistic Pathways For Monohydride Catalysts

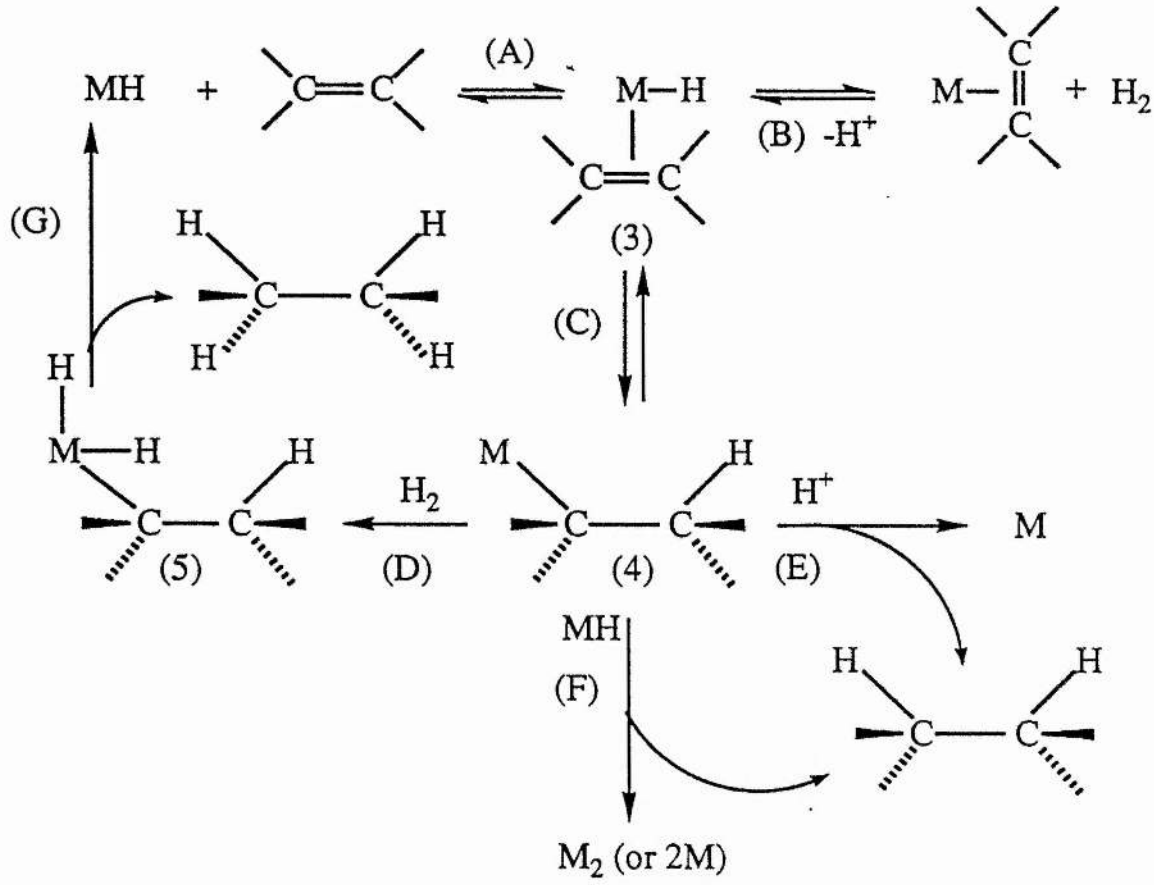


Step (C) is highly stereospecific, with the four-centre transition state shown in Figure 1.3.1 requiring a coplanar arrangement of metal, hydride and alkene $\pi$-bond, and leads to exclusive cis addition of the metal hydride.

Figure 1.3.1

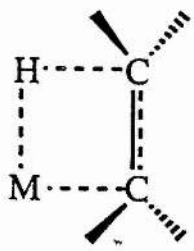


An explanation for the isomerization of simple alkenes in the absence of $H_2$ by

metal hydride addition-elimination (Figure 1.3.2) is provided by the reversibility of steps (A) and (C). This reversibility also accounts for isotope exchange between the metal hydride and the hydrogens on the alkene. Alkene isomerization can also occur via $\pi$-allyl intermediates (Figure 1.3.3) and possibly via $\alpha$-hydrogen abstractions involving carbene intermediates (Figure 1.3.4), although metal monohydride systems generally follow the process shown in Figure 1.3.2. [19]

Figure 1.3.2

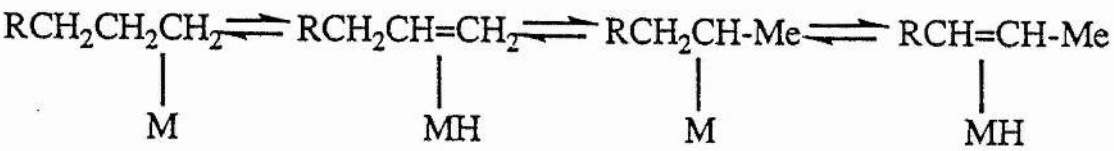


Figure 1.3.3

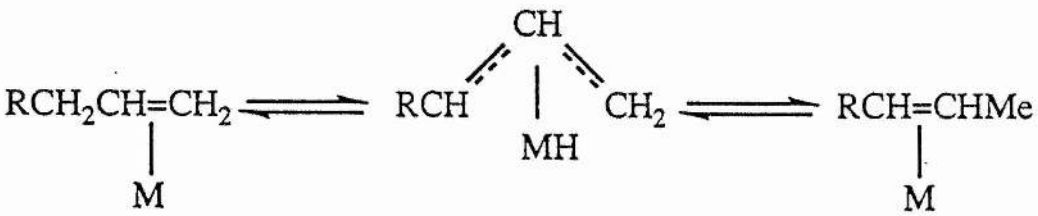


Figure 1.3.4

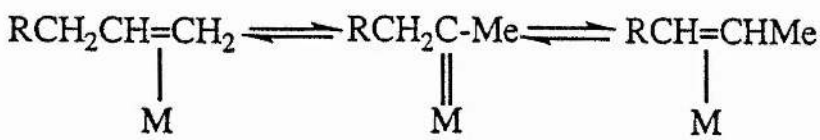


The formation of the saturated product from the alkyl(4) has been discussed in terms of steps (D), (E), or (F). Step (D) may involve oxidative addition of $H_2$ to give the dihydridoalkyl intermediate (5), which then reductively eliminates the saturated product in step (G) with regeneration of the monohydride catalyst.

Dihydridoalkyls (5) have never been detected thus far; the evidence for step (D) is by analogy with known oxidative addition of $H_2$ to $d^6$ and $d^8$ systems. Steps (E) and (F), which will be discussed later in further detail, represent decomposition routes for the metal alkyl(4) during catalytic cycles.

Catalysts that appear to operate via the ACDG cycle include the monohydrides $[RuHCl(PPh_3)_3]$[20], $[CoH(PPh_3)_3]$[8], $[RhH(CO)(PPh_3)_3]$[21] and $[IrH(CO)(PPh_3)_3]$.[8,22] The kinetic data for such cycles, neglecting complications due to ligand dissociation, are generally of the form shown in Equation 1.3.1. K is the overall equilibrium constant for alkyl formation (steps A and C) and k is the rate-determining oxidative addition of $H_2$.

Equation 1.3.1

$$\frac{-d[H_2]}{dt} = \frac{kK[metal][alkene][H_2]}{1 + K[alkene]}$$

The hydride transfer (step G) involving a three-centre transition state, as shown in Figure 1.3.5, is considered comparatively fast.

Figure 1.3.5

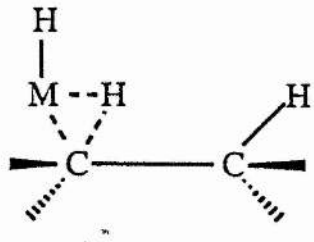


A significant study, albeit using a dihydride catalyst[23], has shown that reductive

elimination of the saturated product from an alkyl monohydride complex occurs with retention of configuration at the metal-bonded carbon (Figure 1.3.6).

Figure 1.3.6

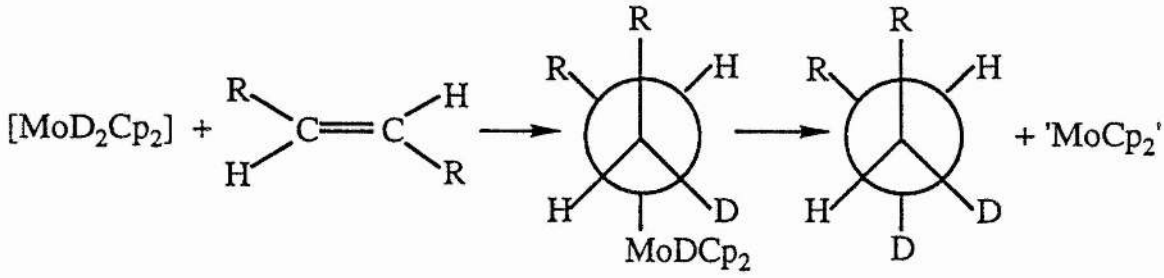


Such retention of configuration is necessary to give the observed cis addition of $H_2$ to alkenic bonds.

The protonolysis and thus decomposition of a metal alkyl(4) during a catalytic cycle gives rise to the metal centre (step E) which can reenter a catalytic cycle either through the unsaturate or the hydride route. Systems using trichlorostannate(II) complexes of Pt(II)[24] and Mo(III)[25], chlororuthenate(II)[17] and $[PdCl_4]^{2-}$ [26] have exhibited such a decomposition.

Step (F) involves the reaction of a metal alkyl with a metal hydride resulting in a binuclear reductive elimination. The metal reenters the catalysis by oxidative addition of $H_2$ to the dimer or 2M species. This process is best illustrated by $[CoH(CN)_5]^{3-}$ [27] and $[CoH(CO)_3(PR_3)]$ systems,[28] although the substrates are usually conjugated dienes and polyenes.

The pathways illustrated in Scheme 1.3.1 are readily modified for the hydrogenation of dienes and polyenes. Certain monohydride catalysts exhibit high selectivity towards hydrogenation of conjugated dienes and polyenes to give monoenes, and these will be reviewed in greater detail in Section 1.5. Addition of the metal hydride now yields $\sigma$ or $\pi$-allyl intermediates (Figure 1.3.7), whose formation and interconversion may be dependent on the concentration of an associated ligand L; lower ligand concentration gives a more unsaturated metal environment that allows formation of $\pi$-allyls, leading to 1,4-addition of hydrogen. Certain cobalt carbonyl phosphine systems have given rise to isolated $\sigma$- and $\pi$-allyl complexes.[27]

Figure 1.3.7

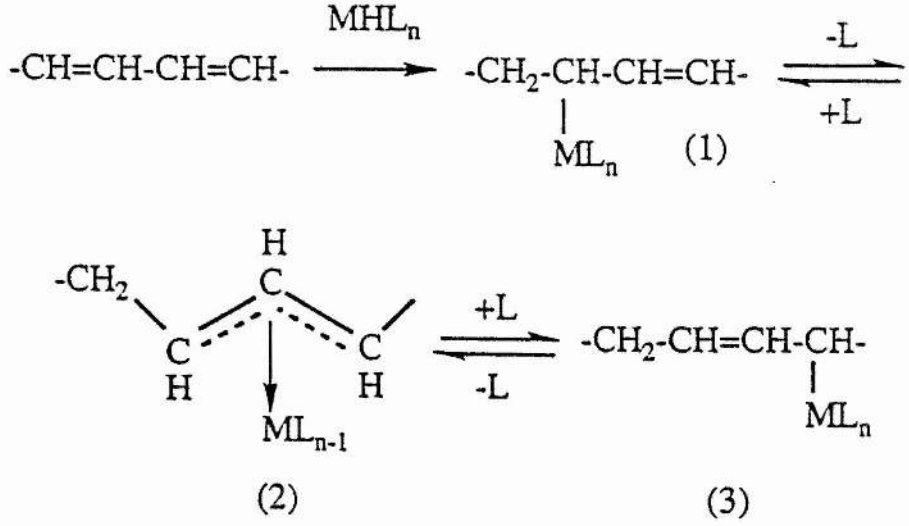


Dihydride Catalysts

The reaction pathways available for the hydrogenation of alkenic double bonds using dihydride catalysts are summarized in Scheme 1.3.2.[15] The hydride route and the unsaturate route, which involves oxidative addition of $H_2$ to a metal-alkene

complex, are defined by steps $K_1$ and $K_2$ respectively. The resulting dihydride alkene intermediate (X) decomposes to the product by two successive hydrogen atom transfers, the $K_3$ and $K_4$ steps. The metal is released as M with appropriate ancillary ligands and reenters the catalytic cycle via coordination to $H_2$ and/or the alkene. As with monohydride systems, an overall cis addition of $H_2$ results from the coplanar migratory insertion ($K_3$) step, and a reductive elimination of the product occurring with retention of configuration at the metal carbon ($K_4$ step).

Equilibria are established quickly for dihydride formation ($K_{H_2}$) and alkene binding ($K_s$) and only rarely have intermediates like (X) and (Y) been detected. If the hydrogen transfer steps ($K_3$ and $K_4$) are relatively fast, a rate law of the form shown in Equation 1.3.2 results, with the $K_1K_{H_2}$ and $K_2K_s$ terms referring to the hydride and unsaturate routes respectively. Oxidative addition of $H_2$ to a preformed complex containing a $\pi$-acceptor alkene ligand causes the unsaturate pathway to become less efficient. In cases where the simple dihydride $MH_2$ is not detected, ie $K_{H_2}$ is very small, and where there is evidence for formation of the alkene complex, ie $K_s$ is measurable, the unsaturate pathway is usually postulated. Similarly in systems where treatment with $H_2$ in the absence of the unsaturated organic substrate leads to metal production, the unsaturate pathway is employed. This is especially true for platinum metal systems that function in the abscence of $\pi$-acceptor ligands, known to stabilize metal hydrides. In these cases the unsaturated organic substrate is playing the role of such a ligand. Examples of catalyst systems that are thought to operate solely via the unsaturate $K_2K_s$ path include $[IrCl(PPh_3)(cod)]$[29] and trans-$[IrCl(CO)(PPh_3)_2]$.[30]

Scheme 1.3.2 Mechanistic Pathways For Dihydride Catalysts

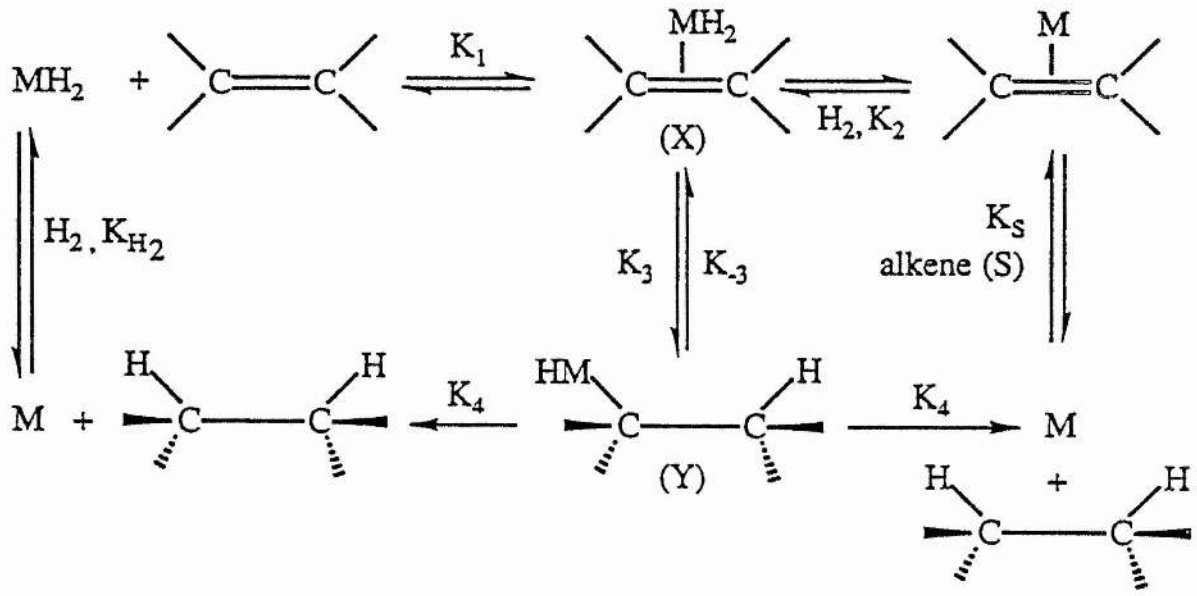


Complexes that give isolable dihydrides are generally considered to operate by the dihydride route, although both routes have been invoked in cases where both alkene and hydrogen are known to coordinate separately, eg $[Co(N_2)(PPh_3)_3]$[31], $[RhCl(PPh_3)_3]$[10] and $[RuH_2(PPh_3)_4]$[32].

Equation 1.3.2

$$\text{Rate} = \frac{-d[H_2]}{dt} = \frac{(K_1K_{H_2} + K_2K_S)[M][H_2][S]}{1 + K_{H_2}[H_2] + K_S[S]}$$

It should be noted that Equation 1.3.2, as with Equation 1.3.1 for monohydride catalysts, ignores any ligand dissociation reactions. These reactions cause the rate laws to be complicated by further denominator terms in ligand concentration.

In contrast to monohydride catalysts, dihydride systems with readily reducible

substrates generally show little alkene isomerization or hydrogen isotope scrambling with any component of the catalyst system. Within Scheme 1.3.2, this implies that $K_4 >> K_3$ and is consistent with the lack of observance of hydridoalkyl intermediates.

However recent, direct evidence for intermediates (X) and (Y) has been obtained in some cationic iridium[33] and rhodium[34] systems. These $[MH_2L_2S_2]^+$ catalysts (L=monodentate tertiary phosphine, S=solvent) are themselves formed by hydrogenation of diene precursors, which must involve the unsaturate mechanism of Scheme 1.3.2 with a modification for diene rather than alkene substrate.

Reaction schemes for hydrogenation of dienes using dihydride catalysts usually follow the basic hydride or unsaturate pathways outlined in Scheme 1.3.2. However, species (Y) is now a hydrido $\sigma$-alkenyl or a hydrido $\pi$-allyl intermediate (cf Figure 1.3.7 for the monohydride systems). Such pathways have been invoked for the widely studied $[Fe(CO)_5]$ and $[(diene)Fe(CO)_3]$ catalytic systems in which the active transient species is thought to be the metal tricarbonyl.[35,36] The reductions are not very selective due to accompanying isomerization via the $\pi$-allyl hydride intermediate (cf Figure 1.3.7).

## 1.4 $\pi$-Bonding of Monoenes and Dienes.

The first complex between a hydrocarbon and a transition metal was isolated by W C Zeise in 1825 and in the following years he characterized the pale-yellow compound now formulated as $[K[Pt(\eta^2\text{-}C_2H_4)Cl_3].H_2O]$. The true constitution of Zeise's salt and a few closely related complexes such as the chloro-bridged binuclear compound $[Pt_2(\eta^2\text{-}C_2H_4)(\mu_2\text{-}Cl)_2Cl_2]$ were not realised for over a hundred years.

The analysis of the bonding in metal alkene complexes carried out by Dewar[37] and Chatt and Duncanson[38] owed much to the bonding model proposed by Winstein and Lucas[39,40] in collaboration with Pauling, but it differed in the sense that it used perturbation molecular orbital formalism rather than the valence bond method to describe the interactions between the frontier orbitals of the alkene and the metal. As a result this mode of analysis led to the important conclusion that the alkene must be bonded in a $\pi$-fashion to the metal and accounted for the IR characteristics of the coordinated alkene molecule in Ziese's salt and related molecules. The Dewar, Chatt and Duncanson(DCD) bonding theory concludes that the alkene is $\pi$-bound to the metal by the combination of two interdependent components, which are shown in Figure 1.4.1. The first component (part (a) of Figure 1.4.1) involves a $\sigma$ overlap between the filled $\pi$-orbital of the alkene and a suitably directed vacant, hybrid metal orbital. This is reinforced by the second component (part (b) of Figure 1.4.1) which derives from the overlap of a filled metal d orbital with the vacant antibonding orbital of the alkene; these orbitals have $\pi$ symmetry with respect to the bonding axis and allow $M \rightarrow C_2$ $\pi$ back bonding to assist the $\sigma$ $C_2 \rightarrow M$

bond synergically. These interactions result in electron population of the alkene $\pi^*$-orbital and depopulation of the alkene $\pi$-orbital. These changes in electron distribution are reflected in a lengthening of the carbon-carbon bond in the coordinated alkene and a lowering of the carbon-carbon stretching frequency.

Figure 1.4.1

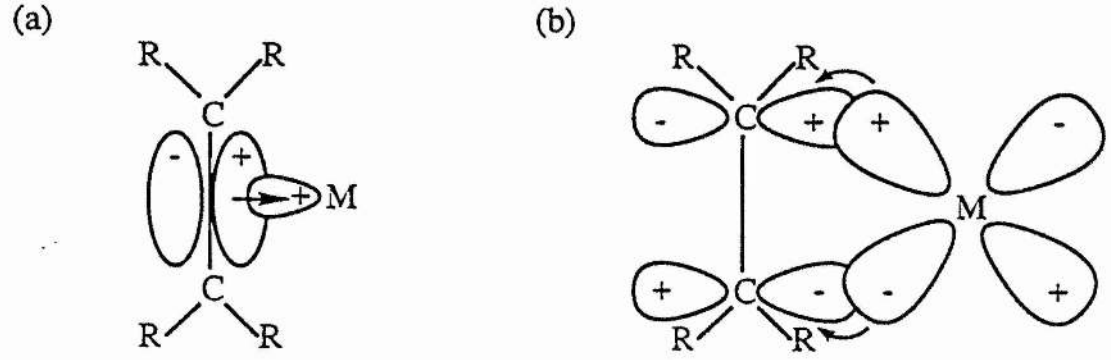


The relative importance of the two bonding components in the DCD bonding model can be qualitatively determined on the basis of the formal oxidation state of the metal, the electron donating characteristics of the ligands coordinated to the metal and the substituents on the alkene.

In lower valent transition metal complexes the amount of back donation from metal to alkene is more extensive. As a result there are larger changes in the geometry of the alkene upon coordination, in particular an increase in the alkene carbon-carbon bond length. Similar bond lengthening has been observed for alkene complexes of the earlier transition metals which have a higher formal oxidation state but have ancillary ligands with good $\sigma$-donating characteristics.[41]

The effects of substituents on the length of the C-C bond in coordinated alkenes do not show any strong or predictable trend. The alkene substituents bend back away form the metal on coordination to give a quasi-tetrahedral coordination geometry to the alkenic carbon atoms. It has been reported that the bending back is least for hydrogen and is greatest for halogen substituents. This trend parallels that for the metal-alkenic carbon bond lengths where it is found that the shortest metal-carbon bond lengths are associated with the alkenes bearing halogen substituents.

One area where the DCD bonding model cannot be applied reliably is for complexes bearing electronegative substituents on the alkene and containing metals of low oxidation state. The geometrical changes associated with coordination are so severe that a better stratagem is to regard the complex as having a metallocyclopropane structure as illustrated in Figure 1.4.2.[42,43]

Figure 1.4.2

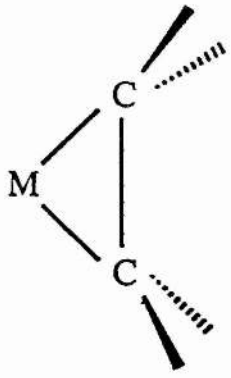

If an unsymmetrically substituted alkene is complexed, the metal-carbon bond lengths often differ significantly.[44-53] In general the metal-carbon interatomic distance to a substituted alkene carbon atom is longer than that to an unsubstituted carbon, an effect which appears to be independent of whether the substituent is a net $\pi$-donor(D) or $\pi$-acceptor(A). This asymmetry in bond lengths is accompanied by a slip distortion of the alkene moiety relative to the metal atom in such a way that the centre of the C-C bond lies below the plane defined by the metal atom and the other ligands coordinated to the metal, as is shown in Figure 1.4.3.

Figure 1.4.3

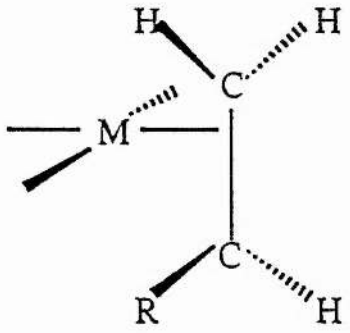


Hoffmann et al.[54] have argued that these asymmetric effects reflect the perturbation introduced into the olefin $\pi$ and $\pi^*$ levels by the introduction of $\pi$-donor and acceptor ligands. Compared to ethylene, $\pi$-acceptors generally lower the energies of $\pi$ and $\pi^*$ and second order perturbation effects polarize the $\pi$ and $\pi^*$ levels in the manner illustrated in Figure 1.4.4. However, $\pi$-donor substituents raise the energies of $\pi$ and $\pi^*$, and polarize these orbitals in the opposite sense, as is illustrated in Figure 1.4.5. In a square planar platinum(II) complex, for example, a $\pi$-accepting substituent will lower the $\pi$ and $\pi^*$ by enhancing the back donation component illustrated in Figure 1.4.6. Since the $\pi^*$ orbital in such an alkene has a

larger coefficient at the unsubstituted carbon atom, the metal-ligand overlap shown in Figure 1.4.6 will result in a strengthening of the metal to unsubstituted carbon bond. A $\pi$-donor substituent raises the energies of $\pi$ and $\pi^*$ and thus enhances the forward bonding component of the synergic bonding model. The relevant metal-alkene interaction illustrated in Figure 1.4.7 will also lead to a strengthening of the metal to unsubstituted carbon bond relative to the substituted carbon because of the larger coefficient at the unsubstituted carbon in the alkene $\pi$-bonding molecular orbital.

Figure 1.4.4

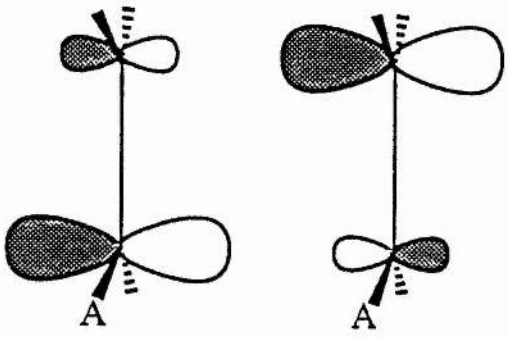


Figure 1.4.5

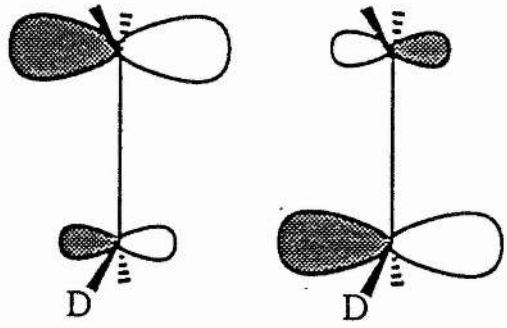


Figure 1.4.6

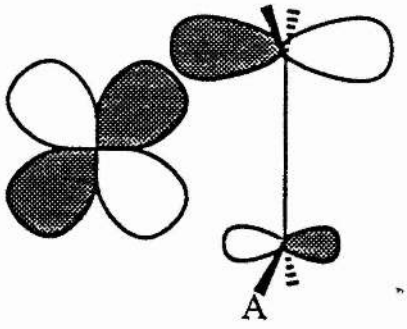


Figure 1.4.7

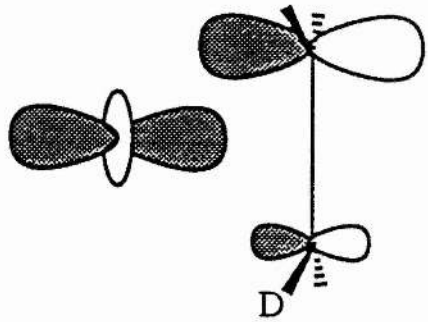

With $\pi$ metal complexes it is often hard to separate the steric and electronic properties of a substituent. A general study of substituted alkenes shows that the introduction of any substituent to a double bond creates an unfavourable, sterically induced effect on the stability of the metal-alkene bond. The appearance of steric effects is put down to the presence of larger substituents both preventing the alkene from approaching the metal centre at the optimum bonding angle[55] and imposing greater physical restrictions to ligand movement in any resulting complex.[56,57]

The presence of steric effects also means that the coordination of cis and trans isomers must be considered separately. Generally the greater stability of cis alkene complexes compared with their trans analogues is attributed to a significant enthalpy difference in favour of the cis isomer. This enthalpy difference is firstly due to less strain being induced by the lengthening of the alkene double bond upon coordination[58] and secondly the cis isomer will be able to approach closer to the metal and thus will achieve greater $\pi$-orbital overlap and hence a stronger bond.[59,60,61]

The electronic properties of substituents have been elucidated by comparing complexes whose ligands are almost identical in size but of different electronic nature.[62] The metals are found to fall into two groups: those such as Ag(I) and Cu(I) whose stability decreases as the electronegativity of the substituent increases and those such as Pt(O) and Rh(I) whose stability increases as the electronegativity of the substituent increases. The difference in behaviour is related to which of the components is the most important in the synergic bond. In the former case, the $\sigma$-

bonding component is more important and as a result electron withdrawing substituents reduce the ability of electrons to participate in this $\sigma$ bond formation and thus a decrease in bond stability is observed. For the latter, the major bonding component is found to be $\pi$-back bonding and thus an increase in the $\pi$-acceptor ability of the alkene, caused by electron withdrawing substituents, strengthens the metal alkene bond.

There are basically two types of metal-diene complexes, from the point of view of the ligand; those containing an unconjugated (eg 1,4- or 1,5-) diene, which acts as a chelating agent, and those containing a conjugated 1,3-diene. In terms of reactivity, the complexes of unconjugated dienes closely resemble those of monoolefins, while 1,3-diene complexes have special properties due to their different bonding arrangement.

Probably the most important conjugated diene is buta-1,3-diene, which can bind in several ways. It usually acts as a 4-electron donor in its cisoid configuration, as shown in Figure 1.4.8(a). As back donation from the metal to the diolefin increases, the contribution from the resonance hybrid, shown in Figure 1.4.8(b), to the bonding of buta-1,3-diene becomes more significant.

Figure 1.4.8

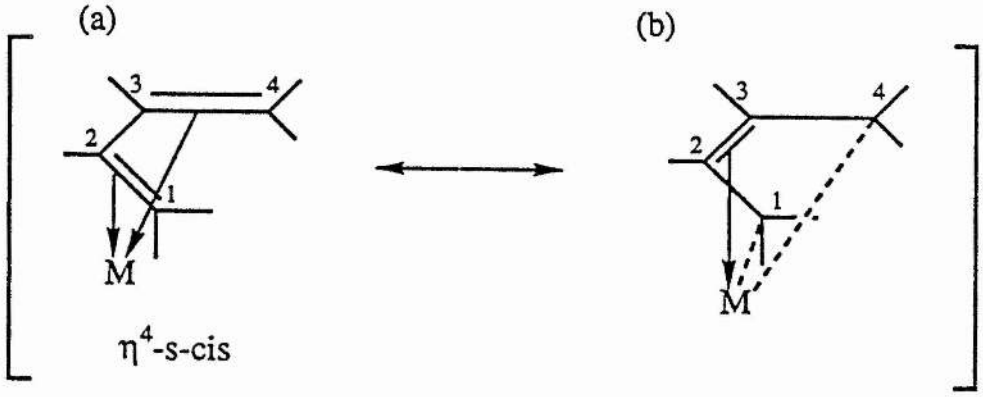


In numerous complexes the $C_2C_3$ distance is slightly shorter than the two other C-C distances, and the substituents at $C_1$ and $C_4$ are twisted ~20-30° out of the plane of the ligand so that the corresponding p orbitals can overlap better with the metal.

The molecular orbital diagram presented in Figure 1.4.9 shows that both the depletion of electron density in $\psi_2$ by $\sigma$ donation to the metal, and population of $\psi_3$ by back donation from the metal, have the effect of lengthening $C_1C_2$ and shortening $C_2C_3$, because $\psi_2$ is $C_1C_2$ bonding and $C_2C_3$ antibonding and $\psi_3$ is $C_1C_2$ antibonding and $C_2C_3$ bonding in character.

The $\eta^4$-s-cis form of butadiene binding illustrated in Figure 1.4.8(a) is usually more stable than the $\eta^4$-s-trans form illustrated in Figure 1.4.10(a), however the reverse is known in the case of $[CpMo(NO)(\eta^4\text{-}C_4H_6)]$.[63] Figure 1.4.10(b) illustrates the $\mu.\eta^4$-s-trans form of butadiene binding and this is exemplified by $[Os_3(CO)_{10}(C_4H_6)]$[64], where the diene is $\eta^2$ bound to each of two different Os centres.

Figure 1.4.9

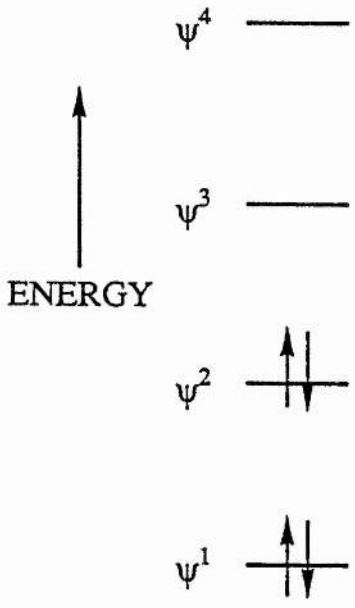


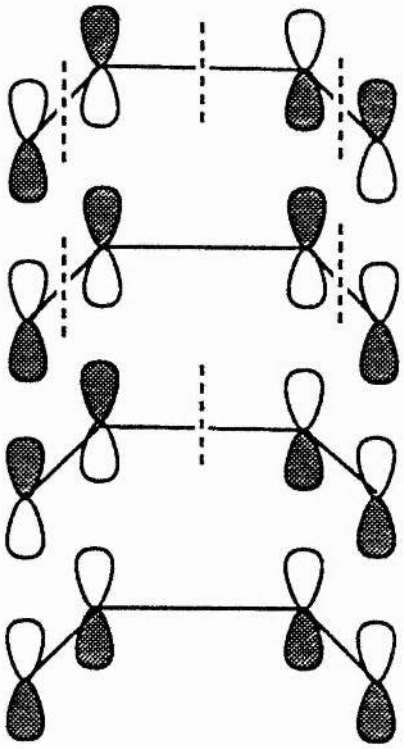

Figure 1.4.10

(a)

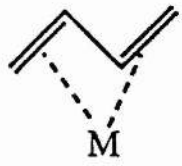


$\eta^4$-s-trans

(b)


$\mu,\eta^4$-s-trans

The "sandwich" form of butadiene binding, shown in Figure 1.4.11(a), is found in a rhodium chelate phosphine complex whereby $\eta^3$ bonding from a cis-$C_4H_6^{2-}$ ligand is observed.[65]

Figure 1.4.11(b) shows how in [CpMo(NO)($C_4H_2Me_4$)] a twisted transoidal, nonplanar diene can bind with the central atoms closer to Mo than the outer ones.[63]

Figure 1.4.11

(a) (b)

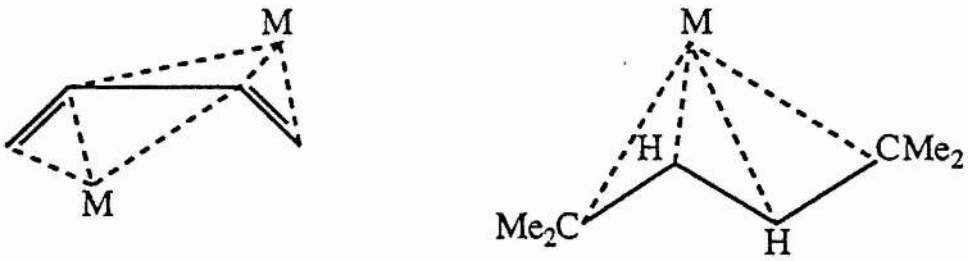


1.5 Catalytic Systems used for the Homogeneous Hydrogenation of Diene Substrates.

Rhodium

The discovery of $[RhCl(PPh_3)_3]$, now known as Wilkinson's catalyst, has represented the most significant step forward in homogeneous hydrogenation.[66] It is a highly active catalyst and the mechanism of hydrogenation has been elucidated by Halpern et al.[67,68,69] It is summarised in Scheme 1.5.1. The actual catalytic cycle is enclosed in the rectangle and the species outside it can also lead to hydrogenation albeit at a slower rate.

Considerable data point generally to the reactivity sequence shown in Equation 1.5.1 for the usual cis addition of $H_2$, $D_2$, or $T_2$. The readily hydrogenated terminal alkenes include nonconjugated, nonchelating dienes,[70,71] while with cyclic alkenes [72-75] the rate decreases with increasing ring size. Conjugated dienes [75] are reduced but much more slowly than terminal alkenes. The following groups or compounds are not hydrogenated or cleaved by hydrogenolysis: arenes, ketones, carboxylic acids, esters, amides, nitriles and ethers, and azo, chloro, hydroxy and nitro compounds.

The catalyst is of limited use when an aldehyde function is present due to an accompanying decarbonylation reaction which produces the relatively inactive trans-$[RhCl(CO)(PPh_3)_2]$ complex.[76]

Scheme 1.5.1

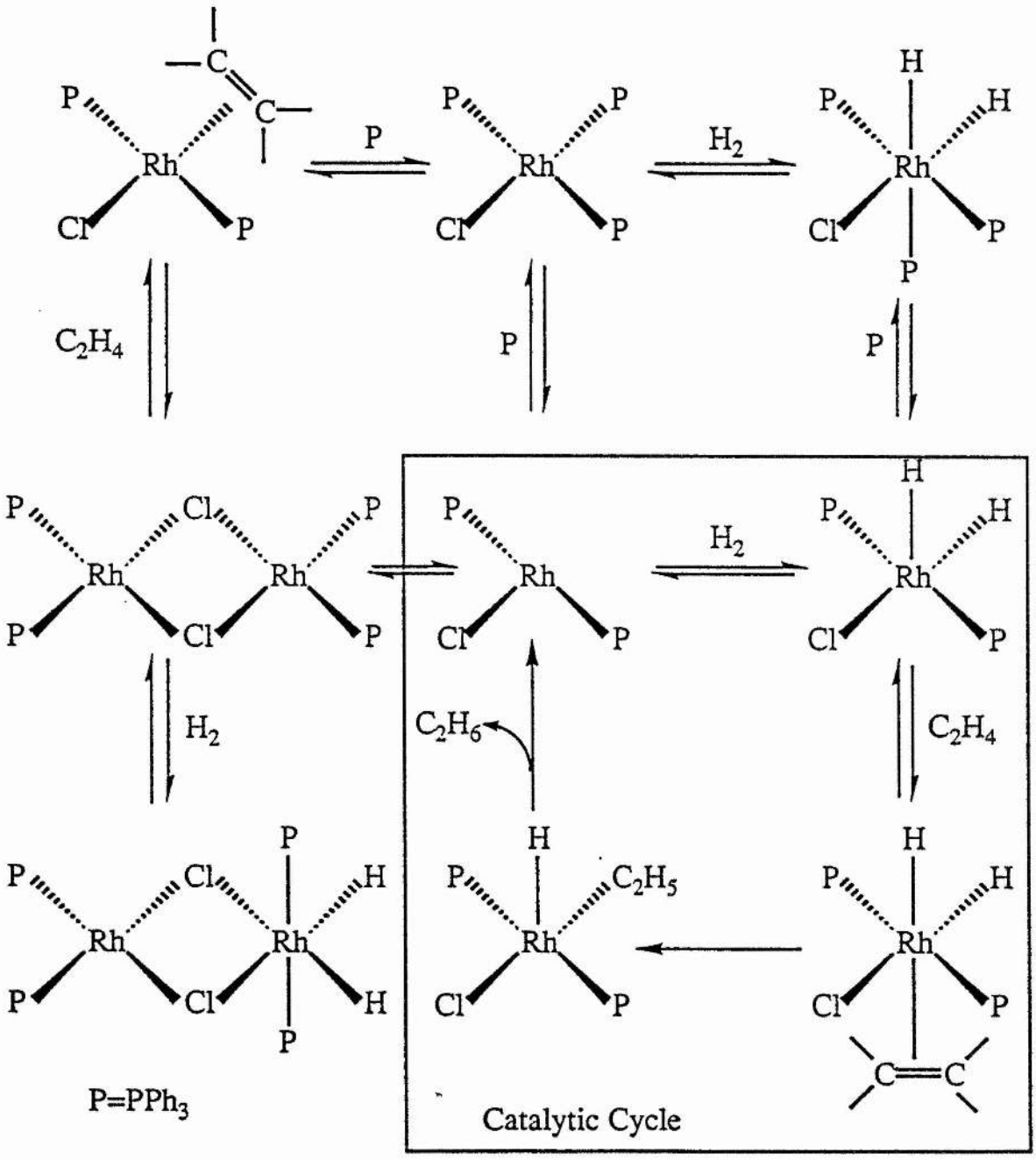

Equation 1.5.1

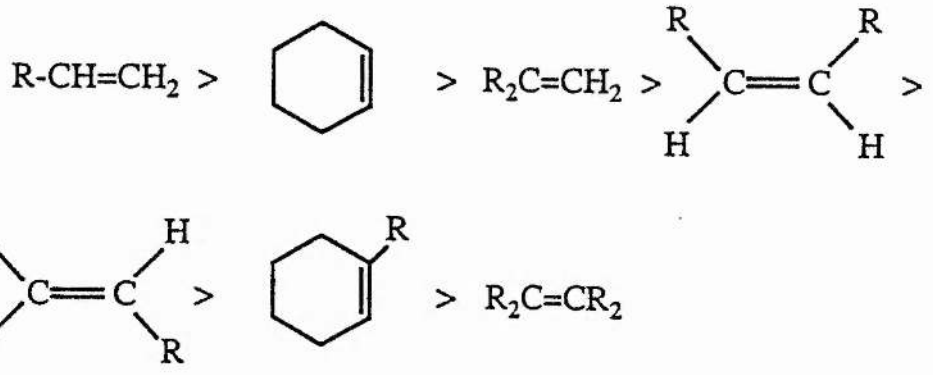


The coordinative ability of naked transition metals towards reducible substrates is most unselective, however the active intermediate in the catalytic cycle, $[RhCl(H)_2(PPh_3)_2]$, selectively coordinates C = C bonds to the vacant sixth coordination position. This position is adjacent to large triphenylphosphine ligands, and thus there is a built-in regioselectivity toward the coordination of the least sterically hindered bond in a polyene. This selectivity is further augmented by the low complex formation constants of hindered alkenes with transition metal compounds. An example of this is the hydrogenation of eremophilone,[77] illustrated in Figure 1.5.1.

Figure 1.5.1

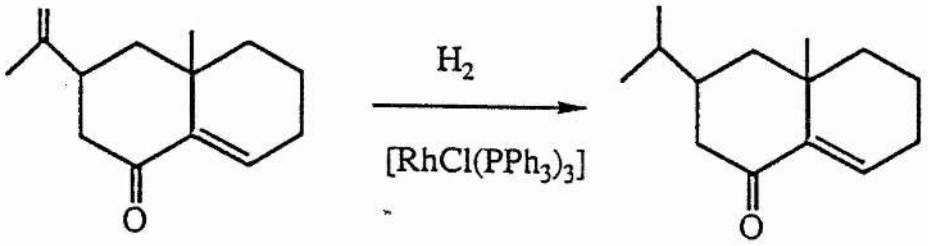

The selectivity towards less hindered alkenes is well established by the facile reduction of similar isopropenyl groups in carvone and γ - gurjunene.

Equation 1.5.2 illustrates another example of this selectivity, whereby the terminal alkene bond in the allene is hydrogenated.[78]

Equation 1.5.2

$$CH_2=C=CEt_2 \xrightarrow[[RhCl(PPh_3)_3]]{H_2} CH_3\text{-}CH=CEt_2$$

Osborn and co-workers introduced a series of cationic rhodium-diene complexes of the general type $[Rh(diene)(phosphine)_2]^+X^-$ ($X^-$ is a non-coordinating anion).[79-82] Norbornadiene was the preferred diene, although 1,5-cyclo-octadiene was used. $PPh_3$, $PPh_2Me$, $PPhMe_2$ or a chelating diphosphine were generally the phosphorus ligands and the anions were typically $ClO_4^-$ or $PF_6^-$. The diene substrates hydrogenated, included norbornadiene and substituted butadienes. An interesting aspect of conjugated diene hydrogenations which was exemplified by this work was the striking variation in product ratios on varying slightly the nature of the chelating phosphine ligand.

Table 1.5.1 shows the percentages of 2,3-dimethylbut-l-ene and tetramethylethylene obtained on reduction of 2,3-dimethylbuta-1,3-diene using $(C_6H_5)_2PCH_2CH_2P(C_6H_5)_2$ = diphos, $(C_6H_5)_2PCH_2CH_2As(C_6H_5)_2$ = arphos and $(C_6H_5)_2AsCH_2CH_2As(C_6H_5)_2$ = dpae as the chelating ligands.

Table 1.5.1 Hydrogenation of $H_2C=CMe-CMe=CH_2$

| Catalyst Precursor | Product % 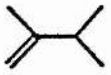 | 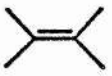 |
|---|---|---|
| $[Rh(NBD)(diphos)]^+$ | 39 | 61 |
| $[Rh(NBD)(arphos)]^+$ | 17 | 83 |
| $[Rh(NBD)(dpae)]^+$ | 80 | 20 |

In contrast, similar product distributions are obtained for the reduction of the methyl ester of trans, trans-hexa-2,4-dienoic acid with the chelating phosphine as diphos or arphos. Therefore the product distribution may be determined in part by the nature of the substrate being reduced, as in the latter example, yet may also depend strongly on the nature of the chelating phosphine, as in the former examples.

It should be noted that under hydrogenation conditions the diene complex is reduced to give cationic solvated rhodium (I) - phosphine complexes which initiate the catalytic cycle.

The implication of metal hydrides in homogeneous hydrogenation led to their direct use as catalyst precursors $[RhH(PPh_3)_4]$, in the presence of an equimolar amount of $PEt_3$ brought about the hydrogenation of 1,3-dienes to alk-l-enes.[83]

By addition of carboxylate anions to solutions of cationic rhodium-triphenylphosphine complexes under hydrogen, complexes of the type $[RhH_2(O_2CR)(PPh_3)_2]$ have been isolated which have the structure shown in

Figure 1.5.2. In benzene-methanol solutions, these complexes reduce the carbon-carbon double bond of activated alkenes.[84] Carboxylate complexes of the type $[Rh(O_2CR)(PPh_3)_3]$, which may be regarded as precursors of $[RhH_2(O_2CR)(PPh_3)_2]$ have been prepared either by addition of $PPh_3$ and a carboxylate anion to an acidic solution of $[Rh_2(OAc)_4]$[85] or more directly from $[RhCl_3.3H_2O]$.[86] $[Rh(OAc)(PPh_3)_3]$, as shown in Figure 1.5.3, in a methanol solution and in the presence of p-toluenesulfonic acid has been used to hydrogenate a wide range of dienes to monoenes. The selectivity associated with this was found to vary with the acid/acetate ratio. The acid dependence is thought to be due to conversion of $[Rh(OAc)(PPh_3)_3]$ to a cationic species by protonation of the acetate group.

Figure 1.5.2

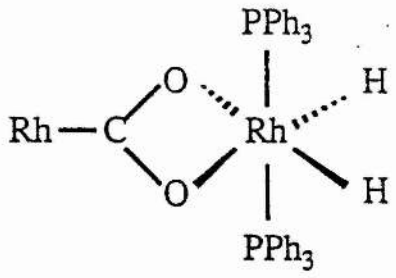


Figure 1.5.3

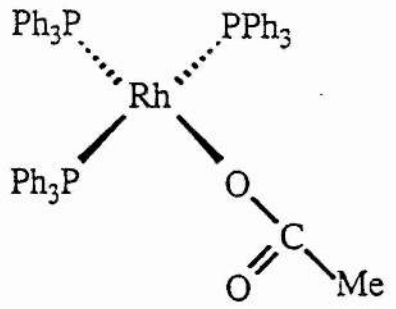


The nitrosyl complex $[Rh(NO)(PPh_3)_3]$ has been used to hydrogenate a variety of unsaturated compounds[87] and a comparison of crude rate studies and intramolecular competition (e.g. 4-vinylcyclohexene and d-limonene) led to the following order for reactivity of different alkenes: 1-alkyne > 2-alkyne > 1-olefin ≥ exo-methylene ≥ cyclohexene ≥ cis-alk-2-ene > trans-alk-2-ene > trisubstituted olefin >>>> tetra-substituted olefin. Isoprene and 2,4-hexadiene were very slowly hydrogenated and

gave all possible isomeric monoenes.

Iridium

The iridium analogue of Wilkinson's catalyst, $[IrCl(PPh_3)_3]$, does not function as a hydrogenation catalyst under mild conditions, as the necessary dissociation of one $PPh_3$ ligand following oxidative addition of $H_2$ does not occur.

The catalytic activities of the nitrosylcatecholato complexes $[Ir(NO)(1,2\text{-}O_2C_6Br_4)(PPh_3)]$ and $[Ir(NO)(1,2\text{-}O_2C_6H_4)(PPh_3)]$ in the homogeneous hydrogenation of cyclic alkenes, dienes and trienes have been related to the electron density on the central metal atom.[88] The bromine atoms, which are electron withdrawing, remove electron density from the metal and thus create a more active catalyst. Unfortunately studies have not yet stated whether there is a 1,2 or 1,4 addition of hydrogen.

The iridium (I) complex $[IrCl(CO)(PPh_3)_2]$, generally known as Vaska's compound, has played a most important role in the study of oxidative addition, however it has also been used in diene hydrogenation with high selectivity towards monoene formation via $\eta^3$ -allyl intermediates.[89] The activity of $[IrCl(CO)(PPh_3)_2]$ is markedly increased under UV radiation. An example being that of 1,3-cyclohexadiene which is hydrogenated to cyclohexadiene at a rate ten times quicker than in the dark.[90,91]

Ruthenium

Wilkinson and co-workers have shown that $[RuCl_2(PPh_3)_3]$ and complexes derived from it play key roles in ruthenium-catalysed hydrogenation. The complex reacts with hydrogen in the presence of a base such as $Et_3N$ according to Equation 1.5.3.[92]

Equation 1.5.3

$$[RuCl_2(PPh_3)_3] + H_2 + Et_3N \longrightarrow [RuH(Cl)(PPh_3)_3] + Et_3NH^+Cl^-$$

The selective hydrogenation of 1,4-androstadiene-3,17-dione to 4-androstene-3,17-dione has been achieved using $[RuCl_2(PPh_3)_3]$[93] as illustrated in Figure 1.5.4.

Figure 1.5.4

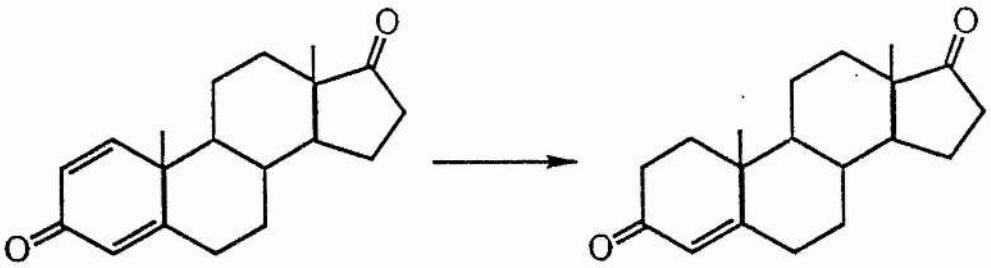

The rate of hydrogenation is dependent on both the base added and on para substituents in the phosphorus ligand. For the bases the sequence was found to be $Et_3N \approx Et_2NH > PhNH_2 > BuNH_2$, with pyridine inhibiting the reaction. The effect of substituents in the phosphine was MeO > Me > H > F.

The catalyst precursor has also been used for the selective hydrogenation of 1,5,9 - cyclododecatriene and 1,5-cyclooctadiene to the monoenes.[94]

A carbonyl complex of ruthenium, $[RuCl_2(CO)_2(PPh_3)_2]$, illustrated in Figure 1.5.5, has been shown to catalyse hydrogenation of a series of alkenes and the rates were found to vary in the order conjugated dienes > non-conjugated dienes > terminal alkenes > internal alkenes.[95] This is opposite to the observed rates seen for hydrogenations catalysed by $[RuH(OCOCF_3)(PPh_3)_3]$.[96] This observation has been rationalized in terms of greater steric hindrance in the addition of hydrogen to five-coordinate $[Ru(alkenyl)X(PPh_3)_2]$ complexes as compared to four-coordinate $[Ru(alkyl)X(PPh_3)_2]$ complexes. By replacing the bulky $PPh_3$ ligands with the smaller CO groups, this steric hindrance is relieved, and the addition of hydrogen to five-coordinate $[RuCl(alkenyl)(CO)_2]$ complexes is sterically allowed.

Figure 1.5.5

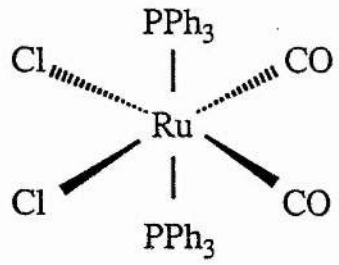


$[Ru(OAc)_2(PPh_3)_2]$ has been used as a hydrogenation catalyst for terminal alkenes in benzene, methanol and methanol containing p-toluensulphonic acid where the rate passed through a maximum at low acid concentration. This was attributed to the stepwise protonolysis of the acetate ligands, leading to cationic, methanol-solvated complexes, as shown in Equation 1.5.4. Benzene or methanol without acid gave much poorer rates. Similar behaviour was observed with both conjugated and non-conjugated dienes and these were generally hydrogenated to the monoenes, though with little regioselectivity. The superior coordinating ability of the diene

compared with the monoene was deemed to be the cause of their hydrogenation.[86]

Equation 1.5.4

$$[Ru(OAc)_2(PPh_3)_2] \xrightarrow[MeOH]{H^+} [Ru(OAc)(PPh_3)_2(MeOH)_x]^+$$

$$\xrightarrow[MeOH]{H^+} [Ru(PPh_3)_2(MeOH)_y]^{2+}$$

Platinum

The complexes $[PtHL(\eta^3\text{-}C_3H_5)]$ ($L = P(C_6H_{11})_3, PBu^t_3$) catalyse the hydrogenation of butadiene to but-l-ene, isoprene to 2-methylbut-lene and 2,3 dimethylbutadiene to 2,3 dimethylbut-l-ene at -78°C. The complexes show a degree of fluxionality in that a -32°C an equilibrium exists between the two structures shown in brackets in Scheme 1.5.2.[97]

Scheme 1.5.2

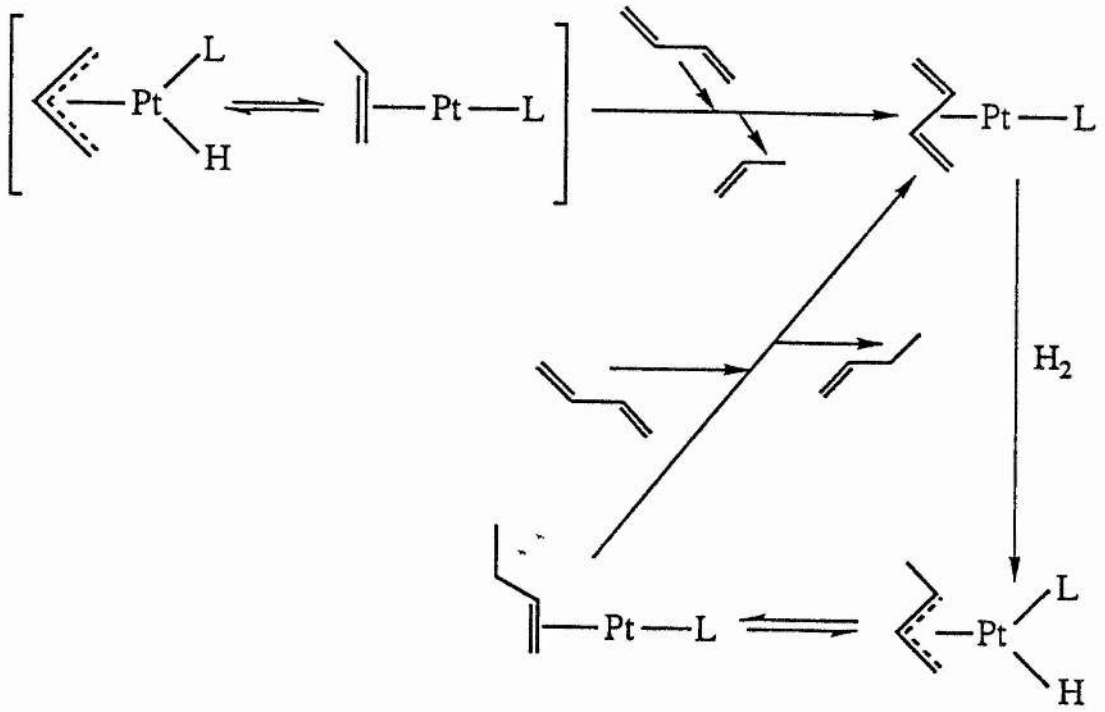

The mechanism illustrated in Scheme 1.5.2 shows that the addition of the diene to the $\eta^3$-allyl complex caused immediate displacement of propene. No reaction with hydrogen occurred in the absence of the diene.

Platinum complexes of the general type $[PtX_2L_2]$ (X = halogen, pseudohalogen; L = phosphine, arsine, sulphide, selenide) in the presence of $SnCl_2$ were found to hydrogenate linear and cyclic dienes.[98,99] The complex $[PtCl_2(PPh_3)_2]$ has been most generally used.[98,99,100] With $SnCl_2$, it gives the complex $[PtCl(SnCl_3)(PPh_3)_2]$ which with hydrogen gives the hydride $[PtH(SnCl_3)(PPh_3)_2]$. The aforementioned catalyst precursors add hydrogen to a conjugated system by 1,4-addition.

Cobalt

The pentacyanocobaltate (II) ion has for many years been known to catalyse alkene hydrogenation, mainly of conjugated dienes. The catalyst system exhibits hardly any activity for the hydrogenation of non-activated monoenes.

The activity and selectivity observed in these systems are markedly solvent dependent. In water alone, deactivation eventually occurs. This has led to the use of mixtures of water and organic solvents, or to polar solvents alone. The product of hydrogenation is not only dependent on the solvent but also on the CN/Co ratio. In the hydrogenation of butadiene in aqueous solution, the major product was trans but-2-ene at CN/Co = 5.1 and but-l-ene at CN/Co > 5.1. The total concentration also affects the product distribution. In a glycerol-methanol solution similar results were obtained, the change occurring at CN/Co = 5.4. In an ethylene glycol-

methanol solution the production of cis but-2-ene was favoured.[101]

$[Co(CN)_5]^{3-}$ has been used in the regioselective hydrogenation of trans-1-phenylbut-1,3-diene and has yielded 1-phenylbuta-l-ene as the product.

The mechanism of hydrogenation of olefinic double bonds using this catalyst precursor has generated much discussion, and it has been suggested that radical reactions are involved.[102] Hydrogen is believed to be activated prior to reaction with the alkene, the mechanism involving homolytic fission by two $[Co(CN)_5]^{3-}$ ions, as is shown in Scheme 1.5.3. The transfer of hydrogen to the alkene can also occur via a radical process,[103] and not by an insertion reaction. The observation of alkenyl and allyl species in diene hydrogenation suggests however, that a different mechanism of hydrogen transfer may operate, as these reactions appear slow enough for intermediates to be observed directly by NMR.

The hydrogenation of hexa-2,4-dienoic acid (sorbic acid) using $[Co(CN)_5]^{3-}$ in water selectively produces hex-2-enoic acid in an 82% yield, and in methanol a 96% yield.[104] Only trace amounts of hex-4-enoic acid are found and this is in contrast with results obtained using rhodium complexes, given in Chapter 2.

Scheme 1.5.3

$$[Co(CN)_5]^{3-} + H_2 \longrightarrow [CoH(CN)_5]^{3-} + H^{\cdot}$$

$$[Co(CN)_5]^{3-} + H^{\cdot} \longrightarrow [CoH(CN)_5]^{3-}$$

$$[CoH(CN)_5]^{3-} + X \longrightarrow [Co(CN)_5]^{3-} + HX^{\cdot}$$

$$[CoH(CN)_5]^{3-} + HX^{\cdot} \longrightarrow [Co(CN)_5]^{3-} + H_2X$$

X = conjugated diene / activated alkene

A distinct problem with many cobalt complexes is that when used as catalysts they do not tolerate an excess of diene and their lifetime is short. The use of phase-transfer reaction conditions for the homogeneous water-soluble hydrogenation catalyst $K_3[Co(CN)_5H]$ has provided a readily accessible catalytic system useful for synthetic scale reactions, with greater regioselectivity.

Reger et al. have performed phase transfer catalysis using $K_3[CoH(CN)_5]$ and a variety of ammonium salts.[105] As a result the water-soluble metal catalyst reacts with organic-soluble conjugated diene substrates, because the ammonium salt ion pairs with the water-soluble anion and transfers it to the organic phase. The catalytic hydrogenation of 2-methyl-1,3-butadiene (isoprene), in the presence of tetramethylammonium chloride, after 5 hours gave rise to 78% conversion to 2-methylbut-2-ene, as illustrated in Equation 1.5.5. Without the ammonium salt 74% conversion to the same product was achieved after 48 hours. Similar rate increases

were observed for a variety of conjugated dienes. Overall 1,4 addition of hydrogen was observed using $K_3[CoH(CN)_5]$, and penta-1,3-diene was hydrogenated to trans pent-2-ene with a fourfold increase in rate when $Et_3PhCH_2NCl$ was present.

Equation 1.5.5

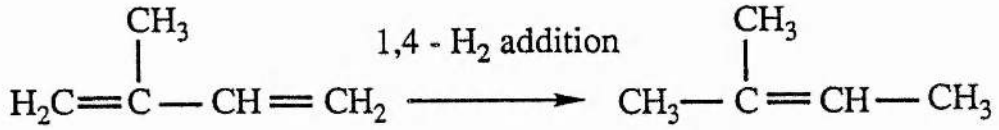


Reger's attempts to hydrogenate sorbic acid using $[CoH(CN)_5]^{3-}$ under both phase-transfer and micellular conditions had failed.[106] However when β-cyclodextrin was used as the phase-transfer agent, sorbic acid was hydrogenated to mainly trans hex-2-enoic acid.[107] β-cyclodextrin can bind conjugated dienes and thus bound dienes could be transferred to the aqueous phase where they could be hydrogenated in the presence of $[CoH(CN)_5]^{3-}$. Alternatively, it has been suggested that β-cyclodextrin could serve as a second-sphere ligand for $[CoH(CN)_5]^{3-}$ thus transferring it to the organic phase where diene hydrogenation would take place.

Modification of the $[Co(CN)_5]^{3-}$ catalyst by addition of diamines has been reported to lead to higher catalytic activity in diene hydrogenation and a predominant 1,2-addition of hydrogen.[108,109]

A fairly high selectivity is shown by the triphenylphosphine complexes $[CoX(PPh_3)_3]$ (X=Cl, Br, I) in the hydrogenation of dienes. Internal double bonds are reduced preferentially. Activation of the complexes requires addition of a Lewis acid, which is thought to cause the removal of the halide ligand and formation of a diene

complex[110] as is shown in Equation 1.5.6

Equation 1.5.6

$$[CoBr(PPh_3)_3] + \text{diene} + BF_3.OEt_2 \longrightarrow [Co(\text{diene})(PPh_3)_3]^+[BF_3Br]^- + Et_2O$$

$[Co(SCN)(PPh_3)_3]$ has also been used as a selective catalyst for acyclic conjugated dienes.[111] Table 1.5.2 shows data obtained using this catalyst. The hydrogenation of $C_2$- or/and $C_3$- substituted 1,3-butadienes was faster than that of 1,3-butadiene, while the hydrogenation of $C_1$- or/and $C_4$- substituted buta-1,3-dienes was slower. 1,4-addition is favoured in all cases.

Table 1.5.2

| Diene | Substituent $C_1$ | $C_2$ | $C_3$ | $C_4$ | Rel. Rate | Products (%) |
|---|---|---|---|---|---|---|
| 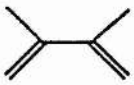 | H | Me | Me | H | 5.0 |   |
| 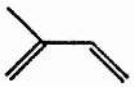 | H | Me | H | H | 2.3 | 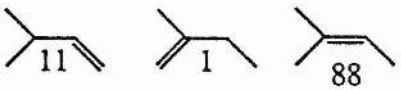  |
|  | H | H | H | H | 1.0 |   |
| 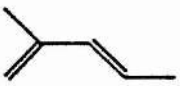 | H | Me | H | Me | 0.2 | 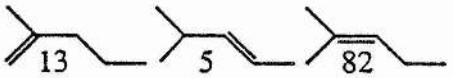  |
| 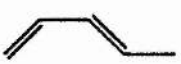 | H | H | H | Me | 0.04 | 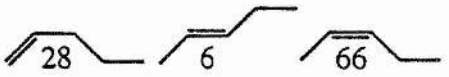  |
| 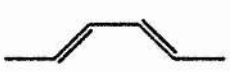 | Me | H | H | Me | 0.00 | |

Nickel

The complex $[NiI_2(PPh_3)_2]$, at high pressure, hydrogenates linear and cyclic dienes, both conjugated and non-conjugated.[112] With the former, 1,4-addition of hydrogen predominates, the reaction involving $\eta^3$-allyl intermediate.

Treatment of $[Ni(acac)_2]$ with $Al_2Et_3Cl_3$ in the presence of $PPh_3$ in the mole ratio of 1:10:5 produces a solution which is capable of selectively hydrogenating cyclic dienes to monoenes.[113] The active species involved in the catalytic cycle is thought to be a nickel hydride complex, $[NiH(PPh_3)(AlCl_4)]$. In comparison with $[Ni(acac)_2]$ itself this system requires a normal pressure of hydrogen.

Sensitized photoreduction of $[Ni(acac)_2]$ with triplet excited state ketones under hydrogen causes catalytic hydrogenation of dienes added in situ.[114] The efficiency of this photohydrogenation is dependent on the rate of photon input. Further complications arise due to precipitations of metallic nickel. Whilst unconjugated dienes with straight chains are hydrogenated without selectivity, 5-methylenebicyclo-[2.2.1] heptene and dicyclopentadiene are selectively reduced at the bicyclic olefinic bond exclusively, as is illustrated in Figure 1.5.6.

Figure 1.5.6

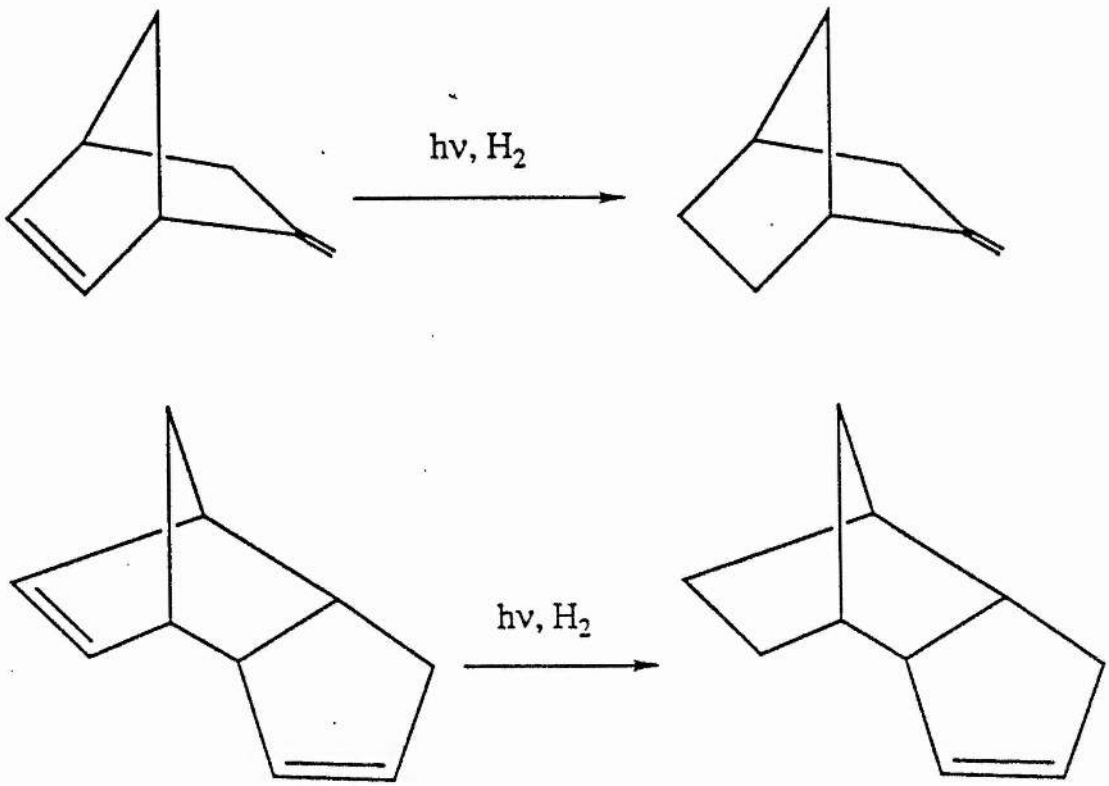


Chromium

The complex $[Cr(CO)_3(CH_3CN)_3]$ catalyses the 1,4-addition of hydrogen to 1,3-dienes such as 2-methyl-1,3-butadiene, trans-1,3-pentadiene and trans, trans-2,4-hexadiene at low temperature and pressure.[115] The catalytic action of $[Cr(CO)_3(CH_3CN)_3]$ parallels that of the photocatalytic complex, $[Cr(CO)_6]$[116] and the high temperature catalyst, $[(arene)Cr(CO)_3]$.[117]

Palladium

Palladium complexes of the general kind $[PdX_2L_2]$ (X=halogen, L=phosphine), either alone or in the presence of $SnCl_2$, hydrogenate linear and cyclic dienes, including sterically hindered ones, at raised hydrogen pressure.[112,118] In the case of 1,5-cyclooctadiene an isomerization to 1,3-cyclooctadiene preceded the reduction

to cyclooctene at 90°C, but the isomerization was slower than the hydrogenation at room temperature.

The $\pi$-allylic reaction intermediate, $[PdCl(PPh_3)(\eta^3\text{-}C_8H_{13})]$, illustrated in Figure 1.5.7 has been isolated and has been shown to be a more active catalyst than $[PdCl_2(PPh_3)_2]$ itself. Although an excess of chloride ion did not affect the reactivities of $[PdCl_2(PPh_3)_2]$ and $[PdCl(PPh_3)(\eta^3\text{-}C_8H_{13})]$, an excess of $PPh_3$ poisoned them.

Figure 1.5.7

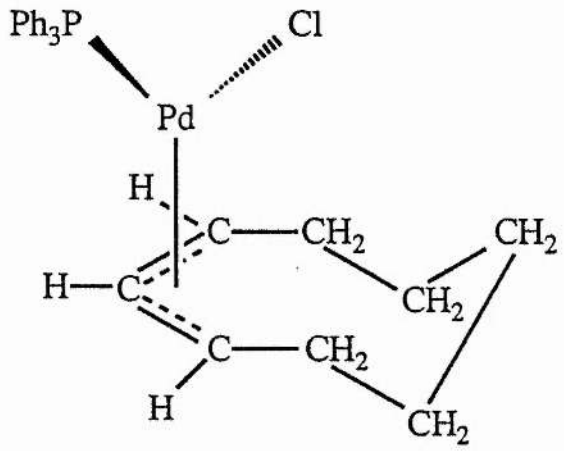


Independently, the complex $[PdCl(PPh_3)(\eta^3\text{-}C_4H_7)]$ and related complexes have been shown to hydrogenate linear and cyclic octadienes,[119] though regioselective studies have not been pursued.

Summary

In water $[CoH(CN)_5]^{3-}$ remains an extremely useful catalyst. The system is selective for the hydrogenation of carbon-carbon double bonds that are conjugated with one another or with C=O, C≡N or phenyl groups. Conversely, the system is relatively unreactive towards unconjugated dienes, as are the chromium catalysts $[Cr(CO)_6]$, $[Cr(CO)_3Cp]$ and $[Cr(CO)_3(arene)]$. With all these catalysts a 1,4-addition of hydrogen is observed and this is also the case for another cobalt complex, $[Co(SCN)(PPh_3)_3]$.

It should be noted that different complexes containing the same transition-metal do not necessarily catalyse the hydrogenation of conjugated dienes in a similar fashion. For example, the platinum complexes $[PtHL(\eta^3\text{-}C_3H_5)]$ ($L=P(C_6H_{11})_3$, $PBBu_3$[4]), promote a 1,4-addition. Indeed in certain systems, a slight variation in catalyst composition or catalytic conditions can lead to what was previously a 1,2-addition becoming a 1,4-addition, an example being the $[Rh(diene)(phosphine)_2]^+$ system. $[RhH(PPh_3)_4]$ however, exhibits no such properties and is an efficient precursor for the 1,2 addition of hydrogen to a conjugated diene.

In terms of the hydrogenation of isolated double bonds both $[RhCl(PPh_3)_3]$ and $[RuHCl(PPh_3)_3]$ are particularly regioselective. It can be readily appreciated that intermediates formed in the catalytic cycle tend to be sterically congested. As a result any hydrogenation is susceptible to steric effects in the olefinic substrate, and the general trend is alk-1-enes > cis-alk-2-enes > > trans-alk-2-enes > trans-alk-3-enes.

## CHAPTER 1 REFERENCES


1 P Zhou, A A Vitale, J San Filippo Jr. and W H Saunders Jr., J. Am. Chem. Soc., 1985, **107**, 8049.

2 A J Kunin, C E Johnson, J A Maguire, W D Jones and R Eisenberg, J. Am. Chem. Soc., 1987, **109**, 2963.

3 J Halpern, Acc. Chem. Res., 1970, 3, 386.

4 B R James, "Homogeneous Hydrogenation", Wiley, New York, 1973, Chapter XI, Section E.

5 J A Osborn, F H Jardine, J F Young and G Wilkinson, J. Chem. Soc. (A), 1966, 1711.

6 F Porta, S Cenini, S Giordano and M Pizzotti, J. Organomet. Chem., 1978, **150**, 261.

7 M A Bennett and D L Milner, J. Am. Chem. Soc., 1969, 91, 6983.

8 J Kwiatek, Catalysis Reviews Vol. 1, ed. H Heinemann, Marcel Dekker, New York, 1968, p37.

9 J J Bonnett, A Thorez, A Maisonnat, J Galy and R Poilblanc, J. Am. Chem. Soc., 1979, **101**, 5940.

10 B R James, Adv. Organomet. Chem., 1979,17, Section IIA.

11 M A Bennett, T N Huang and T W Turney, J. Chem. Soc., Chem. Commum., 1979, 312.

12 Reference 4, Chapter II.

13 T I Eliades, R O Harris and M˙C Zia, Chem. Commun., 1970, 1709.

14 J F Harrod, D F R Gilson and R Charles, Can. J. Chem., 1969, 47, 1431.

15 B R James, "Comprehensive Organometallic Chemistry", Pergamon Press, Oxford, 1982, Vol. 8, 51, 285.

16 Reference 4, Chapter XI, Section B.

17 Reference 4, Chapter IX, Section B.

18 Reference 4, Chapter XVII.

19 Reference 4, Chapter I.

20 P S Hallman, B R McGarvey and G Wilkinson, J. Chem. Soc. (A), 1968, 3143.

21 C O'Connor and G Wilkinson, J. Chem. Soc. (A), 1968, 2665.

22 L Vaska, Inorg. Nucl. Chem. Letters, 1965, 1, 89.

23 A Nakamura and S Otsuka, J. Am. Chem. Soc., 1973, 95, 7262.

24 Reference 4, Chapter XIII, Section B.

25 Reference 4, Chapter VII, Section B.

26 D R Armstrong, O Novaro, M E Ruiz-Vizcaya and R Linarte, J. Catal., 1977, 48, 8.

27 Reference 4, Chapter X, Section F.

28 Reference 4, Chapter X, Section B.

29 R N Haszeldine, R J Lunt and R V Parish, J. Chem. Soc. (A), 1971, 3711.

30 M Burnett, R J Morrison and C J Strugnell, J. Chem. Soc., Dalton Trans., 1973, 701.

31 F K Shmidt, V V Sarayev, L O Nindakova, V A Gruznykh, S M Krasnapolskaya and Y S Levkovskii, React. Kinet. Catal. Lett., 1978, 9, 113.

32 S Komiya and A Yamamoto, J. Mol. Catal., 1979, 5, 279.

33 R H Crabtree, Acc. Chem. Res., 1979, 12, 331.

34 A S Chan, J J Pluth and J Halpern, J. Am. Chem. Soc., 1980, 102, 5952.

35 Reference 4, Chapter XIV, Section B.

36 Reference 4, Chapter IX, Section A.

37 M J S Dewar, Bull. Soc. Chim. Fr. 1951, 18, C79.

38 J Chatt and L A Duncanson, J. Chem. Soc., 1953, 2939.

39 S Winstein and H J Lucas, J. Am. Chem. Soc., 1956, 78, 1665.

40 H J Lucas, R S Moore and D Pressman, J. Am. Chem. Soc., 1943, 65, 227.

41 A J Schultz, R K Brown, J M Williams and R R Schrock, J. Am. Chem. Soc., 1981, 103, 169.

42 A D Walsh, Trans. Faraday Soc., 1949, 45, 179.

43 J A McGinnety and J A Ibers, Chem. Commun., 1968, 235.

44 C Pedone and E Benedetti, J Organomet. Chem., 1971, 29, 443.

45 S Merlino, R Lazzaroni and G Montagnoli, J. Organomet. Chem., 1971, 30, C93.

46 A De Renzi, B DiBabio, G Paiaro, A Panunzi and C Pedone, Gazz. Chim. Ital. 1976, 106, 765.

47 S C Nyburg, K Simpson and W Wong-Ny, J. Chem. Soc., Dalton Trans., 1976, 1865.

48 F Sartori and L Leoni, Acta Crystallogr., Section B, 1976, B32, 145.

49 F A Catton, J N Francis, B A Frenz and M Tsutsui, J. Am. Chem. Soc., 1973, 95, 2483.

50 A McAdam, J N Francis and J A Ibers, J. Organomet. Chem., 1971, 29, 149.

51 L J Guggenberger, Inorg. Chem., 1973, 12, 499.

52 D J Sepelak, C G Pierpont, E K Barfield, J T Budz and C A Poffenberger, J. Am. Chem. Soc., 1976, 98, 6178.

53 R Countryman and B R Penfold, Chem. Commun., 1971, 1598.

54 T A Albright, R Hoffmann, J C Thibeault and d L Thorn, J. Am. Chem. Soc., 1979, 101, 3801.

55 J R Holden and N C Baenziger, J. Am. Chem. Soc., 1955, 77, 4987.

56 A R Brause, F Kaplan and M Orchin, J. Am. Chem. Soc., 1967, 89, 2661.

57 B F G Johnson, G E Holloway, G Hulley and J Lewis, Chem. Commun., 1967, 1143.

58 T Okuyama, T Fueno and J Furukawa, Bull. Chem. Soc. Jap., 1969, 42, 3106.

59 C E Holloway, G Hulley, B F G Johnson and J Lewis, J. Chem. Soc. (A), 1969, 53.

60 A R Brause, Diss. Abstr. B., 1968, 28(8), 3215.

61 R Cramer, J. Am. Chem. Soc., 1964, 86, 217.

62 R W Taft, "Steric Effects in Organic Chemistry", M S Newman, Ed., Wiley, New York, 1956, Chapter 3.

63 P Legzdins et al., J. Am. Chem. Soc., 1986, 108, 3843.

64 C G Pierpoint et al., Inorg. Chem., 1978, 17, 1976.

65 M D Fryzuk et al., J. Am. Chem. Soc., 1985, 107, 8259.

66 J F Young, J A Osborn, F H Jardine and G Wilkinson, Chem. Commun., 1965, 131.

67 J Halpern, Inorg. Chim. Acta., 1981, 50, 11.

68 J Halpern and C S Wong, J. Chem. Soc., Chem. Commun., 1973, 629.

69 J Halpern, T Okamoto and A Zakhariev, J. Mol. Catal., 1977, 2, 65.

70 C Rousseau, M Evrard and R Pettit, J. Mol. Catal., 1979, 5, 163.

71 R L Augustine, R J Pellet, J F Van Peppen and J P Mayer, Adv. Chem. Ser., 1974, **132**, 111.

72 A S Hussey and Y Takeuchi, J. Am. Chem. Soc., 1969, **91**, 672.

73 C H Heathcock and S R Poulter, Tetrahedron Lett., 1969, 2755.

74 W Strohmeier and E Hitzel, J. Organomet. Chem., 1976, **110**, 389.

75 F H Jardine, J A Osborn and G Wilkinson, J. Chem. Soc. (A), 1967, 1574.

76 Reference 4, Chater XI, Section E.

77 M Brown and L W Piszkiewicz, J. Org. Chem., 1967, **32**, 2013.

78 M M Bhagwat and D Devaprabhakara, Tetrahedron Lett., 1972, 1391.

79 J R Shapley, R R Schrock and J A Osborn, J. Am. Chem. Soc., 1969, **91**, 2816.

80 R R Schrock and J A Osborn, J. Am. Chem. Soc., 1976, **98**, 2134.

81 R R Schrock and J A Osborn, J. Am. Chem. Soc., 1976, **98**, 2143.

82 R R Schrock and J A Osborn, J. Am. Chem. Soc., 1976, **98**, 4450.

83 G F Pregaglia, G F Ferrari, A Andreetta, G Capparella, F Genoni and R Ugo, J. Organomet. Chem., 1974, **70**, 89.

84 Z Nagy-Magos, B Heil and L Marko, Transition Met. Chem., 1976, **1**, 215.

85 R W Mitchell, J D Ruddick and G Wilkinson, J. Chem. Soc. (A), 1971, 3224.

86 A Spencer, J. Organomet. Chem., 1975, **93**, 389.

87 G Dolcetti, Inorg. Nucl. Chem. Lett., 1973, **9**, 705.

88 B Giovannitti, M Ghedini, G Dolcetti and G Denti, J. Organomet. Chem., 1978, **157**, 457.

89 J E Lyons, J. Catal., 1973, **30**, 490.

90 Reference 8, Section VIII.

91 W Strohmeier and J P Stasch, Z Naturforsch, Teil B, 1979, **34B**, 755.

92 P S Hallman, B R McGarvey and G Wilkinson, J. Chem. Soc. (A), 1968, 3143.

93 S Nishimura, T Ichino, A Akimato and K Tsuneda, Bull. Chem. Soc. Jpn., 1975, 48, 2852.

94 J Tsuji and H Suzuki, Chem. Lett., 1977, 1083.

95 D R Fahey, J. Org. Chem., 1973, 38, 3343.

96 D Rose, J O Gilbert, R P Richardson and G Wilkinson, J. Chem. Soc. (A), 1969, 2610.

97 R Bertani, G Carturan and A Serivanti, Angew. Chem., 1983, 95, 241.

98 R W Adams, G W Batley and J C Bailar Jr., J. Am. Chem. Soc., 1968, 90, 6051.

99 H A Tayim and J C Bailar Jr., J. Am. Chem. Soc., 1967, 89, 4330.

100 H C Clark, C Billard and C S Wong, J. Organomet. Chem., 1980, 190, C105.

101 T Funabiki and K Tarama, Bull. Chem. Soc. Jpn., 1971, 44, 945.

102 K Ohkubo, K Tsuchihashi, H Ikebe and K Sakamoto, Bull. Chem. Soc. Jpn., 1975, 48, 1114.

103 J Busters, C J Groenenboom, H Van Bekkum and L L Van Reijen, Recl. Trav. Chim. Pay-Bas, 1973, 92, 219.

104 L I Simandi, F Nagy and E Budo, Acta. Chim. (Budapest), 1968, 58(1),39.

105 D L Reger, M M Habib and D J Fauth, J. Org. Chem., 1980, 45, 3860.

106 D L Reger, M M Habib, J. Mol. Catal., 1980, 7, 365.

107 J T Lee and H Alper, J. Org. Chem., 1990, 55, 1854.

108 T Funabiki, S Kasaoka, M Matsumoto and K Tarama, J. Chem. Soc., Dalton Trans., 1974, 2043.

109 D L Reger and A Gabrielli, J. Mol. Catal., 1981, 12, 173.

110 K Kawakami, T Mizoroki and A Ozaki, J. Mol. Catal., 1979, 5, 175.

111 T Nakayama and H Kanai, Bull. Chem. Soc. Jpn., 1985, 58, 16.

112 H Itatani and J C Bailar Jr., Ind. Eng. Chem., Prod. Rrs. Dev., 1972, 11, 146.

113 M Sakai, F Harada, Y Sakakibara and N Uchino, Bull. Chem. Soc. Jpn., 1982, 55, 343.

114 Y L Chow, H Li and M S Yang, Can. J. Chem., 1988, 66, 2920.

115 M A Schroeder and M S Wrighton, J. Organomet. Chem., 1974, 74, C29.

116 M Wrighton and M A Schroeder, J. Am. Chem. Soc., 1973, 95, 5764.

117 E N Frankel and R O Butterfield, J. Org. Chem., 1969, 34, 3930.

118 Y Fujii and J C Bailar Jr, J. Catal., 1978, 55, 146.

119 G Strukul and G Carturan, Inorg. Chim. Acta., 1979, 35, 99.

# CHAPTER 2

# MECHANISTIC STUDIES FOR THE HYDROGENATION OF ACRYLIC ACIDS USING RHODIUM-MIXED ANHYDRIDE COMPLEXES

## 2.1 Introduction.

Cole-Hamilton et al. have developed catalyst precursors that have been shown to be more effective for the catalytic hydrogenation of acrylic acids in the presence of added base than is Wilkinson's catalyst, $[RhCl(PPh_3)_3]$.[1,4] The aforementioned catalyst precursors have been derived from the reaction of Wilkinson's catalyst with mixed anhydride ligands of the general formula, $[Ph_2PO_2CCR=CR'R'']$. These ligands are synthesized under a dry dinitrogen atmosphere by the reaction of the appropriate acrylic acid $[HO_2CCR=CR'R'']$ with chlorodiphenylphosphine in the presence of the base, triethylamine, as is illustrated in Figure 2.1.1.

Figure 2.1.1

$$HO_2CCR=CR'R'' + Ph_2PCl + NEt_3 \xrightarrow{0^oC} Ph_2PO_2CCR=CR'R'' + Et_3N^+H\,Cl^-$$

The reaction of $[RhCl(PPh_3)_3]$ with one mole equivalent of $[Ph_2PO_2CCR=CR'R'']$ leads to the isolation of rhodium complexes of composition $[RhCl(PPh_3)_n(Ph_2PO_2CCR=CR'R'')]$ (n = 2, R=H, R'=R''=Me; R=R'=H, R''=CH=CHMe; R=Me, R'=H, R''=Ph; n = 1, R=R'=H, R''=Me or CH=CHMe). As mentioned, these complexes have been used as catalyst precursors

for the catalytic hydrogenation of various substituted acrylic acids, and in the case of hexa-2,4-dienoic acid a certain degree of regioselectivity has been observed.

Initially, this chapter covers the structure and characterisation of the rhodium-mixed anhydride catalyst precursors as well as their use in the hydrogenation of acrylic acids. Then work directed towards establishing a mechanism for the catalysis is presented and discussed.

## 2.2 Overview of the Preparation and Spectral Analysis of the Mixed Anhydride Complexes of Rhodium.

The products of reactions of $[RhCl(PPh_3)_3]$ with mixed anhydrides of diphenylphosphinous and acrylic acids appear to be determined largely by steric factors, in that the lesser the number of substituents on the carbon-carbon double bond the more likelihood there is of chelate binding of the anhydride to rhodium.

In the complex $[RhCl(PPh_3)_2(Ph_2PO_2CCH=CMe_2)]$, the mixed anhydride ligand derived from 3-methylbut-2-enoic acid, is bound to the rhodium metal centre via the phosphorus atom alone, and this is illustrated in Figure 2.2.1.

Figure 2.2.1

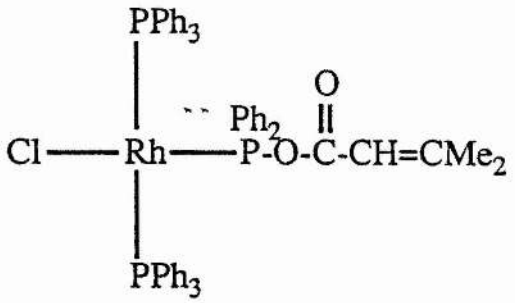

A similar monodentate complexation occurs when using [$Ph_2PO_2CCMe=CHPh$], the mixed anhydride derived from 2-methyl-3-phenylpropenoic acid.

Alternatively, when Wilkinson's catalyst reacts with [$Ph_2PO_2CCH=CHMe$], the resulting complex has the mixed anhydride ligand bound in a bidentate manner, via the phosphorus atom and the carbon-carbon double bond, as is illustrated in Figure 2.2.2. Such chelate binding is also observed in the complex [$RhCl(PPh_3)(Ph_2PO_2CCH=CHCH=CHMe)$], in which the mixed anhydride is derived from hexa-2,4-dienoic acid, [$HO_2CCH=CHCH=CHMe$].

Figure 2.2.2

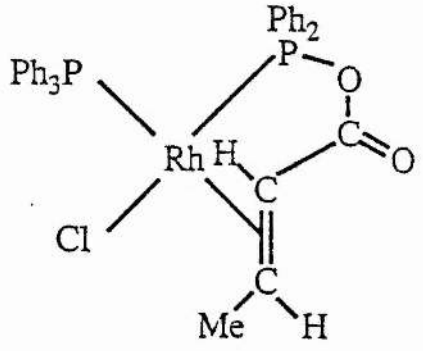


As indicated previously, [$Ph_2PO_2CCH=CHCH=CHMe$] can also bind in a monodentate fashion, as is exemplified by the complex [$RhCl(PPh_3)_2(Ph_2PO_2CCH=CHCH=CHMe)$].

The treatment of the complexes [$RhCl(PPh_3)_2(Ph_2PO_2CCH=CMe_2)$] and [$RhCl(PPh_3)_2(Ph_2PO_2CCMe=CHPh)$] with one mole equivalent of $TlPF_6$ or $AgSbF_6$ leads to the cationic species, [$Rh(PPh_3)_2(Ph_2PO_2CCH=CMe_2)]^+$ $Y^-$ and [$Rh(PPh_3)_2(Ph_2PO_2CCMe=CHPh)]^+$ $Y^-$ ($Y^-$ = $SbF_6^-$ or $PF_6^-$) respectively. In

both cases the mixed anhydride is bound through the phosphorus atom and the carbonyl oxygen as is illustrated in Figure 2.2.3 for the former cationic species.

Figure 2.2.3

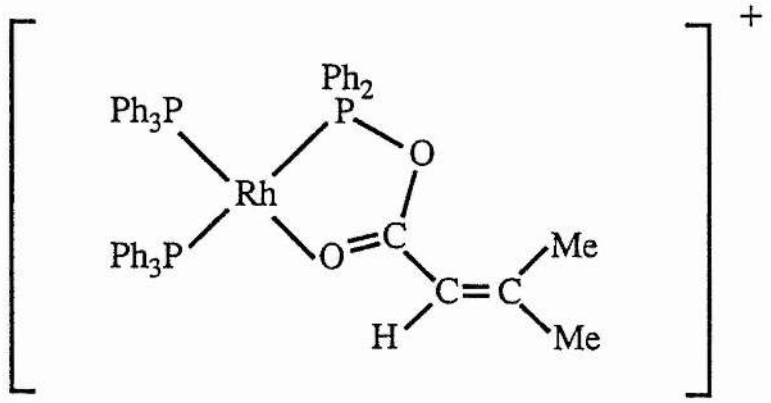


The characterisation of all the complexes referred to in this section is a result of analysis by IR, $^{31}P$ NMR and $^{1}H$ NMR techniques.

Infrared has shown that for complexes containing a monodentate mixed anhydride ligand, ν(C=C) and ν(C=O) are in approximately the same position as is observed for the free ligands. In cases where the mixed anhydride is bound through phosphorus and the carbon-carbon double bond, shifts in frequency for ν(C=C) and ν(C=O) are observed. The carbonyl band of [$RhCl(PPh_3)(Ph_2PO_2CCH=CHMe)$] is located at 1740 $cm^{-1}$, which is a significant shift to higher frequency from the carbonyl band of the free ligand, located at 1705 $cm^{-1}$. This can be explained in either of two ways. Firstly, for a monodentate mixed anhydride the carbonyl bond and the carbon-carbon double bond are conjugated, however upon chelate binding of the anhydride ligand this conjugation is lost and as a result the carbonyl bond itself becomes stronger. Secondly, the carbonyl group can be considered to be a

member of a five and a half membered ring. Studies of five and six membered lactone rings have shown carbonyl absorbancies at 1780 $cm^{-1}$ and 1730 $cm^{-1}$ respectively.[5] The lack of a band in the 1600 $cm^{-1}$ region, corresponding to $\nu(C=C)$, indicates that upon complexation the environment of the double bond has been altered. A shift to lower frequency of over 100 $cm^{-1}$ from the free ligand position, can only be explained by $\pi$ coordination of the double bond to the metal centre, in a manner described by Dewar, Chatt and Duncanson.

Cationic complexes of the form $[Rh(PPh_3)_2(Ph_2PO_2CCR=CR'R'')]^+$, predictably have quite different IR spectra from those of the complexes previously mentioned. There are no strong bands near 1700 $cm^{-1}$, although there are features near 1600 $cm^{-1}$. The absorption at about 1630 $cm^{-1}$, attributed to $\nu(C=C)$, is in a similar position to that of the free ligand. As anticipated, the absorption attributed to $\nu(C=O)$ occurs at a lower frequency (about 1585 $cm^{-1}$), due to the fact that the oxygen atom of the carbonyl group is bound to rhodium.

$^{31}P$ NMR has proved invaluable for the characterisation of these rhodium-mixed anhydride complexes. For instance, complexes of general formula $[RhCl(P_APh_3)_2(Ph_2P_BO_2CCR=CR'R'')]$ have $^{31}P$ NMR spectra that are very similar to that of Wilkinson's catalyst. The general spectrum consists of firstly, a doublet of doublets corresponding to the resonance of the phosphorus atom ($P_A$) from the triphenylphosphine ligand being coupled to rhodium and the phosphorus atom ($P_B$) of the mixed anhydride. Secondly, a doublet of triplets corresponding to the resonance of the phosphorus atom of the monodentate mixed anhydride

ligand ($P_B$) being coupled to rhodium and then to the two identical phosphorus atoms ($P_A$) of the triphenylphosphine ligands. The shielding effect resulting from the complexation of the mixed anhydride to the rhodium centre, causes the phosphorus resonance to move upfield i.e. to a lower shift ($\delta$ ppm). The rhodium-phosphorus B coupling constant, $J_{RhP_B}$, is about 190 Hz and is greater than the rhodium-phosphorus A coupling constant, $J_{RhP_A}$, which is about 145 Hz, and this suggests that the mixed anhydride is bound more strongly to the rhodium metal centre than triphenylphosphine.[6] This is due to the greater trans influence of triphenylphosphine compared with chlorine. The phosphorus A - phosphorus B coupling constant, $J_{P_AP_B}$, is about 40 Hz and is characteristic of a cis phosphorus coupling.

Complexes of the form $[RhCl(P_APh_3)(Ph_2P_BO_2CCR=CR'R'')]$ have $^{31}$P NMR spectra consisting of two doublet of doublets, where each phosphorus atom in a unique environment will give rise to a unique resonance which will be split by a coupling to rhodium and by mutual phosphorus coupling. The exception to this is that at room temperature $[RhCl(P_APh_3)(Ph_2P_BO_2CCH=CHMe)]$ has a $^{31}$P NMR spectrum consisting of a broad resonance ($P_B$) and a doublet ($P_A$). This complex has been presented as a fluxional one and the fluxionality has been attributed to a rapid cis-trans isomerism as illustrated in Figure 2.2.4.[7] Indeed at low temperature $^{31}$P resonances from small amounts of the trans isomer are observed and on warming these resonances exchange with the resonances from the predominant cis isomer.

Figure 2.2.4

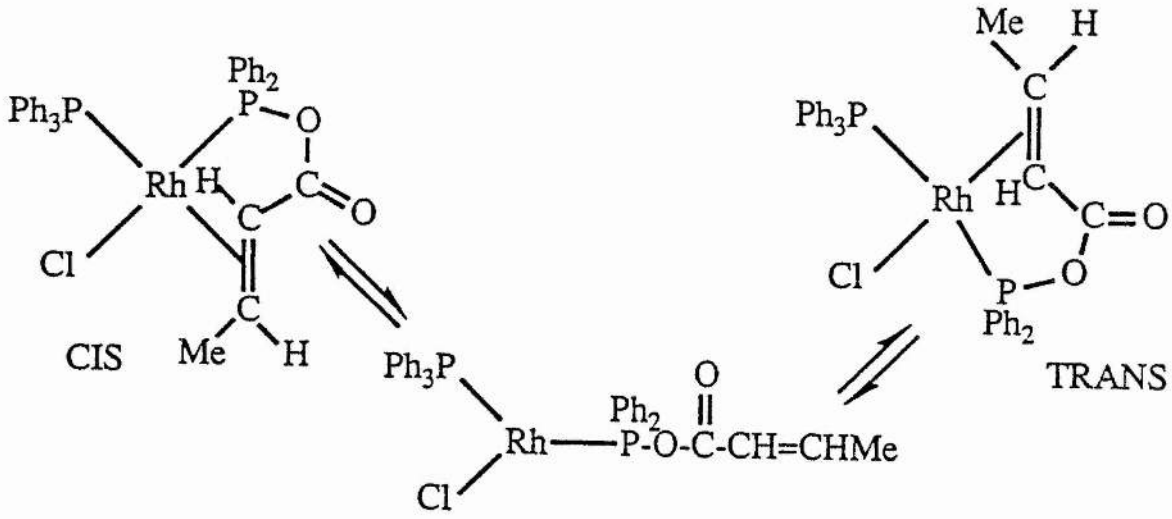


In all cases for complexes of general formula $[RhCl(PPh_3)(Ph_2PO_2CCR=CR'R'')]$, the $^{31}P$ resonance for the chelate bound anhydride ligand is downfield of the free ligand position. This is due to the presence of ring contributions[8], whereby the formation of a ring due to bidentate binding of a phosphorus containing ligand causes a shift of the phosphorus resonance to lower field. The size of the ring contribution is related to the size of the ring formed. In general, the smaller the ring formed the greater the low field shift. This is further exemplified by the cationic complexes of general formula, $[Rh(PPh_3)_2(Ph_2PO_2CCR=CR'R'')]^+$, where the phosphorus of the mixed anhydride resonates at a very high shift (about 175ppm). This is because the phosphorus atom is contained in a five-membered ring as opposed to the five and a half-membered ring evident in $[RhCl(PPh_3)(Ph_2PO_2CCR=CR'R'')]$.

The $^1H$ NMR spectra of cationic complexes of general formula

$[Rh(PPh_3)_2(Ph_2PO_2CCR=CR'R'')]^+$ and of complexes containing a monodentate mixed anhydride, $[RhCl(PPh_3)_2(Ph_2PO_2CCR=CR'R'')]$, show features which are very similar to those present in the non-bound mixed anhydrides. The presence of resonances at about $\delta$6.0 assignable to the vinylic protons suggest that the carbon-carbon double bond is not bound to the metal. Conversely, for complexes where the mixed anhydride is chelate bound through the phosphorus atom and the double bond, the vinylic protons shift upfield.

For $[RhCl(PPh_3)(Ph_2PO_2CCH^c=CH^bMe^a)]$, the low-temperature $^1H$ NMR is consistent with its X-ray structure, although $J_{H_bH_c}$ at 4.9Hz is smaller than is perhaps anticipated for trans hydrogen atoms. This is attributable to significant pyramidalisation at the carbon atoms on coordination. At room temperature the $^1H$ NMR spectrum consists of broad resonances, due to the fluxionality of the complex.

The spectrum of $[RhCl(PPh_3)(Ph_2PO_2CCH=CHCH=CH^bMe)]$ includes a resonance ($H^b$) at very high field ($\delta$0.23). This high-field shift is similar to those observed for endo protons when 1,3-butadiene is complexed to transition metals[9] and therefore suggests that the complex is five-coordinate, with the ligand being bound by the phosphorus atom and by both the double bonds in the chain, as is represented in Figure 2.2.5. The broadness of the resonances associated with this complex reflect a degree of fluxionality.

Figure 2.2.5

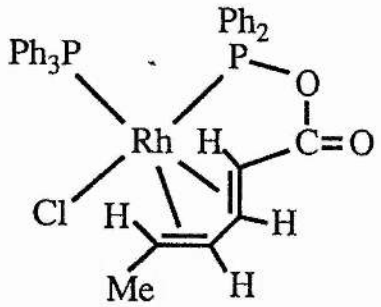


2.3 Catalytic Studies Involving Mixed Anhydride Complexes of Rhodium.

The rhodium complexes mentioned thus far in this chapter are more effective for the catalytic hydrogenation of substituted acrylic acids in the presence of added base (KOH or $Et_3N$) than is $[RhCl(PPh_3)_3]$.

Initially, the monodentate mixed anhydride complex, $[RhCl(PPh_3)_2(Ph_2PO_2CCH=CMe_2)]$, when it reacts with hydrogen at one atmosphere pressure, in benzene, gives the hydrogenated species $[RhCl(PPh_3)_2(Ph_2PO_2CCH_2CHMe_2)]$. However, when this reaction is carried out in the presence of excess $[Ph_2PO_2CCH=CMe_2]$, catalytic hydrogenation of the carbon-carbon double bond does not occur. This observation contrasts with work done by Jackson on the phosphine, $[Ph_2PCH_2CH=CH_2]$,[10,11] where catalytic hydroformylation was observed using $[RhH(CO)(PPh_3)_3]$. The failure to obtain catalysis using the mixed anhydride catalyst arises because of the low lability of the mixed anhydride itself compared with $PPh_3$ or even hydroformylated $Ph_2PCH_2CH=CH_2$. For the mixed anhydrides the reaction is further complicated by the possible formation of $[RhCl(PPh_3)(Ph_2POPPh_2)]$ when more than one molar

equivalent of $[Ph_2PO_2CCR=CR'R'']$ is reacted with $[RhCl(PPh_3)_3]$.[12] This reaction has been observed for a range of different alkene substituents, although not for $R=H$, $R'=R''=Me$.

Catalytic chemistry is also not observed when the hydrogenation of $[RhCl(PPh_3)_2(Ph_2PO_2CCH=CMe_2)]$ is carried out in the presence of excess 3-methylbut-2-enoic acid.

Although trans-esterification of trivalent phosphinites is known,[13] and indeed, uncoordinated $[Ph_2PO_2CCH=CMe_2]$ reacts with acetic acid to give $Ph_2PO_2CMe$,[2] such acid catalysed transesterification reactions occur via initial protonation of the lone pair. In both phosphorus (V) compounds and metal complexes, the lone pair is not available for protonation and hence acid catalysed transesterifications do not occur.[14]

In contrast, base catalysed transesterification of trialkylphosphates is well known[15] and it has been reported[16] that the phosphinite complex $[(CO)_4Mo(Me_2POC_5H_4N)]$ reacts with lithium salts of allyl alcohols, including $Li[OCH_2CH=CMe_2]$, to give the transesterification product $[(CO)_4Mo(Me_2POCH_2CH=CMe_2)]$. It was these observations that led to the study of the hydrogenation of acrylic acids using the mixed anhydride complex $[RhCl(PPh_3)_2(Ph_2PO_2CCH=CMe_2)]$, under basic conditions.

The yields of products from the hydrogenation of various substituted acrylic acids

using $[RhCl(PPh_3)_3]$ and $[RhCl(PPh_3)_2(Ph_2PO_2CCH=CMe_2)]$ as catalysts are compared in Table 2.3.1, together with their relative efficiencies for the hydrogenation of hex-l-ene, a simple alkene for which chelate binding is not possible.

Table 2.3.1

| | | % Conversion[a] |
|---|---|---|
| Substrate | $[RhCl(PPh_3)_3]$ | $[RhCl(PPh_3)_2(Ph_2PO_2CCH=CMe_2)]$ |
| $Me_2C=CHCO_2H$ | 26.7 | 80.0 |
| $PhCH=CMeCO_2H$ | 14 | 68.2(13[b]) |
| $MeCH=CHCO_2H$ | 75.8(31[b]) | 100(76[b]) |
| $MeCHCHCHCHCO_2H$ | 10.6[c] | 64.7[d] |
| Hex-l-ene[e] | 22 | 10 |

[a]Conditions: [catalyst] = $3x10^{-3}$ mol $dm^{-3}$, [substrate] = $6x10^{-2}$ mol $dm^{-3}$, [KOH] = $4x10^{-2}$ mol $dm^{-3}$, in acetone ($5cm^3$), 17h, 22°C, $p(H_2)$ = 3atm. [b]Conditions as a, but t = 2h. [c]Hexanoic acid. [d]Hex-4-enoic acid (52.3%), hexanoic acid (47.7%). [e]Conditions: [catalyst] = $10^{-3}$ mol $dm^{-3}$, [hex-l-ene] = 0.73 mol $dm^{-3}$ in toluene, $10cm^3$, 20 min, 22°C, $p(H_2)$ = 1atm.

As expected, for hex-l-ene, on account of the higher basicity and lower lability of the mixed anhydride compared with triphenylphosphine, $[RhCl(PPh_3)_3]$ is about twice as efficient a hydrogenation catalyst as $[RhCl(PPh_3)_2(Ph_2PO_2CCH=CMe_2)]$. Conversely, for all the substituted acrylic acids, the mixed anhydride complex is a more efficient catalyst than $[RhCl(PPh_3)_3]$. This suggests that a different

mechanism is operating for the hydrogenation of acrylic acids than for the hydrogenation of hex-1-ene.

The relative rates for hydrogenation of the various substituted acrylic acids are dominated by steric factors, with the more highly substituted alkenes undergoing hydrogenation more slowly. Similar observations have been made for the hydrogenation of simple alkenes in the presence of Wilkinson's catalyst (see Chapter 1).

Another indication that different mechanisms are operating for $[RhCl(PPh_3)_2(Ph_2PO_2CCH=CMe_2)]$ than for $[RhCl(PPh_3)_3]$ comes from the fact that when both are used as catalysts for the hydrogenation of hexa-2,4-dienoic acid the products obtained are different. Wilkinson's catalyst gives hexanoic acid with traces of hex-2-enoic acid, whilst under similar conditions, at least at short reaction times, the mixed anhydride containing catalyst gives a mixture of hex-4-enoic and hexanoic acids. It should be noted that different complexes employing different modes of anhydride binding eg $[RhCl(PPh_3)(Ph_2PO_2CCH=CHMe)]$ and $[Rh(PPh_3)_2(Ph_2PO_2CCMe=CHPh)]^+$, under similar conditions and in the early stages of the reactions, produce similar yields and selectivities for the hydrogenation of hexa-2,4-dienoic acid in the presence of the base triethylamine. As mentioned in Chapter 1, these results are of particular interest since studies on other catalysts for the hydrogenation of hexa-2,4-dienoic acid have shown that hex-2-enoic or hex-3-enoic acids are generally the products.[4]

For mixed anhydride catalysts the effect of base upon the efficiency of the catalysis is significant. It is seen that the use of triethylamine is more advantageous than the use of the potassium salt of the substrate acrylic acid, which is prepared either in situ from the acid and KOH or added directly. This is due to the very low solubility of the potassium salts in the reaction solvent (thf or acetone) compared with the totally soluble triethylammonium salts.

The mechanism initially proposed for the hydrogenation of $[Me_2C=CHCO_2H]$ using $[RhCl(PPh_3)_2(Ph_2PO_2CCH=CMe_2)]$ as the catalyst, is shown in Scheme 2.3.1. The evidence for the cationic nature of the active species comes from the observation that the catalyst reacts with $KSbF_6$ in acetone to give $[Rh(PPh_3)_2(Ph_2PO_2CCH=CMe_2)]^+ {}^-[SbF_6]$.

As all the catalytic reactions are carried out in the presence of excess acrylic acid anions, it seems unlikely that a cationic species could be the active species involved in the catalytic cycle.

Scheme 2.3.1

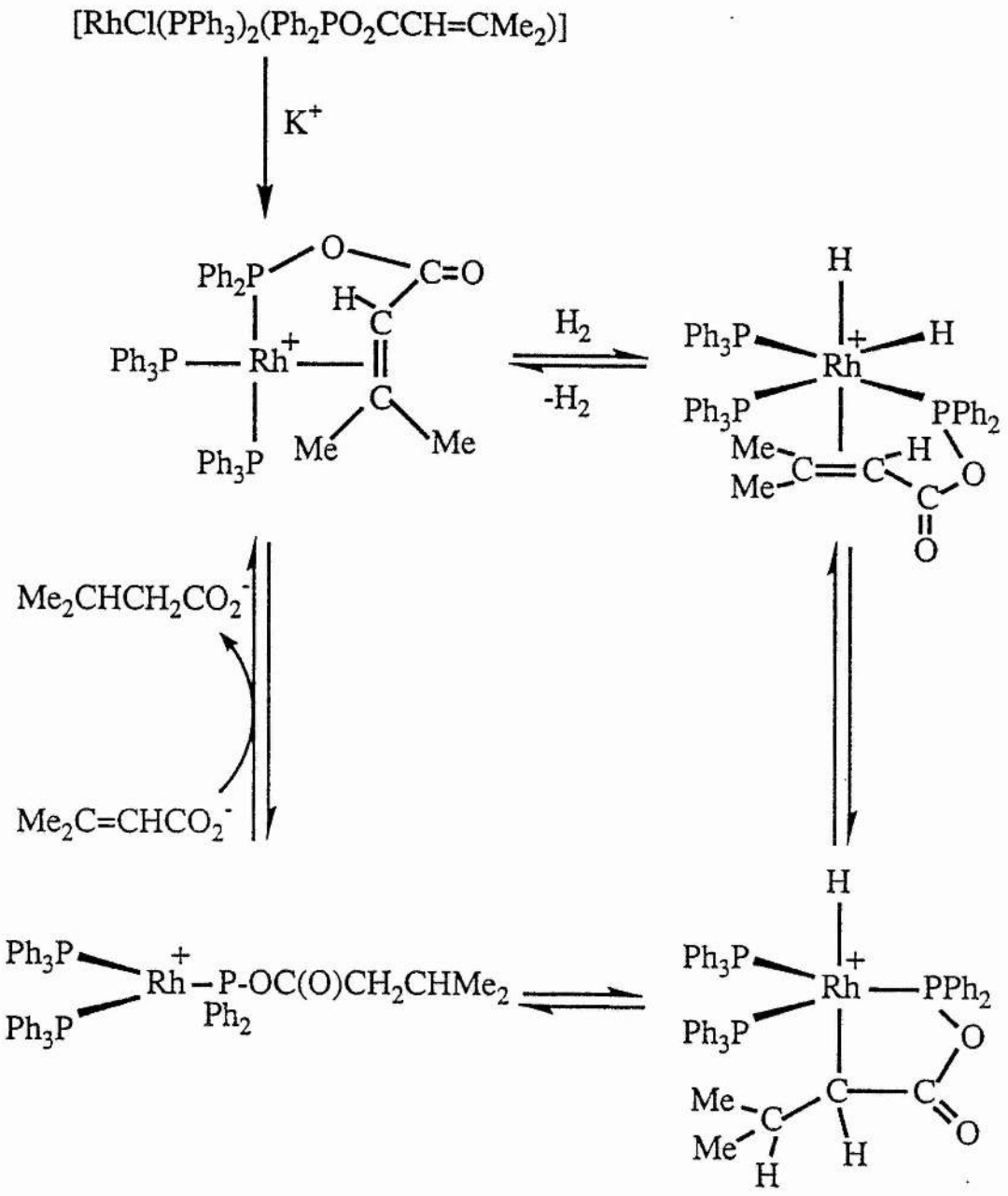


2.4 Attempted Identification of the Active Catalytic Species, Reaction of $[RhCl(PPh_3)_n(Ph_2PO_2CCR=CR'R'')]$ with $[O_2CCR=CR'R'']^-$.

Since all the catalyses are carried out in the presence of excess acrylic acid anions, various catalyst precursors have been reacted with various acrylic acid anions, either

as potassium or triethylammonium salts, in the absence of hydrogen. The aim of these reactions is to isolate the active species in the catalytic cycle.

The reactions of $[RhCl(PPh_3)(Ph_2PO_2CCH=CHMe)]$ with $[O_2CCH=CHMe]^-$ and $[RhCl(PPh_3)_2(Ph_2PO_2CCMe=CHPh)]$ with $[O_2CCMe=CHPh]^-$ give rise to both $[Rh(O_2CCH=CHMe)(PPh_3)(Ph_2PO_2CCH=CHMe)]$ and $[Rh(O_2CCMe=CHPh)(PPh_3)(Ph_2PO_2CCMe=CHPh)]$ as their respective products, as illustrated in Figure 2.4.1. In both cases the chloride ligand has been replaced by a substituted acrylic acid anion whilst the mixed anhydride ligand is bound in a bidentate fashion to rhodium via phosphorus and the carbon-carbon double bond. The appropriate acrylic acid anion was used in excess, either as the potassium or triethylammonium salt.

Figure 2.4.1

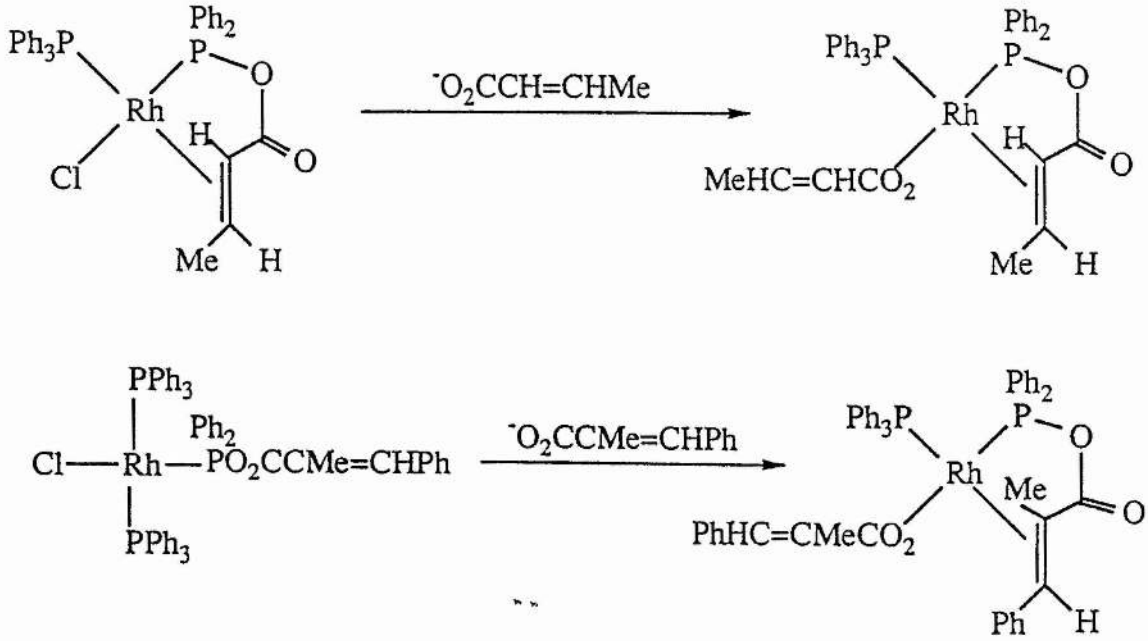

In addition $[Rh(O_2CCMe=CHPh)(PPh_3)(Ph_2PO_2CCMe=CHPh)]$ has also been prepared by reacting the cationic complex $[Rh(PPh_3)_2(Ph_2PO_2CCMe=CHPh)]^+$ with an excess of $[O_2CCMe=CHPh]^-$, as illustrated in Figure 2.4.2.

Figure 2.4.2

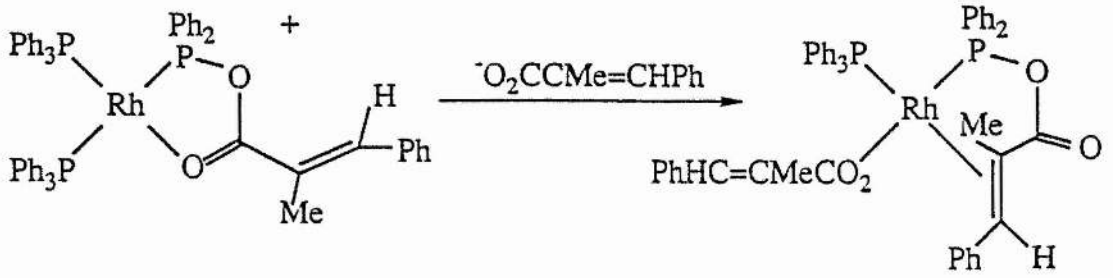


Transition metals and their carboxylate derivatives have been studied in the past[17-25] and have themselves been used as homogeneous catalysts.[26-30] It has been observed that the spectral properties of these complexes depend on the particular M-O, C-O and C-C bond strengths as well as the OCO bond angle and the ionic radius of the metal itself.[31]

Four different coordination modes have been observed for carboxylate ligands, namely monodentate, bidentate, bridging and monodentate coordination supported by hydrogen bonding. These are illustrated in Figure 2.4.3.

Figure 2.4.3

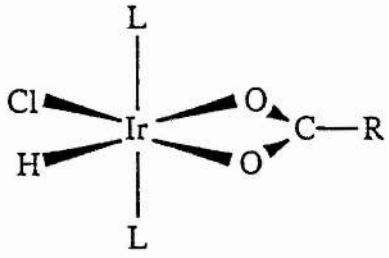


BIDENTATE

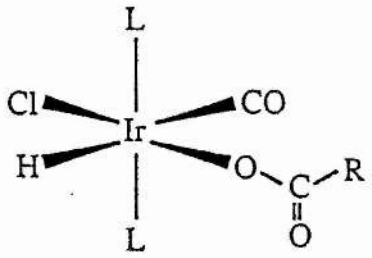


MONODENTATE

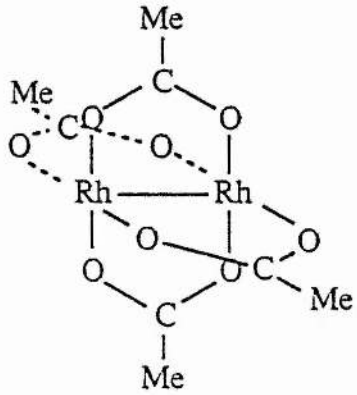


BRIDGING

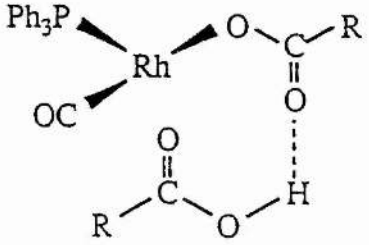


MONODENTATE WITH HYDROGEN BONDING

The active infra-red vibrations associated with the carboxylate group are ν(OCO) symmetric and ν(OCO) antisymmetric, with the values of ν(OCO)asym and [ν(OCO)asym - ν(OCO)sym] found to correlate with the coordination mode present in a particular complex. The highest frequencies have been recorded for the ν(OCO)asym of the monodentate carboxylate and thus these produce the largest values of [ν(OCO)asym - ν(OCO)sym].[31]

Rhodium complexes of the form $[Rh(O_2CR)(PPh_3)_3]$ have shown that ν(OCO)asym of the carboxylates are generally found at about $1600cm^{-1}$.[32] The symmetric stretch, ν(OCO)sym, is located at a lower frequency value to give a Δν (ie νasym - νsym)

of sufficient value to indicate monodentate coordination. The values of the ν(OCO)asym bands for compounds containing electron withdrawing groups are of higher frequency.[32] Table 2.4.1 shows IR data for rhodium carboxylate complexes.

Table 2.4.1

| Complex | ν(OCO)asym | ν(OCO)sym | Δν(νasym-νsym) |
|---|---|---|---|
| $[Rh(OCOCH_3)(PPh_3)_3]$ | 1601 | 1370 | 231 |
| $[Rh(OCOC_2H_5)(PPh_3)_3]$ | 1599 | 1379 | 230 |
| $[Rh(OCOC_5H_{11})(PPh_3)_3]$ | a | 1383 | - |
| $[Rh(OCOPh)(PPh_3)_3]$ | a | 1389 | - |
| $[Rh(OCOC_3H_7)(CO)(PPh_3)_2]$ | a | a | - |
| $[Rh(OCOCH_3)(CO)(PPh_3)_2]$ | 1608 | 1377 | 231 |
| $[Rh(OCOC_2H_5)(CO)(PPh_3)_2]$ | 1607 | 1382 | 225 |
| $[Rh(OCOCF_3)(PPh_3)_3]$ | 1673 | 1418 | 255 |
| $[Rh(OCOC_2F_5)(PPh_3)_3]$ | 1685 | a | - |

a - band obscured

The complex $[Rh(O_2CCH=CHMe)(PPh_3)(Ph_2PO_2CCH=CHMe)]$, has an IR spectrum (Table 2.4.2) that differs significantly from that for $[RhCl(PPh_3)(Ph_2PO_2CCH=CHMe)]$. The loss of a Rh-Cl band ($\sim 300cm^{-1}$) is observed, as well as the presence of new bands corresponding to the new but-2-enoate ligand. There is a slight shift in the absorbance assignable to the carbonyl group of the bidentate anhydride, from $1740cm^{-1}$ to $1744cm^{-1}$, however this is not

too significant. The absorptions at 1661cm$^{-1}$ and 1535cm$^{-1}$ belong to the monodentate but-2-enoate ligand, with the former band corresponding to the ν(OCO)asymmetric stretching frequency and this value is consistent with the electron withdrawing nature of the vinyl group. Conjugation of C=O with C=C cannot, therefore, be very important since this would be expected to reduce ν(OCO)asym. Coordination does however, appear to lower ν(C=C) from 1633cm$^{-1}$ in the free anion to 1535cm$^{-1}$ for the monodentate anion.

The complex [Rh($O_2$CCMe=CHPh)($PPh_3$)($Ph_2PO_2$CCMe=CHPh)], has an IR spectrum (see Table 2.4.2) similar to that observed for [Rh($O_2$CCH=CHMe)($PPh_3$)($Ph_2PO_2$CCH=CHMe)]. Once again new bands are observed, this time corresponding to the newly introduced 2-methyl-3-phenylpropenoate ligand. These are at 1634cm$^{-1}$ and 1506cm$^{-1}$ corresponding to ν(OCO)asym and ν(C=C) respectively. The band at 1729cm$^{-1}$, assignable to the carbonyl group of the bidentate anhydride is in keeping with that observed in both the species [RhCl($PPh_3$)($Ph_2PO_2$CCH=CHMe)] and [Rh($O_2$CCH=CHMe)($PPh_3$)($Ph_2PO_2$CCH=CHMe)].

The $^{31}$P NMR spectrum of [Rh($O_2$CCH=CHMe)($PPh_3$)($Ph_2PO_2$CCH=CHMe)] is shown in Spectrum 2.4.1. The two phosphorus atoms are in unique environments and each give rise to a resonance that is split by a coupling to rhodium and by a mutual cis phosphorus coupling. The mixed anhydride ligand is clearly bidentate as the resonance from its phosphorus atom is shifted to low field ($\delta$127.0) whilst the second phosphorus atom resonates in the characteristic area for a coordinated

triphenylphosphine ligand ($\delta$25.9). The shift in resonance for the phosphorus of the mixed anhydride is again, as mentioned previously, due to the appearance of ring contributions. The effects of coordinating the but-2-enoate anion, as far as the $^{31}P$ NMR is concerned, are that the phosphorus environment of the anhydride exhibits a small change due to the structural changes needed to accomodate the more bulky, anionic acid ligand and that this extra bulk removes the fluxionality seen in the complex $[RhCl(PPh_3)(Ph_2PO_2CCH=CHMe)]$, presumably by making the trans isomer of much higher relative energy. The $^{31}P$ NMR data for $[Rh(O_2CCH=CHMe)(P_APh_3)(Ph_2P_BO_2CCH=CHMe)]$ are shown in Table 2.4.3, with both the Rh-$P_A$ and Rh-$P_B$ coupling constants having a value of 146Hz. The Rh-$P_B$ coupling is less than that which is observed for $[RhCl(P_APh_3)(Ph_2P_BO_2CCH=CHMe)]$ where $J_{RhP_B}$ has a value of 164Hz, thus indicating that by replacing a chloride ligand with a but-2-enoate ligand, there has been a significant increase in the trans-influence.[6]

The bidentate binding of $Ph_2PO_2CCMe=CHPh$ to rhodium via phosphorus and the carbon-carbon double bond has previously not been observed. However, the $^{31}P$ NMR of $[Rh(O_2CCMe=CHPh)(P_APh_3)(Ph_2P_BO_2CCMe=CHPh)]$ closely resembles that of its but-2-enoate derived counterpart, $[Rh(O_2CCH=CHMe)(PPh_3)(Ph_2PO_2CCH=CHMe)]$. The $^{31}P$ NMR of the former consists of a doublet of doublets at $\delta$126.0 and another doublet of doublets at $\delta$25.3 (see Table 2.4.3).

Spectrum 2.4.1 $^{31}P$ NMR of $[Rh(O_2CCH=CHMe)(PPh_3)(Ph_2PO_2CCH=CHMe)]$ in $CD_2Cl_2$ at 298K.

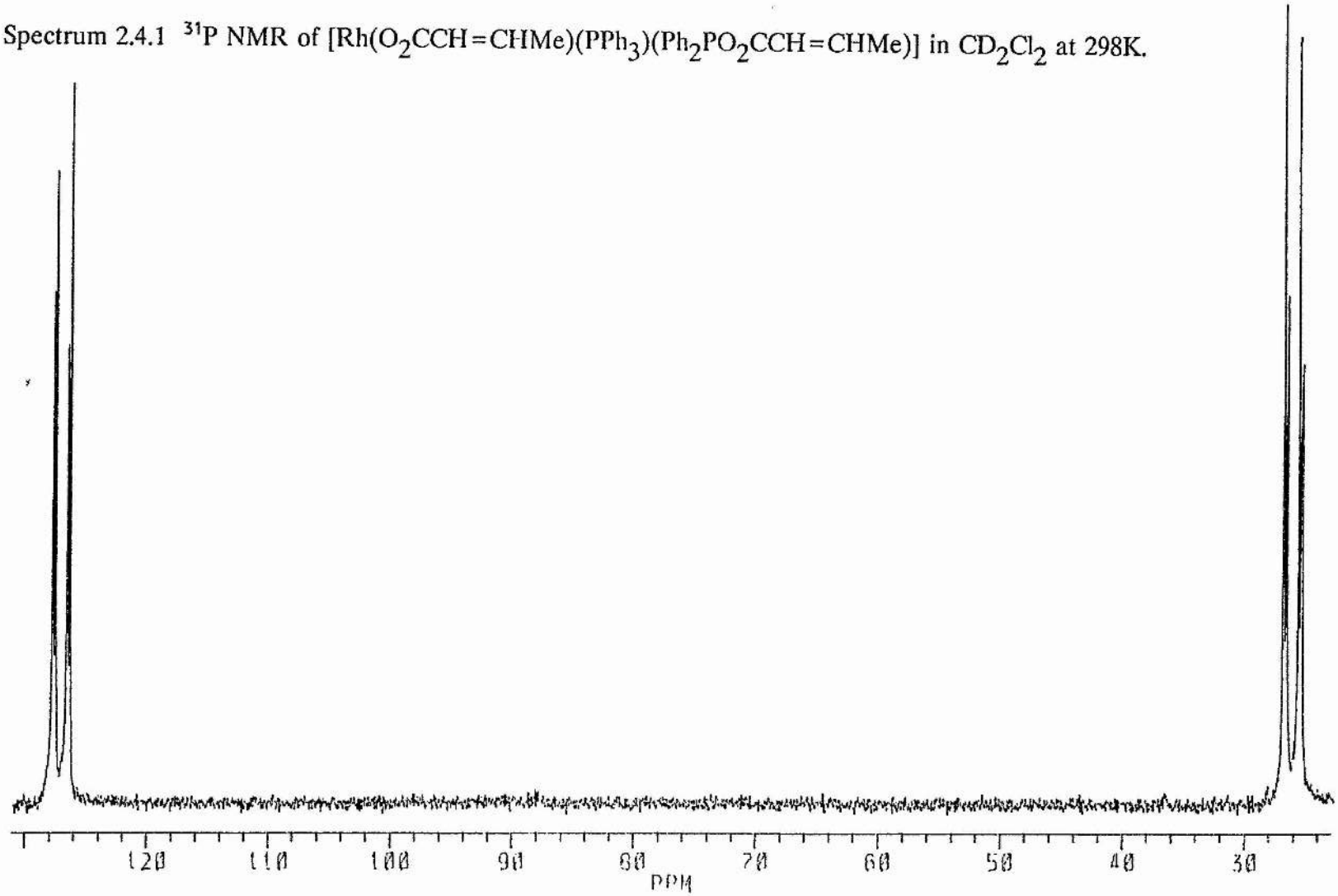

The spectroscopic data obtained from the $^1H$ NMR further helps in the characterisation of both $[Rh(O_2CCH=CHMe)(PPh_3)(Ph_2PO_2CCH=CHMe)]$ and $[Rh(O_2CCMe=CHPh)(PPh_3)(Ph_2PO_2CCMe=CHPh)]$. With regards to the former, the resonances assigned to the monodentate but-2-enoate anion are found at $\delta$6.27, $\delta$5.20 and $\delta$1.58. These positions are shifted upfield from those of the free but-2-enoic acid; $\delta$7.08, $\delta$5.90 and $\delta$1.92 respectively. These shifts can be explained in terms of a reduction in the bond order of C=C due to electron migration away from the double bond. This reduction in bond order is analogous to the double bond obtaining a certain degree of single bond character, which thus produces the observed shift for the substituents of the carbon-carbon double bond. The resonances from the bidentate anhydride are found at $\delta$1.11, $\delta$4.07 and $\delta$3.31 compared with $\delta$1.69, $\delta$4.75 and $\delta$4.07 for $[RhCl(PPh_3)(Ph_2PO_2CCH=CHMe)]$. The shifts to higher field are consistent for all substituents of the carbon-carbon double bond and are again indicative of the structural changes induced in the bidentate ring to accomodate the greater bulk of the acid anion. The experimentally observed $^1H$ NMR spectrum of $[Rh(O_2CCH=CHMe)(PPh_3)(Ph_2PO_2CCH=CHMe)]$ is shown in Spectrum 2.4.2 and the corresponding data are presented in Table 2.4.4.

The $^1H$ NMR spectrum (refer to Table 2.4.4) of $[Rh(O_2CCMe^a=CH^bPh)(PPh_3)(Ph_2PO_2CCMe^c=CH^dPh)]$, where the mixed anhydride is bidentate, is significantly different from that observed for the chloride containing complex, $[RhCl(PPh_3)_2(Ph_2PO_2CCMe^a=CH^bPh)]$, where the mixed anhydride is monodentate. For the bidentate mixed anhydride the peak assignable

to the proton ($H^b$) is seen as a broad signal at $\delta$4.70 whereas for the monodentate anhydride this signal is further downfield and is obscured by the phenyl resonances.

Spectrum 2.4.2 $^{1}H$ NMR of $[Rh(O_2CCH=CHMe)(PPh_3)(Ph_2PO_2CCH=CHMe)]$ in $CD_2Cl_2$ at 298K.

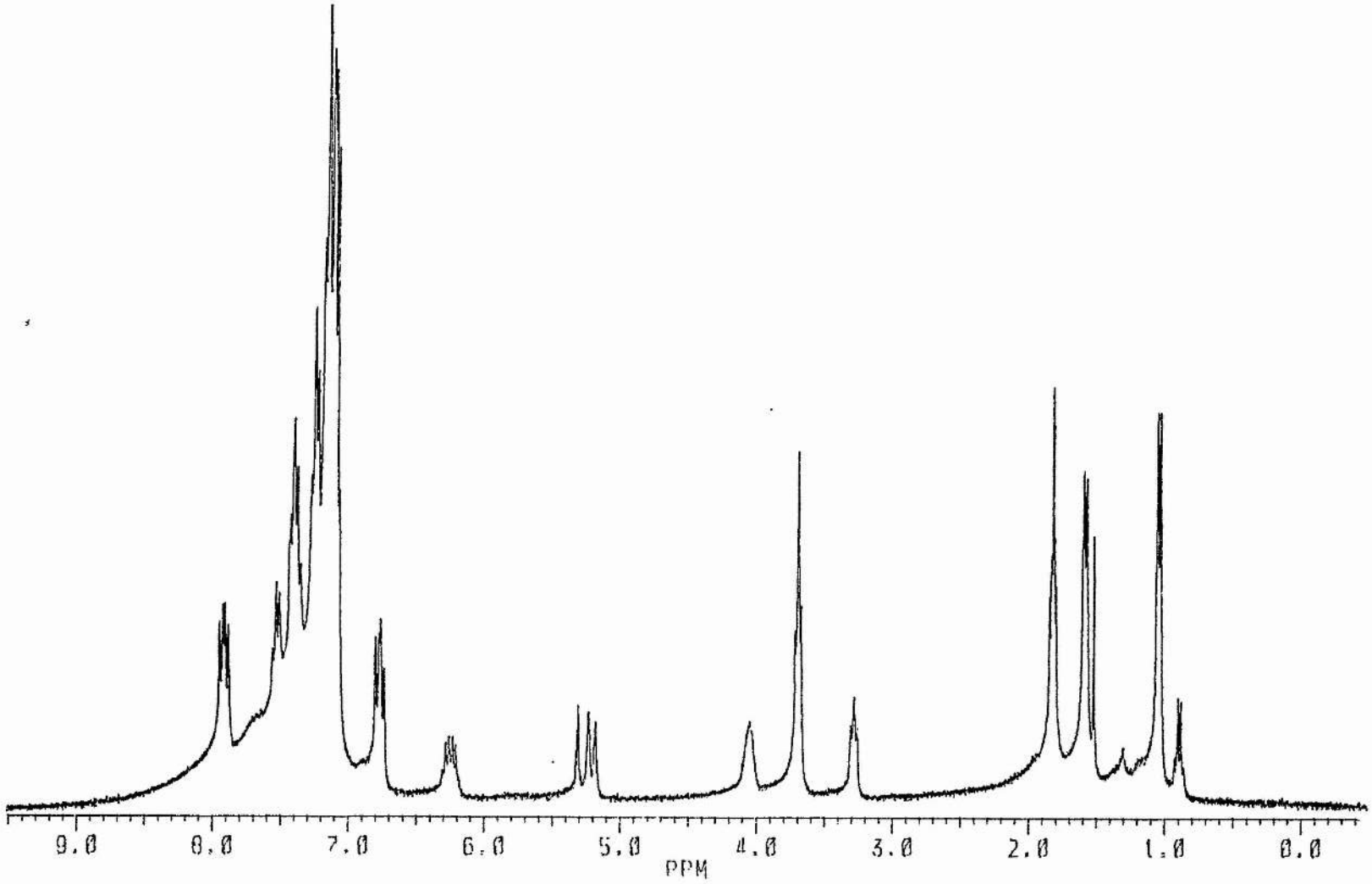

Table 2.4.2 IR data ($cm^{-1}$) for rhodium complexes (Nujol Mulls)

| Complex | Mixed Anhydride Ligand | | Carboxylate Ligand | |
|---|---|---|---|---|
| | ν(C=O) | ν(C=C) | ν(C=O) | ν(C=C) |
| $[Rh(O_2CCH=CHMe)(PPh_3)(Ph_2PO_2CCH=CHMe)]$ | 1744 | - | 1661 | 1535 |
| $[Rh(O_2CCMe=CHPh)(PPh_3)(Ph_2PO_2CCMe=CHPh)]$ | 1729 | - | 1634 | 1506 |
| $[Rh(O_2CCMe=CHPh)(PPh_3)(Ph_2PO_2CCH=CHMe)]$ | 1747 | - | 1658 | 1514 |
| $[Rh(O_2CCH=CMe_2)(PPh_3)(Ph_2PO_2CCH=CHMe)]$ | 1740 | - | 1648 | 1530 |

Table 2.4.3 $^{31}P$ NMR data for rhodium complexes, measured in $CD_2Cl_2$ at 298K

| Complex | $\delta$ | | J/Hz | | |
|---|---|---|---|---|---|
| | $P_A$ | $P_B$ | Rh-$P_A$ | Rh-$P_B$ | $P_A$-$P_B$ |
| [Rh($O_2$CCH=CHMe)($P_A$$Ph_3$)($Ph_2$$P_B$$O_2$CCH=CHMe)] | 25.9(dd) | 127.0(dd) | 146 | 146 | 30 |
| [Rh($O_2$CCMe=CHPh)($P_A$$Ph_3$)($Ph_2$$P_B$$O_2$CCMe=CHPh)] | 25.3(dd) | 126.0(dd) | 139 | 145 | 31 |
| [Rh($O_2$CCMe=CHPh)($P_A$$Ph_3$)($Ph_2$$P_B$$O_2$CCH=CHMe)] | 26.3(dd) | 127.1(dd) | 146 | 146 | 31 |
| [Rh($O_2$CCH=$CMe_2$)($P_A$$Ph_3$)($Ph_2$$P_B$$O_2$CCH=CHMe)] | 25.8(dd) | 126.9(dd) | 146 | 145 | 30 |

Table 2.4.4 $^1$H NMR data ($\delta$) for rhodium complexes, measured in $CD_2Cl_2$ at 298K

| Complex | | | | |
|---|---|---|---|---|
| | Me | H | Me | H |
| $[Rh(O_2CCH^f=CH^eMe^d)(PPh_3)(Ph_2PO_2CCH^c=CH^bMe^a)]$ | $^a$1.11(d) | $^b$4.07(br) $^c$3.31(brt) | $^d$1.58(d) | $^e$6.27(m) $^f$5.20(brd) |
| $[Rh(O_2CCMe^c=CH^dPh)(PPh_3)(Ph_2PO_2CCMe^a=CH^bPh)]$ | $^a$1.95(d) | $^b$4.70(br) | $^c$1.75(s) | a |
| $[Rh(O_2CCMe^d=CH^ePh)(PPh_3)(Ph_2PO_2CCH^c=CH^bMe^a)]$ | $^a$1.10(d) | $^b$4.06(br) $^c$3.27(brt) | $^d$1.73(s) | b |
| $[Rh(O_2CCH^f=\dot{M}e_2^{d,e})(PPh_3)(Ph_2PO_2CCH^c=CH^bMe^a)]$ | $^a$0.99(d) | $^b$3.97(br) $^c$3.23(brt) | $^d$1.60(s) $^e$1.95(s) | $^f$4.98(s) |

a $H^d$ obscured by phenyl resonance

b $H^e$ obscured by phenyl resonance

## 2.5 Reactions of $[RhCl(PPh_3)_n(Ph_2PO_2CR=CR'R'')]$ with Acrylic Acid Anions other than $[O_2CCR=CR'R'']^-$.

The reaction of $[RhCl(PPh_3)(Ph_2PO_2CCH=CHMe)]$ with excess $[PhHC=CMeCO_2]K$ yields $[Rh(O_2CCMe=CHPh)(PPh_3)(Ph_2PO_2CCH=CHMe)]$ as the product. The bidentate mixed anhydride is but-2-enoic acid derived, as in the starting material, and the monodentate acid anion is that of 2-methyl-3-phenylpropenoic acid. This reaction is illustrated in Figure 2.5.1 and both the room temperature $^{31}P$ and $^{1}H$ NMR spectra of the product, $[Rh(O_2CCMe=CHPh)(PPh_3)(Ph_2PO_2CCH=CHMe)]$, are presented as Spectra 2.5.1 and 2.5.2 respectively.

Figure 2.5.1

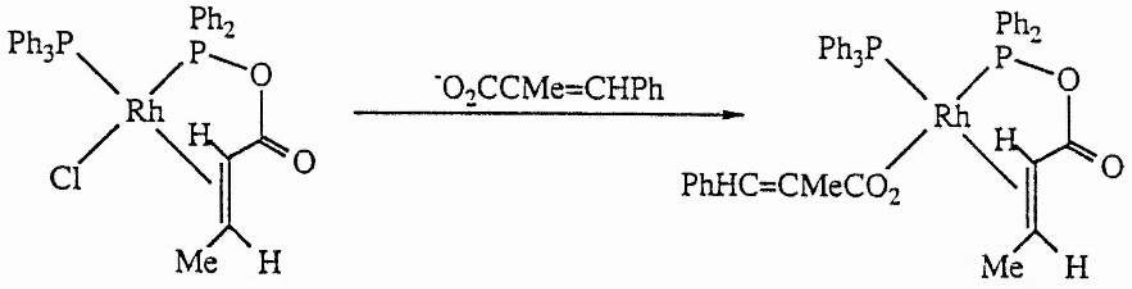


The data obtained from the IR spectrum (shown in Table 2.4.2) illustrate that the absorbance assignable to the carbonyl group of the bidentate anhydride is at $1747cm^{-1}$, which is in close proximity to the value obtained for $\nu(C=O)$ in $[Rh(O_2CCH=CHMe)(PPh_3)(Ph_2PO_2CCH=CHMe)]$. Similarly, bands corresponding to $\nu(OCO)asym$ and $\nu(C=C)$ of the 2-methyl-3-phenylpropenoate ligand in

[Rh($O_2$CCMe=CHPh)($PPh_3$)($Ph_2PO_2$CCH=CHMe)] (1658$cm^{-1}$ and 1514$cm^{-1}$) are generally in similar positions to those bands observed in [Rh($O_2$CCMe=CHPh)($PPh_3$)($Ph_2PO_2$CCMe=CHPh)] (1634$cm^{-1}$ and 1506$cm^{-1}$).

Once again two sets of doublet of doublets are observed in the $^{31}P$ NMR, and the shifts of the resonances and also the coupling constants involved vary little from those for example of [Rh($O_2$CCMe=CHPh)($PPh_3$)($Ph_2PO_2$CCMe=CHPh)], and as before the data are shown in Table 2.4.3.

There is, however, in the $^1H$ NMR (Table 2.4.4) a small shift to higher field in the resonances associated with the but-2-enoate mixed anhydride in the complex, [Rh($O_2$CCMe=CHPh)($PPh_3$)($Ph_2PO_2$CCH=CHMe)], compared with those resonances observed in [Rh($O_2$CCH=CHMe)($PPh_3$)($Ph_2PO_2$CCH=CHMe)]. This is again attributed to the structural changes induced in the bidentate ring to accommodate the greater bulk of [$O_2$CCMe=CHPh]$^-$ compared with [$O_2$CCH=CHMe]$^-$.

Spectrum 2.5.1 $^{31}P$ NMR of $[Rh(O_2CCMe=CHPh)(PPh_3)(Ph_2PO_2CCH=CHMe)]$ in $CD_2Cl_2$ at 298K.

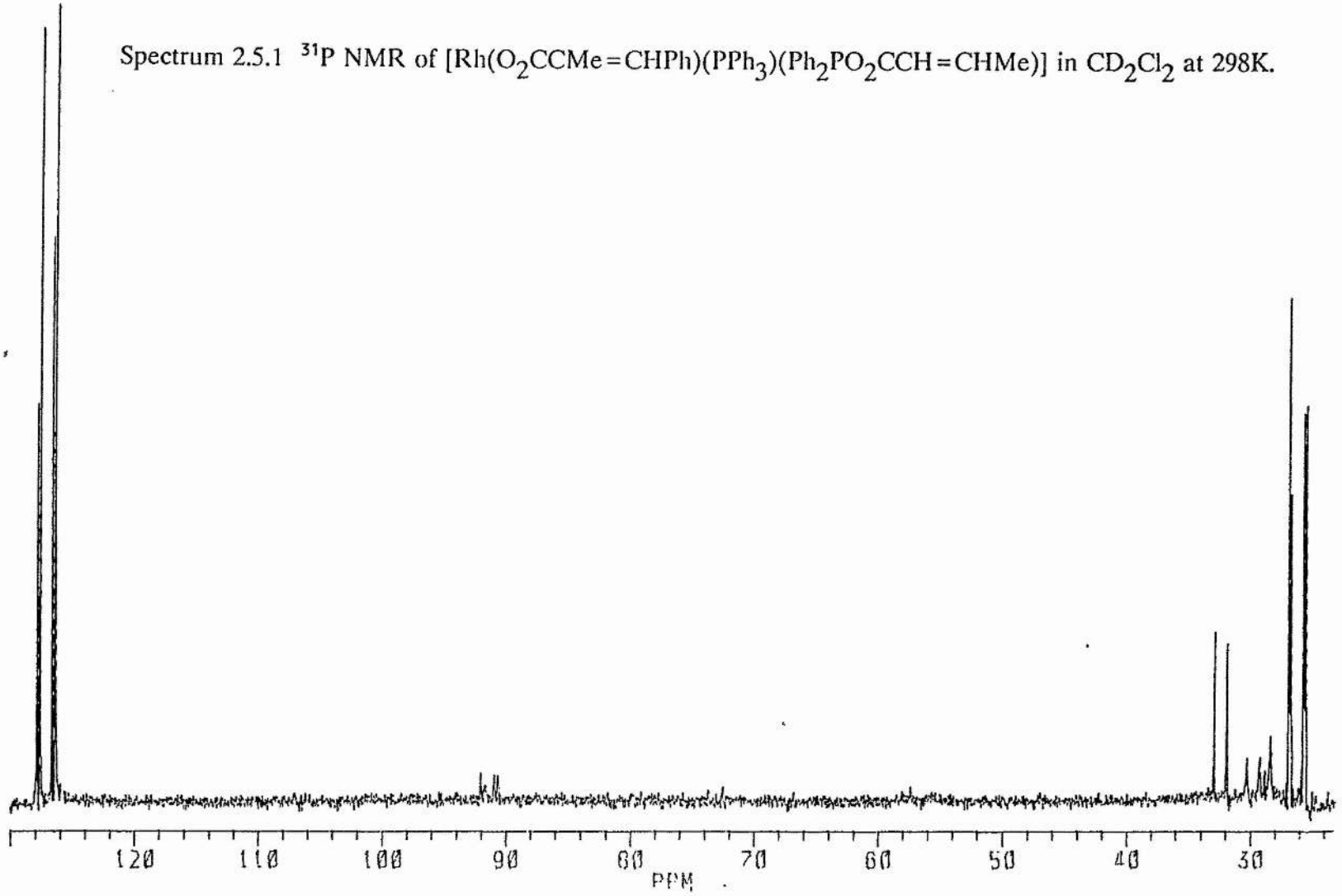

Spectrum 2.5.2 $^{1}H$ NMR of $[Rh(O_2CCMe=CHPh)(PPh_3)(Ph_2PO_2CCH=CHMe)]$ in $CD_2Cl_2$ at 298K.

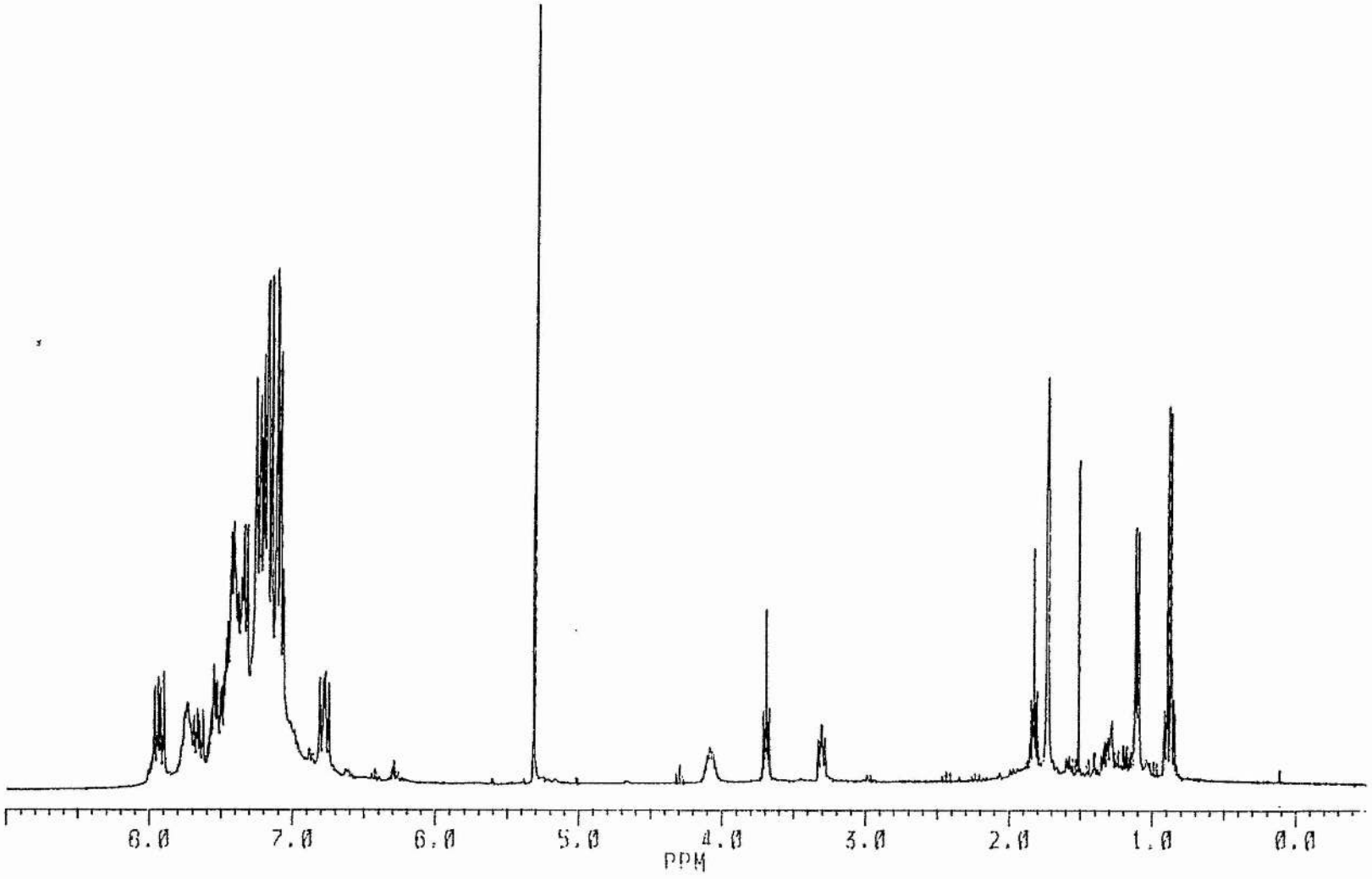

The reaction of $[RhCl(PPh_3)_2(Ph_2PO_2CCMe=CHPh)]$ with a 10 times excess of $[MeHC=CHCO_2]K$ at room temperature for 3 hours does not produce $[Rh(O_2CCH=CHMe)(PPh_3)(Ph_2PO_2CCMe=CHPh)]$ as the product. The products of the reaction are shown in Figure 2.5.2, whereby both of the rhodium species $[Rh(O_2CCMe=CHPh)(PPh_3)(Ph_2PO_2CCH=CHMe)]$ and $[Rh(O_2CCH=CHMe)(PPh_3)(Ph_2PO_2CCH=CHMe)]$ are obtained, in the % ratio of 60%:40%.

Figure 2.5.2

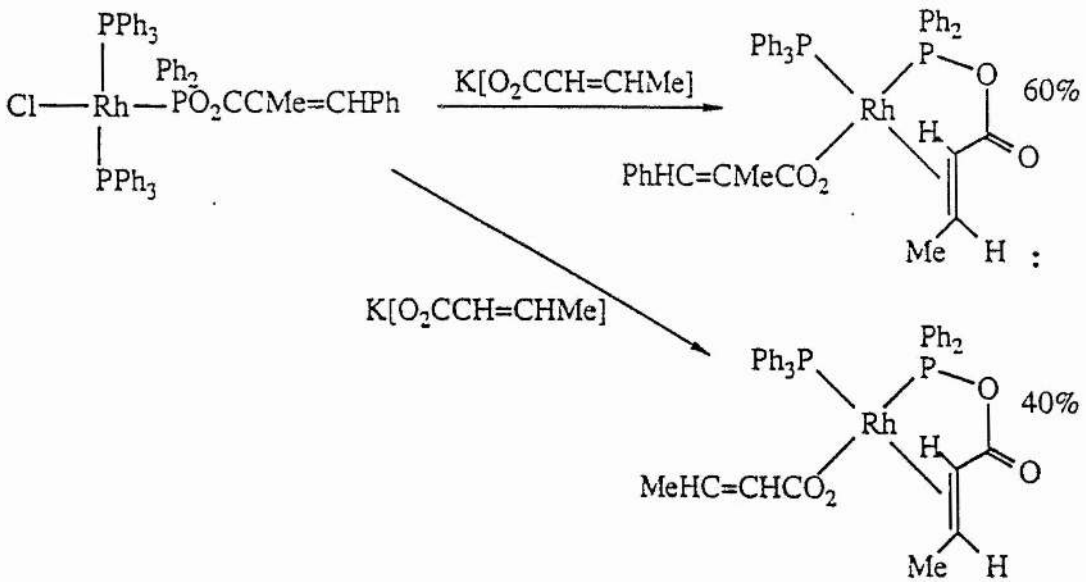


This reaction clearly shows that there is a strong preference for $[O_2CCH=CHMe]^-$ over $[O_2CCMe=CHPh]^-$ to be involved in the bidentate mixed anhydride. This might be expected due to the smaller number of substituents on the carbon-carbon double bond, although the marked preference is surprising in view of the isolation

and apparent stability of [Rh($O_2$CCMe=CHPh)($PPh_3$)($Ph_2PO_2$CCMe=CHPh)]. $^{31}$P and $^1$H NMR studies have shown that at shorter reaction times the ratio of the amounts of [Rh($O_2$CCMe=CHPh)($PPh_3$)($Ph_2PO_2$CCH=CHMe)] to [Rh($O_2$CCH=CHMe)($PPh_3$)($Ph_2PO_2$CCH=CHMe)] is greater than 3:2. Furthermore, when a mixture of the two complexes is reacted with excess but-2-enoic acid in the presence of the base, triethylamine ($NEt_3$), [Rh($O_2$CCH=CHMe)($PPh_3$)($Ph_2PO_2$CCH=CHMe)] is produced as the sole product. These observations, presented in Figure 2.5.3, can be partially explained in terms of the lower solubility of K[$O_2$CCH=CHMe] compared with the triethylammonium salt of but-2-enoic acid, since complete conversion of the catalyst precursor, [RhCl($PPh_3$)$_2$($Ph_2PO_2$CCMe=CHPh)], to [Rh($O_2$CCH=CHMe)($PPh_3$)($Ph_2PO_2$CCH=CHMe)] does not occur when using K[$O_2$CCH=CHMe] but does occur when using [$HO_2$CCH=CHMe] and $NEt_3$. What is more difficult to elucidate is whether the but-2-enoate anion first of all replaces the chloride ligand or the 2-methyl-3-phenylpropenoate anion of the mixed anhydride or whether it replaces both simultaneously.

Figure 2.5.3

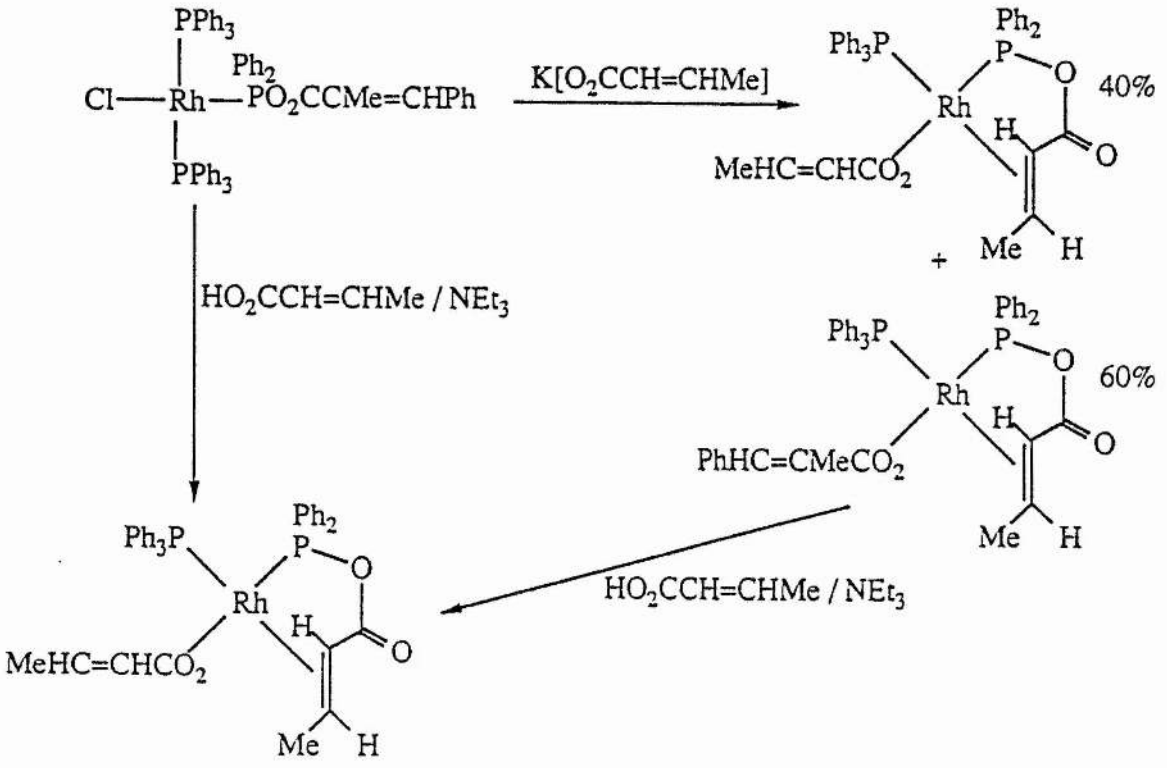


The reaction of $[RhCl(PPh_3)(Ph_2PO_2CCH=CHMe)]$ with a 10 times excess of the potassium salt of 3-methylbut-2-enoic acid, illustrated in Figure 2.5.4, yields $[Rh(O_2CCH=CMe_2)(PPh_3)(Ph_2PO_2CCH=CHMe)]$ as the sole product.

Figure 2.5.4

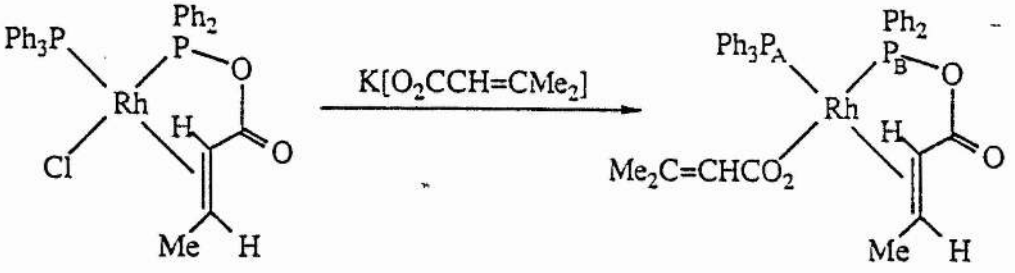

In this reaction the 3-methylbut-2-enoate anion has replaced the chloride ligand, however it should be noted that no exchange occurs at the mixed anhydride ligand. This is another case whereby the but-2-enoate derived mixed anhydride is preferred due to the fewer number of substituents on the carbon-carbon double bond.

The $^{31}P$ NMR (Table 2.4.3) is very similar to that observed for $[Rh(O_2CCH=CHMe)(PPh_3)(Ph_2PO_2CCH=CHMe)]$ in Section 2.4. The phosphorus resonance assigned to the mixed anhydride, $P_B$, is at $\delta$126.9 with the values of $J_{RhP_B}$ and $J_{P_AP_B}$ equal to 145Hz and 30Hz respectively. The phosphorus resonance assigned to the $PPh_3$ ligand, $P_A$, is at $\delta$25.8 with $J_{RhP_A}$ 146Hz and $J_{P_AP_B}$ 30Hz.

The $^1H$ NMR spectrum of the isolated product complex $[Rh(O_2CCH=CMe_2)(PPh_3)(Ph_2PO_2CCH=CHMe)]$ shows the resonances assignable to the protons in the mixed anhydride to be very similar to those seen in $[Rh(O_2CCH=CHMe)(PPh_3)(Ph_2PO_2CCH=CHMe)]$. The resonances assigned to the methyl groups of the 3-methylbut-2-enoate ligand ($-O_2CCH^f=CMe_2^{d,e}$) are at $\delta$1.60(s) and $\delta$1.95(s), whilst that assigned to the vinylic proton is at $\delta$4.98(s), which is significantly upfield from that observed in the free acid and the mixed anhydride.

Infra-red studies show $\nu$(C=O) for the bidentate mixed anhydride to be at 1740cm$^{-1}$ whilst $\nu$(C=O) and $\nu$(C=C) for the 3-methylbut-2-enoate anion are at 1648cm$^{-1}$ and 1530cm$^{-1}$ respectively. These absorptions are entirely consistent with the

structure presented in Figure 2.5.4, and the results are tabulated in Table 2.4.2.

The reaction between the monodentate mixed anhydride complex $[RhCl(PPh_3)_2(Ph_2PO_2CCH=CMe_2)]$ and a 10 times excess of potassium but-2-enoate produces the two products illustrated in Figure 2.5.5, in the percentage ratio shown.

Figure 2.5.5

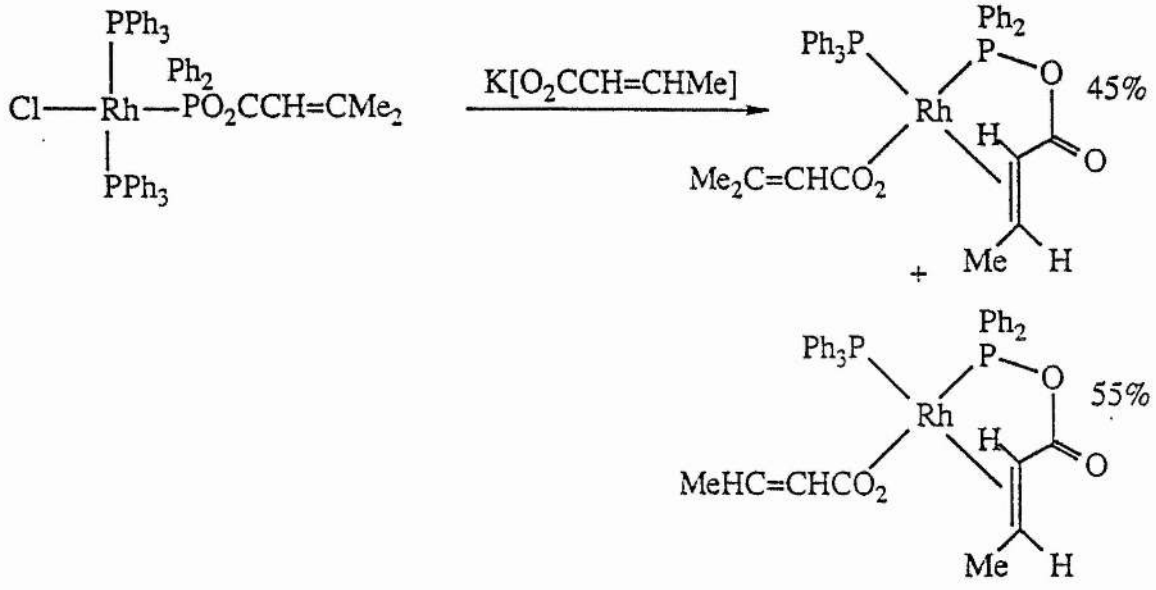


Once again the chelate mixed anhydride is derived from but-2-enoic acid. The $^{31}P$ and $^{1}H$ NMR spectra of the mixture are presented in Spectra 2.5.3 and 2.5.4 respectively.

Overall, it seems probable that the active catalytic species for the hydrogenation of acrylate ions is not the catalyst precursor, $[RhCl(PPh_3)_n(Ph_2PO_2CCR=CR'R'')]$, nor the previously suggested cationic chelate complex,

$[Rh(PPh_3)_2(Ph_2PO_2CCR=CR'R'')]^+$, but rather the complex $[Rh(O_2CCR=CR'R'')(PPh_3)(Ph_2PO_2CCR=CR'R'')]$ in which the carboxylate ions are those derived from the substrate rather than from the catalyst precursor.

Spectrum 2.5.3 $^{31}P$ NMR of a product mixture, obtained from the reaction between $[RhCl(PPh_3)_2(Ph_2PO_2CCH=CMe_2)]$ and $K[O_2CCH=CHMe]$, in $CD_2Cl_2$ at 298K.


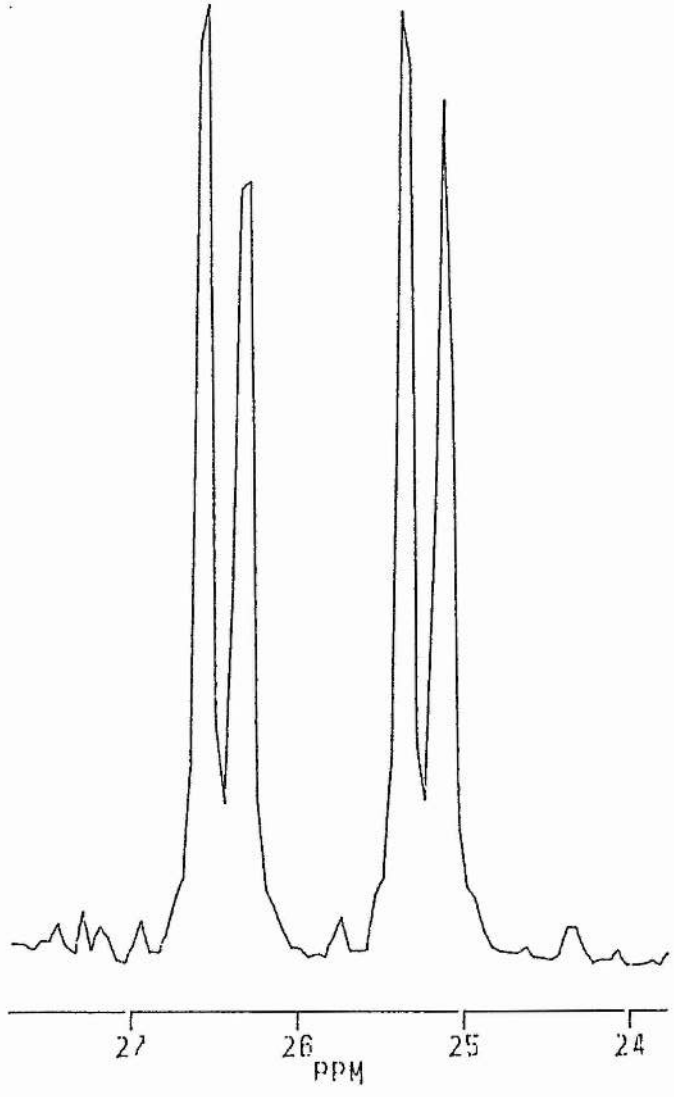

Spectrum 2.5.4 $^{1}H$ NMR of a product mixture, obtained from the reaction between $[RhCl(PPh_3)_2(Ph_2PO_2CCH=CMe_2)]$ and $K[O_2CCH=CHMe]$, in $CD_2Cl_2$ at 298K.

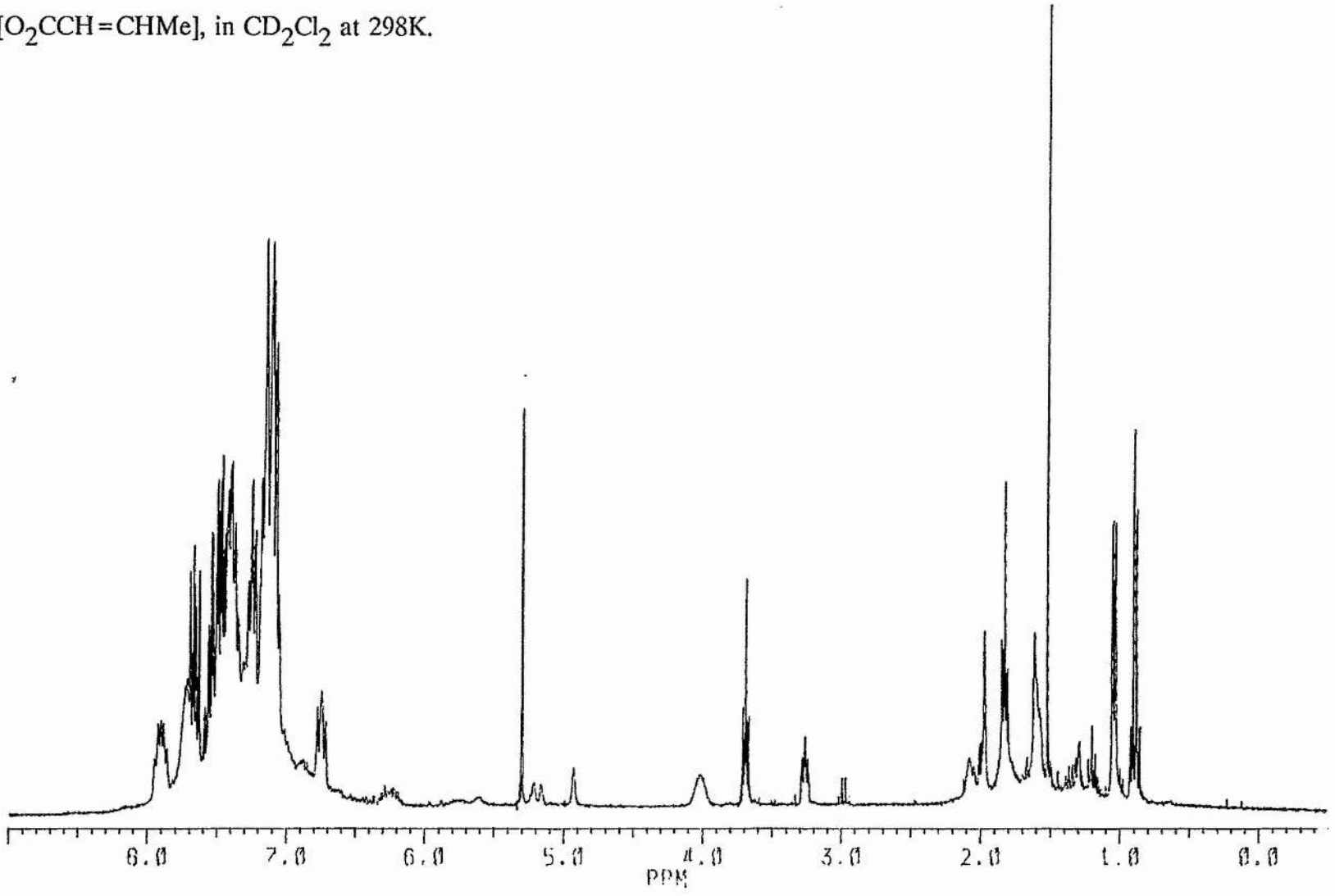

## 2.6 The Syntheses and Reactions of $[RhCl(PPh_3)_2(Ph_2PO_2CCH_2CH_2CH_3)]$ and $[Rh(PPh_3)_2(Ph_2PO_2CCH_2CH_2CH_3)]^+$.

In an attempt to investigate the step by which the product carboxylic acid anion is released from the metal complex, $[RhCl(PPh_3)_2(Ph_2PO_2CCH_2CH_2CH_3)]$ has been synthesized from the reaction of Wilkinson's catalyst with $[Ph_2PO_2CCH_2CH_2Me]$.[4] The complex isolated from this reaction has the correct stoichiometry, but it exists in 2 forms, A and B, as illustrated in Figure 2.6.1. The $^{31}P$ and $^1H$ NMR spectra of the isomeric mixture are presented as Spectra 2.6.1 and 2.6.2 respectively, and correspondingly, the data obtained from them are presented in Tables 2.6.1 and 2.6.2 at the end of this section.

Figure 2.6.1

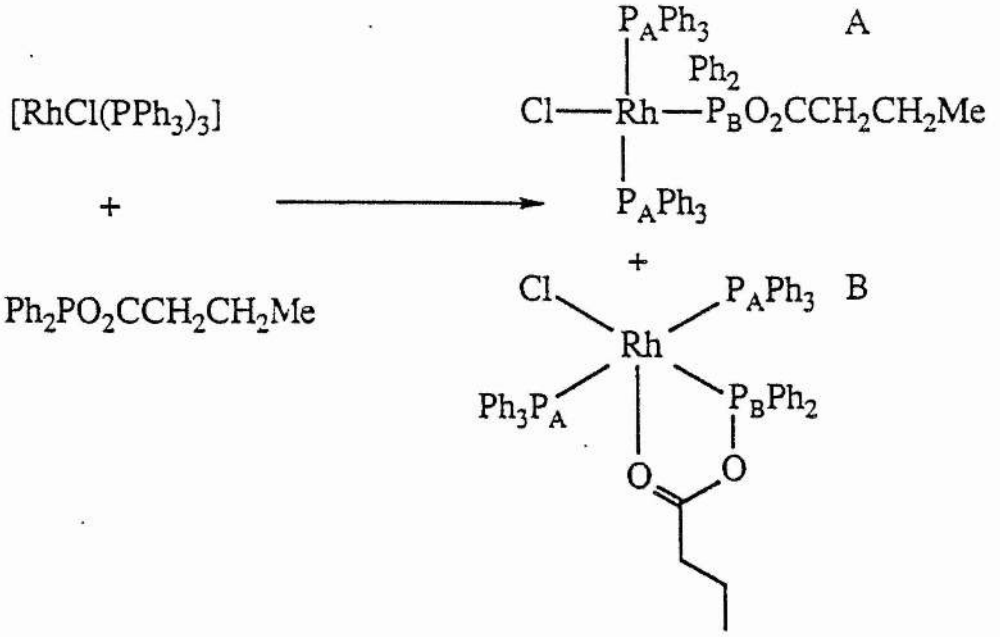


Form A, in which the mixed anhydride is only bound through the phosphorus atom, has spectroscopic properties consistent with the structure shown. Both the spectrum

shown as Spectrum 2.6.1 and the data presented in Table 2.6.1 show that at room temperature the resonance of the phosphorus atom from the triphenylphosphine ligand ($P_A$) is coupled to rhodium and the phosphorus atom ($P_B$) of the mixed anhydride, resulting in a doublet of doublets; the shift of which ($\delta$31.8) is consistent with a coordinated $PPh_3$ ligand. The coupling constants $J_{RhP_A}$ (142Hz) and $J_{P_AP_B}$ (38Hz) are comparable with those observed for compounds of general formula $[RhCl(PPh_3)_2(Ph_2PO_2CCR{=}CR'R'')]$, as are the shift and couplings associated with the phosphorus atom ($P_B$) of the mixed anhydride ligand.

In the $^1H$ NMR of the free butanoic acid derived mixed anhydride, $[Ph_2PO_2CCH_2^cCH_2^bMe^a]$, $-CH_3^a$ gives rise to a triplet resonance at a shift of $\delta$1.0, $-CH_2^b$ a triplet of quartets at $\delta$1.74 and $-CH_2^c$ a triplet at $\delta$2.52. Upon complexation, in form A of $[RhCl(PPh_3)_2(Ph_2PO_2CCH_2CH_2Me)]$, the corresponding signals are shifted to $\delta$1.26, $\delta$1.60 and $\delta$2.27 respectively; this being due to the shielding by the metal d electrons.

As can be seen in Spectrum 2.6.1, form B of $[RhCl(PPh_3)_2(Ph_2PO_2CCH_2CH_2Me)]$ has a room temperature $^{31}P$ NMR spectrum consisting of 2 broad peaks at $\delta$33.0 and $\delta$131.0. On cooling to -60°C the $^{31}P$ NMR spectrum consists of a doublet of triplets at $\delta$131.7 and a doublet of doublets at $\delta$33.6, as is shown in Spectrum 2.6.3. On warming, these signals broaden and at temperatures above ambient (75°C for 0.5h) they disappear irreversibly with the formation of $PPh_3$, a complex containing two phosphorus atoms, probably $[RhCl(PPh_3)(Ph_2PO_2CCH_2CH_2Me)]$, and a third complex in which all the phosphorus atoms are equivalent ($\delta$89, $J_{RhP}$=154Hz).

The non-fluxional isomer, A, is stable under these conditions.

As illustrated in Figure 2.6.1 the fluxional compound has been assigned as being 5-coordinate with the mixed anhydride being bound through phosphorus and the carbonyl oxygen atom. The fluxionality probably arises from a Berry pseudorotation but $PPh_3$ is more easily lost from this complex to form the dimer than from the 4-coordinate isomer. The $^1H$ NMR spectrum (Spectrum 2.6.2) shows that the signals associated with the mixed anhydride ($\delta$0.6(t), $\delta$0.85(tq) and $\delta$1.26(m)) are at higher field than those for form A. This is presumably brought about by the significant influence of ring currents associated with the phenyl rings of triphenylphosphine due to the closer proximity of the butanoate derived ligand to the rhodium centre.

Spectrum 2.6.1 $^{31}P$ NMR of $[RhCl(PPh_3)_2(Ph_2PO_2CCH_2CH_2CH_3)]$ in $CD_2Cl_2$ at 298K.

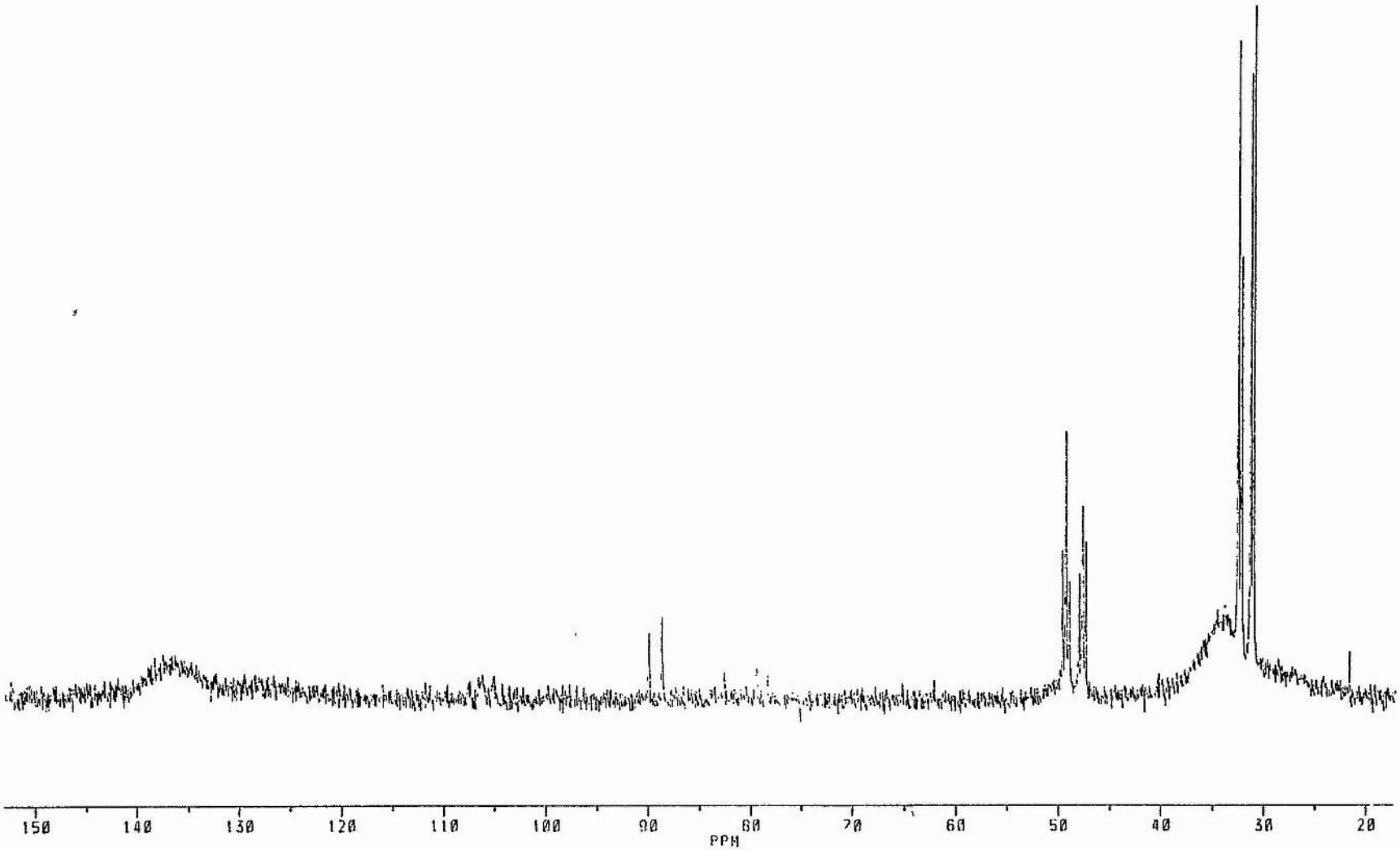

Spectrum 2.6.2 $^{1}H$ NMR of $[RhCl(PPh_3)_2(Ph_2PO_2CCH_2CH_2CH_3)]$ in $CD_2Cl_2$ at 298K.

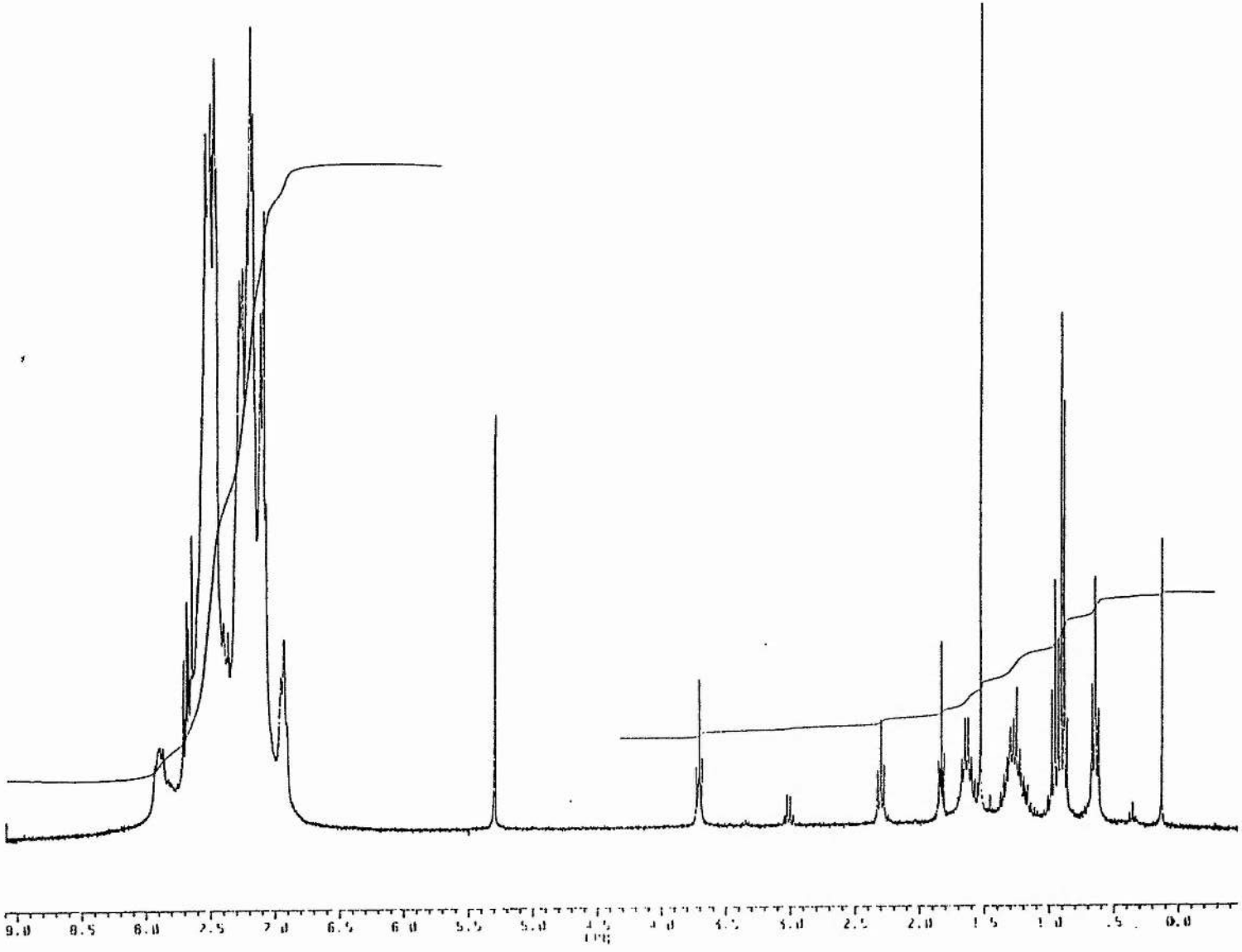

Spectrum 2.6.3 $^{31}P$ NMR of $[RhCl(PPh_3)_2(Ph_2PO_2CCH_2CH_2CH_3)]$ in $CD_2Cl_2$ at 213K.

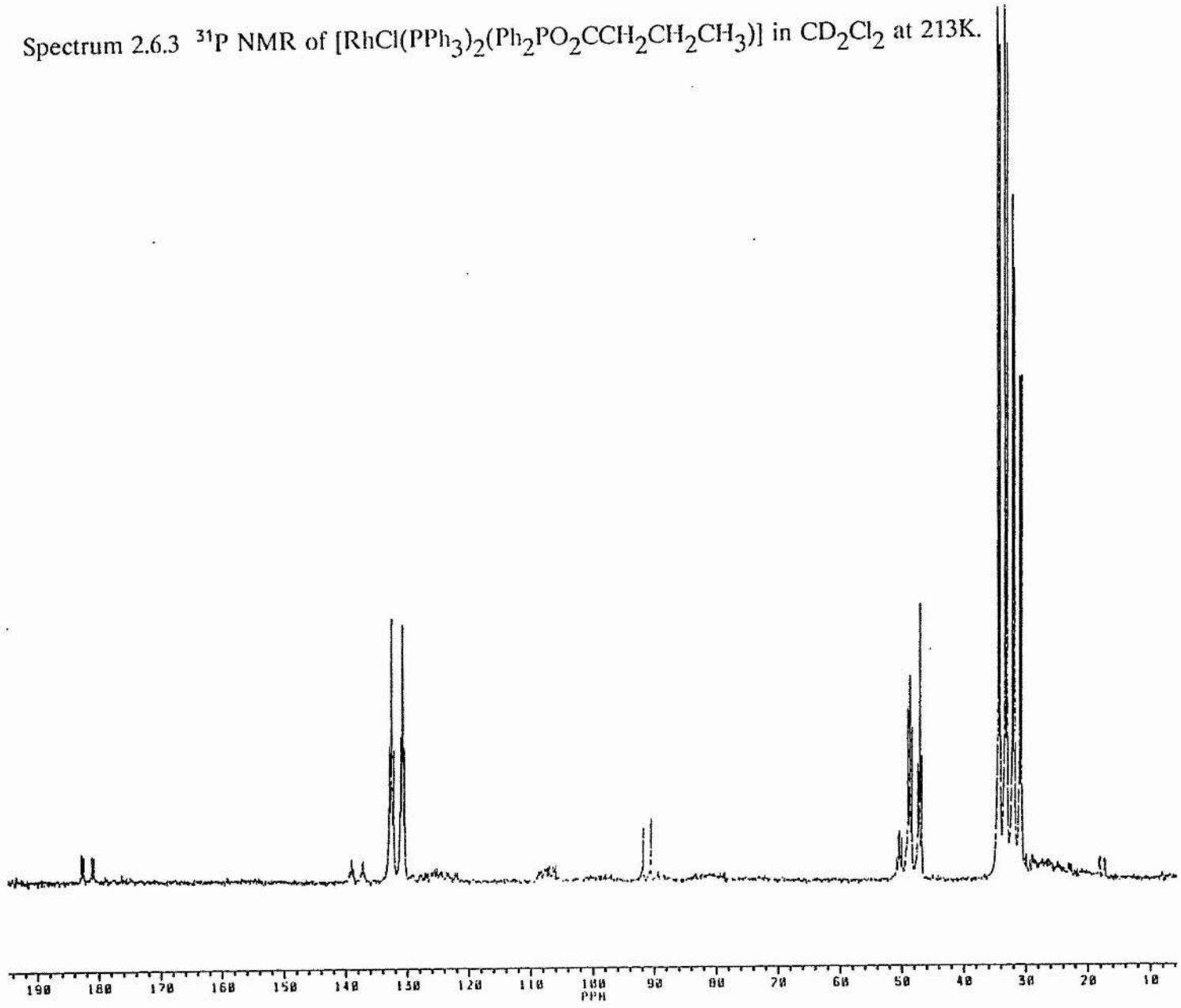

In a similar manner to that described in Section 2.2, the reaction of $[RhCl(PPh_3)_2(Ph_2PO_2CCH_2CH_2Me)]$ with $TlPF_6$ produces almost exclusively $[Rh(PPh_3)_2(Ph_2PO_2CCH_2CH_2Me)]^+PF_6^-$, as shown in Figure 2.6.2, with binding of the mixed anhydride through phosphorus and the carbonyl oxygen. The $^{31}P$ and $^1H$ NMR spectra of the product are shown as Spectra 2.6.4 and 2.6.5 respectively. The major impurity present in the $^{31}P$ NMR is the rhodium species $[Rh(PPh_3)_2(Ph_2POPPh_2]^+$.

Figure 2.6.2

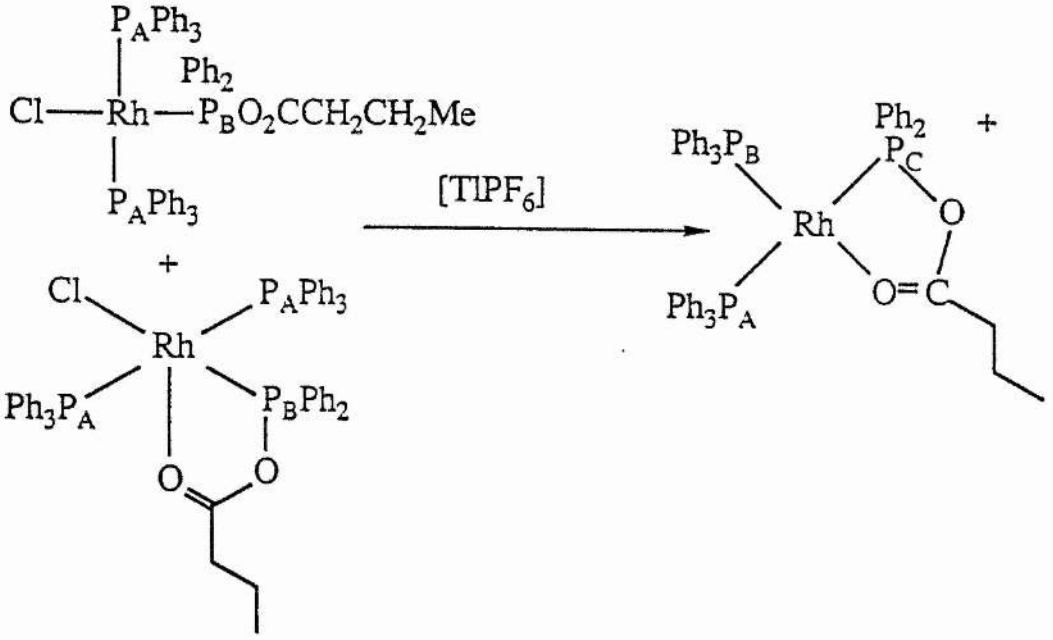


The $^{31}P$ and $^1H$ NMR data associated with the species $[Rh(PPh_3)_2(Ph_2PO_2CCH_2CH_2Me)]^+$ are presented at the end of this section in Tables 2.6.1 and 2.6.2.

From Figure 2.6.2, the resonance of the phosphorus atom of the mixed anhydride ($P_c$) exists as a doublet of doublet of doublets in the $^{31}P$ NMR and the value of

$J_{P_APc}$(320Hz) is comparable with those observed for both [Rh(diop)($Ph_2PO_2CCMe=CHPh$)]$PF_6$ and [Rh(chiraphos)($Ph_2PO_2CCMe=CHPh$)]$PF_6$. The shift of the aforementioned resonance is at $\delta$176.5, this being due to the cationic nature of the complex and also the size of the ring formed by the chelate binding of the mixed anyhdride ligand. A similar splitting of the resonance of the phosphorus atom, $P_A$, of triphenylphosphine is observed at $\delta$26.3, whilst the resonance associated with $P_B$($\delta$48.7) is observed as a doublet of doublet of triplets.

The $^1$H NMR data is broadly similar to that observed for the fluxional isomer of [RhCl($PPh_3$)$_2$($Ph_2PO_2CCH_2CH_2Me$)], the only significant difference being that the -$CH_2$- group attached to the carbonyl carbon atom is at lower field; an effect presumably brought about by the electronic environment in that particular group.

Spectrum 2.6.4 $^{31}P$ NMR of $[RhCl(PPh_3)_2(Ph_2PO_2CCH_2CH_2CH_3)]^+PF_6^-$ in $CD_2Cl_2$ at 298K.

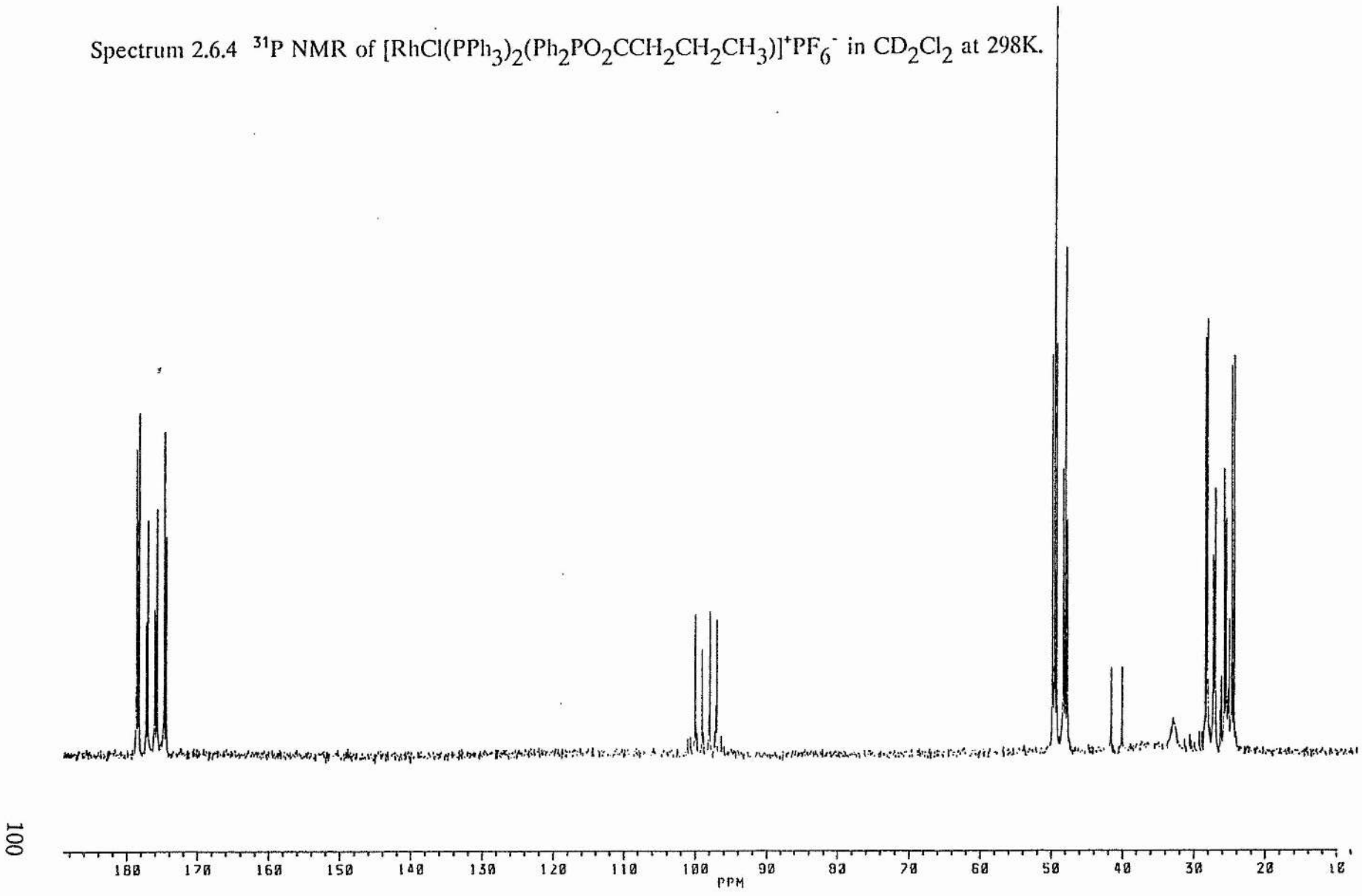

Spectrum 2.6.5 $^{1}H$ NMR of $[RhCl(PPh_3)_2(Ph_2PO_2CCH_2CH_2CH_3)]^+PF_6^-$ in $CD_2Cl_2$ at 298K.

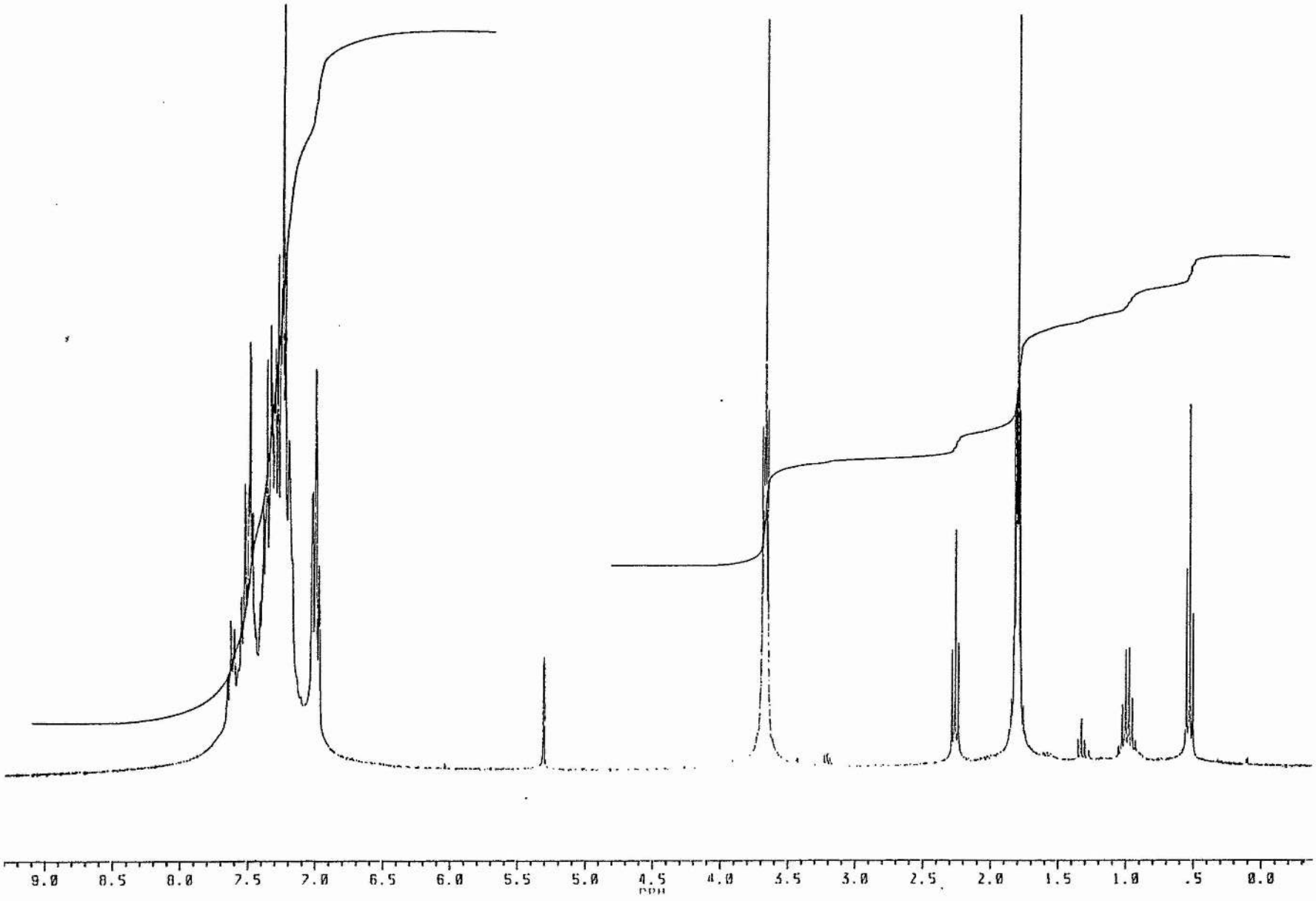

It has been suggested that the expulsion of product from the coordination sphere of the rhodium and the reintroduction of substrate during reactions catalysed by these mixed anhydride complexes may occur by a transesterification at phosphorus (see Scheme 2.3.1). In order to test this hypothesis, $[RhCl(PPh_3)_2(Ph_2PO_2CCH_2CH_2Me)]$, which contains the supposed product of hydrogenation of a mixed anhydride containing $[O_2CCH=CHMe]^-$, was reacted with excess but-2-enoate anions. The product of the reaction is $[Rh(O_2CCH=CHMe)(PPh_3)(Ph_2PO_2CCH=CHMe)]$ (Figure 2.6.4), which was also isolated from the reaction of $[RhCl(PPh_3)(Ph_2PO_2CCH=CHMe)]$ with excess $[O_2CCH=CHMe]^-$ (see Section 2.4). Thus both the chloride ligand and the saturated butanoate anion are replaced by the unsaturated but-2-enoate anion and this provides evidence that transesterification of a product similar to that likely to be present in the catalytic cycle after the hydrogen transfer steps, can occur.

Figure 2.6.4

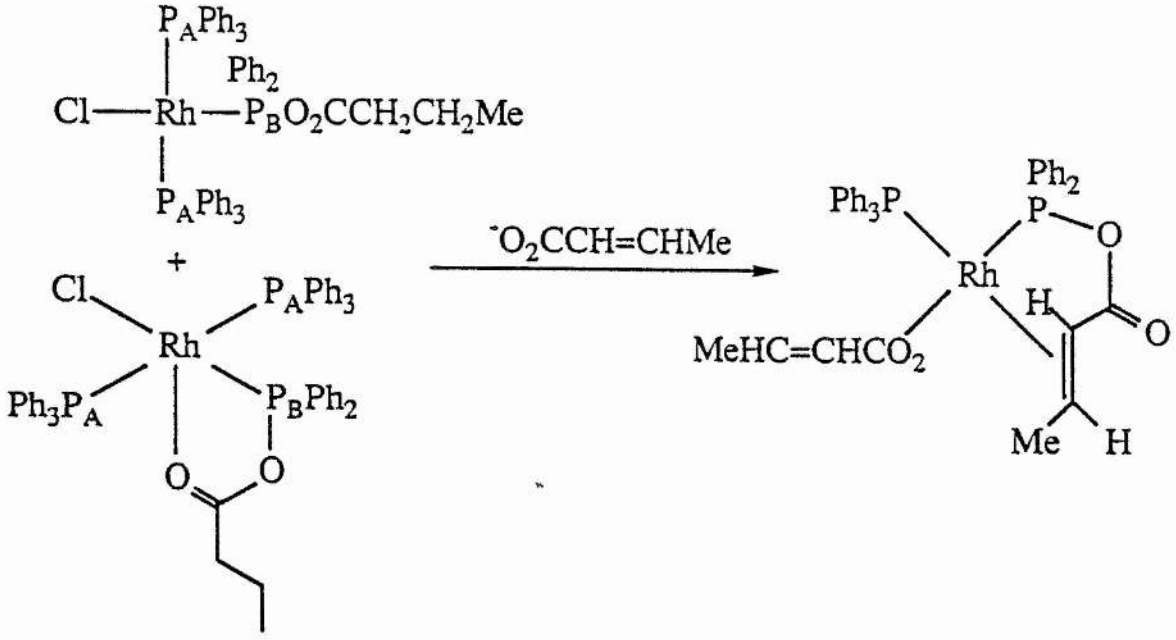

$[Rh(O_2CCH=CHMe)(PPh_3)(Ph_2PO_2CCH=CHMe)]$ is also the product when the cationic complex, $[Rh(PPh_3)_2(Ph_2PO_2CCH_2CH_2Me)]^+$ , reacts with excess but-2-enoate anions as illustrated in Figure 2.6.5.

Figure 2.6.5

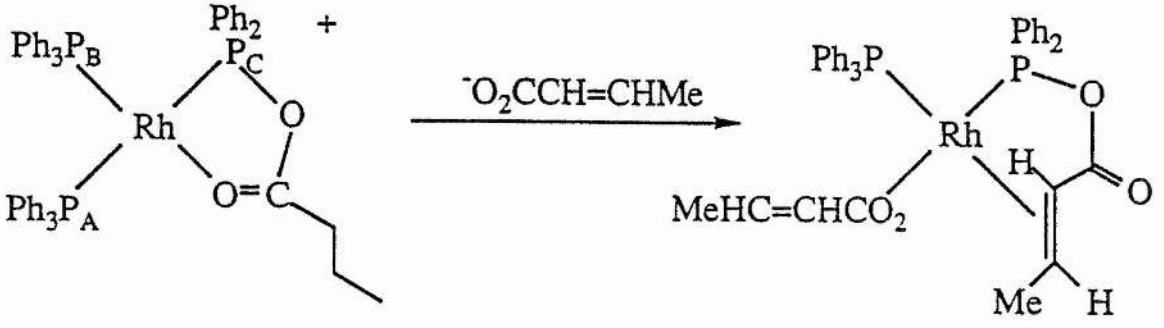


The ease with which $[Rh(O_2CCH=CHMe)(PPh_3)(Ph_2PO_2CCH=CHMe)]$ can be synthesized by a variety of routes is strong evidence for its role as the active species in the catalytic cycle concerned with the hydrogenation of but-2-enoic acid.

The transesterification reaction is rare, although a similar step has been invoked in the mechanism proposed for the deuteration of the ortho positions in phenol catalysed by $[RuH(C_6H_4OP(OPh)_2)(P(OPh)_3)]$[33]; however in this case the transesterification is of free $P(OPh)_3$ and is acid catalysed.

Table 2.6.1 $^{31}P$ NMR data for rhodium complexes measured in $CD_2Cl_2$ at 298K

| Complex | $\delta$ | | | J/Hz | | | | | |
|---|---|---|---|---|---|---|---|---|---|
| | $P_A$ | $P_B$ | $P_C$ | $RhP_A$ | $RhP_B$ | $RhP_C$ | $P_AP_B$ | $P_AP_C$ | $P_BP_C$ |
| Complex 1 form A | 31.8(dd) | 48.5(dt) | - | 142 | 190 | - | 38 | - | - |
| form B | 33.0(br) | 131.0(br) | - | - | - | - | - | - | - |
| Complex 1 form A[a] | 31.3(dd) | 47.8(dt) | - | 145 | 192 | - | 40 | - | - |
| form B[a] | 33.6(dd) | 131.7(dt) | - | 140 | 220 | - | 42 | - | - |
| Complex 2 | 26.3(dd) | 48.7(ddt) | 176.5(ddd) | 136 | 183 | 162 | 36 | 320 | 36 |

Complex 1 = $[RhCl(P_APh_3)_2(Ph_2P_BO_2CCH_2CH_2Me)]$

Complex 2 = $[Rh(PPh_3)_2(Ph_2PO_2CCH_2CH_2Me)]PF_6$[b]

[a] at 213K [b] For assignments see Figure 2.6.2

Table 2.6.2 $^1H$ NMR spectra ($\delta$) for rhodium complexes measured in $CD_2Cl_2$ at 298K

| | | Mixed anhydride ligand | | |
|---|---|---|---|---|
| Complex | | Me | $CH_2$ | |
| $[RhCl(PPh_3)_2(Ph_2PO_2CCH_2^cCH_2^bCH_3^a)]^x$ | Form B | $^a$0.6(t) | $^b$0.85(tq) | $^c$1.26(m) |
| $[RhCl(PPh_3)_2(Ph_2PO_2CCH_2^cCH_2^bCH_3^a)]PF^6$ | Form A | $^a$1.26(m) | $^b$1.60(tq) | $^c$2.27(t) |
| $[Rh(PPh_3)_2(Ph_2PO_2CCH_2^cCH_2^bCH_3^a)]PF_6$ | Form A | $^a$0.53(t) | $^b$0.98(tq) | $^c$2.26(t) |

$^x$ At 213K

## 2.7 The Synthesis, Reactions and Properties of $[Rh(O_2CCH_2CH_2Me)(PPh_3)_2$ $-(Ph_2PO_2CCH_2CH_2Me)]$.

Although the reactions considered in the previous section suggest that transesterification is a key step in the catalytic reaction, the most likely intermediate in the catalytic cycle is neither of those described, but rather $[Rh(O_2CCH_2CH_2Me)(PPh_3)_n(Ph_2PO_2CCH_2CH_2Me)]$ in which both the mixed anhydride and the coordinated anion have been hydrogenated.

The title complex, $[Rh(O_2CCH_2CH_2Me)(PPh_3)_2(Ph_2PO_2CCH_2CH_2Me)]$, has been prepared as yellow microcrystals from the reaction of $[RhCl(PPh_3)_2(Ph_2PO_2CCH_2CH_2CH_3)]$ with potassium butanoate in tetrahydrofuran, as illustrated in Figure 2.7.1. Infra-red studies indicate that the butanoate anion is bound through only one oxygen atom, the value of $\nu(C=O)$ being at 1546 $cm^{-1}$, which is comparable with the carboxylate complexes presented in Table 2.4.1. The mixed anhydride is bound only through the phosphorus atom with $\nu(C=O)$ at 1710$cm^{-1}$ which is similar a frequency to those observed for other complexes containing a monodentate mixed anhydride.

Figure 2.7.1

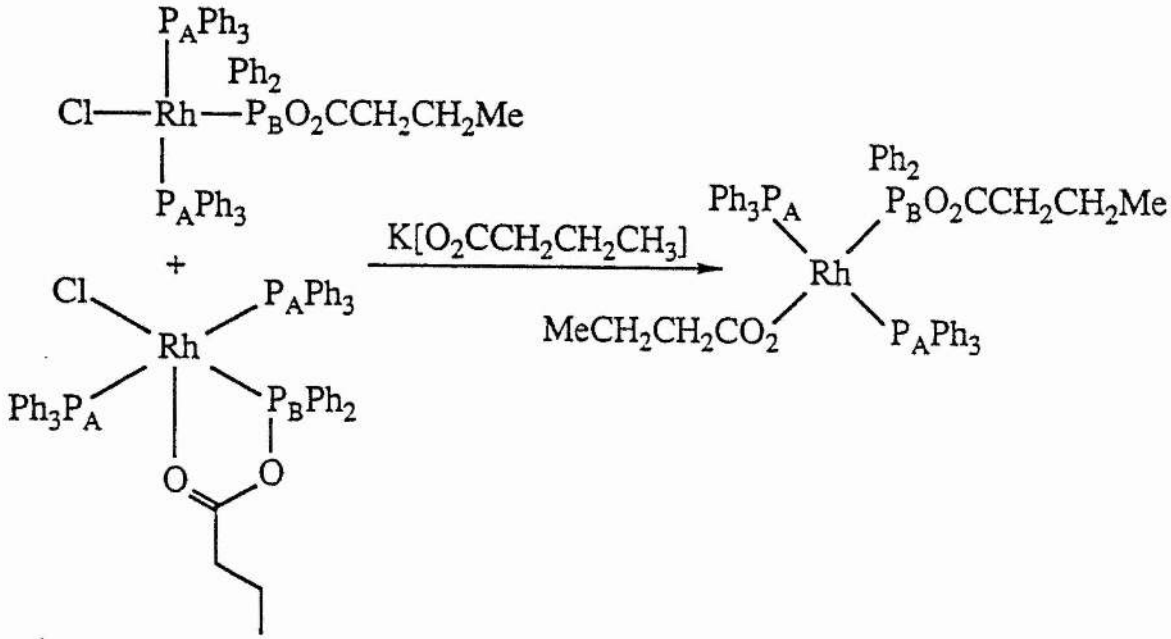


At room temperature the $^{31}P$ NMR spectrum consists of two very broad resonances at $\delta$33.6 and $\delta$51.6, as is shown in Spectrum 2.7.1. At -40°C the $^{31}P$ NMR, as presented in Spectrum 2.7.2, consists of a doublet of triplets at $\delta$51.5 and a doublet of doublets at $\delta$34.3. The value of the coupling constant $J_{RhP_B}$ is greater than that of $J_{RhP_A}$ (175.5Hz c.f. 152.3 Hz) due to the fact that $PPh_3$ exerts a greater trans influence than the butanoate anion. Consequentially the Rh-$P_B$ bond is stronger than the Rh-$P_A$ bond.

Spectrum 2.7.1 $^{31}P$ NMR of $[Rh(O_2CCH_2CH_2CH_3)(PPh_3)_2(Ph_2PO_2CCH_2CH_2CH_3)]$ in $CD_2Cl_2$ at 298K.

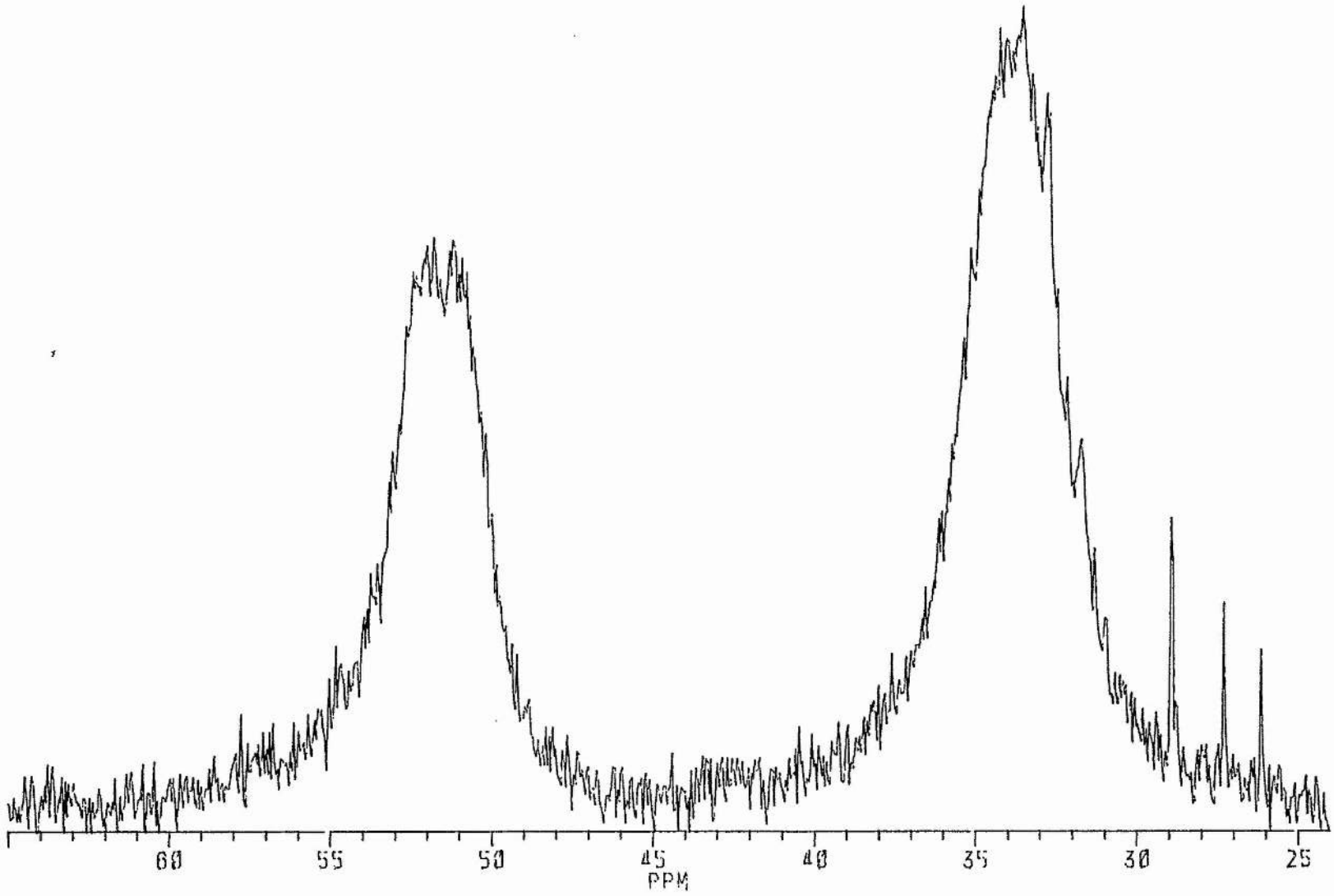

Spectrum 2.7.2 $^{31}P$ NMR of $[Rh(O_2CCH_2CH_2CH_3)(PPh_3)_2(Ph_2PO_2CCH_2CH_2CH_3)]$ in $CD_2Cl_2$ at 233K.

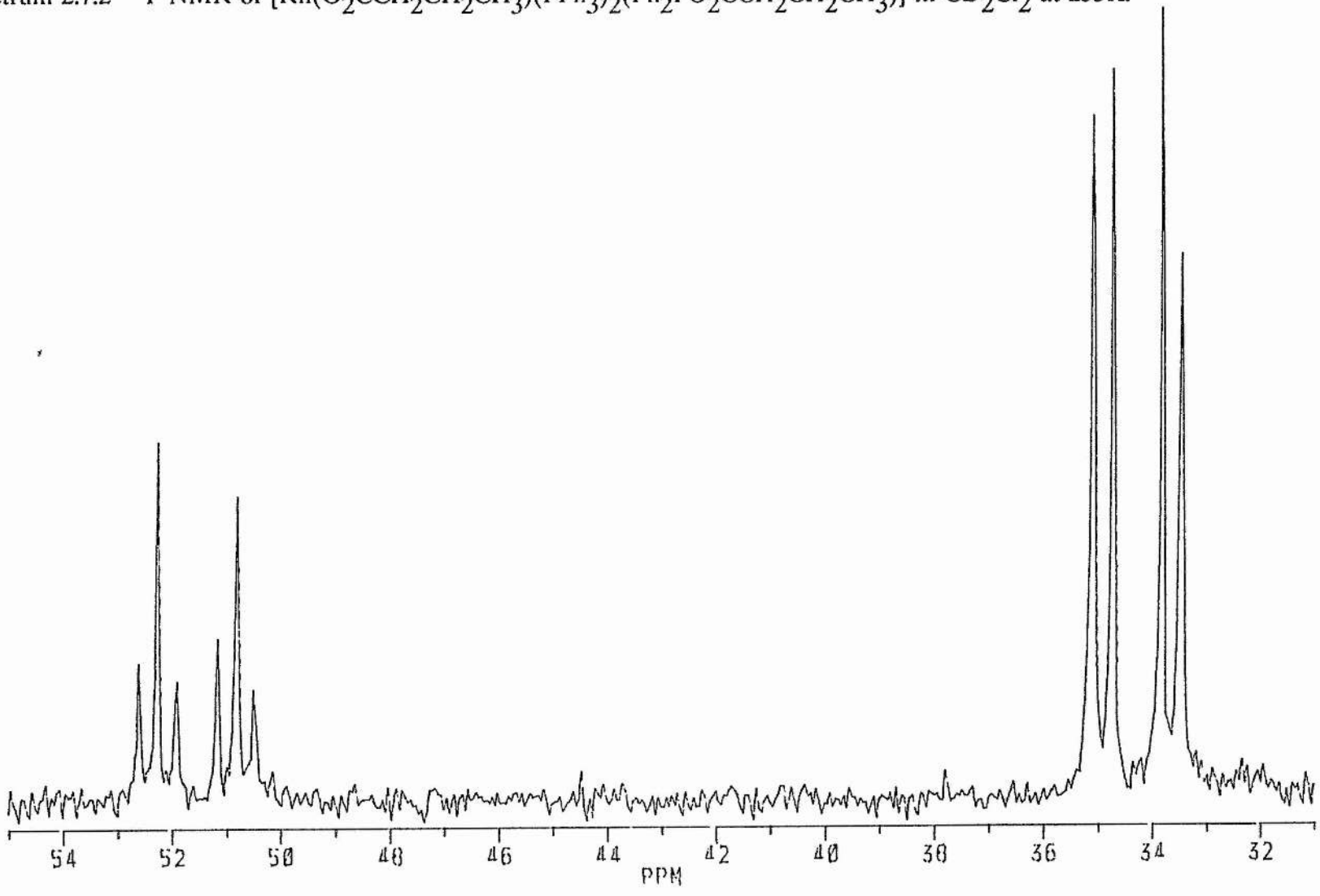

The room temperature $^{1}H$ NMR spectrum (see Spectrum 2.7.3) is like its $^{31}P$ counterpart in that the resonances are broad. Spectrum 2.7.4 however, shows that at -40°C the resonances associated with both the butanoate anionic ligand and the mixed anhydride ligand are clearly visible. The resonances attributed to the -$O_2CCH_2{}^{f}CH_2{}^{e}CH_3{}^{d}$ ligand ($^{d}$0.1(t),$^{e}$0.2(tq) and $^{f}$0.38(t)) are at considerably higher field than those attributed to the phosphorus bound ($Ph_2PO_2CCH_2{}^{c}CH_2{}^{b}CH_3{}^{a}$) ligand ($^{a}$0.97(t),$^{b}$1.68(tq),$^{c}$2.34(t)). It should be noted that no $^{1}H$ NMR data exists for rhodium-carboxylate complexes. Decoupling experiments at -40°C have shown the H environments to be assigned correctly. The unusually high field resonances of the butanoate ligand are presumably the result of significant interaction with the ring currents associated with the phenyl rings of triphenylphosphine. The data obtained from the room temperature and low temperature $^{31}P$ and $^{1}H$ NMR spectra are presented in Tables 2.7.1 and 2.7.2 respectively.

The broadness of the resonances in both the $^{31}P$ and $^{1}H$ NMR room temperature spectra are attributable to the complex [$Rh(O_2CCH_2CH_2CH_3)$-$(PPh_3)_2(Ph_2PO_2CCH_2CH_2CH_3)$] being a fluxional species. $^{31}P$ and $^{1}H$ NMR spectra at -40°C are entirely consistent with the complex having a square planar structure with the triphenylphosphine ligands mutually trans. On warming all of these signals broaden and eventually coalesce and, although the high temperature limiting spectrum has not been observed, it is clear that the two differing types of butanoate group are exchanging with one another. Spectrum 2.7.5 shows this effect; in the $^{1}H$ spectrum at -40°C the proton resonances are distinct whilst at -30°C those associated with the mixed anhydride become less distinct. On further warming to

0°C the resonances from both butanoate moieties become broad. At 35°C coalescence has occurred. The high-temperature limit $^1$H NMR spectrum would show three sharp resonances, because the ligand exchange would be much faster than the NMR timescale and only the averaged resonances would be seen.

The room temperature $^1$H NMR spectrum is found to be independent of concentration and thus the exchange between the two butanoate moieties must be intramolecular. The mechanism proposed for this intramolecular exchange is illustrated in Figure 2.7.2. It is proposed that the exchange occurs by nucleophilic attack of the carbonyl oxygen atom of the rhodium bound carboxylate ligand onto the phosphorus atom of the mixed anhydride in a 5- coordinate intermediate with the mixed anhydride bound through phosphorus and the oxygen atom. It is necessary to propose this intermediate in order for the phosphorus atom of the mixed anhydride and the rhodium bound butanoate to be able to be mutually cis. There is precedent for this since $[RhCl(PPh_3)_2(Ph_2PO_2CCH_2CH_2CH_3)]$ exists in two forms, one of which is a 5-coordinate, fluxional species with binding of the carbonyl oxygen of the mixed anhydride to rhodium as described in Section 2.6.

Spectrum 2.7.3 $^{1}H$ NMR of $[Rh(O_2CCH_2CH_2CH_3)(PPh_3)_2(Ph_2PO_2CCH_2CH_2CH_3)]$ in $CD_2Cl_2$ at 298K.

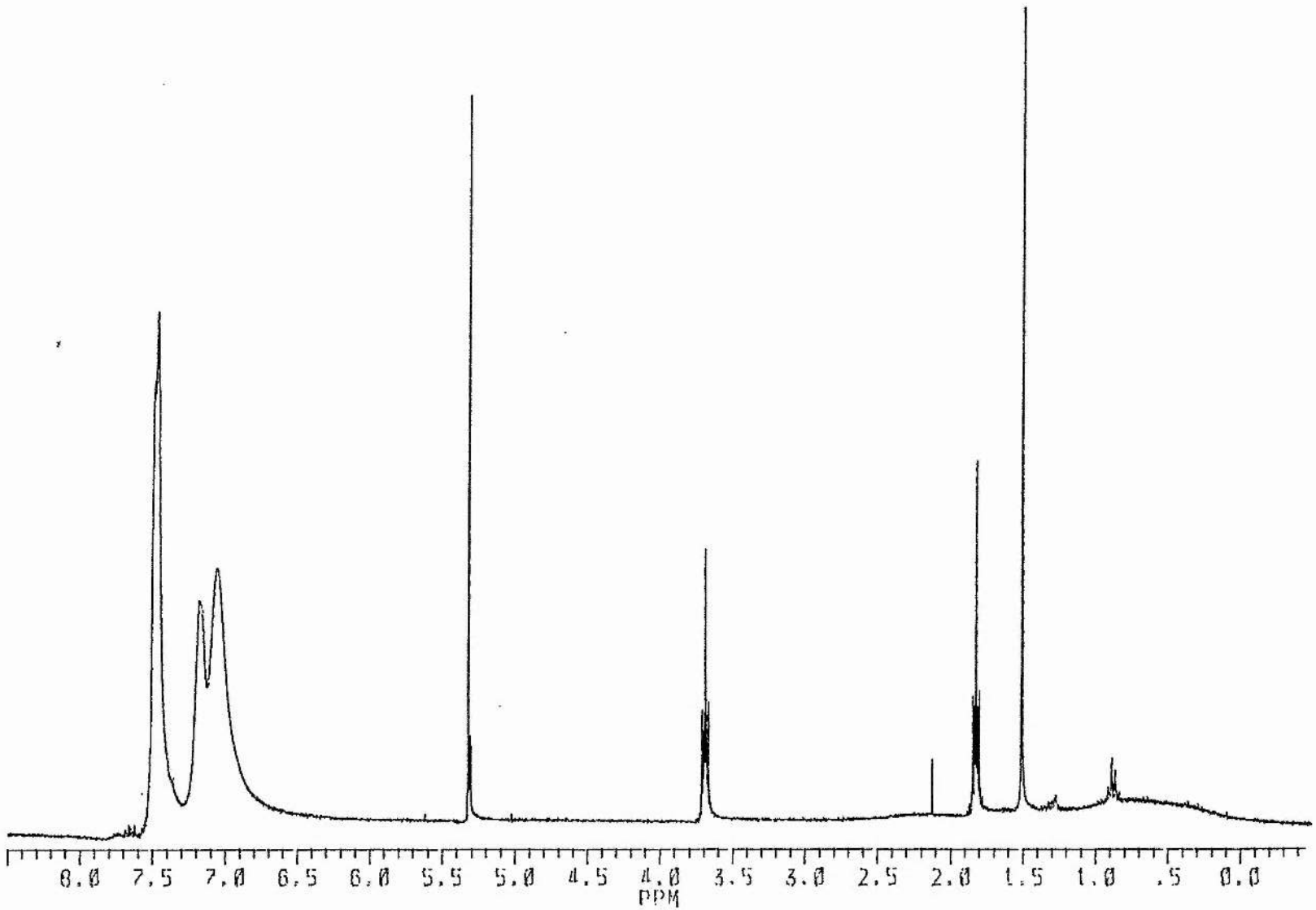

Spectrum 2.7.4 $^{1}H$ NMR of $[Rh(O_2CCH_2CH_2CH_3)(PPh_3)_2(Ph_2PO_2CCH_2CH_2CH_3)]$ in $CD_2Cl_2$ at 233K.

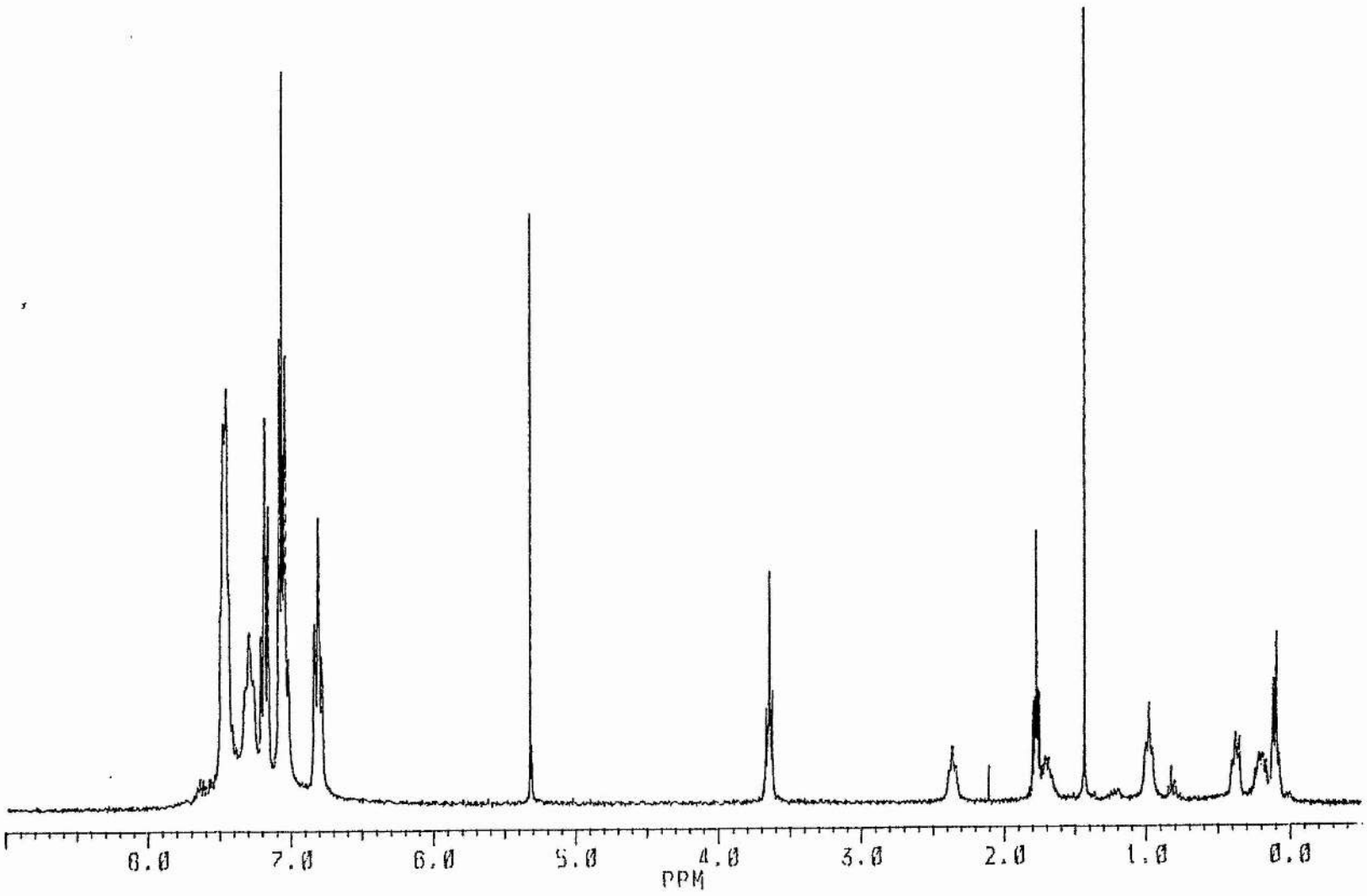

Spectrum 2.7.5 $^{1}H$ NMR of $[Rh(O_2CCH_2CH_2CH_3)(PPh_3)_2(Ph_2PO_2CCH_2CH_2CH_3)]$ in $CD_2Cl_2$ at 308K.

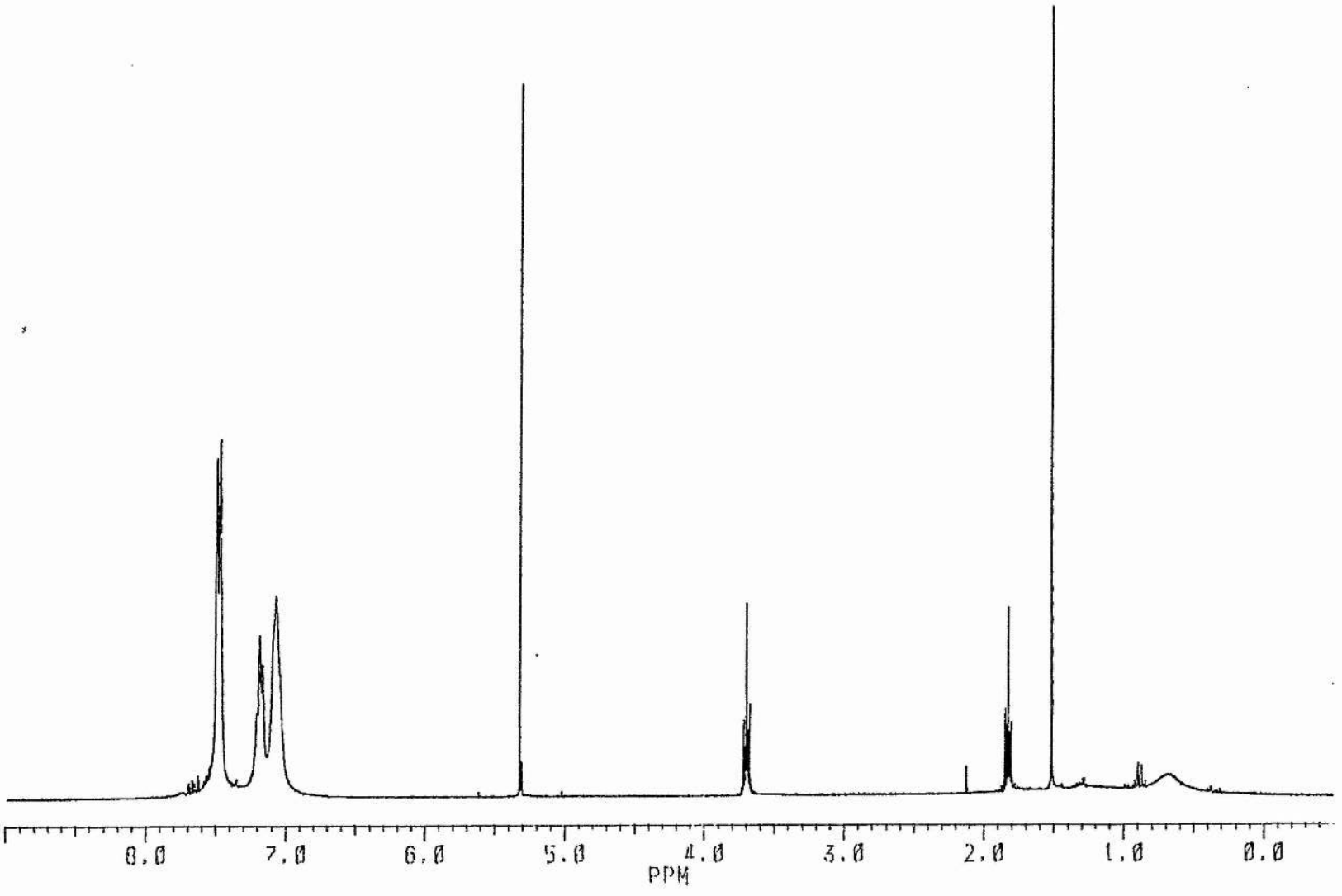

Figure 2.7.2

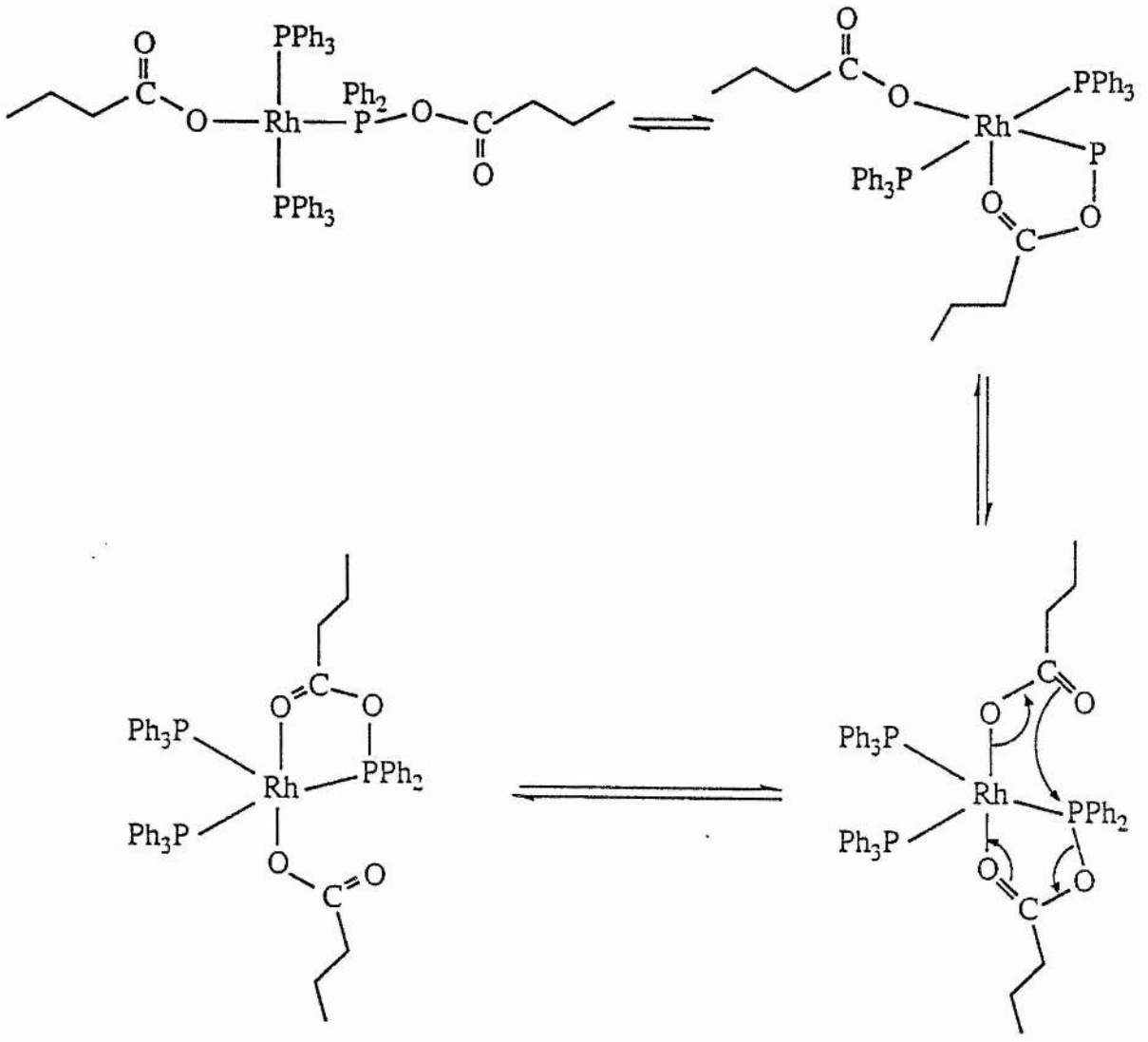

Phosphine adducts of nickel triad 1,1-dithiolates exhibit fluxionality in which mono and bidentate ligands on the same metal atom exchange with one another, as illustrated in Figure 2.7.3.[34]

Figure 2.7.3

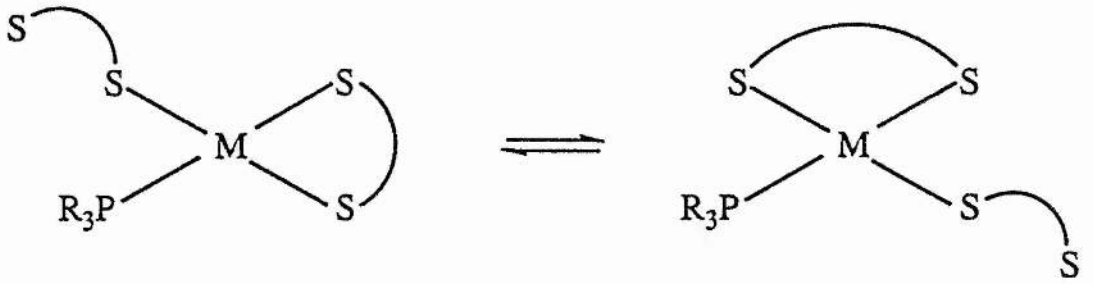


However, there appears to be no precedent for the type of exchange illustrated in Figure 2.7.2, in which a ligand bound to a metal centre exchanges with the same anion bound to phosphorus.

This type of fluxionality then poses new questions concerning the mechanism of the transesterification reaction. For example, does the transesterification take place directly on the coordinated P atom via attack from the external nucleophilic anion or does it occur by intramolecular nucleophilic displacement of the hydrogenated substrate? (See Figure 2.7.4). In both cases there is likely to be a strong thermodynamic driving force for the introduction of new substrate since the substrate will bind strongly in a bidentate fashion, releasing $PPh_3$ if more than one $PPh_3$ molecule is present in the complex and cause a large positive change in entropy of the system.

Figure 2.7.4

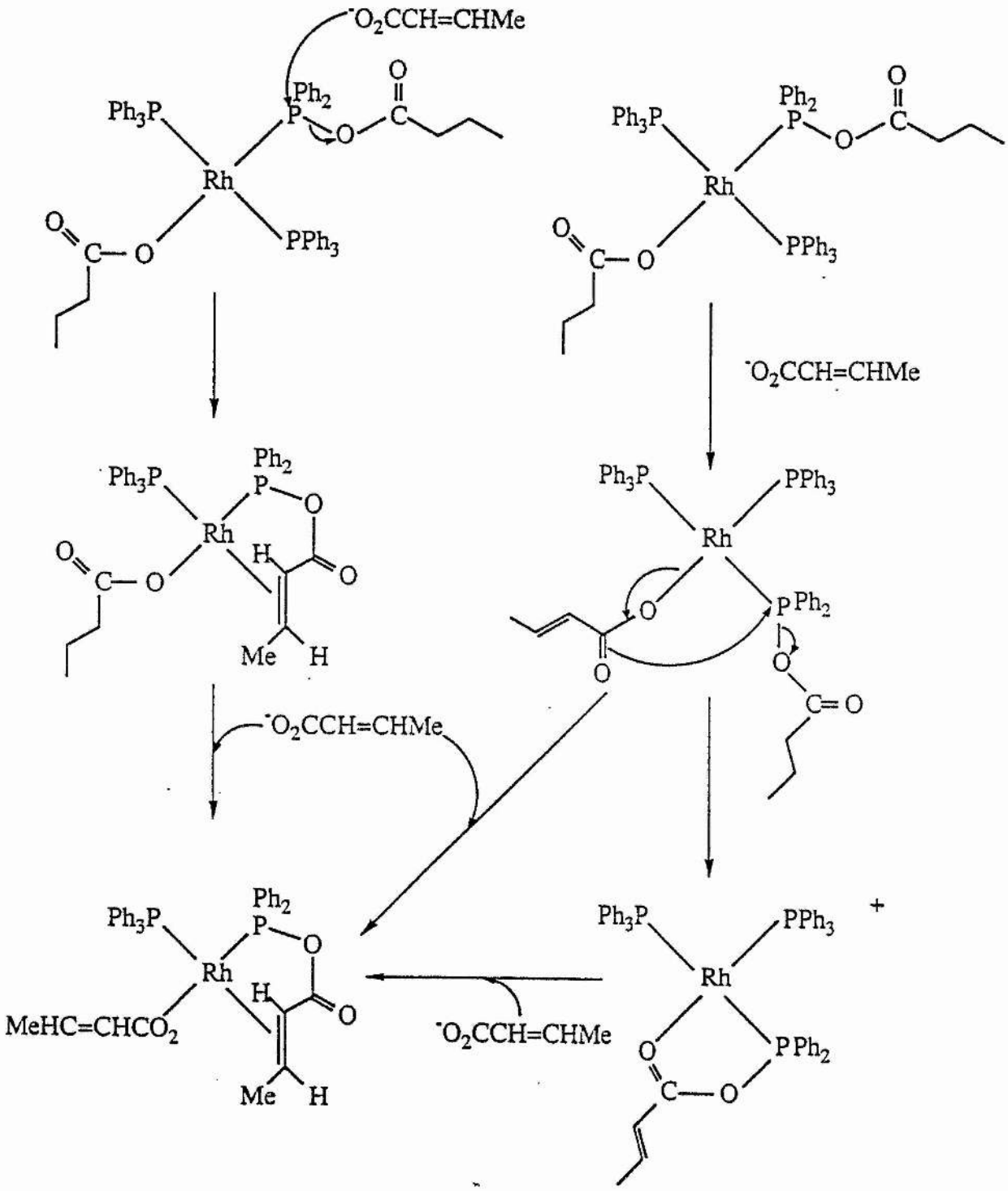
$^{-}O_2CCH=CHMe$
$Ph_3P$
$Ph_2$
P
O
C
Rh
$PPh_3$
$^{-}O_2CCH=CHMe$
H
Me
$PPh_2$
C= O
+
$MeHC=CHCO_2$

In order to try to examine which of the two routes shown in Figure 2.7.4 operates, $[Rh(O_2CCH_2CH_2Me)(PPh_3)_2(Ph_2PO_2CCH_2CH_2Me)]$ has been reacted with $[HO_2CCH=CHMe]$ in the presence of triethylamine in an NMR tube. The product is $[Rh(O_2CCH=CHMe)(PPh_3)_2(Ph_2PO_2CCH_2CH_2Me)]$ as illustrated in Figure 2.7.5. Both the mixed anhydride and the but-2-enoate ligands are monodentate and, as in the case of $[Rh(O_2CCH_2CH_2Me)(PPh_3)_2(Ph_2PO_2CCH_2CH_2Me)]$ the complex is fluxional at room temperature.

Figure 2.7.5

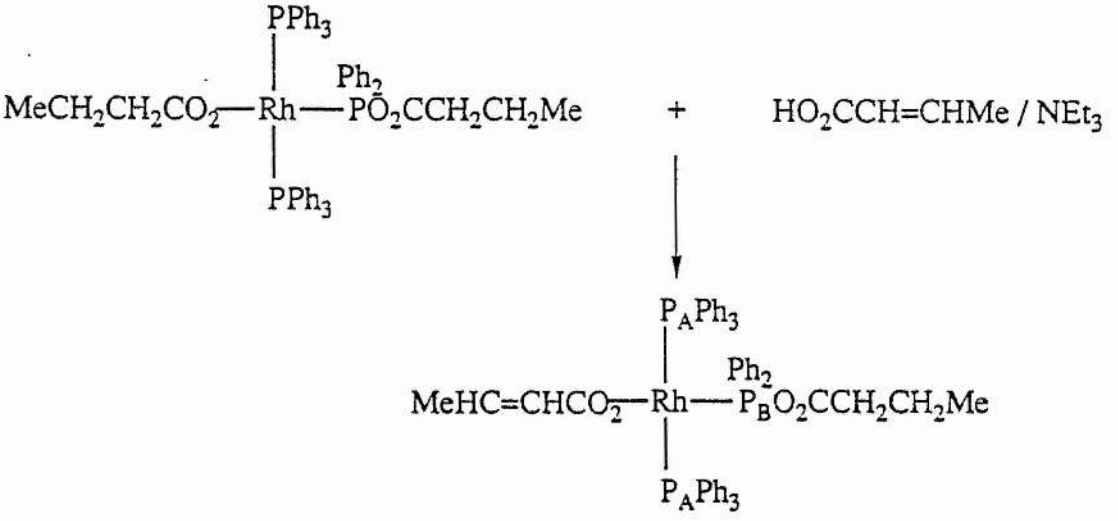


The low temperature $^{31}P$ NMR spectrum (Spectrum 2.7.6) shows the resonance associated with the anhydride, $P_B$, at a shift of $\delta$50.8 and that of coordinated triphenylphosphine, $P_A$, at $\delta$33.7. The low temperature $^1H$ NMR (Spectrum 2.7.7) provides further evidence for the structure of the product shown in Figure 2.7.5, where the resonances attributed to the mixed anhydride ligand, $(Ph_2PO_2CCH_2{}^cCH_2{}^bCH_3{}^a)$ ($^a$0.83(t),$^b$1.52(tq),$^c$2.15(t)), are at similar shifts to those observed for the same mixed anhydride ligand in

$[Rh(O_2CCH_2CH_2CH_3)(PPh_3)_2(Ph_2PO_2CCH_2CH_2CH_3)]$. The resonances attributed to the but-2-enoate ligand, $(O_2CCH^f=CH^eMe^d)$ ($^d$1.05(d),$^e$4.85(m),$^f$4.53(br d)), are at significantly lower shifts than those observed in $[Rh(O_2CCH^f=CH^eMe^d)(PPh_3)(Ph_2PO_2CCH=CHMe)]$ ($^d$1.58(d),$^e$6.27(m),$^f$5.20(br d), due to the presence of two triphenylphosphine ligands. $^{31}P$ and $^1H$ NMR spectral data are presented in Tables 2.7.1 and 2.7.2 respectively.

This reaction clearly shows that the metal bound anion is more easily exchanged than that bound to the phosphorus atom of the mixed anhydride, but surprisingly there is no evidence that the metal bound $(O_2CCH=CHMe)^-$ ligand displaces the $-O_2CCH_2CH_2Me$ group from the mixed anhydride nor that this $-O_2CCH_2CH_2Me$ group is displaced by excess external $[O_2CCH=CHMe]^-$.

One possible explanation of these results is that the catalytic cycle occurs only via hydrogenation of the metal bound anion and that the mixed anhydride, probably in its reduced form, is an innocent spectator ligand. However, the results of catalytic reactions tend not to favour this explanation. Thus, a catalytic mechanism that involves hydrogenation of a metal bound acrylic acid anion should also be operative using Wilkinson's catalyst. Since Wilkinson's catalyst is a better hydrogenation catalyst for hex-l-ene than the mixed anhydride complexes, it seems likely that it should also be a better catalyst for the hydrogenation of acrylic acids via the mechanism of Scheme 2.7.1. However, all of the acrylic acids that have been studied are hydrogenated more rapidly by the mixed anhydride complexes than by

Wilkinson's catalyst. Furthermore, the selectivity of hydrogenation of hexa-2,4-dienoic acid (see Section 2.8) strongly suggests that a different mechanism operates when Wilkinson's catalyst is the precursor, from that which operates when using the mixed anhydride catalyst precursors.

Scheme 2.7.1

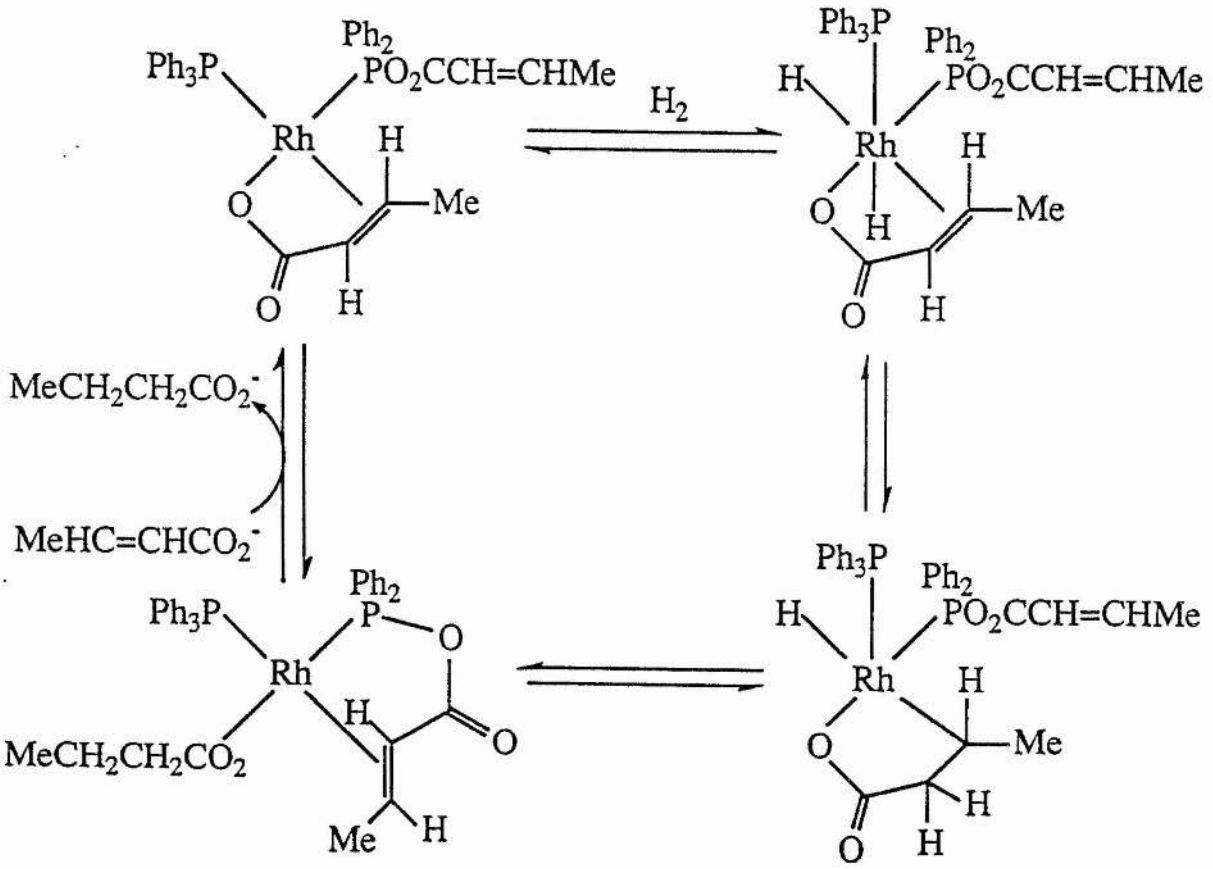

Spectrum 2.7.6 $^{31}P$ NMR of $[Rh(O_2CCH=CHMe)(PPh_3)_2(Ph_2PO_2CCH_2CH_2CH_3)]$ in $CD_2Cl_2$ at 233K.

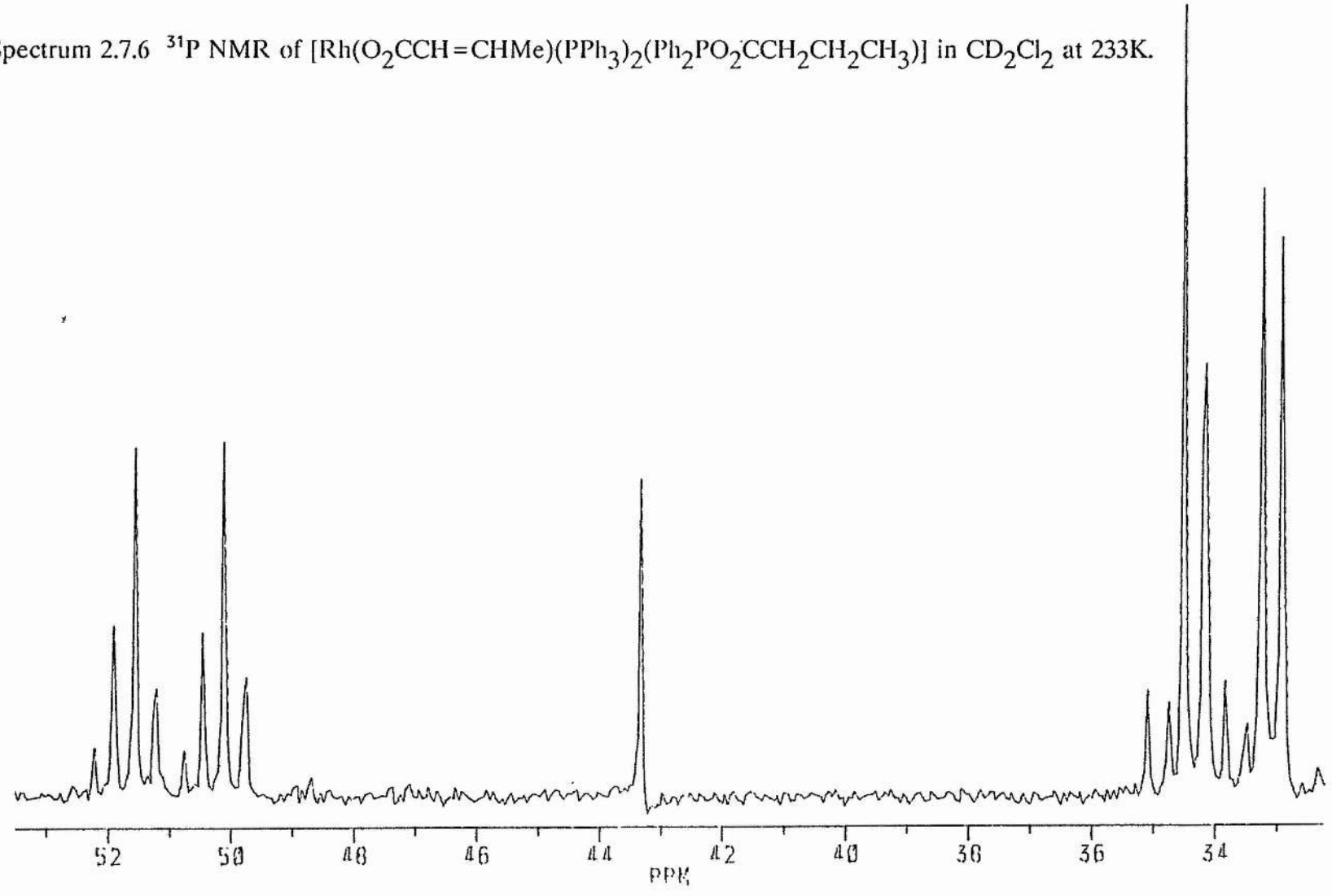

Spectrum 2.7.7 $^{1}H$ NMR of $[Rh(O_2CCH=CHMe)(PPh_3)_2(Ph_2PO_2CCH_2CH_2CH_3)]$ in $CD_2Cl_2$ at 233K.

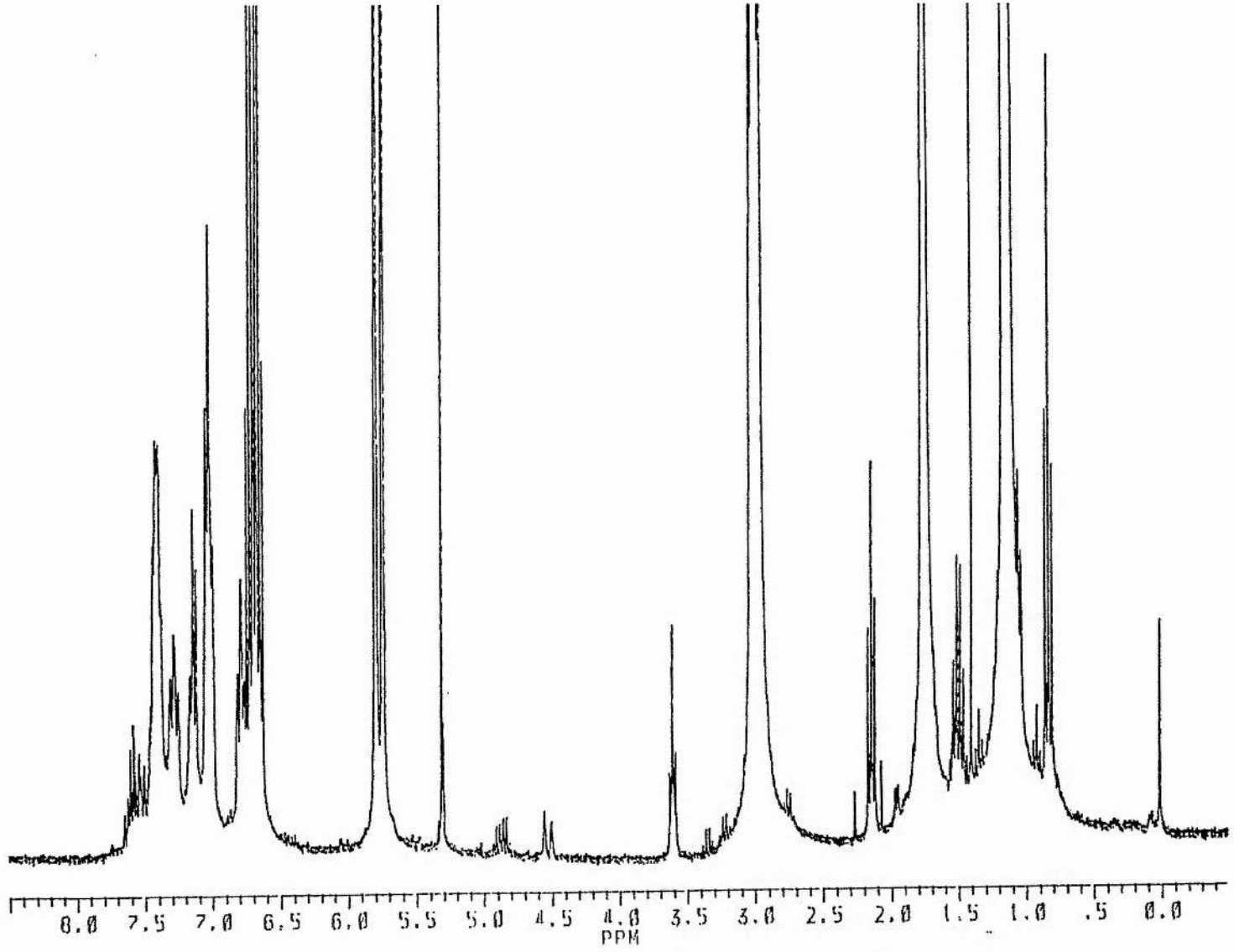

Considering the various reactions of the butanoate complexes together, it appears that $-O_2CCH_2CH_2Me$ can be displaced by $[O_2CCH=CHMe]^-$ from the mixed anhydride in $[RhX(PPh_3)_2(Ph_2PO_2CCH_2CH_2Me)]$ for X = Cl, but not for X = $O_2CCH_2CH_2Me$ or $O_2CCH=CHMe$. This must also mean that for X = Cl, transesterification is not via the metal but from an external nucleophile. Clearly subtle steric and/or electronic effects operate in these systems and, since the catalytic cycle appears to operate effectively with only one mole of triphenylphosphine per rhodium it may be that the key intermediate from which product is lost is $[Rh(O_2CCH_2CH_2Me)(PPh_3)(Ph_2PO_2CCH_2CH_2Me)]$ and, since this complex has not been synthesized it is difficult to predict whether or not transesterification would occur. There is, however, some evidence that transesterification can occur in complexes of this type. This has been obtained from the reaction of $[Rh(O_2CCMe=CHPh)(PPh_3)(Ph_2PO_2CCMe=CHPh)]$ and $[HO_2CCH=CHMe]$ in the presence of triethylamine. As illustrated in Figure 2.7.6 the product obtained is $[Rh(O_2CCH=CHMe)(PPh_3)(Ph_2PO_2CCH=CHMe)]$, which is fully characterised in Section 2.4.

Figure 2.7.6

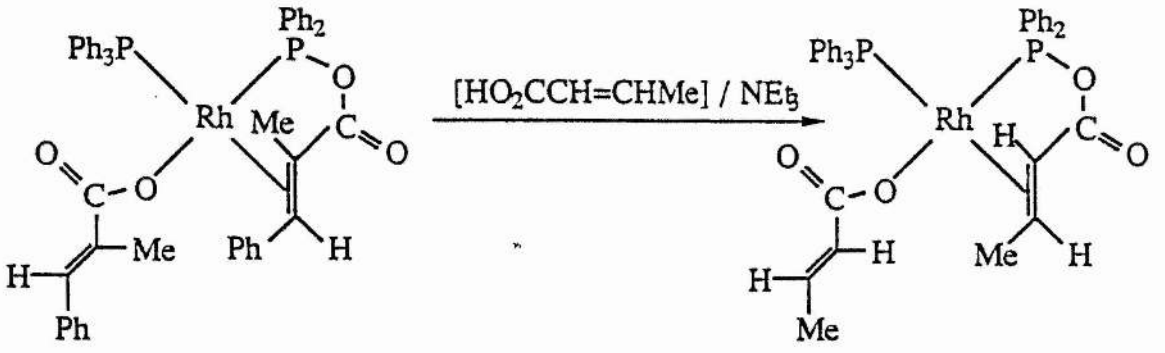

Both the 2-methyl-3-phenylpropenoate and the 2-methyl-3-phenyl-propenoate derived mixed anhydride ligands are replaced by but-2-enoate anions.

Furthermore transesterifications do occur in the reactions of $[RhCl(PPh_3)_n(Ph_2PO_2CCR=CR'R'')]$ and acrylic acid anions, as discussed in Section 2.5. Of particular significance in this context are reactions in which the incoming acrylate anion displaces the acrylate anion from the mixed anhydride onto the metal. (See Figure 2.7.7).

These reactions were all carried out in the presence of an excess of the attacking anion (up to 15 fold) and in the initial stages at least, some of the acrylate anion displaced from the mixed anhydride ($>> 1/15$) remains in the coordination sphere of the metal.

Figure 2.7.7

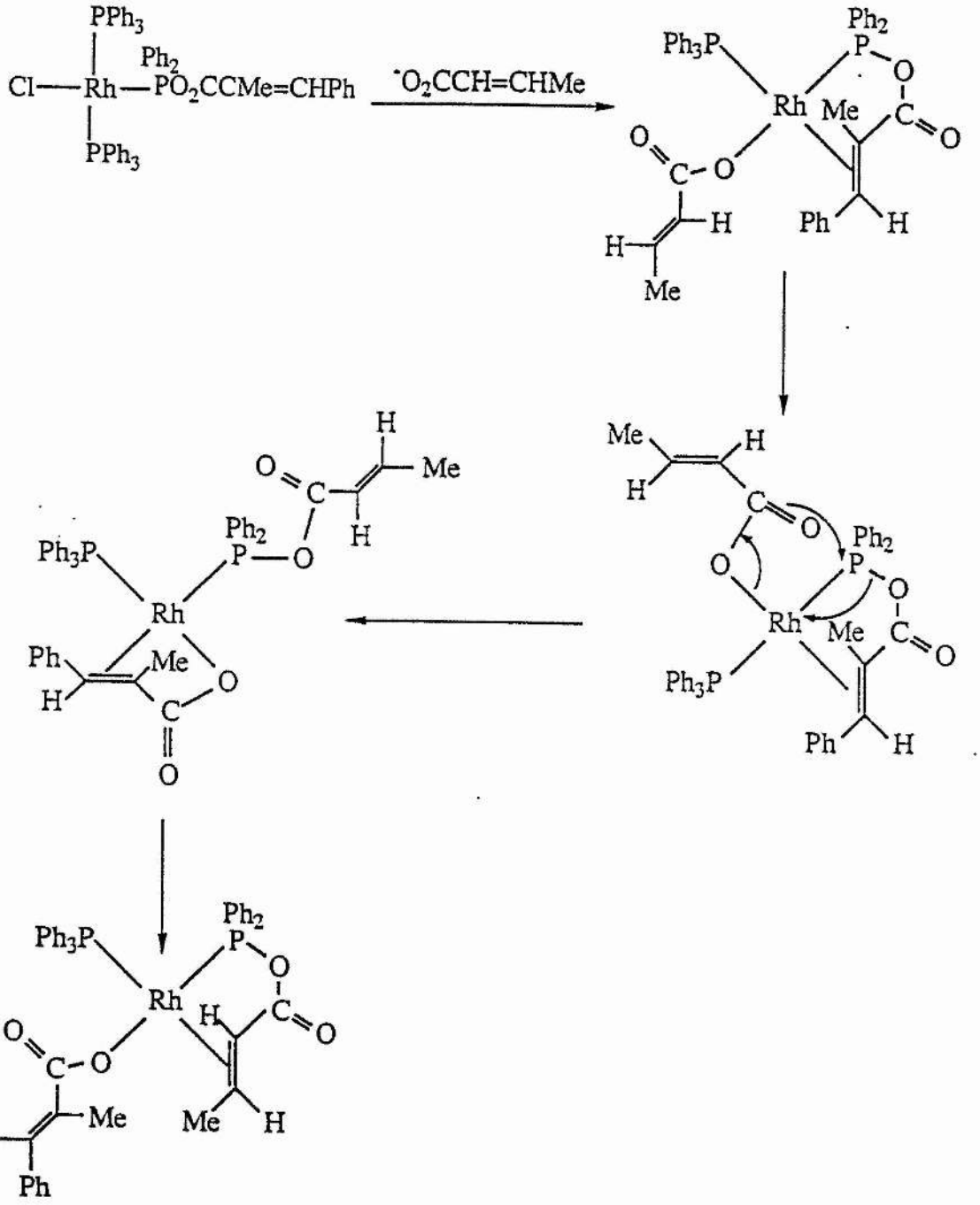

Since there is unlikely to be a marked preference for the more sterically demanding

anion (i.e. that which has been displaced) to bind to the rhodium centre, it is difficult to see why it should be retained so readily in the coordination sphere unless it never becomes free of the complex, but rather is displaced by an intra-molecular transesterification reaction after metathesis of the chloride ion. The reaction between $[RhCl(PPh_3)_2(Ph_2PO_2CCH=CMe_2)]$ and excess $[KO_2CCH=CHMe]$ (Section 2.5) gave both $[Rh(O_2CCH=CMe_2)(PPh_3)(Ph_2PO_2CCH=CHMe)]$ and $[Rh(O_2CCH=CHMe)(PPh_3)(Ph_2PO_2CCH=CHMe)]$ as the products. Similarly both products are produced from the reaction between $[RhCl(PPh_3)_2(Ph_2PO_2CCH=CMe_2)]$ and $[HO_2CCH=CHMe]$ in the presence of triethylamine. This observation indicates that the continued presence of the acrylate anion, displaced from the mixed anhydride, in the coordination sphere of the metal is not solely due to the lower solubility of the incoming potassium species.

Table 2.7.1 $^{31}P$ NMR data for rhodium complexes measured in $CD_2Cl_2$ at 298K.

| | $\delta$ | | J/Hz | | |
|---|---|---|---|---|---|
| | $P_A$ | $P_B$ | Rh-$P_A$ | Rh-$P_B$ | $P_A$-$P_B$ |
| $[Rh(O_2CCH_2CH_2Me)(P_APh_3)_2(Ph_2P_BO_2CCH_2CH_2Me)]$ | 33.6(br) | 51.6(br) | - | - | - |
| $[Rh(O_2CCH_2\dot{C}H_2Me)(P_APh_3)_2(Ph_2P_BO_2CCH_2CH_2Me)]$[a] | 34.3(dd) | 51.5(dt) | 152.3 | 175.5 | 40.2 |
| $[Rh(O_2CCH=CHMe)(P_APPh_3)_2(Ph_2P_BO_2CCH_2CH_2Me)]$[a] | 33.7(dd) | 50.8(dt) | 150.5 | 177.0 | 41.0 |

[a] at 233K

Table 2.7.2 $^{1}H$ NMR data for rhodium complexes measured in $CD_2Cl_2$ at 233K.

| | Mixed anhydride ligand | Carboxylate ligand |
|---|---|---|
| $[Rh(O_2CCH_2{}^{f}CH_2{}^{e}Me^{d})(PPh_3)_2(Ph_2PO_2CCH_2{}^{c}CH_2{}^{b}Me^{a})]$ | $^{a}0.97(t)$, $^{b}1.68(tq)$, $^{c}2.34(t)$ | $^{d}0.1(t)$, $^{e}0.2(tq)$, $^{f}0.38(t)$ |
| $[Rh(O_2CCH^{f}{=}CH^{e}Me^{d})(PPh_3)_2(Ph_2PO_2CCH_2{}^{c}CH_2{}^{b}Me^{a})]$ | $^{a}0.83(t)$, $^{b}1.52(tq)$, $^{c}2.15(t)$ | $^{d}1.05(d)$, $^{e}4.85(m)$, $^{f}4.53(br\ d)$ |

## 2.8 Proposed Mechanisms for the Regioselective Hydrogenation of Acrylic Acids Catalysed by Rhodium Mixed Anhydride Precursors.

The stoichiometric reactions described in Sections 2.4, 2.5, 2.6 and 2.7 lead to the proposed mechanisms illustrated in Scheme 2.8.1 for the hydrogenation of acrylic acids under basic conditions catalysed by rhodium complexes containing ligands which are mixed anhydrides of diphenylphosphinous acids with acrylic acids. The nature of the active species has been identified unequivocally as $[Rh(O_2CCR=CR'R'')(PPh_3)(Ph_2PO_2CCR=CR'R'')]$ with R, R' and R'' arising from the substrate acrylic acid, not necessarily from the catalyst precursor. These compounds react with $H_2$ to hydrogenate both carbon-carbon double bonds with similar rates, hence the two pathways shown in Scheme 2.8.1. Evidence for this is provided by the reaction of $[Rh(O_2CCH=CHMe)(PPh_3)(Ph_2PO_2CCH=CHMe)]$ with hydrogen (25°C, 3 atm and 2h) in $CD_2Cl_2$. There is a colour change from yellow to orange and the $^1H$ NMR spectrum shows signals in the aliphatic region from $-O_2CCH_2^cCH_2^bMe^a$ ($^a$0.97(t),$^b$1.61(tq),$^c$2.29(t)). Although a rhodium hydride complex has not been isolated, it is clear that both the double bond of the mixed anhydride and that of the coordinated anion are hydrogenated.

The other catalytic step, which has been demonstrated is the expulsion of the hydrogenated product and reintroduction of the substrate via a base-catalysed transesterification at both the coordinated phosphorus atom and the rhodium metal centre.

Scheme 2.8.1

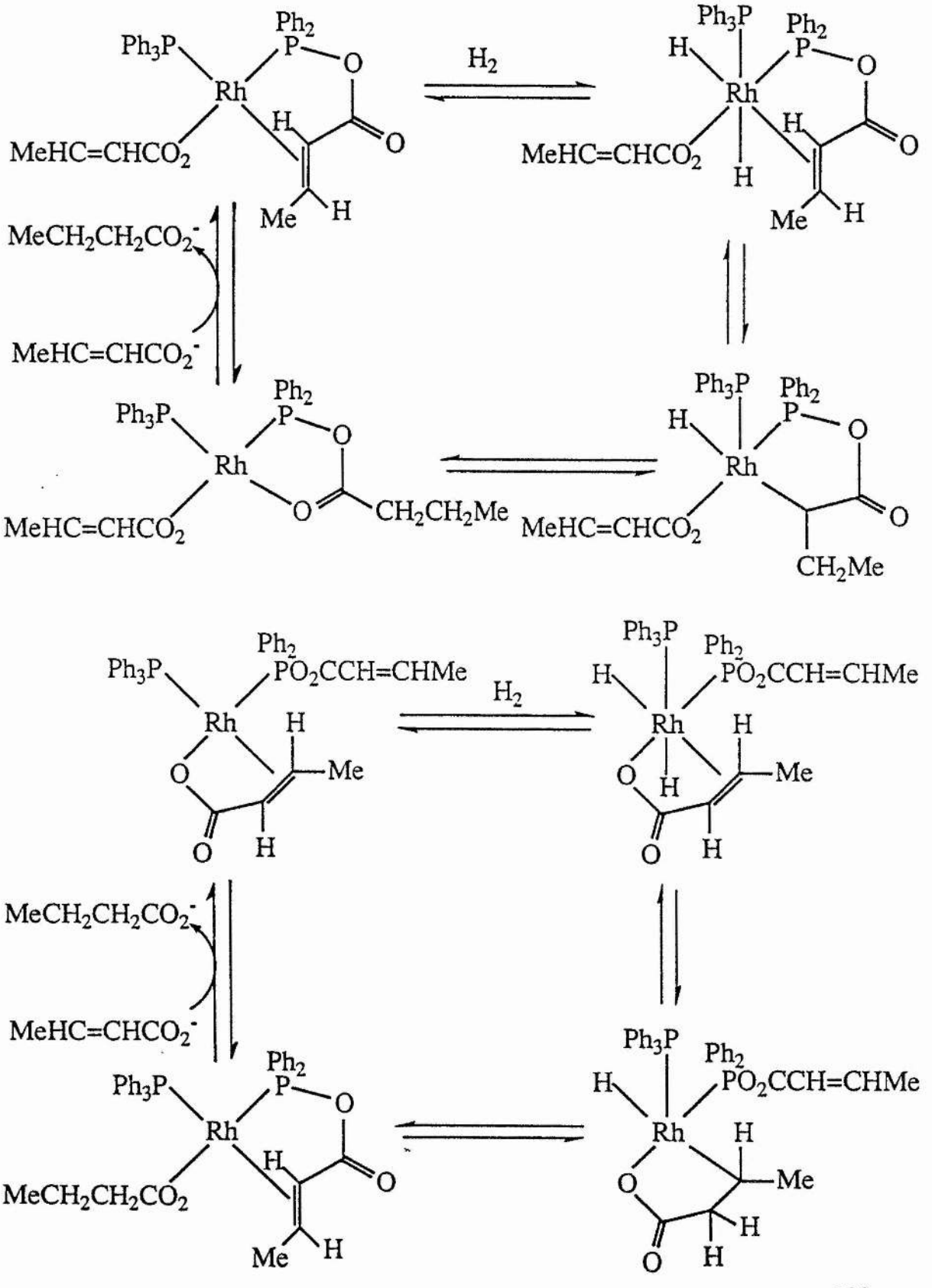
Ph3P
Ph2
P
O
Rh
H
MeHC=CHCO2
Me
H2
MeCH2CH2CO2-
MeHC=CHCO2-
CH2CH2Me
CH2Me
PO2CCH=CHMe

As mentioned in Section 2.3 an indication that different mechanisms operate for the rhodium-mixed anhydride catalyst precursors than for Wilkinson's catalyst comes from the observation that the products obtained from the hydrogenation of hexa-2,4 dienoic acid using the two types of catalyst are different. Wilkinson's catalyst gives hexanoic acid with traces of hex-2-enoic acid, whilst under similar conditions, at least at short reaction times, the mixed anhydride containing catalyst precursors give a mixture of hex-4-enoic and hexanoic acids.

Schemes 2.8.2 and 2.8.3 illustrate the hydrogenation of hexa-2,4-dienoic acid under basic conditions, catalysed by rhodium-mixed anhydride catalyst precursors. The composition of the active species has been identified as $[Rh(O_2CCH=CH-CH=CHMe)(PPh_3)(Ph_2PO_2CCH=CH-CH=CHMe)]$, whereas in the case of but-2-enoic acid, as illustrated in Scheme 2.8.1, the active species is $[Rh(O_2CCH=CHMe)(PPh_3)(Ph_2PO_2CCH=CHMe)]$.

Scheme 2.8.2

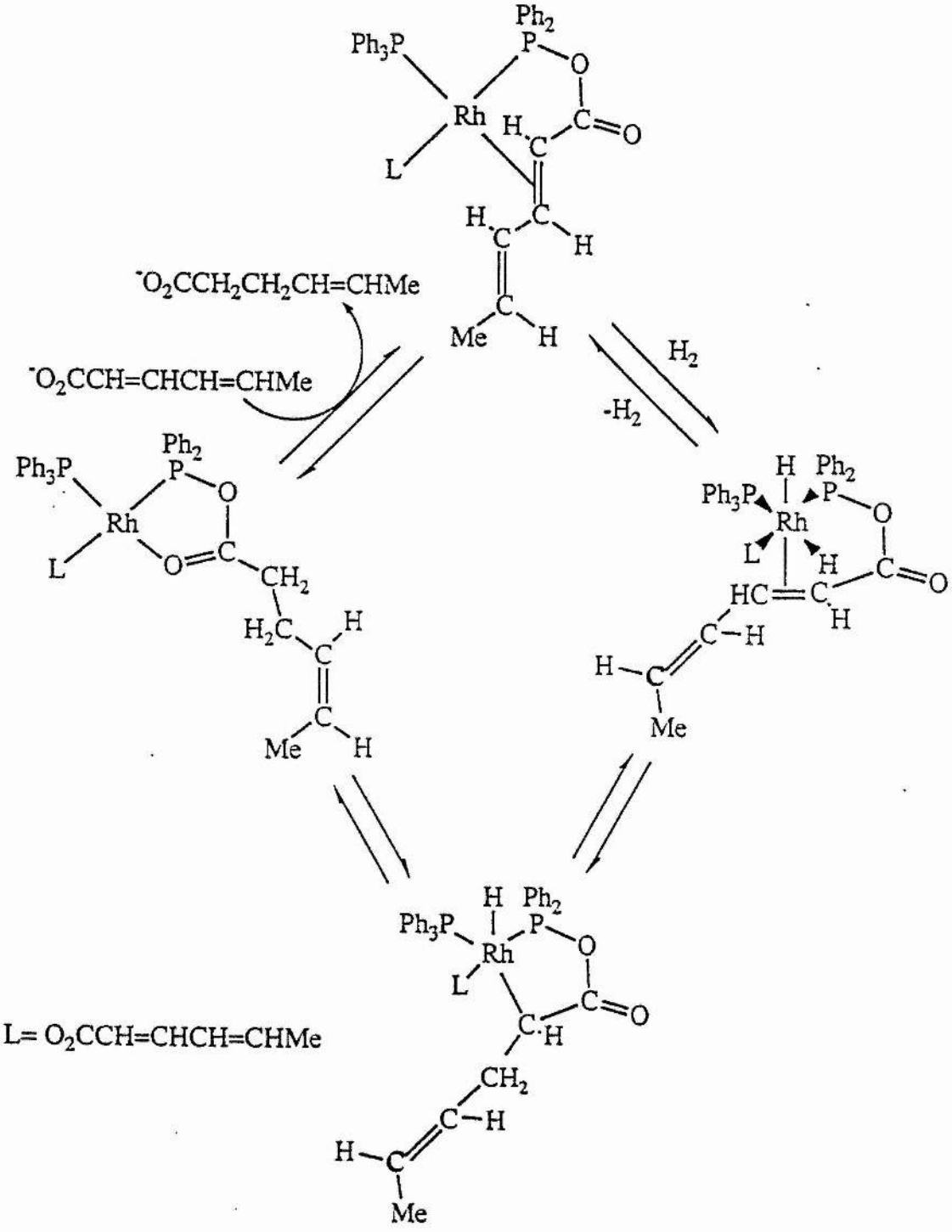


L= $O_2CCH=CHCH=CHMe$

Scheme 2.8.3

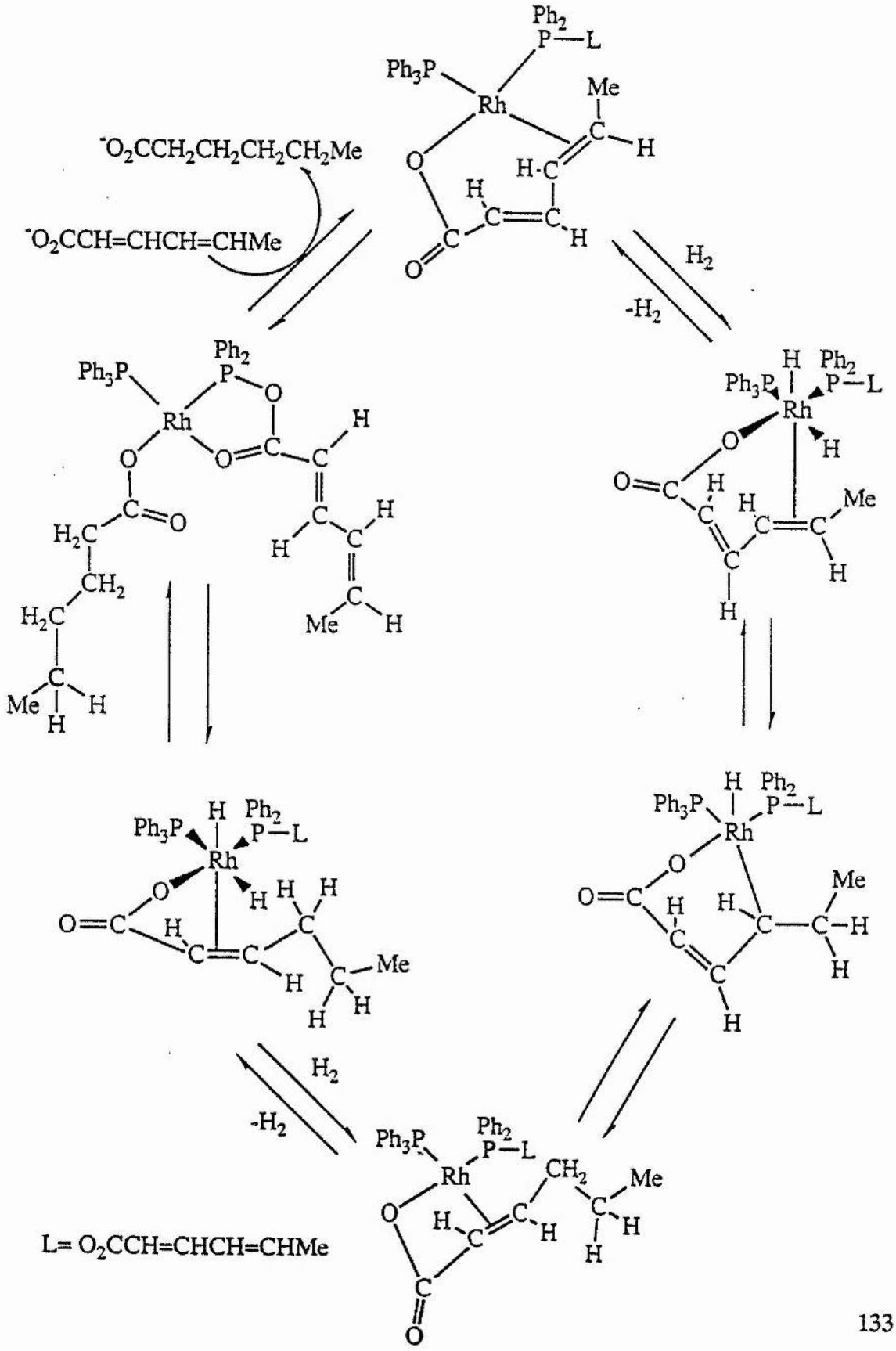

The selectivity in the hydrogenation of hexa-2,4-dienoic acid is of particular interest since these mixed anhydride catalysts offer the possibility of selectively removing a double bond which is conjugated with two other double bonds. It is proposed that this selectivity occurs because the mixed anhydride binds preferentially through phosphorus and the $C^2$ double bond as illustrated in Figure 2.8.1.

Figure 2.8.1

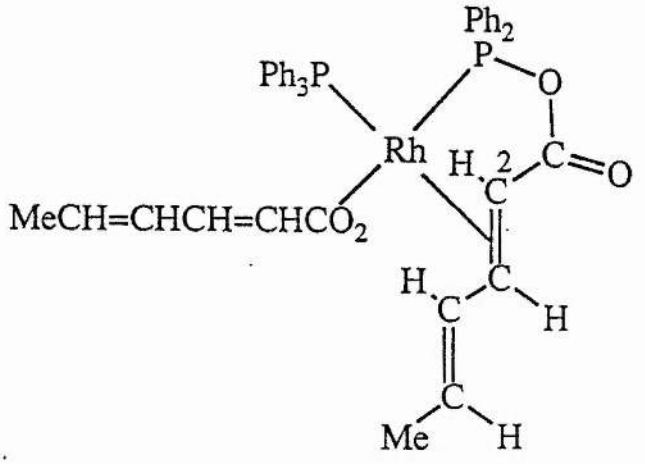


Indeed this binding has been crystallographically demonstrated in the complex $[\{RhCl(Ph_2PO_2CCH=CHCH=CHMe)\}_2]$.[2]

Unfortunately, the observed selectivity for the hydrogenation of hexa-2,4-dienoic acid is not very high since hexanoic acid is formed at a similar rate to hex-4-enoic acid. These reactions evidently proceed in parallel according to the mechanisms shown in Schemes 2.8.2 and 2.8.3 since hex-4-enoic acid is not readily hydrogenated in this system.[4]

Since $[RhCl(PPh_3)_3]$ produces largely hexanoic acid under similar conditions, it

seems that this product probably arises from hydrogenation of the hexa-2,4-dienoate ligand bound directly to the rhodium (Scheme 2.8.3). In this case, having one less atom in the ring formed on double bond co-ordination will lead to a lesser preference for binding of the $C^2$ double bond and probably will favour binding of the $C^4$ double bond, as illustrated in Figure 2.8.2 and Scheme 2.8.3.

Figure 2.8.2

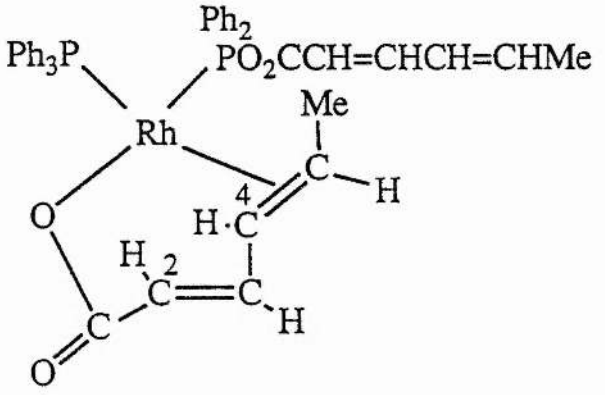


Thus on hydrogenation, hex-2-enoic acid is initially produced and subsequently complete hydrogenation occurs to give hexanoic acid.

The failure to observe hex-2-enoic acid as an intermediate when mixed anhydride complexes are employed as catalysts presumably arises because any hex-2-enoic acid formed will readily be introduced into the mixed anhydride and hydrogenated according to the mechanism illustrated in Scheme 2.8.2.

Assuming this explanation to be correct, it is clear that higher selectivities to hex-4-enoic acid will only be observed if the substrate anion can be prevented from binding directly to the metal. Studies aimed at achieving this goal are presented in

Chapters 3 and 4.

The active species, [Rh($O_2$CCH=CH-CH=CHMe)($P_A$Ph$_3$)(Ph$_2P_B$$O_2$CCH=CH-CH=CHMe)], illustrated in Figure 2.8.1 and Scheme 2.8.2 has not been isolated, however it has been identified spectroscopically, from the reaction between [RhCl(PPh$_3$)(Ph$_2$P$O_2$CCH=CH-CH=CHMe)] and hexa-2,4-dienoic acid in the presence of triethylamine. The reaction is not a clean one, partly due to the presence of both [RhCl(PPh$_3$)$_2$(Ph$_2$P$O_2$CCH=CH-CH=CHMe)] and [RhCl(PPh$_3$)$_2$(Ph$_2$POPPh$_2$)] in the starting material. As the hexa-2,4-dienoate derived mixed anhydride ligand in the active species is chelate bound through phosphorus and a carbon-carbon double bond the resonance assigned to the phosphorus atom ($P_B$) of the anhydride in the $^{31}$P NMR is at a shift of $\delta$124.4(dd). This is at slightly lower field than is observed for [RhCl(PPh$_3$ )(Ph$_2$P$O_2$CCH=CH-CH=CHMe)] although the values of $J_{RhP_B}$ and $J_{P_AP_B}$ are similar. The resonance assigned to the phosphorus atom of the triphenylphosphine ligand ($P_A$) is at a shift of $\delta$22.3(dd). At -50°C the $P_A$-$P_B$ couplings in the $^{31}$P NMR are lost, probably due to increased viscosity of the sample.

The $^1$H NMR spectrum of the reaction mixture clearly shows the resonances assignable to the chelate bound mixed anhydride ligand, Ph$_2$P$O_2$CCH$^e$=CH$^d$CH$^c$=CH$^b$CH$_3{}^a$ ($^a$1.07(br), $^b$0.23(br), $^c$5.61(br), $^d$4.96(br) and $^e$2.53(br)). These shifts are similar, although not identical to those observed for [RhCl(PPh$_3$)(Ph$_2$P$O_2$CCH$^e$=CH$^d$CH$^c$=CH$^b$CH$_3{}^a$)] ($^a$1.14(br), $^b$0.23(br), $^c$5.67(br), $^d$5.05(br), $^e$2.42(br)). The resonances assignable to the monodentate hexa-2,4-

dienoate anion, however, are obscured by the presence of both free hexa-2,4-dienoic acid and triethylamine.

The reaction of $[RhCl(PPh_3)(Ph_2PO_2CCH=CH\text{-}CH=CHMe)]$ and excess $K[O_2CCH=CHMe]$ affords the two products illustrated in Figure 2.8.3.

Figure 2.8.3

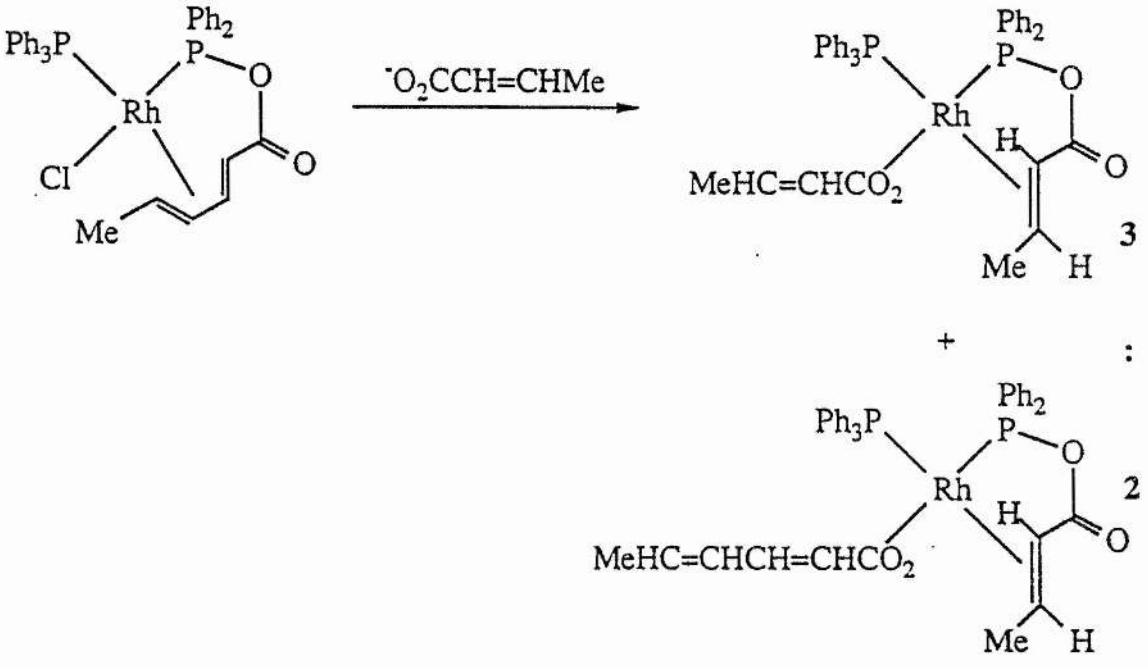


In this reaction a but-2-enoate anion replaces both the chloride anion and the hexa-2,4-dienoate anion in the mixed anhydride to give $[Rh(O_2CCH=CHMe)(PPh_3)(Ph_2PO_2CCH=CHMe)]$, whose characterisation has been discussed in Section 2.4. The other product is $[Rh(O_2CCH=CH\text{-}CH=CHMe)(PPh_3)(Ph_2PO_2CCH=CHMe)]$, and the $^{31}P$ NMR spectrum (see Spectrum 2.8.1) shows two resonances, one at $\delta$127.0 (doublet of doublets) assignable to the phosphorus atom of the mixed anhydride ligand, the other at

$\delta$25.8(dd) assignable to the phosphorus of the coordinated triphenylphosphine ligand. As was observed earlier in this chapter, there is once again a marked preference for the but-2-enoate anion as the component of the bidentate mixed anhydride.

Spectrum 2.8.1 $^{31}P$ NMR of a product mixture, obtained from the reaction between $[RhCl(PPh_3)_2(Ph_2PO_2CCH=CHCH=CHMe)]$ and $K[O_2CCH=CHMe]$, in $CD_2Cl_2$ at 298K.

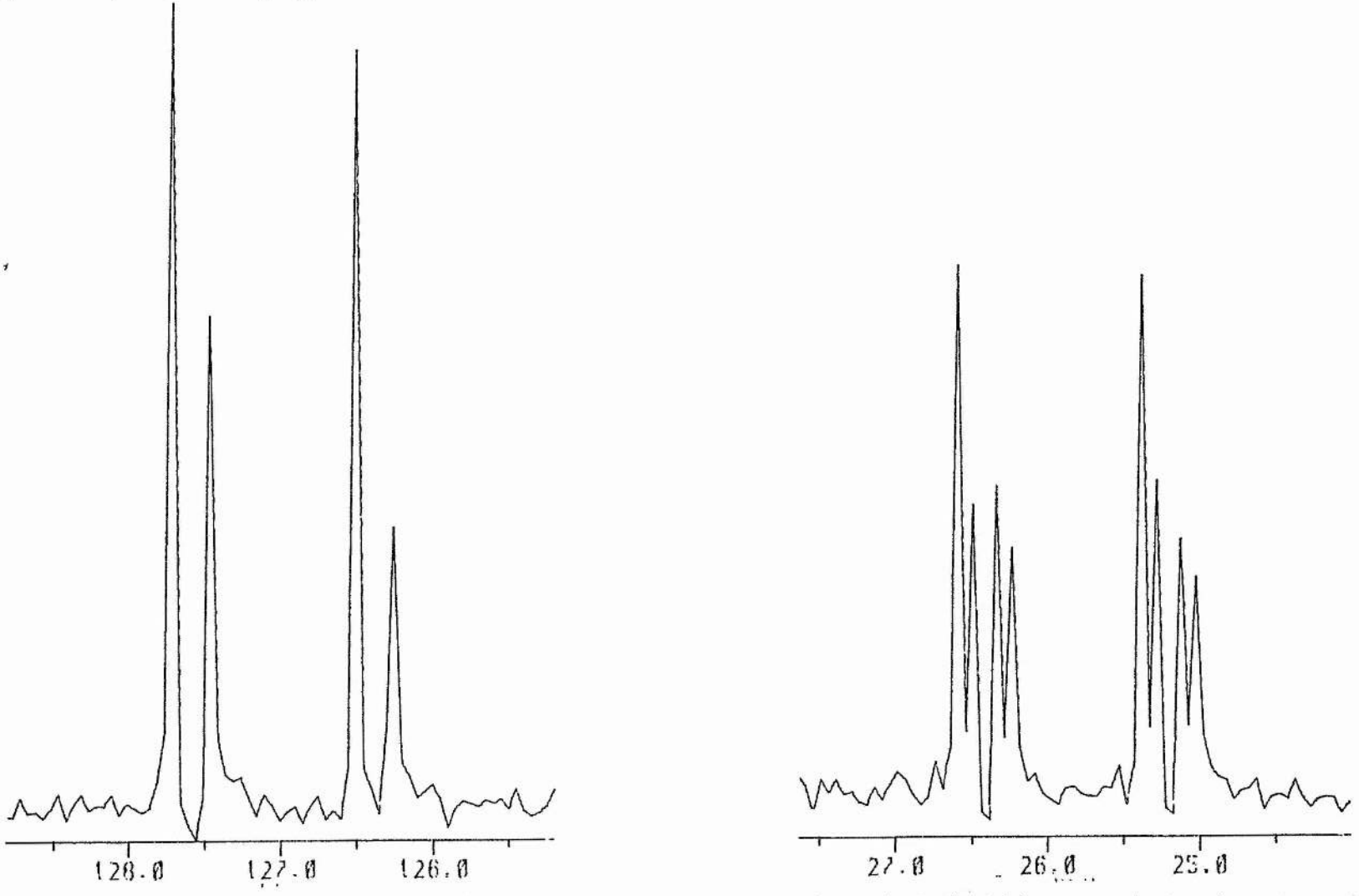

In order to explain the production of hexanoic acid, when using rhodium-mixed anhydride precursors it has been proposed that the hexa-2,4-dienoate ligand bound directly to rhodium is hydrogenated. This implies that there should be an equilibrium between the two active species presented in Schemes 2.8.2 and 2.8.3 (See Figure 2.8.4).

Figure 2.8.4

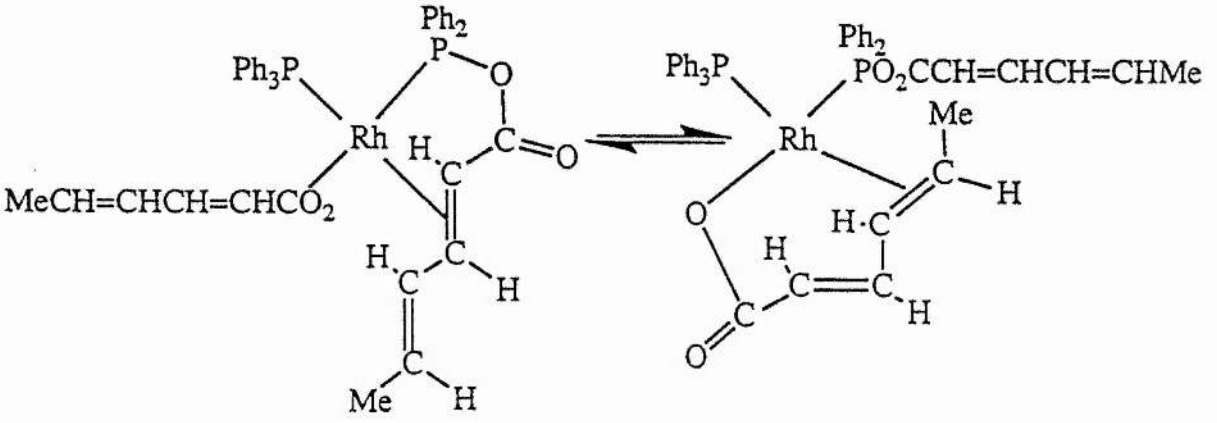


The findings that possibly verify the existence of the species presented in Figure 2.8.2 and Scheme 2.8.3 are provided by the reaction of $[RhCl(PPh_3)(Ph_2PO_2CCH=CHMe)]$ with 5 mole equivalents of both hexa-2,4-dienoic acid and triethylamine. The four products of this reaction (W, X, Y and Z) are illustrated in Scheme 2.8.4, and the $^{31}P$ NMR is presented as Spectrum 2.8.2.

Scheme 2.8.4

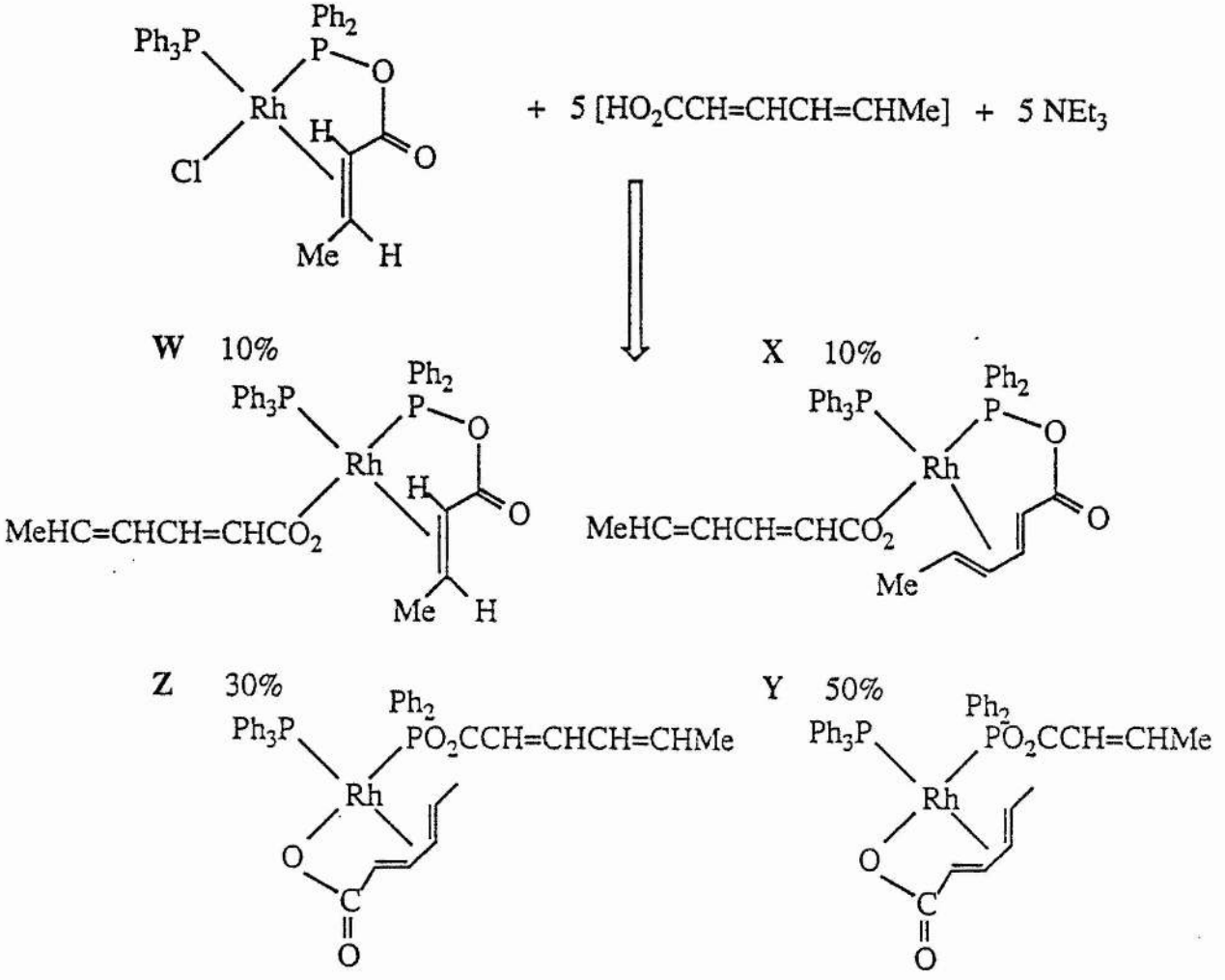


Complex W, $[Rh(O_2CCH=CH\text{-}CH=CHMe)(P_APh_3)(Ph_2P_BO_2CCH=CHMe)]$, previously prepared from the reaction of $[RhCl(PPh_3)(Ph_2PO_2CCH=CH\text{-}CH=CHMe)]$ with but-2-enoic acid and triethylamine, gives resonances at $\delta$127.0(dd) and $\delta$25.8(dd) in the $^{31}P$ NMR with the values of $J_{RhP_A}$, $J_{RhP_B}$ and $J_{P_AP_B}$ equal to 146.5 Hz, 146.1 Hz and 30.9 Hz respectively.

Complex X, [Rh($O_2$CCH=CH-CH=CHMe)($P_A$Ph$_3$)(Ph$_2$$P_B$$O_2$CCH=CH-CH=CHMe)], that was previously prepared from the reaction of [RhCl(PPh$_3$)(Ph$_2$PO$_2$CCH=CH-CH=CHMe)] with hexa-2,4-dienoic acid and triethylamine, gives resonances at $\delta$124.4(dd) and $\delta$22.3(dd) with the values of $J_{RhP_A}$, $J_{RhP_B}$ and $J_{P_AP_B}$ equal to 168.1 Hz, 137.5 Hz and 25.3 Hz respectively.

Complexes Y and Z are similar in that they have both been assigned as having a chelate bound hexa-2,4-dienoate anion, however they differ with respect to their monodentate mixed anhydride ligands; Y having a but-2-enoate derived anhydride and Z a hexa-2,4-dienoate derived anhydride.

Complex Y, [Rh($O_2$CCH=CH-CH=CHMe)($P_A$Ph$_3$)(Ph$_2$$P_B$$O_2$CCH=CHMe)], gives resonances at $\delta$63.7(dd) and $\delta$17.7(dd) with the values of $J_{RhP_A}$, $J_{RhP_B}$ and $J_{P_AP_B}$ equal to 146.8 Hz, 99.5 Hz and 23.4 Hz respectively. The shift of the resonance assignable to the phosphorus atom of the mixed anhydride, $P_B$, is in the region associated with a monodentate mixed anhydride ligand ($\delta$63.7), whilst the value of the coupling $J_{RhP_B}$ (99.5 Hz) is significantly smaller than is observed for [RhCl(PPh$_3$)$_2$(Ph$_2$PO$_2$CCH=CH-CH=CHMe)] (191 Hz), presumably because of the greater trans influence of the chelate bound hexa-2,4-dienoate anion compared with that of chlorine. Similarly complex Z, [Rh($O_2$CCH=CH-CH=CHMe)($P_A$Ph$_3$)(Ph$_2$$P_B$$O_2$CCH=CH-CH=CHMe)] has resonances at $\delta$61.7(dd) and $\delta$17.7(dd) with the values of $J_{RhP_A}$, $J_{RhP_B}$ and $J_{P_AP_B}$ equal to 146.8 Hz, 103.6 Hz and 23.4 Hz respectively.

Spectrum 2.8.2 $^{31}P$ NMR of a product mixture, obtained from the reaction between [$RhCl(PPh_3)(Ph_2PO_2CCH{=}CHMe)$] and 5 $NEt_3$ and 5 hexa-2,4-dienoic acid, in $CD_2Cl_2$ at 298K.

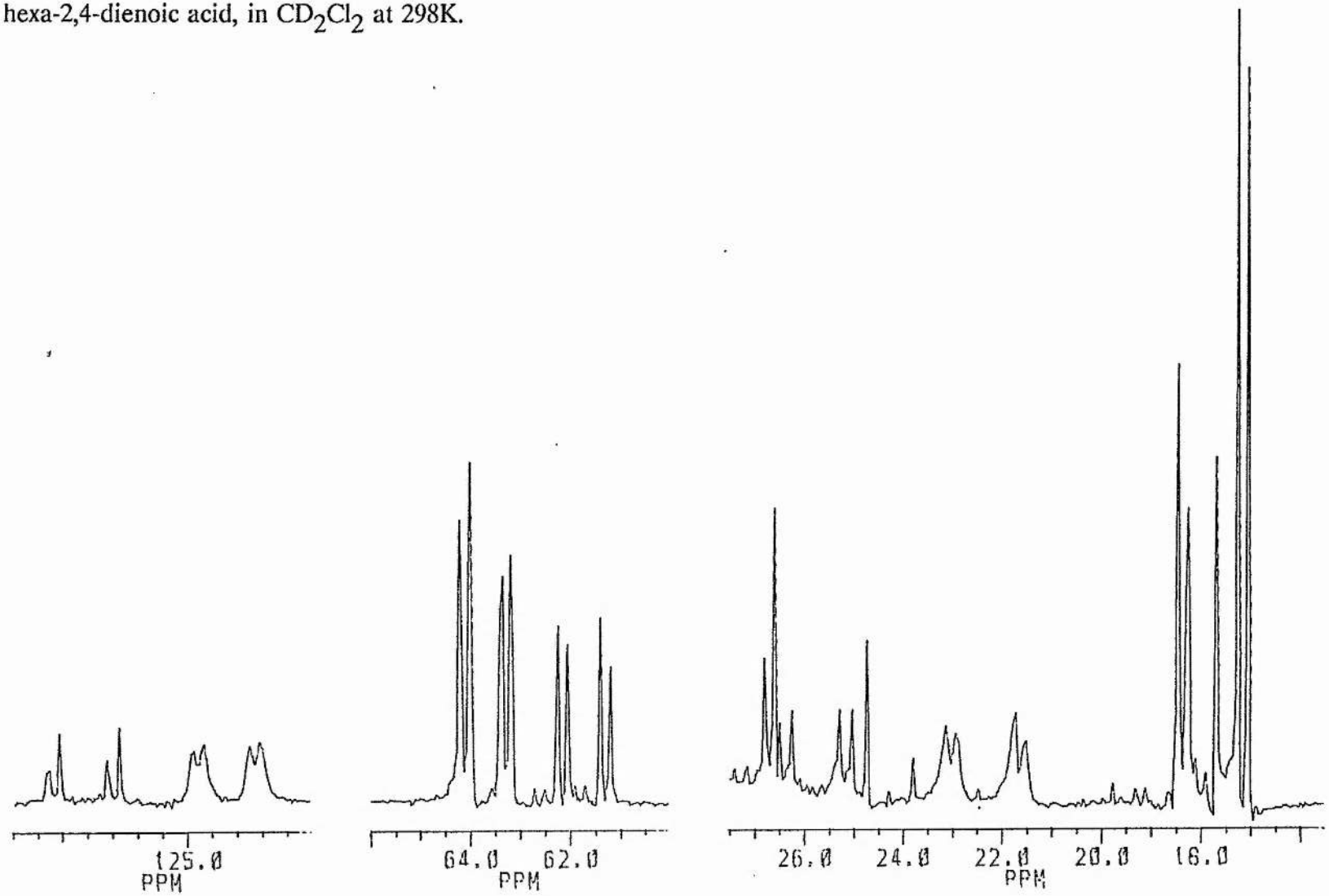

## 2.9 Experimental.

Microanalyses were by the University of St. Andrews microanalytical service. NMR spectra were recorded on Bruker Associates WP80 and AM300 spectrometers operating in the Fourier transform mode with (for $^{31}P$ and $^{19}F$) noise proton decoupling. IR spectra were recorded on a Perkin-Elmer 1330 spectrometer as Nujol mulls between caesium iodide plates.

All manipulations were carried out under dry oxygen-free nitrogen using standard Schlenk line and catheter tubing techniques. All solvents were purified by distillation from calcium hydride ($CH_2Cl_2$) or sodium diphenylketyl (toluene, petroleum (boiling range 40-60°C), diethylether and tetrahydrofuran (thf).

The mixed anhydride ligands of general formula $[Ph_2PO_2CCR=CR'R'']$[2] and the complexes $[RhCl(PPh_3)_3]$[35], $[RhCl(PPh_3)_2(Ph_2PO_2CCMe=CHPh)]$[3], $[RhCl(PPh_3)_2(Ph_2PO_2CCH=CMe_2)]$[3], $[Rh(PPh_3)_2(Ph_2PO_2CCMe=CHPh)]PF_6$[3], $[RhCl(PPh_3)(Ph_2PO_2CCH=CHMe)]$[3] and $[RhCl(PPh_3)(Ph_2PO_2CCH=CH-CH=CHMe)]$[3] were all made by literature procedures.

The potassium salts of all the substituted acrylic acids $K[O_2CCR=CR'R'']$ referred to in this chapter were all prepared in a similar manner. A detailed account of the preparation of potassium but-2-enoate $K[O_2CCH=CHMe]$ is presented here.

Potassium but-2-enoate, $K[O_2CCH=CHMe]$.

To a solution of but-2-enoic acid, $[CH_3CH=CHCO_2H]$ (3.27g, 38.0mmol) in tetrahydrofuran ($70cm^3$) was added solid KOH (2.13g, 38.0mmol). The mixture was stirred under nitrogen for 8 hours during which time a white microcrystalline powder appeared. The product, identified spectroscopically as $K[O_2CCH=CHMe]$, was filtered off, washed with diethyl ether (3 x $30cm^3$) and then dried under vacuum. Yield 4.09g (86.8%).

Other yields $K[O_2CCMe=CHPh]$, 82.6%; $K[O_2CCH=CMe_2]$, 84.1% $K[O_2CCH_2CH_2Me]$, 86.2%; $K[O_2CCH=CH-CH=CHMe]$, 81.3%.

But-2-enoato(diphenylphosphino but-2-enoate)(triphenylphosphine)rhodium(I).

$[Rh(O_2CCH=CHMe)(PPh_3)(Ph_2PO_2CCH=CHMe)]$

Different reactions can lead to this compound. It has been isolated in the following experiments:

(i) To a solution of $[RhCl(PPh_3)(Ph_2PO_2CCH=CHMe)]$ (0.25g, 0.37mmol) in tetrahydrofuran ($70cm^3$) was added $K[O_2CCH=CHMe]$ (0.41g, 3.30mmol). The mixture was stirred for 2 hours and then filtered to eliminate the excess of $K[O_2CCH=CHMe]$. The solution was then evaporated under vacuum to $3cm^3$ and light petroleum ($50cm^3$) was added to give an orange microcrystalline powder that was filtered and dried under vacuum. Yield 0.20g (73%). Found: C,64.1; H, 5.3%. $C_{38}H_{35}O_4P_2Rh$ requires C,63.3;

H, 4.9%.

(ii) A similar reaction, but using $[MeHC=CHCO_2][NEt_3H]$, prepared in situ from $[MeCH=CHCO_2H]$ and $NEt_3$, the product was isolated and characterised spectroscopically.

(iii) To a suspension of $K[O_2CCH=CHMe]$ (0.16g, 1.29mmol) in $CH_2Cl_2$ ($20cm^{-1}$) was added a solution of $[RhCl(PPh_3)_2(Ph_2PO_2CCH_2CH_2CH_3)]$(0.12g,0.13mmol) in $CH_2Cl_2$($30cm^3$). The mixture was stirred for 3 hours, filtered to eliminate the excess of $K[O_2CCH=CHMe]$ and evaporated in vacuo to 2 $cm^3$. Light petroleum (50 $cm^3$) was added to give an orange powder that was filtered and dried in vacuo. The product was characterised spectroscopically, giving identical $^1H$ and $^{31}P$ NMR spectra to that obtained from method (i).

(iv) A similar reaction, again in $CH_2Cl_2$, using $[Rh(PPh_3)_2(Ph_2PO_2CCH_2CH_2CH_3)]PF_6$ and $K[O_2CCH=CHMe]$ led after 10 hours to the same product with 100% conversion. The product was identified spectroscopically.

(v) To a solution of $[RhCl(PPh_3)_2(Ph_2PO_2CCMe=CHPh)]$ (0.46g, 0.48mmol) in THF (60 $cm^3$) was added $[HO_2CCH=CHMe]$(0.21g, 2.4mmol) and $NEt_3$ (0.24g, 2.4mmol). The mixture was stirred for 3 hours and then filtered. After evaporation to 3 $cm^3$, light petroleum (60

$cm^3$) was added to give an orange powder which was filtered off, washed with cold (-40°C) diethylether (3 x 20 $cm^3$) and dried under vacuum. Yield 0.24g (65.9%).

Diphenylphosphino E-2-methyl-3-phenylpropenoate (2-methyl-3-phenylpropenoato)-(triphenylphosphine) rhodium (I).

$[Rh(O_2CCMe=CHPh)(PPh_3)(Ph_2PO_2CCMe=CHPh)]$

This compound was obtained from several experiments:

(i) To a suspension of $K[O_2CCMe=CHPh]$ (0.5g, 2.5mmol) in $CH_2Cl_2$ ($40cm^3$) was added a solution of $[RhCl(PPh_3)_2(Ph_2PO_2CCMeCHPh)]$ (0.15g, 0.16mmol) in $CH_2Cl_2$ ($20cm^3$). The mixture was stirred for 2 hours and then filtered to eliminate excess $K[O_2CCMe=CHPh]$. The solution was evaporated to dryness and the product identified spectroscopically but was contaminated with part of the unreacted starting material $[RhCl(PPh_3)_2(Ph_2PO_2CCMe=CHPh)]$. 80% Conversion was observed by NMR analyses.

(ii) When treating $[Rh(PPh_3)_2(Ph_2PO_2CCMe=CHPh)]PF_6$ with $K[O_2CCMe=CHPh]$ in $CH_2Cl_2$ under similar conditions for 20 hours, the isolated product of the reaction contained only 35% $[Rh(O_2CCMe=CHPh)(PPh_3)(Ph_2PO_2CCH=CHMe)]$, the rest being the starting material.

(iii) Reaction of $[Rh(PPh_3)(Ph_2PO_2CCMe=CHPh)]PF_6$ with an excess of $[PhCH=CMeCO_2][NEt_3H]$ (prepared in situ) in $CD_2Cl_2$ led after 3 hours to the conversion of 90% of the starting material to $[Rh(O_2CCMe=CHPh)(PPh_3)(Ph_2PO_2CCH=CHMe)]$.

(iv) A similar reaction involving $[RhCl(PPh_3)_2(Ph_2PO_2CCMe=CHPh)]$ and an excess of $[PhCH=CMeCO_2][NEt_3H]$ in $CD_2Cl_2$ led after 20 minutes to the conversion of 40% of the starting material to $[Rh(O_2CCMe=CHPh)(PPh_3)(Ph_2PO_2CCH=CHMe)]$. In all these experiments the products were characterised by NMR spectroscopy.

Diphenylphosphino but-2-enoate (2-methyl-3-phenylpropenoato) (triphenylphosphine) rhodium(I).

$[Rh(O_2CCMe=CHPh)(PPh_3)(Ph_2PO_2CCH=CHMe)]$

To a solution of $[RhCl(PPh_3)(Ph_2PO_2CCH=CHMe)]$ (0.42g, 0.62mmol) in tetrahydrofuran (70 $cm^3$) was added $K[O_2CCMe=CHPh]$ (1.24g, 6.2mmol). The mixture was stirred for 3 hours and then filtered to eliminate the excess of $K[O_2CCMe=CHPh]$. The solution was then evaporated under vacuum to 3 $cm^3$ and light petroleum (50$cm^3$) was added to give an orange microcrystalline powder that was filtered off and dried under vacuum. Yield 0.35g (67.6%).

Reaction of $[RhCl(PPh_3)_2(Ph_2PO_2CCMe=CHPh)]$ with $K[O_2CCH=CHMe]$

To a solution of $[RhCl(PPh_3)_2(Ph_2PO_2CCMe=CHPh)]$ (0.23g, 0.24mmol) in THF (50 $cm^3$) was added $K[O_2CCH=CHMe]$ (0.31g, 2.46mmol). The mixture was stirred for 3 hours and then filtered to eliminate the excess of $K[O_2CCH=CHMe]$. After evaporation to 3 $cm^3$, light petroleum (50$cm^3$) was added to give an orange powder which was collected and dried in vacuo. The product was characterised as a mixture of $[Rh(O_2CCMe=CHPh)(PPh_3)(Ph_2PO_2CCH=CHMe)]$ and $[Rh(O_2CCH=CHMe)(PPh_3)(Ph_2PO_2CCH=CHMe)]$ in a 3:2 molar ratio by $^1H$ and $^{31}P$ NMR spectroscopy.

Diphenylphosphino but-2-enoate (3-methylbut-2-enoato) (triphenylphosphine) rhodium(I).

$[Rh(O_2CCH=CMe_2)(PPh_3)(Ph_2PO_2CCH=CHMe)]$

To a solution of $[RhCl(PPh_3)(Ph_2PO_2CCH=CHMe)]$ (0.37g, 0.55mmol) in tetrahydrofuran (70 $cm^3$) was added $K[O_2CCH=CMe_2]$ (0.76g, 5.5mmol). The mixture was stirred for 3.5 hours and then filtered to eliminate the excess of $K[O_2CCH=CMe_2]$. The solution was then evaporated under vacuum to 3 $cm^3$ and light petroleum (50 $cm^3$) was added to give an orange microcrystalline powder that was filtered off and dried under vacuum. Yield 0.30g (70.6%)

Reaction of $[RhCl(PPh_3)_2(Ph_2PO_2CCH=CMe_2)]$ with $^-[O_2CCH=CHMe]$

(a) To a solution of $[RhCl(PPh_3)_2(Ph_2PO_2CCH=CMe_2)]$ (0.27g, 0.29mmol) in THF (70$cm^3$) was added $K[O_2CCH=CHMe]$ (0.36g, 2.9mmol). The mixture was stirred for 3 hours and then filtered to eliminate the excess of $K[O_2CCH=CHMe]$. After evaporation to 3

$cm^3$, light petroleum (50 $cm^3$) was added to give an orange powder which was collected and dried in vacuo. The product was characterised as a mixture of both $[Rh(O_2CCH=CMe_2)(PPh_3)(Ph_2PO_2CCH=CHMe)]$ and $[Rh(O_2CCH=CHMe)(PPh_3)(Ph_2PO_2CCH=CHMe)]$ in a 1:1.22 molar ratio by $^1H$ and $^{31}P$ NMR spectroscopy.

(b) To a solution of $[RhCl(PPh_3)_2(Ph_2PO_2CCH=CMe_2)]$ (0.20g, 0.21mmol) in THF (60 $cm^3$) was added $[HO_2CCH=CHMe]$ (0.09g, 1.05mmol) and $NEt_3$ (0.11g, 1.05mmol). The mixture was stirred for 3 hours and then filtered. After evaporation to 3 $cm^3$, light petroleum (40 $cm^3$) was added to give an orange powder which was collected and dried under vacuum. The product material itself was characterised as a mixture of both $[Rh(O_2CCH=CMe_2)(PPh_3)(Ph_2PO_2CCH=CHMe)]$ and $[Rh(O_2CCH=CHMe)(PPh_3)(Ph_2PO_2CCH=CHMe)]$ in a 2:3 ratio by $^1H$ and $^{31}P$ NMR spectroscopy.

Chloro(diphenylphosphino butyrate)bis(triphenylphosphine)rhodium(I).

$[RhCl(PPh_3)_2(Ph_2PO_2CCH_2CH_2CH_3)]$

(a) Preparation of $[Ph_2PO_2CCH_2CH_2CH_3]$

To a cooled (-10°C) solution of $[CH_3CH_2CH_2CO_2H]$ (3g, 34.0mmol) in tetrahydrofuran (50 $cm^3$) was added a solution of $PPh_2Cl$ (7.5g, 34.0mmol) in tetrahydrofuran (30 $cm^3$) over 5 minutes followed by a solution of $NEt_3$ (3.44g, 34.0mmol) in tetrahydrofuran (50$cm^3$). The

mixture was stirred at -10°C for 1 hour, the ammonium salt formed ($NHEt_3Cl$) was then removed by filtration and the solution was evaporated to dryness under reduced pressure to give the product as a viscous colourless liquid. Yield 8.8g (95%). $^{31}P$ NMR ($C_6D_6$); singlet at $\delta$ = 97.5, $^1H$ NMR: 0.8 (t, 3H), 1.66 (m, 2H), 2.35 (t, 2H) and 7.0 - 8.0 (m, 10H).

(b) To a solution of $[RhCl(PPh_3)_3]$ (0.7g, 0.75 mmol) in tetrahydrofuran (40 $cm^3$) was added a solution of $[Ph_2PO_2CCH_2CH_2CH_3)]$ (0.21g, 0.76 mmol) in tetrahydrofuran (30 $cm^3$). On addition the solution gradually became orange. The solution was stirred for 90 minutes, and the solvent was then removed in vacuo to 3 $cm^3$. Petroleum spirit (50 $cm^3$) was added to precipitate the product as an orange powder that was filtered and dried in vacuo. Yield 0.6g (85%). Found C, 66.85; H, 5.23%. $C_{52}H_{47}ClO_2P_3Rh$ requires: C, 66.78; H, 5.06%.

Diphenylphosphino butyrate bis (triphenylphosphine) rhodium(I) hexafluorophosphate.

$[Rh(PPh_3)_2(Ph_2PO_2CCH_2CH_2CH_3)]PF_6$

To a solution of $[RhCl(PPh_3)_2(Ph_2PO_2CCH_2CH_2CH_3)]$ (0.164 g, 0.17 mmol) in THF (40 $cm^3$) was added $TIPF_6$ (0.062g, 0.17mmol). On addition a fine white precipitate formed. The mixture was stirred for 1 hour, filtered and evaporated to dryness in vacuo. The orange solid was analysed by $^{31}P$ NMR spectroscopy showing ca. 95% yield with traces of $[Rh(PPh_3)_2(Ph_2POPPh_2)]^+$ as an impurity and a compound given a doublet at $\delta$40.2 (J = 181 Hz).

Butyrato(diphenylphosphino butyrate) bis (triphenylphosphine) rhodium(I).

$[Rh(O_2CCH_2CH_2CH_3)(PPh_3)_2(Ph_2PO_2CCH_2CH_2CH_3)]$

To a solution of $[RhCl(PPh_3)_2(Ph_2PO_2CCH_2CH_2CH_3)]$ (0.33g, 0.35mmol) in THF (50 $cm^3$) was added $K[O_2CCH_2CH_2CH_3]$ (0.44g, 3.5mmol). The mixture was stirred for 4 hours and then filtered to eliminate the excess of $K[O_2CCH_2CH_2CH_3]$. The solution was then evaporated under vacuum to 3 $cm^3$ and light petroleum (50 $cm^3$) was added to give an orange powder that was filtered off and dried in vacuo. This powder was analysed as being starting material. The filtered liquid was kept in a flask, under dry nitrogen at -40°C and orange microcrystals of $[Rh(O_2CCH_2CH_2CH_3)(PPh_3)_2(Ph_2PO_2CCH_2CH_2CH_3)]$ were isolated. Yield 0.09g (26.1%) Found : C, 68.79; H, 5.42%. $C_{56}H_{54}O_4P_3Rh$ requires: C, 68.16; H, 5.52%.

But-2-enoato(diphenylphosphinobutyrate) bis (triphenylphosphine)rhodium(I).

$[Rh(O_2CCH=CHMe)(PPh_3)_2(Ph_2PO_2CCH_2CH_2CH_3)]$

Reaction of $[Rh(O_2CCH_2CH_2CH_3)(PPh_3)_2(Ph_2PO_2CCH_2CH_2CH_3)]$ and an excess of $[MeHC=CHCO_2][NEt_3H]$ (prepared in situ) in $CD_2Cl_2$ led after 30 minutes to the complete conversion of the starting material to $[Rh(O_2CCH=CHMe)(PPh_3)_2(Ph_2PO_2CCH_2CH_2CH_3)]$. The product was characterised by NMR spectroscopy.

## CHAPTER 2 REFERENCES


1 S A Preston, D C Cupertino, P Palma-Ramirez and D J Cole-Hamilton, J. Chem. Soc., Chem. Commun., 1986, 977.

2 D C Cupertino and D J Cole-Hamilton, J. Chem. Soc., Dalton Trans., 1987, 443.

3 A F Borowski, A Iraqi, D C Cupertino, D J Irvine and D J Cole-Hamilton, J. Chem. Soc., Dalton Trans., 1990, 29.

4 A Iraqi, N R Fairfax, S A Preston, D C Cupertino, D J Irvine and D J Cole-Hamilton, J. Chem. Soc., Dalton Trans, 1991, 1929.

5 Aldrich Library of Infra-red Spectra.

6 T G Appleton, H C Clark and L E Manzer, Coord. Chem. Rev., 1973, 10, 335.

7 D J Irvine, A F Borowski and D J Cole-Hamilton, J. Chem. Soc., Dalton Trans., 1990, 3549.

8 P E Garrou, Chem. Rev., 1981, 81, 229.

9 D J Cole-Hamilton and G Wilkinson, Nouveau J. Chim., 1977, 1, 141.

10 W R Jackson, P Perlmutter and G H Suh, J. Chem. Soc., Chem. Commun., 1987, 724.

11 W R Jackson, P Perlmutter and E E Tasdelen, J. Chem. Soc., Chem. Commun., 1990, 763.

12 D J Irvine, D J Cole-Hamilton, J C Barnes and P K G Hodgson, Polyhedron, 1989, 8, 1575.

13 G M Kosolapoff and L Maier, Organic Phosphorus Compounds, Wiley, New York, 1972, Vol. 4, 497.

14 D H Gerlach, W G Peet and E L Muetterties, J. Am. Chem. Soc., 1972, **94**, 4545.

15 G M Kosolapoff and L Maier, Organic Phosphorus Compounds, Wiley, New York, 1973, Vol. 6, 237.

16 R T De Pue, D B Collum, J W Ziller and M R Churchill, J. Am. Chem. Soc., 1985, **107**, 2131.

17 H C Clark, K R Dixon and W J Jacobs, Chem. Commun., 1968, 548.

18 L Malatesta, G Caglio and M Angoletta, J. Chem. Soc., 1965, 6974.

19 W Heiber and H Duchatsch, Chem. Ber., 1965, **98**, 1744.

20 W Heiber and V Frey, Chem. Ber, 1966, **99**, 2614.

21 R B King, M B Bisnette and A Fronzaglia, J Organomet. Chem., 1965, **3**, 256.

22 R B King, M B Bisnette and A Fronzaglia, J Organomet. Chem., 1966, **5**, 341.

23 W Heiber, V Frey and P Joan, Chem. Ber., 1967, **100**, 1961.

24 T Kruck, M Holfer and M Noack, Chem. Ber., 1966, **99**, 1153.

25 J Halpern and S F A Kettle, Chem. and Ind., 1961, 745.

26 D Rose, J D Gilbert, R P Richardson and G Wilkinson, J. Chem. Soc.(A), 1969, 2610.

27 P Legzdins, R W Mitchell, G L Rempel, J D Ruddick and G Wilkinson, J. Chem. Soc.(A), 1970, 3322.

28 R W Mitchell, J D Ruddick and G Wilkinson, J. Chem. Soc.(A), 1971, 3224.

29 R S Coffey, Chem. Commun., 1967, 923.

30 J J Byerley, G L Rempel, N Takebe and B R James, Chem. Commun., 1971 1482.

31 S D Robinson and M F Uttley, J. Chem. Soc., Dalton Trans., 1973, 1912.

32 M J Lawrence and G Foster, G.P.1, 806, 293.

33 L N Lewis, Inorg. Chem., 1985, 24, 4433.

34 J P Fackler Jr., L D Thompson, I J B Lin, T A Stephenson, R O Gould, J M C Alison and A J F Fraser, Inorg. Chem., 1982, 21, 2397.

35 J A Osborn and G Wilkinson, Inorg. Synth., 1967, 10, 68.

# CHAPTER 3

# THE REACTIONS OF MIXED ANHYDRIDES AND FLUOROTRISTRIPHENYLPHOSPHINERHODIUM (I), $[RhF(PPh_3)_3]$

## 3.1 Introduction.

As stated in Section 2.3, mixed anhydride derived rhodium complexes, when used as catalysts in the hydrogenation of hexa-2,4-dienoic acid, give rise to the formation of both hex-4-enoic and hexanoic acids. In order to increase production of hex-4-enoic acid it is necessary to increase the regioselectivity of the catalyst. In an attempt to achieve this, modification of the initial catalysts has been pursued.

It is shown in Section 2.8 that two mechanisms exist for the catalytic hydrogenation of hexa-2,4-dienoic acid. The production of hexanoic acid is brought about by the active participation, via bidentate binding, of the acrylate ligand in the catalytically active species, as shown in Figure 3.1.1.

Figure 3.1.1

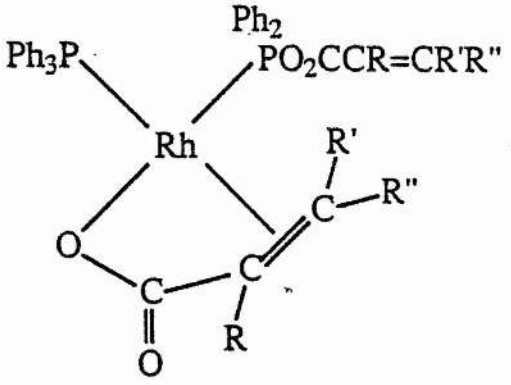

As presented in Chapter 2, the formation of the catalytically active species involves the substitution of a labile chloride ligand by an acrylic acid anion. Thus it is conceivable that if the catalyst's chloride ligand is replaced by another anionic ligand that cannot be substituted by an acrylic acid anion, then the formation of hexanoic acid should be eliminated. Consequently more hex-4-enoic acid should be produced and hence a more regioselective catalyst would be created. This chapter covers the use of a fluoride anion as such a ligand.

It should be noted however, that organotransition-metal fluoro compounds have received far less literature coverage than their halide counterparts, and there are several reasons for this, the principal one being the supposed belief, by hard/soft/acid base rules, that the combination of a low-valent metal centre and a fluoride anion is inherently unstable. Despite this, there have been numerous cases where the opposite has been observed, especially when $\pi$ back-bonding ligands are also present, and this is discussed in Section 3.2. Another reason for the lesser degree of study of organometallic fluoro compounds is the lack of convenient ways to introduce fluoride ligands. The problems of working with elemental fluorine and hydrogen fluoride are major deterrents to extending reactions readily performed with the heavier halogens and hydrogen halides to $F_2$ and HF.

Associated with this is the strength by which fluoride reagents bind to water and other protic reagents via strong hydrogen bonding, thus making the preparation of clean fluoride reagents difficult.[1-3]

## 3.2 The Stability of the Rh-F Bond in $[RhF(CO)(PPh_3)_2]$.

Of all organometallic fluorides, the rhodium and iridium Vaska's derivatives, $[MF(CO)(PPh_3)_2]$ (M=Rh, Ir), have been studied to the greatest degree. The rhodium species can be synthesized by a variety of routes, as shown in Scheme 3.2.1.

Scheme 3.2.1

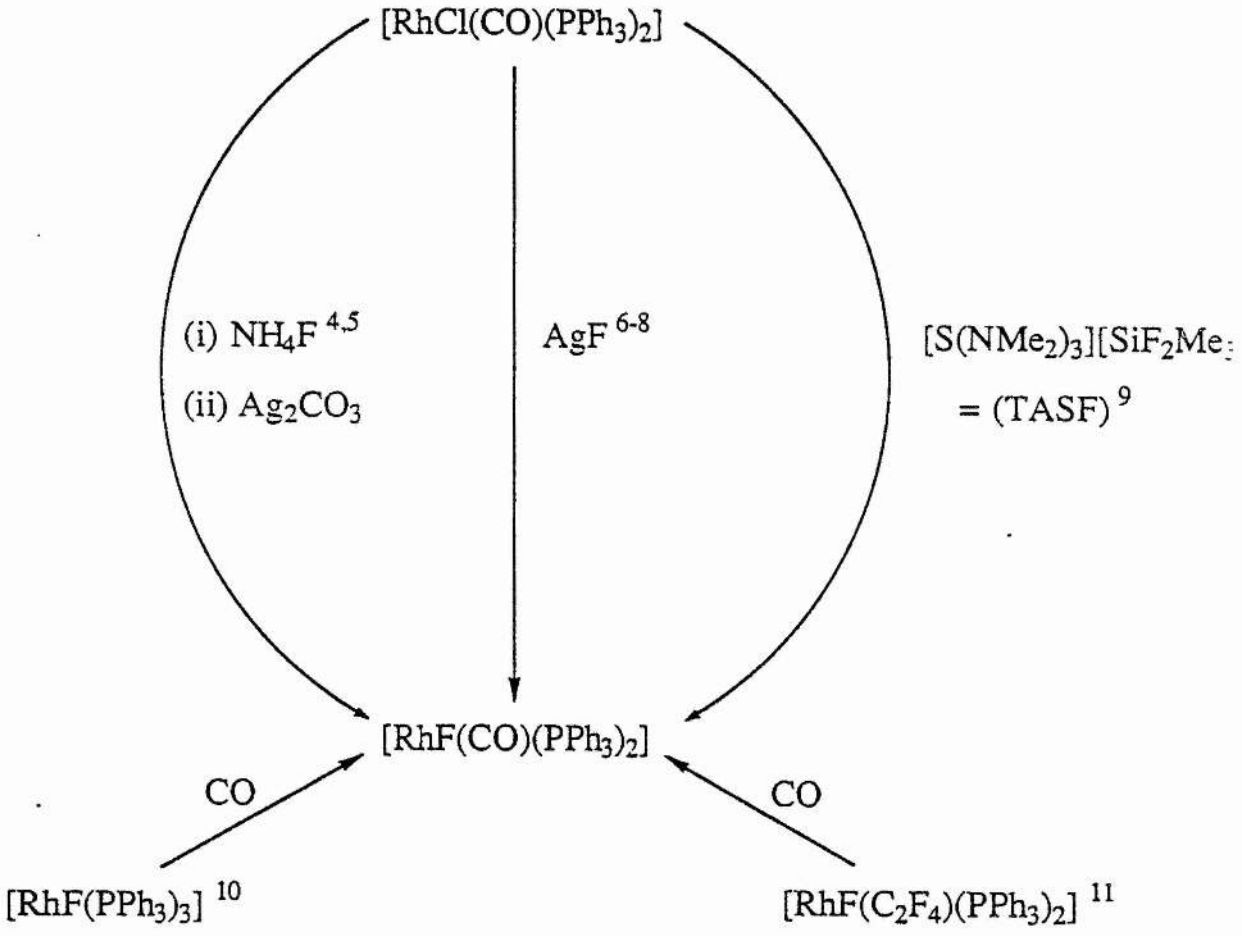


Studies of the series of rhodium (I) Vaska's halides have shown significant differences between the fluoro complex and the heavier halo derivatives, which are often rather similar to each other. Interpretations of these differences have

involved the interplay of the $\sigma$-donor and $\pi$-acceptor characteristics of the halide ligands. The influence of the $\pi$-donor ability of the halides, which is expected to follow the order $F^- > Cl^- > Br^- > Cl^-$, has not received much literature discussion, except for a publication by Doherty and Hoffman.[9]

The metal-halide $\pi$-bonding interactions in trans-halocarbonylmetal complexes such as the Vaska's halides are illustrated in Figure 3.2.1.

Figure 3.2.1

(a)

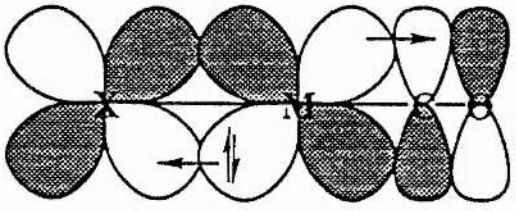

$\pi$-back bonding X=F<<Cl<Br<I

(b)

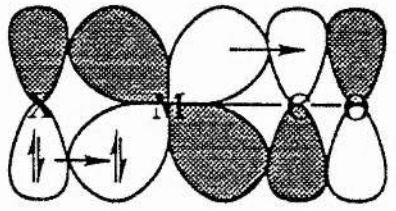

$\pi$-donation X=F>Cl>Br>I

Halides can be considered to (a) compete with CO for $\pi$-backbonding to M and (b) enhance $\pi$-backbonding to CO via $\pi$-donation to M.

The electronic absorption spectra of $[RhX(CO)(PPh_3)_2]$ in benzene have shown $\lambda_{MAX}$ for the $dz^2 \rightarrow b_1\pi$ transition[12,13] (Figure 3.2.2) increasing in the order X=F<Cl<Br<I, as shown in Table 3.2.1.

Table 3.2.1

Spectral Data for $[RhX(CO)(PPh_3)_2]$

| Halogen (X) | $\nu CO(cm^{-1})$[4] | $\lambda_{MAX}(nm)$[12] |
|---|---|---|
| F | 1971 | 358 |
| Cl | 1980 | 367 |
| Br | 1980 | 369 |
| I | 1981 | 372 |

This has been considered in terms of greater stabilization of the $b_1\pi$ level with increasing $\pi$-acceptor strength of X, which is regarded as following the order F<<Cl<Br<I on the basis of the availability of low-lying empty $d\pi$ orbitals on the halide.

Alternatively this can be explained by greater destabilization of $dz^2$ with increasing $\sigma$-donor ability in the order F<Cl<Br<I, paralleling decreasing electronegativity and increasing polarizability.

Figure 3.2.2 Partial Molecular Orbital Energy Level Correlation Diagram for Planar $C_{2V}$ complexes. (x is taken as the $C_2$ axis and z is perpendicular to the molecular plane).

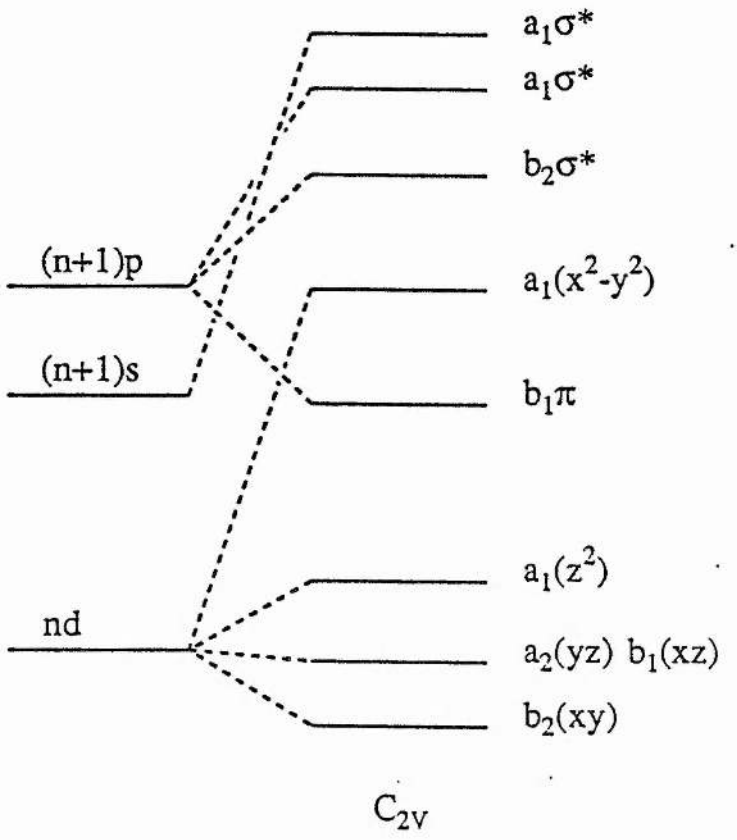


The carbonyl stretching frequencies (νCO) of $[RhX(CO)(PPh_3)_2]$ follow the order $X=F<Cl\leq Br\leq I$[4], as shown in Table 3.2.1, and this is once again consistent with increasing $\pi$-acceptor strength of the halides along this series. The observed trend in halide affinity for $[Rh(CO)(PPh_3)_2]^+$, with fluoride the most preferred, is supplemented by the IR data, on the basis of minimising competition between the halide and the trans carbon monoxide for electron density in the filled rhodium $d\pi$ orbitals (Figure 3.2.1). Corresponding trends in νCO with variation of X have been observed for $[RhX(CO)L_2]$ where L = $AsPh_3$ or $SbPh_3$[14].

In certain cases[15], with variation of L, νCO values have not followed the pattern previously stated. Doherty and Hoffman[9] have stated that carbonyl stretching frequencies are not just a simple measure of the ligand σ-donor and π-acceptor capabilities but also a measure of ligand π-donor capability. They have suggested that the spectral data for $[RhX(CO)L_2]$ are most consistent with the interpretation that the fluoro complex has the most electron-rich metal centre. In supporting this they make reference to electrochemical experiments[16] in which it is shown that fluoro complexes are the most difficult to reduce. They have concluded that these observations are opposite to expectations based on electronegativity arguments and have thus stated that differences in metal-halide π-bonding dominate in the electronic structure of the rhodium (I) compounds, with fluoride the poorest π-acceptor and best π-donor.

Comparisons of $^{31}P$ NMR chemical shifts for the rhodium halides, $[RhX(CO)(PPh_3)_2]$, show no discernible trend[17]. Variation in the magnitude of the $^{103}Rh$-$^{31}P$ coupling constants in the observed order F(135.5Hz) > Cl(126.9Hz) > Br(125.0Hz) > I(123.5Hz), has been interpreted as indicating increased effective electronegativity of the rhodium centre with increased electronegativity of X.

## 3.3 Halide Exchange for $[RhF(PPh_3)_3]$ in $CD_2Cl_2$.

Fluorotristriphenylphosphinerhodium (I), $[RhF(PPh_3)_3]$, is synthesized under nitrogen by the route shown in Scheme 3.3.1.[17,18] It cannot, however, be prepared

by reacting AgF with $[RhCl(PPh_3)_3]$ directly.

Scheme 3.3.1

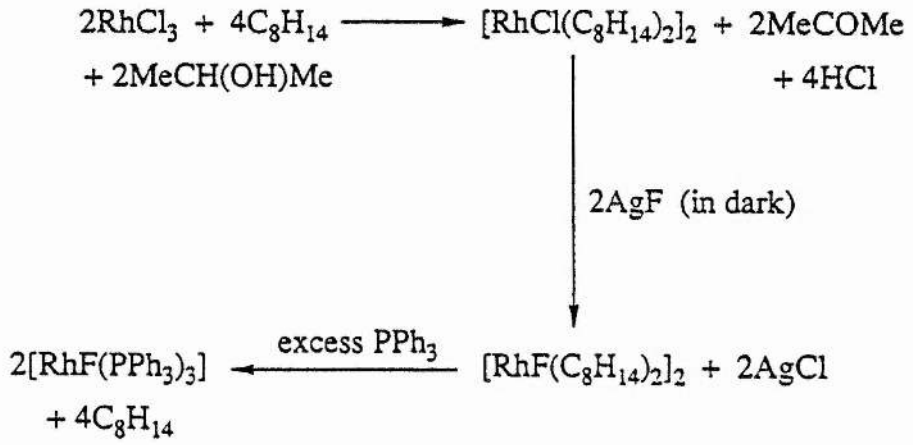


$^{31}P$ NMR spectra of the prepared $[RhF(PPh_3)_3]$ in deuterated dichloromethane, $CD_2Cl_2$, initially showed the presence of a significant amount of $[RhCl(PPh_3)_3]$. Thus it was considered that the reaction between $[RhCl(C_8H_{14})_2]_2$ and AgF had not gone to completion, and as a result when excess $PPh_3$ was added both $[RhF(PPh_3)_3]$ and $[RhCl(PPh_3)_3]$ were produced.

Experiments using $^{31}P$ NMR have shown that a sample of $[RhF(PPh_3)_3]$ in $CD_2Cl_2$ undergoes a halide exchange reaction and as a result increasing amounts of $[RhCl(PPh_3)_3]$ are produced.

Spectrum 3.1.1 clearly demonstrates the existence of a halide exchange process. After 11.5 minutes there is no significant presence of $[RhCl(PPh_3)_3]$, however after 43 minutes there clearly is. After 5 hours and with reference to intensities there is more $[RhCl(PPh_3)_3]$ than $[RhF(PPh_3)_3]$.

Spectrum 3.3.1 $^{31}P$ NMR spectra indicating the halide exchange process of $[RhF(PPh_3)_3]$ in $CD_2Cl_2$ at 298K.

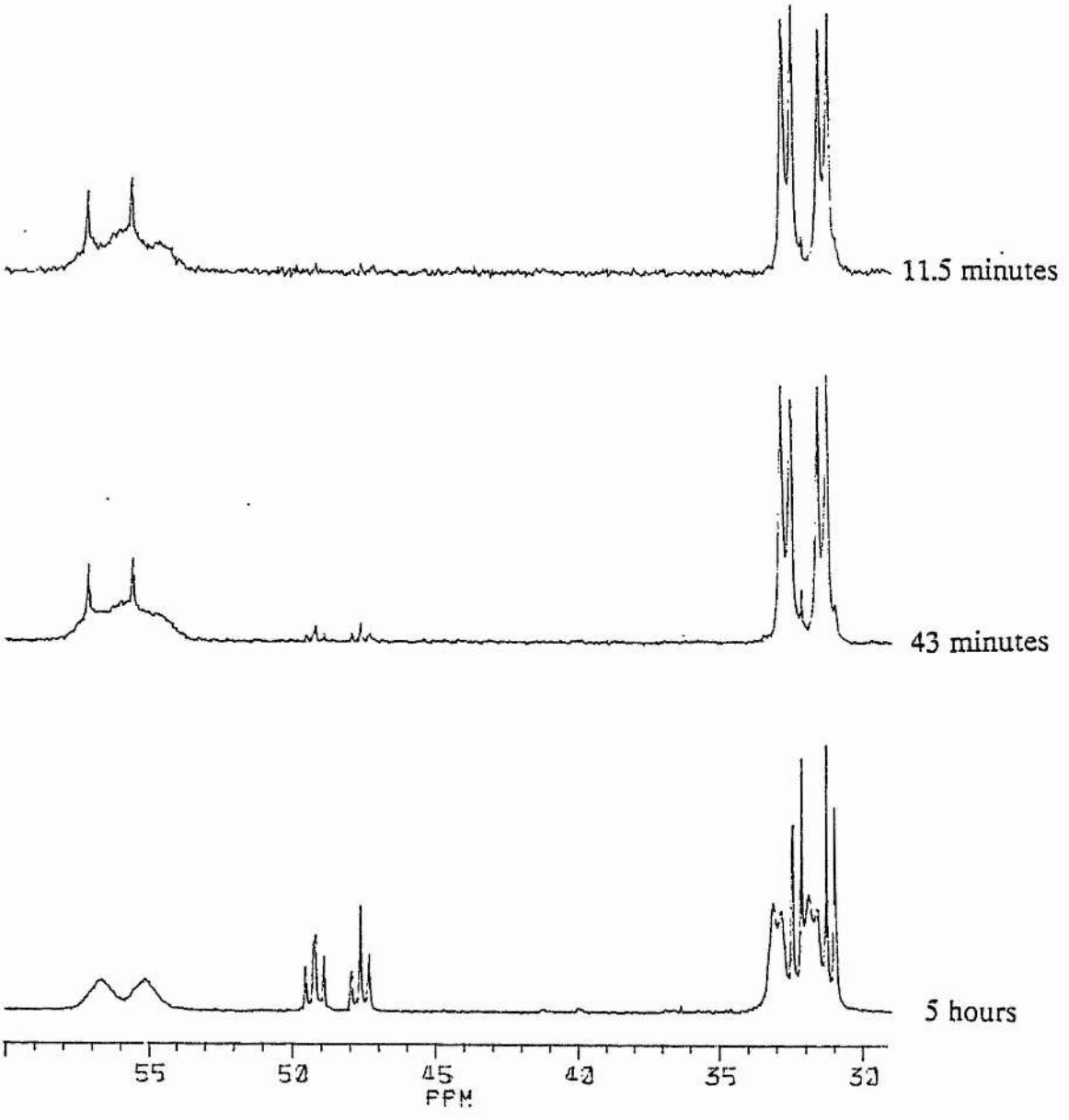

Such a halide exchange has been observed for the complex $[(C_5Me_5)Rh(PMe_3)(C_6F_5)F]$[19], illustrated in Figure 3.3.1, whereby in chloroform ($CHCl_3$) the corresponding chloride species, $[(C_5Me_5)Rh(PMe_3)(C_6F_5)Cl]$, is formed.

Figure 3.3.1

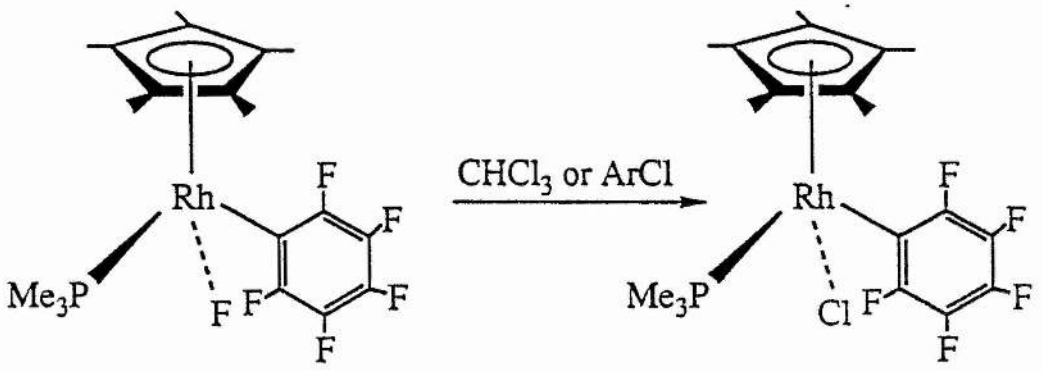


Spectrum 3.3.2 shows the room temperature $^{31}P$ NMR of $[RhF(PPh_3)_3]$ whilst Spectrum 3.3.3 shows the $^{31}P$ NMR spectrum obtained at -40°C, and from the latter the couplings due to the fluoride ligand, which are not evident at room temperature, can be clearly seen. Table 3.3.1 presents the $^{31}P$ NMR data for $[RhF(PPh_3)_3]$ at -40°C.

Table 3.3.1

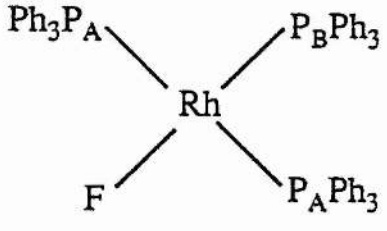


| Shift δ (ppm) | | Coupling Constants J (Hz) | | | | |
|---|---|---|---|---|---|---|
| $P_A$ | $P_B$ | $RhP_A$ | $RhP_B$ | $P_AP_B$ | $P_AF$ | $P_BF$ |
| 30.7 | 55.1 | 153 | 177 | 40 | 28 | 354 |

Spectrum 3.3.2 $^{31}P$ NMR of $[RhF(PPh_3)_3]$ in $CD_2Cl_2$ at 298K.

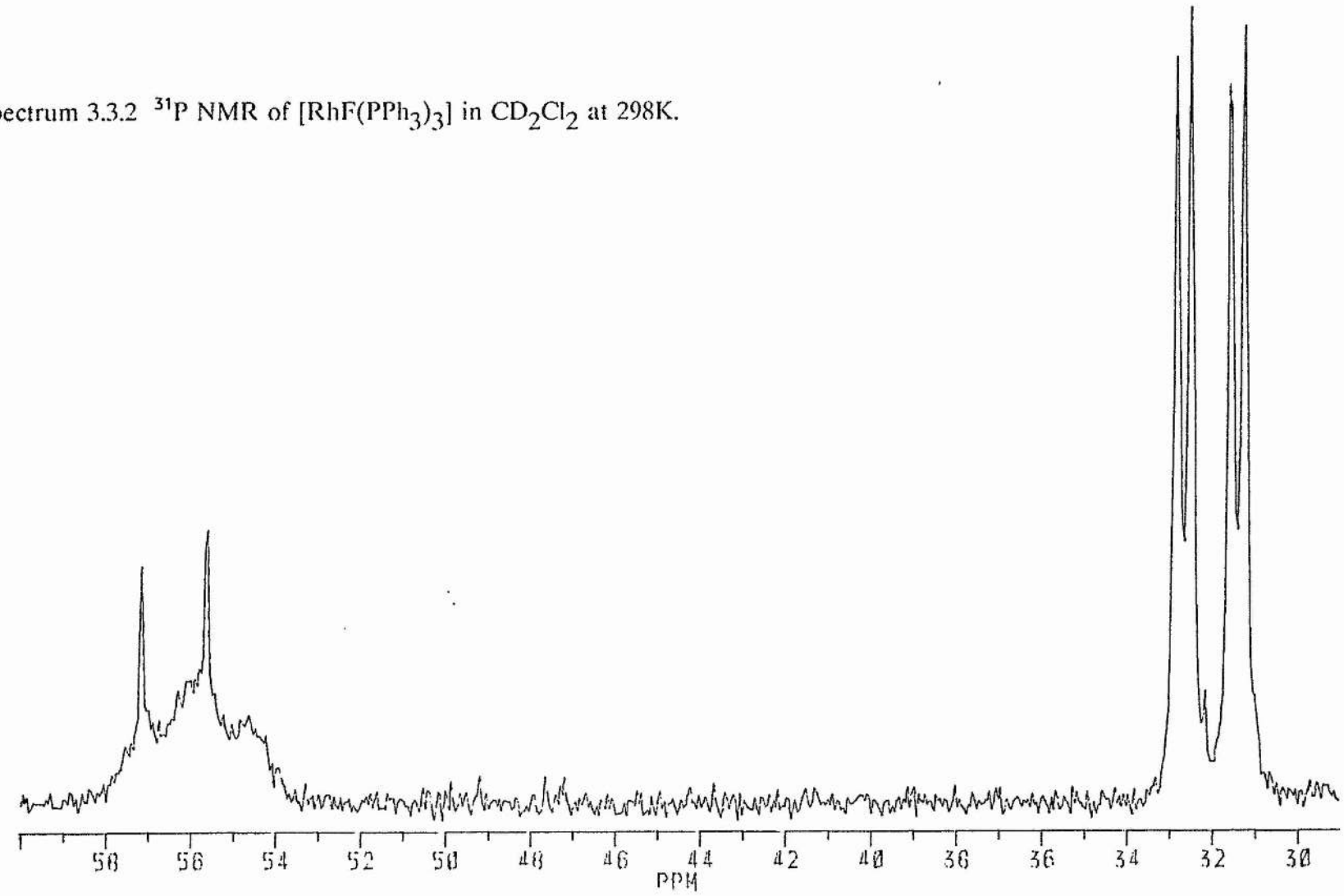

Spectrum 3.3.3 $^{31}P$ NMR of $[RhF(PPh_3)_3]$ in $CD_2Cl_2$ at 233K.

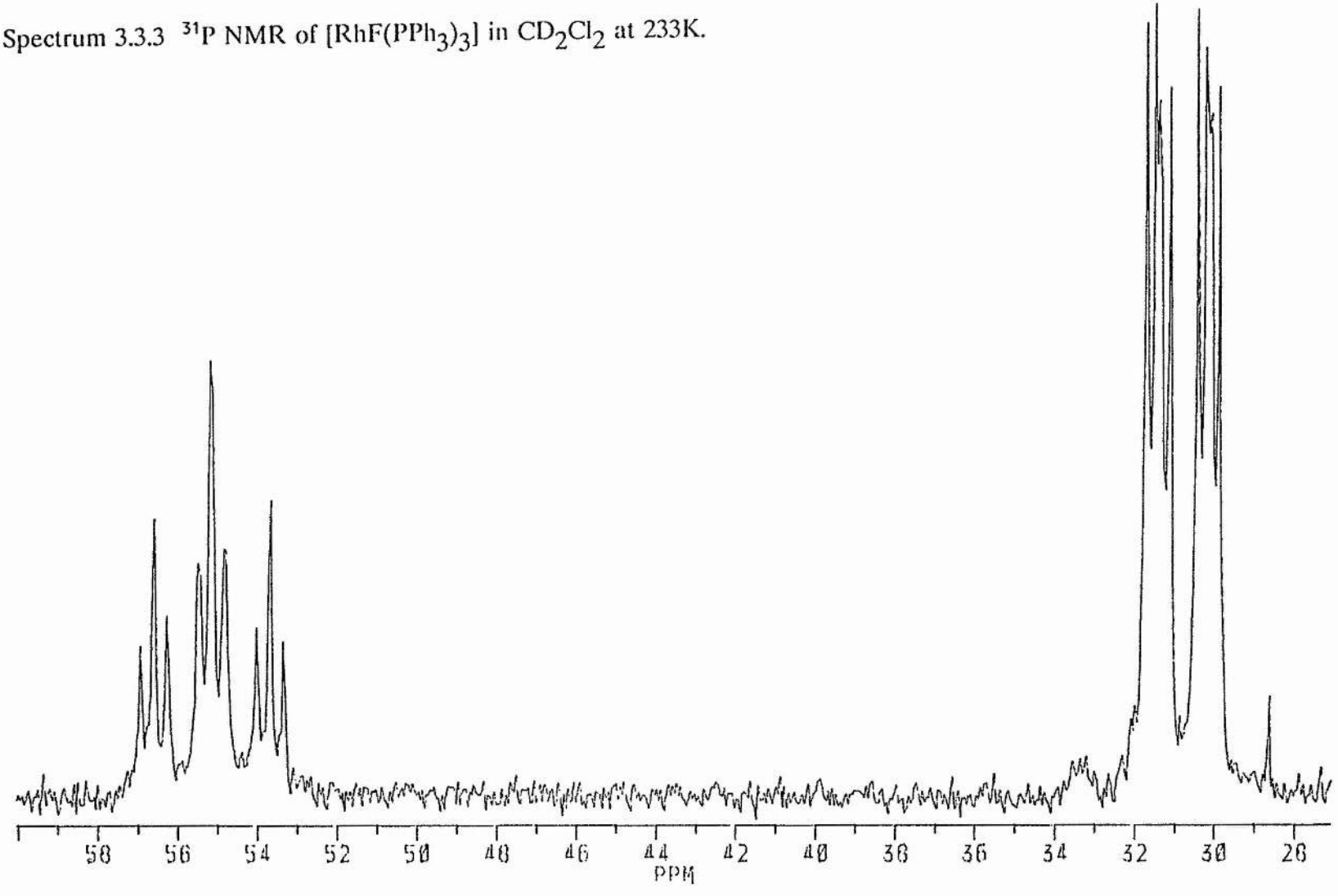

## 3.4 Fluxional Species obtained from the Reactions of $[RhF(PPh_3)_3]$ with Mixed Anhydride Ligands.

The reaction between $[RhF(PPh_3)_3]$ and the mixed anhydride derived from 2-methyl,3-phenylpropenoic acid, $[Ph_2PO_2CCMe=CHPh]$ was carried out at room temperature under dry dinitrogen, with a solution of the mixed anhydride in thf being added to a mole equivalent of $[RhF(PPh_3)_3]$ in thf.

The room temperature $^{31}P$ NMR of the microcrystalline solid obtained from the reaction consists of a broad doublet of doublets at a shift of $\delta$183.6 and a broad indistinguishable multiplet at about $\delta$34, as is shown in Spectrum 3.4.1. On cooling to -40°C a far clearer NMR spectrum is obtained (Spectrum 3.4.2), and it is from this that a species characterised as being $[RhF(P_APh_3)_2(Ph_2P_BO_2CCMe=CHPh)]$, a fluxional, 5-coordinate complex in which the mixed anhydride is bound to the rhodium metal centre via phosphorus and the carbonyl oxygen atom is found (see Figure 3.4.1). There is a resonance at $\delta$186.5 corresponding to the phosphorus atom of the mixed anhydride, $P_B$. The shift of this resonance is in a similar position to that observed for the cationic species $[Rh(PPh_3)_2(Ph_2PO_2CCMe=CHPh)]^+$ in which the mixed anhydride ligand is also bound to rhodium via phosphorus and carbonyl oxygen ($\delta$175.2). This resonance is split by a trans coupling to fluorine ($J_{P_BF}$=848.8Hz), by a coupling to rhodium ($J_{RhP_B}$=207.2Hz) and by two identical couplings to the neighbouring cis phosphorus atoms, $P_A$, ($J_{P_AP_B}$=42.7Hz) thus resulting in a doublet of doublet of triplets. The resonance assigned to the two triphenylphosphine ligands, $P_A$, has a coupling to rhodium ($J_{RhP_A}$=147.6Hz), a cis

coupling to the mixed anhydride phosphorus ($J_{P_AP_B}$=42.7Hz) and a cis coupling to fluorine ($J_{P_AF}$=22.8Hz), thus resulting in a doublet of doublet of doublets which is centred at $\delta$34.9.

Figure 3.4.1

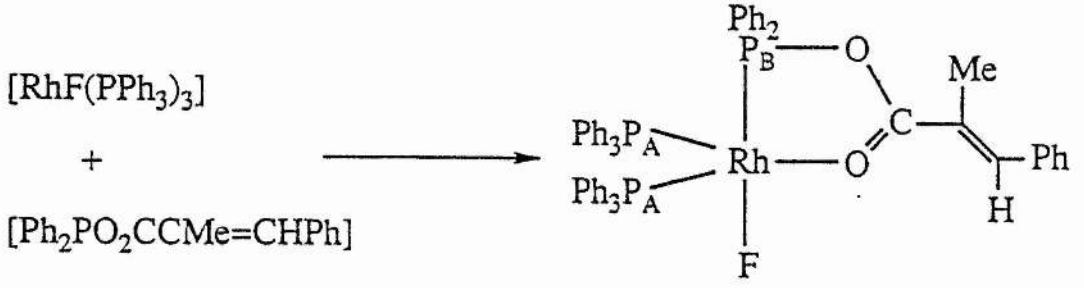


Information regarding the fluxionality of the product illustrated in Figure 3.4.1, is gained from the room temperature $^{31}$P NMR. Almost all detail about the resonance at $\delta$34 ($P_A$) is lost as opposed to the loss of only the mutal phosphorus coupling for the mixed anhydride resonace ($P_B$) at $\delta$183.6; the Rh-$P_B$ and $P_B$-F couplings of the latter clearly being displayed in the form of the retained doublet of doublets. Thus it is apparent from the data presented in Table 3.4.1 that the observed fluxionality in [RhF(PPh$_3$)$_2$(Ph$_2$PO$_2$CCMe=CHPh] is due to the rapid and reversible movement of triphenylphosphine ligands about the rhodium metal centre, and as a result couplings to this ligand are lost.

Spectrum 3.4.1 $^{31}P$ NMR of $[RhF(PPh_3)_2(Ph_2PO_2CCMe=CHPh)]$ in $CD_2Cl_2$ at 298K.

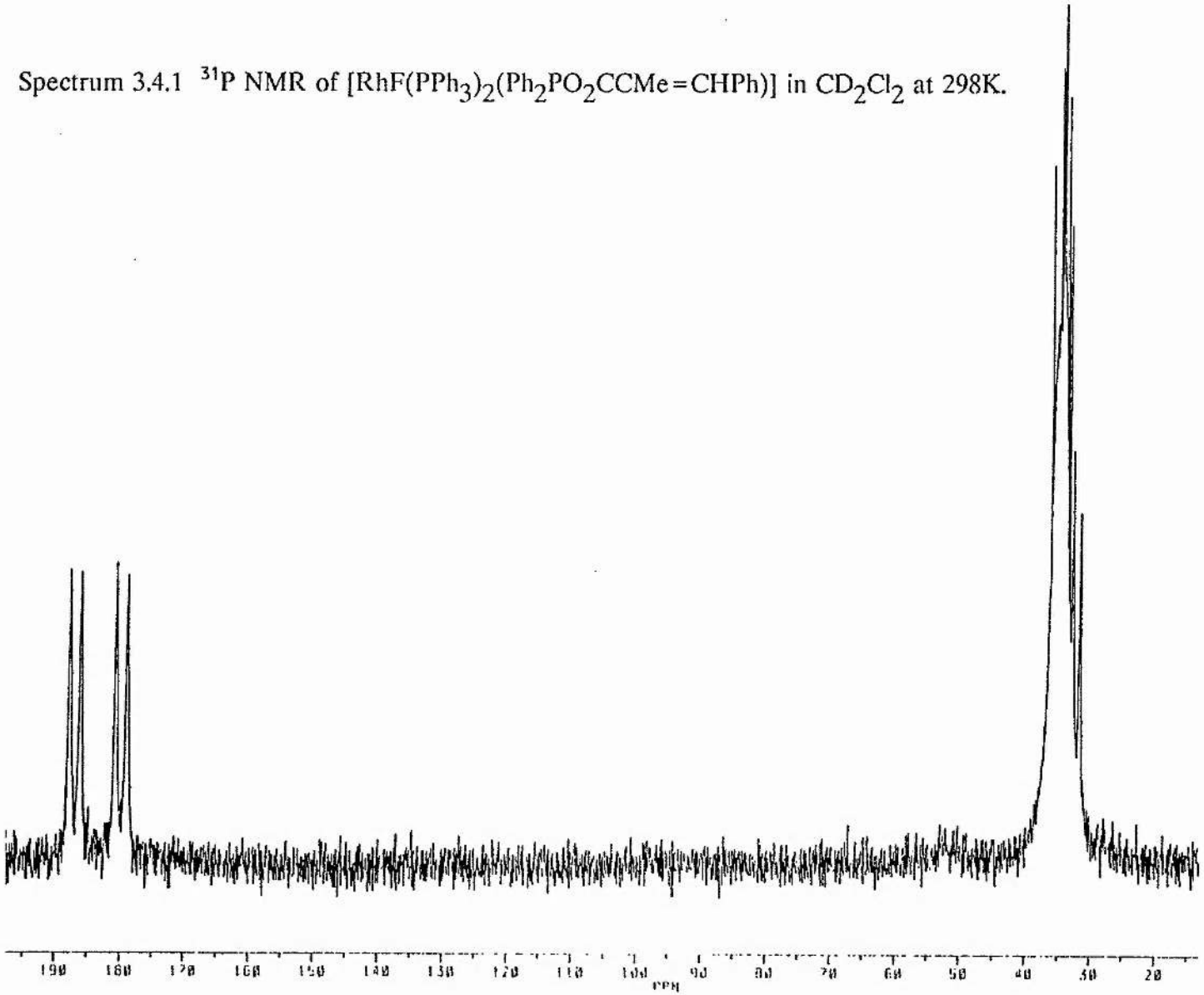

Spectrum 3.4.2 $^{31}P$ NMR of $[RhF(PPh_3)_2(Ph_2PO_2CCMe{=}CHPh)]$ in $CD_2Cl_2$ at 233K.

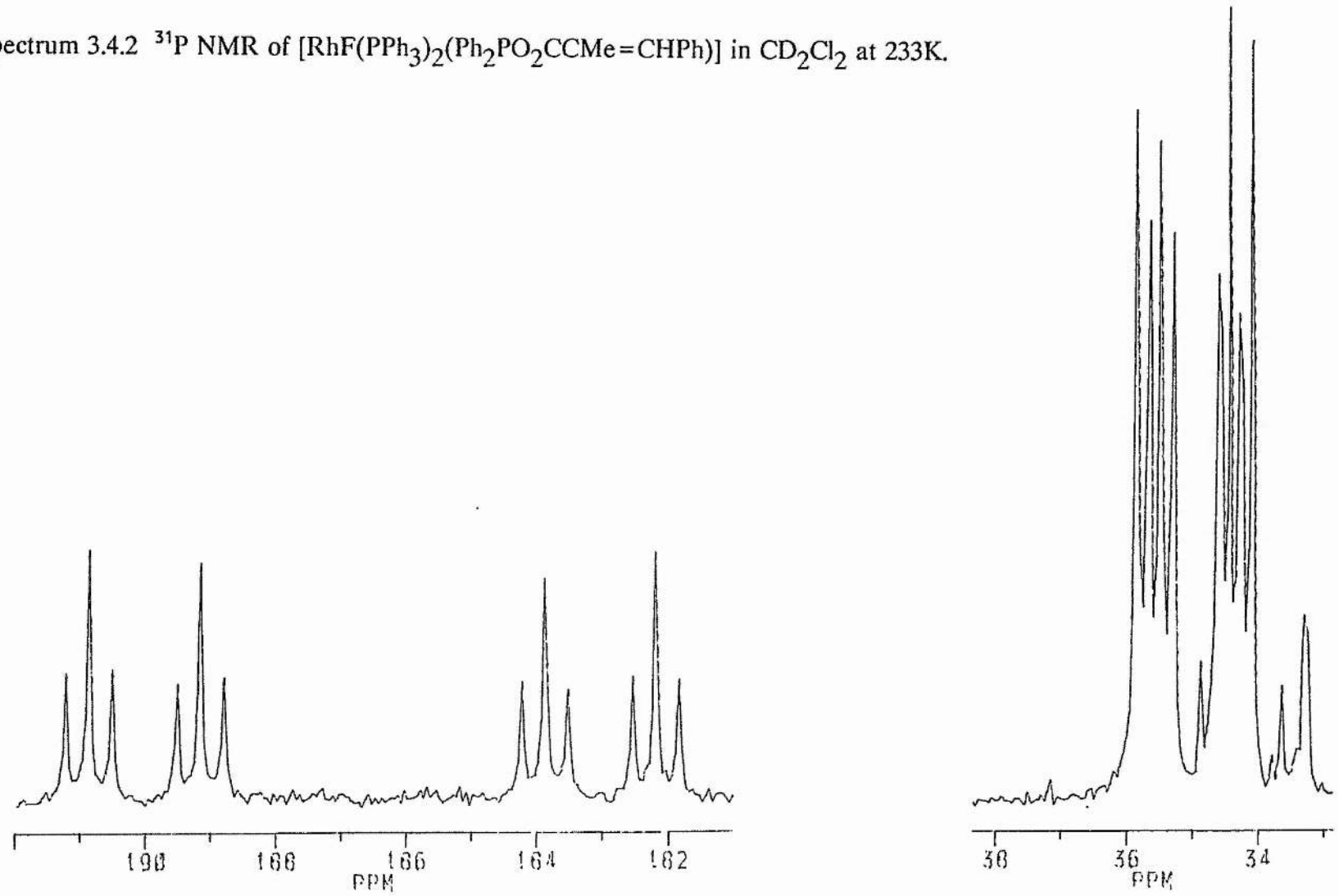

There are three possible mechanisms for this fluxionality. One involves an intra-molecular process - a Berry pseudorotation about the 5-coordinate metal centre. Although this need not lead to loss of P-P couplings or P-F couplings, it is possible that different mutual orientations of the phosphorus and fluorine ligands will give different coupling constants and that when these are arranged they are very different from those of the non-fluxional species. The second explanation would invoke intermolecular dissociative exchange of $PPh_3$ groups. In order to test this possiblity excess triphenylphosphine was added to a solution of $[RhF(PPh_3)_2(Ph_2PO_2CCMe=CHPh)]$ in $CD_2Cl_2$. $^{31}P$ NMR studies indicated that the spectra at different temperatures were identical to those obtained in the absence of $PPh_3$, thus ruling out intra-molecular exchange mechanisms involving triphenylphosphine. Finally it is possible that the fluxionality involves decoordination and recoordination of the mixed anhydride's carbonyl oxygen atom to give a square planar intermediate. Relatively large changes in coupling constants would be expected from this mechanism, particularly if the original complex were trigonal bipyramidal, as illustrated in Figure 3.4.2. Complexes containing either cis or trans $PPh_3$ groups could be formed but the greatest effect on the $PPh_3$ groups might occur if they are cis.

Figure 3.4.2

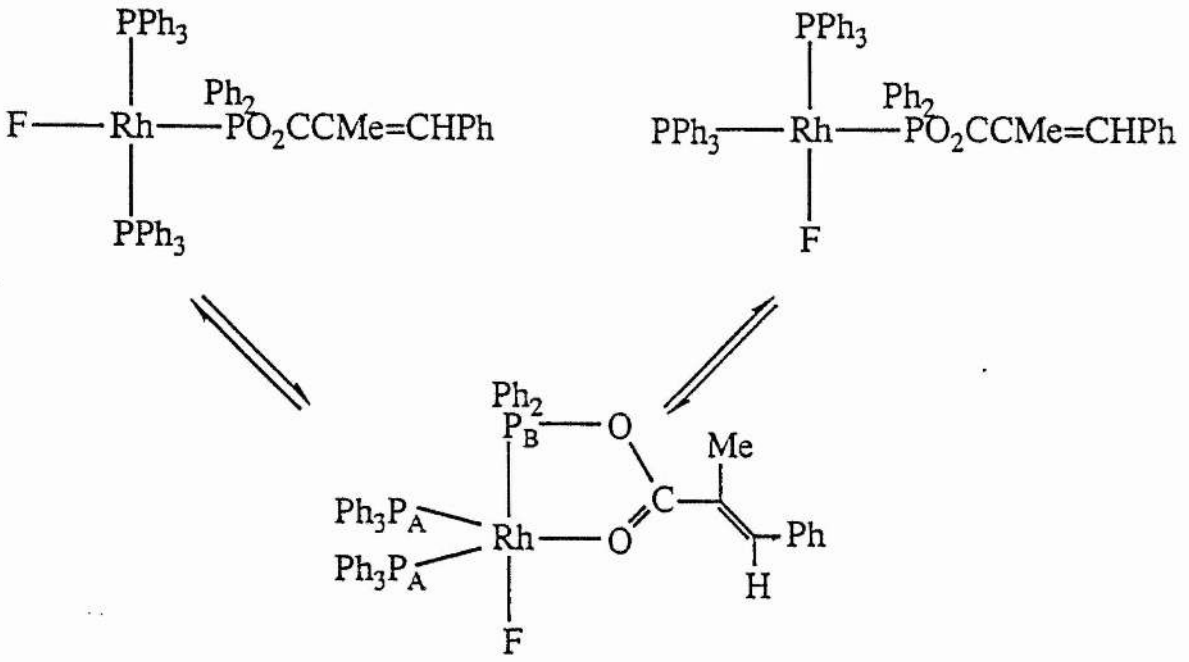


The room temperature $^{1}H$ NMR spectrum is, as its $^{31}P$ analogue, broad in nature, although signals at $\delta$6.4 and $\delta$1.15 (Table 3.4.2) are assigned to the hydrogen and methyl substituents of the vinylic double bond respectively. Accordingly at -40°C these signals sharpen (see Spectrum 3.4.3) and singlets are visible at $\delta$6.2 and $\delta$1.0, with the former at lower field than is observed in $[Rh(O_2CCMe=CHPh)(PPh_3)(Ph_2PO_2CCMe=CHPh)]$ ($\delta$4.70) but at higher field than is observed in $[Rh(PPh_3)_2(Ph_2PO_2CCMe=CHPh)]^+$ where the resonance is obscured by phenyl resonances.

Further evidence for the binding of the mixed anhydride through phosphorus and carbonyl oxygen is provided by the IR spectrum of $[RhF(PPh_3)_2(Ph_2PO_2CCMe=CHPh)]$. An absorption band at 1640cm$^{-1}$ corresponds to the carobn-carbon double bond stretching frequency, $\nu$(C=C). This

is in the region typical of complexes with the carbonyl oxygen atom bound to the rhodium metal centre ($1613cm^{-1}$ for $[Rh(PPh_3)_2(Ph_2PO_2CCMe=CHPh)]^+$). Similarly the band assigned to $\nu(C=O)$, $1591cm^{-1}$, is in the region associated with carbonyl oxygen being bound to rhodium ($1565cm^{-1}$ for $[Rh(PPh_3)_2(Ph_2PO_2CCMe=CHPh)]^+$).

The $^{19}F$ NMR spectrum at -40°C (see Spectrum 3.4.4 and Table 3.4.3) is represented schematically in Figure 3.4.3. It shows that the fluorine atom in the complex is coupled to the phosphorus atom of the mixed anhydride ($J_{P_BF}=852.5Hz$), to both of the phosphorus atoms of the two triphenylphosphine ligands ($J_{P_AF}=20.5Hz$) and to rhodium ($J_{RhF}=14.6Hz$). The shift of the resonance is centred at $\delta 114.8$ to the high field side of the $CCl_3F$ reference.

Figure 3.4.3

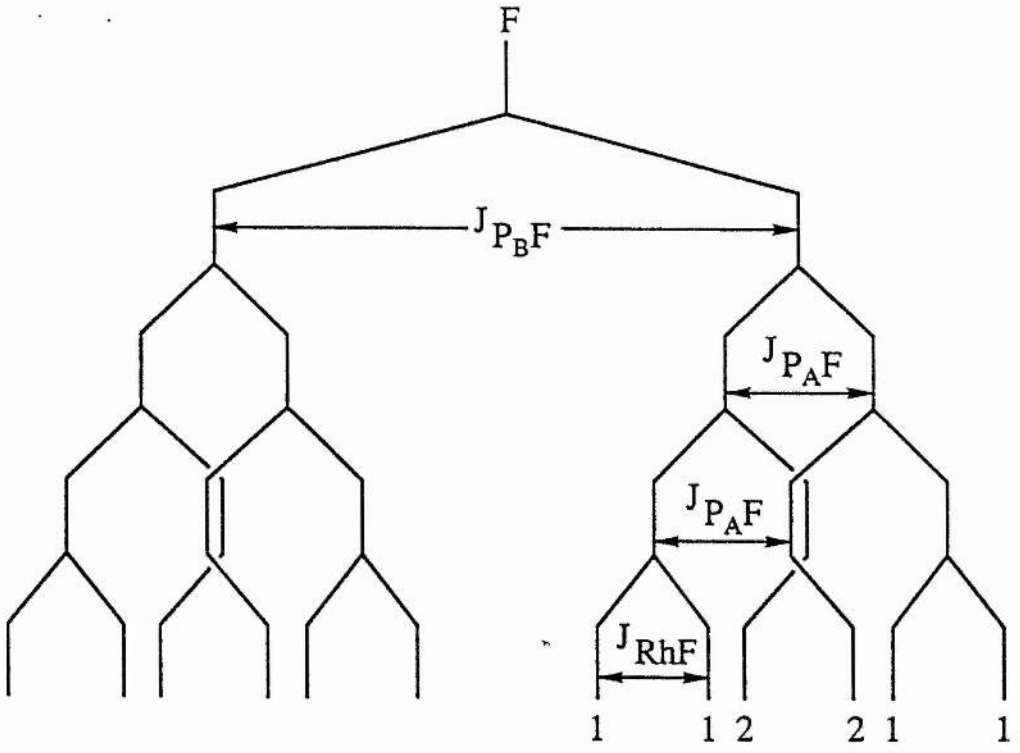

Spectrum 3.4.3 $^{1}H$ NMR of $[RhF(PPh_3)_2(Ph_2PO_2CCMe{=}CHPh)]$ in $CD_2Cl_2$ at 233K.

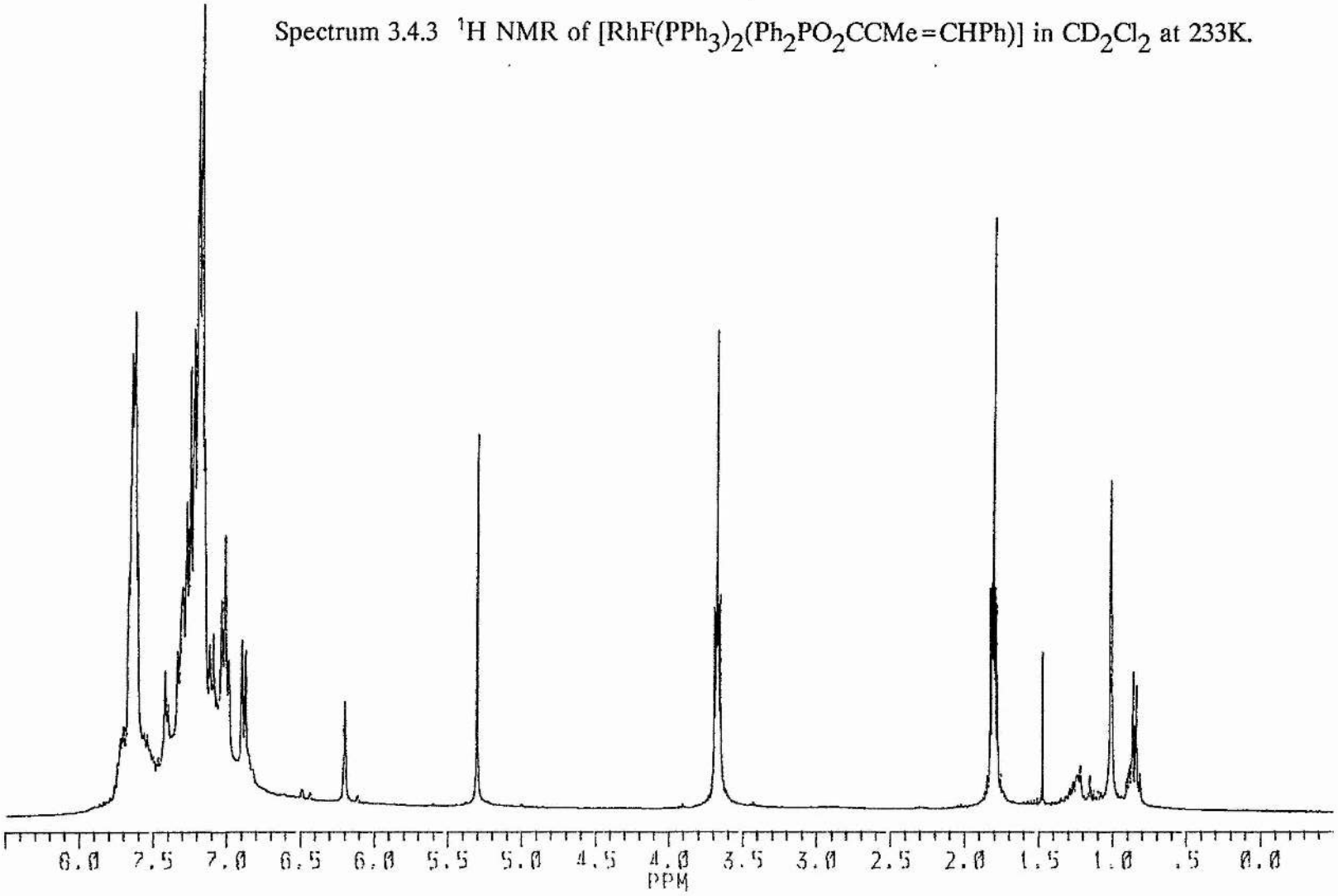

Spectrum 3.4.4 $^{19}F$ NMR of $[RhF(PPh_3)_2(Ph_2PO_2CCMe{=}CHPh)]$ in $CD_2Cl_2$ at 233K.

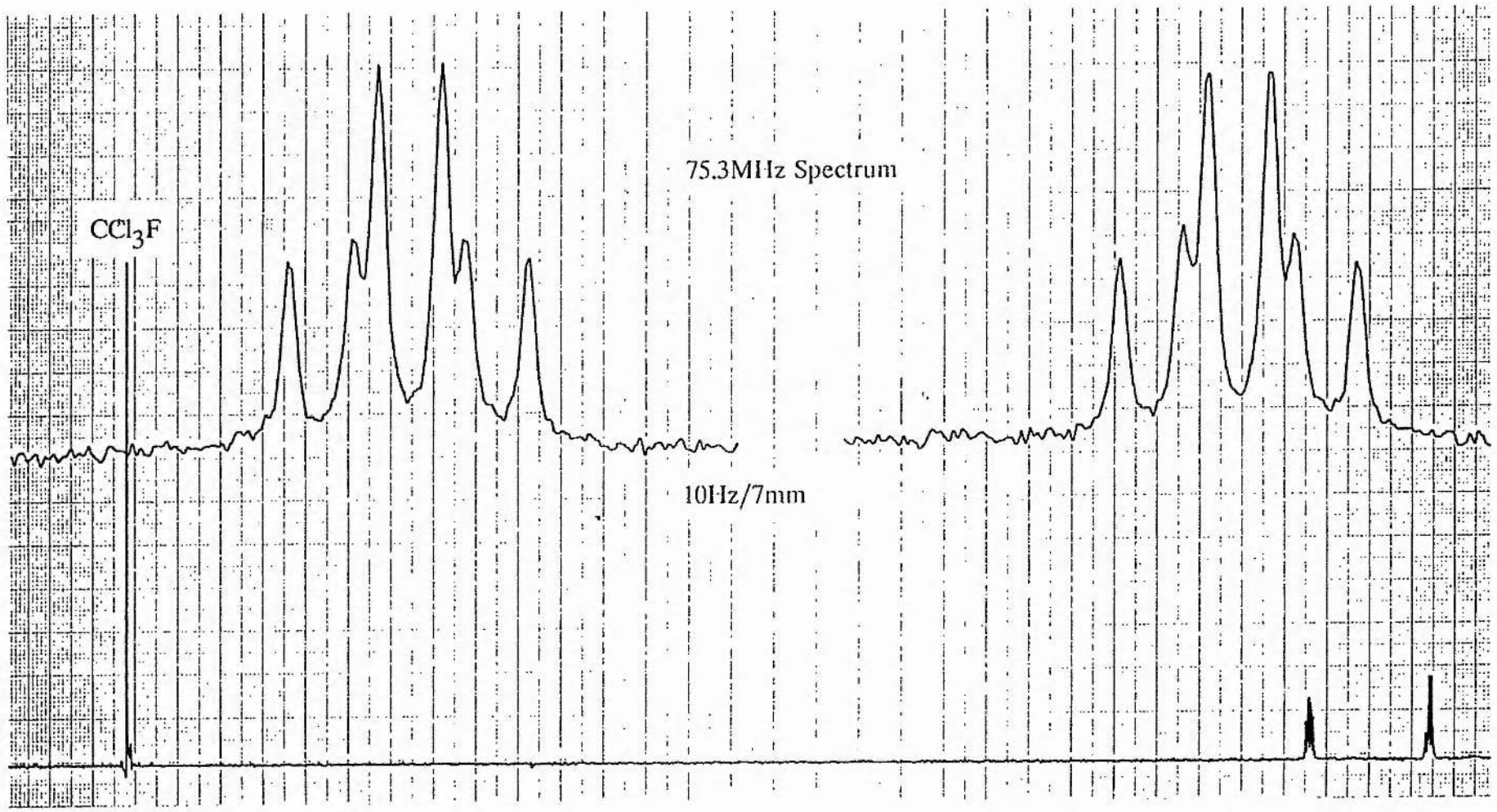

In a similar manner as for $[RhF(PPh_3)_2(Ph_2PO_2CCMe=CHPh)]$, $[RhF(PPh_3)_3]$ and the mixed anhydride derived from hexa-2,4-dienoic acid, $[Ph_2PO_2CCH=CH-CH=CHMe]$, react to give a fluxional 5-coordinate complex in which the mixed anhydride is bound to the rhodium metal centre via phosphorus and the carbonyl oxygen atom (see Figure 3.4.4).

Figure 3.4.4

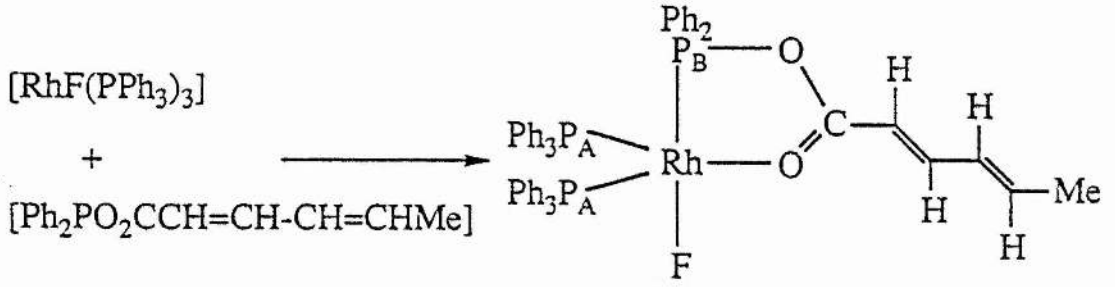


Both the room temperature and low temperature $^{31}P$ NMRs of the product illustrated in Figure 3.4.4 are similar in splitting pattern to those observed for $[RhF(PPh_3)_2(Ph_2PO_2CCMe=CHPh)]$, however there are slight differences in the values of coupling constants, as would be expected. The data presented in Table 3.4.1 shows that at -60°C the resonance assigned to the phosphorus atom ofthe mixed anhydride ligand ($P_B$) is at $\delta$185.3(ddt) and the couplings associated with it $J_{RhP_B}$, $J_{P_AP_B}$ and $J_{P_BF}$ are 207.4, 43.2 and 854.6Hz respectively. The resonance assigned to the phosphorus atom of the triphenylphosphine ligands ($P_A$) is centred at $\delta$33.8 with $J_{RhP_A}=146.4$Hz, $J_{P_AP_B}=43.2$Hz and $J_{P_BF}=18.2$Hz.

The low temperature $^1H$ NMR of $[RhF(PPh_3)_2(Ph_2PO_2CCH^e=CH^d-CH^c=CH^bMe^a)]$ (see Spectrum 3.4.5 and Table 3.4.2) consists of resonances at

$\delta$1.58(d), $\delta$4.65(brd) and $\delta$5.45(m) corresponding to -$Me^a$, -$CH^e$ and =$CH^d$-$CH^c$=$CH^b$ respectively. These shifts are at lower field compared with those observed for [$RhCl(PPh_3)_2(Ph_2PO_2CCH=CH-CH=CHMe)$] in which the mixed anhydride is bound through phosphorus and a carbon-carbon double bond.

IR data also illustrate that the mixed anhydride in [$RhF(PPh_3)_2(Ph_2PO_2CCH=CH-CH=CHMe)$] is bound through phosphorus and carbonyl oxygen since $\nu$(C=O) is assigned to an absorption at 1577$cm^{-1}$ whilst absorption bands at 1652 and 1617 $cm^{-1}$ are assignable to $\nu$(C=C).

The room temperature $^{19}F$ NMR of [$RhF(PPh_3)_2(Ph_2PO_2CCH=CH-CH=CHMe)$] (Table 3.4.3) consists of two broad resonances centred at $\delta$117.0 and the only coupling observed is that of $J_{P_BF}$ which is about equal to 865Hz, thus indicating once again the fluxionality of the complex.

An experiment aimed at further substantiating the ability of the mixed anhydride to bind through phosphorus and carbonyl oxygen involved the reaction of [$RhF(PPh_3)_3$] and [$Ph_2PO_2CCH_2CH_2Me$], the mixed anhydride derived from butanoic acid. Since this ligand has no carbon-carbon double bond the only manners in which it can bind to rhodium are via phosphorus alone or via phosphorus and carbonyl oxygen. The room temperature $^{31}P$ NMR of the product is similar to that observed for both [$RhF(PPh_3)_2(Ph_2PO_2CCMe=CHPh)$] and [$RhF(PPh_3)_2(Ph_2PO_2CCH=CHCH=CHMe)$] in that there is a broad doublet of doublets at $\delta$183.1 and a broad resonance at $\delta$34.1. The $^1H$ NMR shows all the

resonances assignable to the anhydride between $\delta$0.4 and $\delta$1.4 and this is comparable to that which is observed for $[RhCl(PPh_3)_2(Ph_2PO_2CCH_2CH_2Me)]$, the fluxional 5-coordinate species in which the mixed anhydride is bound through phosphorus and carbonyl oxygen (see Chapter 2).

Another reaction involved the addition of $[Ph_2POCH_2CHCMe_2]$,[20] derived from the corresponding allylic alcohol and consequently possessing no C=O group, to $[RhF(PPh_3)_3]$. No isolable product was obtained from this reaction thus proving that a carbonyl group is required to bind to the rhodium metal centre.

The use of the fluxional species $[RhF(PPh_3)_2(Ph_2PO_2CCH=CHCH=CHMe)]$ as a catalyst precursor in the hydrogenation of hexa-2,4-dienoic acid is discussed in Chapter 5.

Spectrum 3.4.5 $^{1}H$ NMR of $[RhF(PPh_3)_2(Ph_2PO_2CCH=CH\text{-}CH=CHMe)]$ in $CD_2Cl_2$ at 213K.

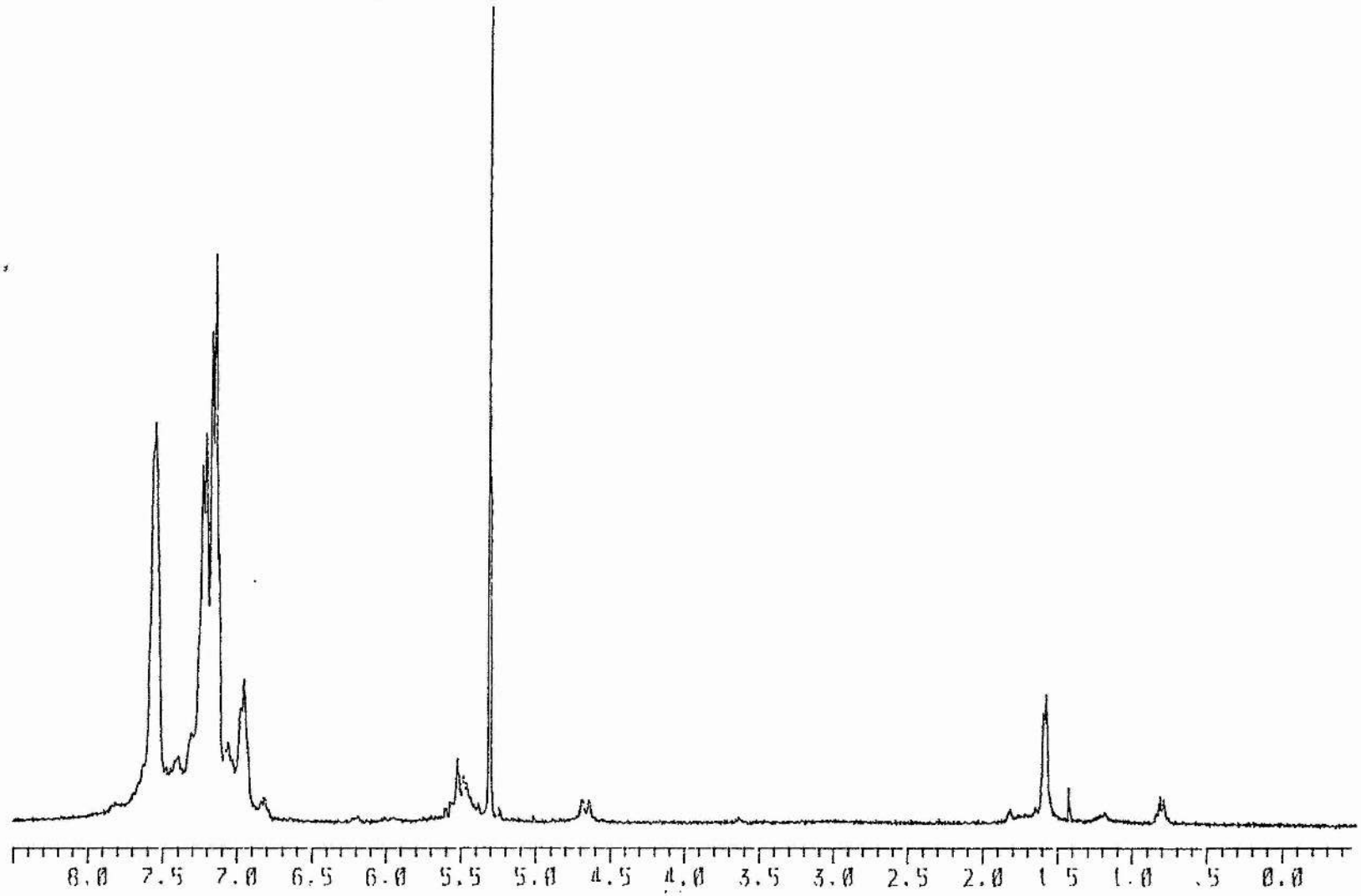

Table 3.4.1 $^{31}P$ NMR data for $[RhF(PPh_3)_2(Ph_2PO_2CCR=CR'R'')]$ complexes in $CD_2Cl_2$ at 298K.

| | δ | | J/Hz | | | | |
|---|---|---|---|---|---|---|---|
| Fluxional Species | $P_A$ | $P_B$ | $RhP_A$ | $RhP_B$ | $P_AF$ | $P_BF$ | $P_AP_B$ |
| $[RhF(P_APh_3)_2(Ph_2P_BO_2CCMe=CHPh)]$ | 34.0(br) | 183.6(dd) | - | 205.2 | - | 865.7 | - |
| $[RhF(P_APh_3)_2(Ph_2P_BO_2CCMe=CHPh)]$[a] | 34.9(ddd) | 186.5(ddt) | 147.6 | 207.2 | 22.8 | 848.8 | 42.7 |
| $[RhF(P_APh_3)_2(Ph_2P_BO_2CCHCHCHCHMe)]$ | 34.4(br) | 182.5(ddd) | - | 207.8 | - | 865.9 | - |
| $[RhF(P_APh_3)_2(Ph_2P_BO_2CCHCHCHCHMe)]$[b] | 33.8(ddd) | 185.3(ddt) | 146.4 | 207.4 | 18.2 | 854.6 | 43.2 |
| $[RhF(P_APh_3)_2(Ph_2P_BO_2CCH_2CH_2Me)]$ | 34.1(br) | 183.1(dd) | - | 206.5 | - | 867.6 | - |
| Non-Fluxional Species | | | | | | | |
| $[RhF(P_APh_3)_2(Ph_2P_BO_2CCMe=CHPh)]$ | 34.3(ddd) | 179.6(ddt) | 138.4 | 221.4 | 20.6 | 856.1 | 39.8 |
| $[RhF(P_APh_3)_2(Ph_2P_BO_2CCMe=CHPh)]$[a,c] | 35.8(ddd) | 181.4(ddt) | 149.1 | 205.4 | 14.6 | 869.5 | 43.3 |
| $[RhF(P_APh_3)_2(Ph_2P_BO_2CCHCHCHCHMe)]$ | 34.3(ddd) | 179.5(ddt) | 137.7 | 221.7 | 21.0 | 855.9 | 39.9 |

[a]233K [b]213K [c]in d-thf

Table 3.4.2 $^{1}H$ NMR data for $[RhF(PPh_3)_2(Ph_2PO_2CCR=CR'R'')]$ complexes in $CD_2Cl_2$ at 298K.

| | δ(ppm) | | | |
|---|---|---|---|---|
| Fluxional Species | | | | |
| $[RhF(PPh_3)_2(Ph_2PO_2CCMe^b=CH^aPh)]$ | $^a$1.15(br) | $^b$6.40(br) | | |
| $[RhF(PPh_3)_2(Ph_2PO_2CCMe^b=CH^aPh)]^x$ | $^a$1.00(s) | $^b$6.20(s) | | |
| $[RhF(PPh_3)_2(Ph_2PO_2CCH^e=CH^d\text{-}CH^c=CH^bMe^a)]^y$ | $^a$1.58(d) | $^{b,c,d}$5.45(m) | $^e$4.65(brd) | |
| Non-Fluxional Species | | | | |
| $[RhF(PPh_3)_2(Ph_2PO_2CCMe^b=CH^aPh)]$ | $^a$1.25(br) | $^b$Obscured by phenyl resonances | | |
| $[RhF(PPh_3)_2(Ph_2PO_2CCMe^b=CH^aPh)]^{x,z}$ | $^a$1.19(s) | $^b$6.50(s) | | |
| $[RhF(PPh_3)_2(Ph_2PO_2CCH^e=CH^d\text{-}CH^c=CH^bMe^a)]$ | $^a$1.79(d) | $^b$5.73(br) | $^{c,d}$6.16(br) | $^e$5.23(br) |

$^x$233K $^y$213K $^z$in d-thf

Table 3.4.3 $^{19}F$ NMR data for $[RhF(PPh_3)_2(Ph_2PO_2CCR=CR'R'')]$ complexes in $CD_2Cl_2$ at 298K.

| | $\delta$ | J/Hz | | |
|---|---|---|---|---|
| | | $P_AF$ | $P_BF$ | RhF |
| Fluxional Species | | | | |
| $[RhF(PPh_3)_2(Ph_2PO_2CCMe=CHPh)]$[a] | 114.8 | 20.5 | 852.5 | 14.6 |
| $[RhF(PPh_3)_2(Ph_2PO_2CCH=CH-CH=CHMe)]$ | 117.0 | - | 865.0 | - |
| Non-Fluxional Species | | | | |
| $[RhF(PPh_3)_2(Ph_2PO_2CCMe=CHPh)]$ | 110.5 | 20.5 | 856.9 | 14.9 |
| $[RhF(PPh_3)_2(Ph_2PO_2CCH=CH-CH=CHMe)]$ | 110.4 | 20.8 | 856.9 | 14.0 |

[a]233K

## 3.5 Non-Fluxional Species obtained from the Reactions of $[RhF(PPh_3)_3]$ with Mixed Anhydride Ligands.

Somewhat different results are obtained if the reactions between $[RhF(PPh_3)_3]$ and mixed anhydrides are carried out in $CH_2Cl_2$. As indicated previously, $[RhF(PPh_3)_3]$ reacts with $CH_2Cl_2$ to give $[RhCl(PPh_3)_3]$, so that both the fluoro and chloro species are present when the mixed anhydride is added.

In most cases, NMR studies of the products of these reactions show the presence of $[RhCl(PPh_3)_n(Ph_2PO_2CCR=CR'R'')](n=1 \text{ or } 2)$[21], expected from the reaction of $[RhCl(PPh_3)_3]$ with the mixed anhydride, together with two other species. One is $[RhF(PPh_3)_2(Ph_2PO_2CCR=CR'R'')]$ which exhibits the fluxionality described in the previous section, whilst the other, which has the same chemical formula, is non-fluxional and exhibits $^{31}P$ and $^{19}F$ NMR parameters at 25°C very similar to those of fluxional $[RhF(PPh_3)_2(Ph_2PO_2CCR=CR'R'')]$ at -40°C (see Tables 3.4.1 and 3.4.3). In some cases, eg where R = Me, R' = H, R'' = Ph, only the non-fluxional species has been observed together with $[RhCl(PPh_3)_2(Ph_2PO_2CCMe=CHPh)]$, see Spectrum 3.5.1 for the $^{31}P$ NMR. Interestingly, in the solutions containing both the fluxional and non-fluxional species there is no interconversion on the NMR timescale, although it should be noted that when non-fluxional $[RhF(PPh_3)_2(Ph_2PO_2CCMe=CHPh)]$ is heated to 50°C in $CD_2Cl_2$ the fluxional species is formed irreversibly.

Spectrum 3.5.1 $^{31}P$ NMR of $[RhF(PPh_3)_2(Ph_2PO_2CCMe=CHPh)]$ and $[RhCl(PPh_3)_2(Ph_2PO_2CCMe=CHPh)]$ mixture in $CD_2Cl_2$ at 298K.

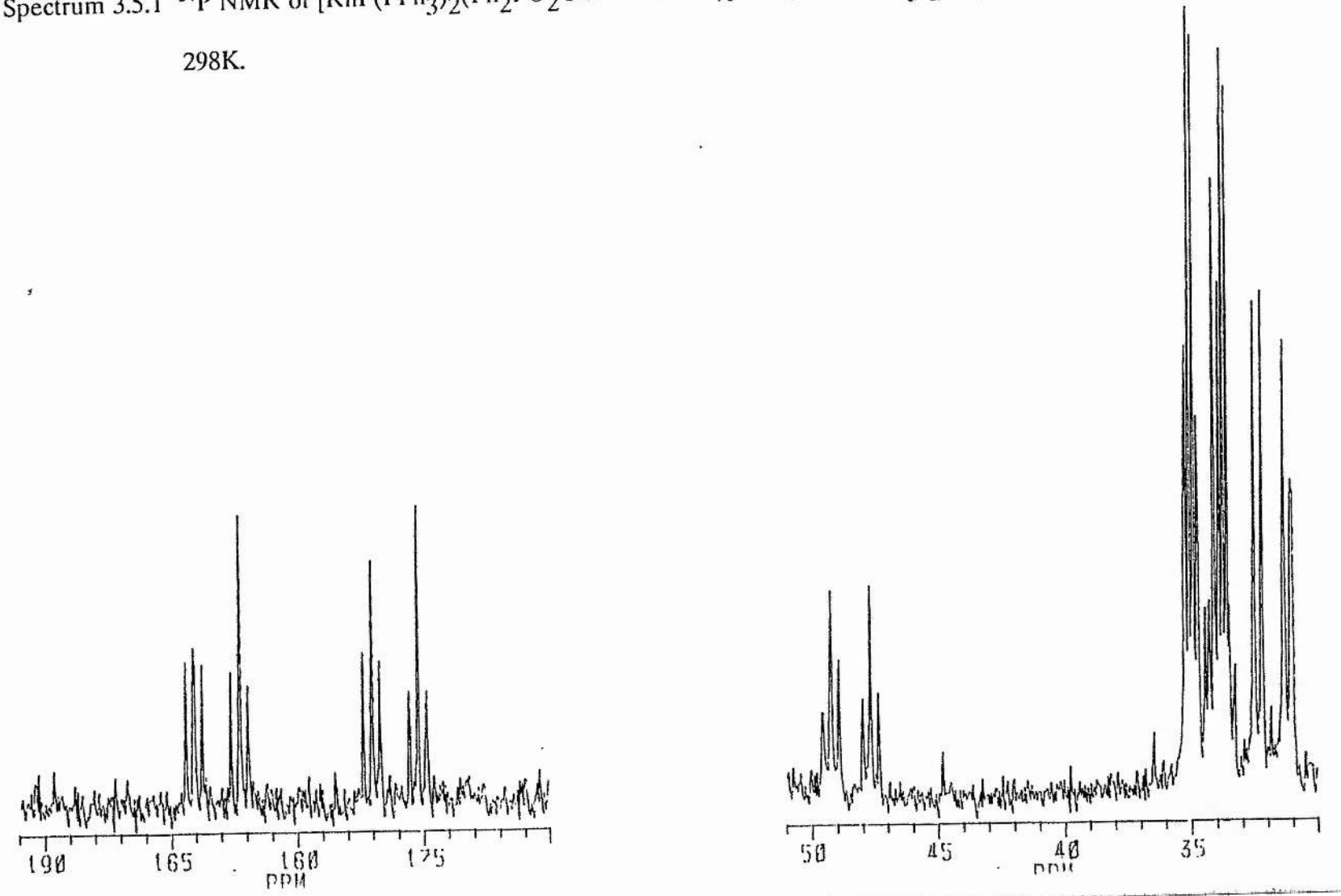

The main differences between the low temperature limiting $^{31}P$ NMR of the fluxional species and the room temperature NMR of the non-fluxional species are the chemical shift of the phosphorus atom of the mixed anhydride ligand and the couplings of the phosphorus atoms to rhodium. The phosphorus resonance in fluxional $[RhF(PPh_3)_2(Ph_2PO_2CCMe=CHPh)]$ is at $\delta$186.5(ddt) compared with $\delta$181.4(ddt) for the corresponding non-fluxional species.

One possible explanation of these observations might be that there are two possible forms of the complex, one with trigonal bipyramidal geometry and one with square pyramidal geometry (see Figure 3.5.1). If this were the case, the process leading to the fluxionality of one of the species must not include the non-fluxional species as an intermediate and so a Berry pseudorotation is unlikely.

Figure 3.5.1

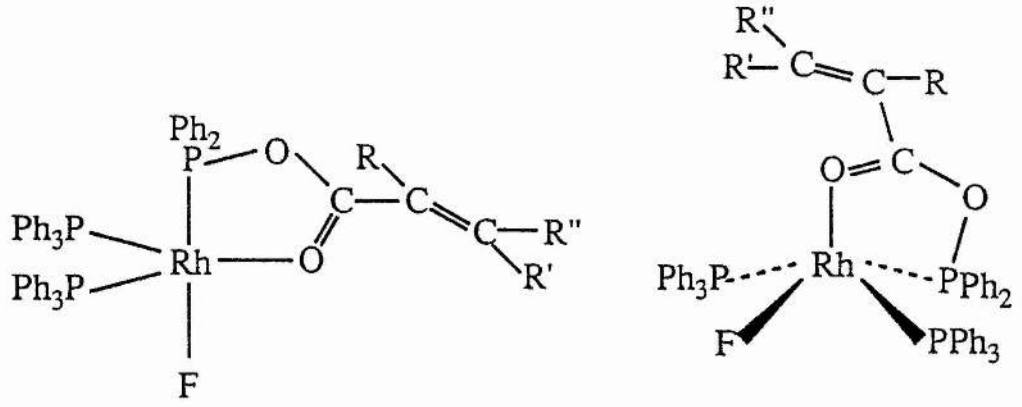


**A** **B**

It is, however, possible that decoordination of the carbonyl oxygen atom occurs in one, but not the other isomer. An explanation that is consistent with all the data is that isomer A in Figure 3.5.1 is the fluxional species and decoordinates the

carbonyl oxygen atom to give the cis square planar intermediate, whilst B is either rigid on the NMR timescale or decomplexes the O atom to give the trans square planar intermediate, the NMR parameters of which will be similar to those of B so that fluxionality might not be observed.

Other explanations, such as the possibility of bonding of the mixed anhydride through phosphorus and carbonyl oxygen in one case or phosphorus and the double bond in the other can be ruled out on the basis of the similar chemical shifts of the phosphorus atoms of the mixed anhydride in both isomers.

It is not clear why the two different isomers form under different conditions, although it may possibly be associated with the different solvating powers of the reaction solvents, $CH_2Cl_2$ and thf, that subtly interfere with the progress of the reaction thus favouring one isomer in $CH_2Cl_2$ and the other in thf.

## 3.6 Experimental.

All manipulations were carried out under dry oxygen-free nitrogen using standard Schlenk line and catheter tubing techniques. All solvents were purfified by distillation from calcium hydride ($CH_2Cl_2$) or sodium diphenylketyl [toluene, petroleum (boiling range 40-60°C), diethyl ether and tetrahydrofuran (thf)].

Preparation of Fluxional [$RhF(PPh_3)_2(Ph_2PO_2CCMe=CHPh)$].

To a suspension of [$RhF(PPh_3)_3$] (0.208g, 0.23mmol) in thf ($30cm^3$) was added a solution of $Ph_2PO_2CCMe=CHPh$ (0.08g, 0.23mmol) in thf ($20cm^3$). On addition the reaction solution became clearer and pale orange in colour. The solution was stirred for 2h and the solvent was then reduced in volume, in vacuo, to $3cm^3$. Light petroleum ($50cm^3$) was added, however no precipitate was formed. The solution became cloudy and on leaving at -40°C for 2h a precipitate was formed. This was then filtered off and dried in vacuo. Yield 0.14g (61.6%) (Found: C, 69.31%; H, 4.89%. $C_{58}H_{49}FO_2P_3Rh$ requires C, 70.17%; H, 4.97%).

Preparation of Fluxional [$RhF(PPh_3)_2(Ph_2PO_2CCH=CH-CH=CHMe)$].

To a suspension of [$RhF(PPh_3)_3$] (0.58g, 0.64mmol) in thf ($40cm^3$) was added a solution of $Ph_2PO_2CCH=CH-CH=CHMe$ (0.19g, 0.64mmol) in thf ($30cm^3$). On addition the reaction solution became clearer and pale orange in colour. The solution was stirred for 1h and the solvent was then reduced in volume, in vacuo, to $3cm^3$. Light petroleum ($50cm^3$) was added, however no precipitation occurred. On leaving at -40°C for 2h a microcrystalline material was formed. This was then

filtered off and dried in vacuo. Yield 0.41g (68.0%).

Preparation of Fluxional $[RhF(PPh_3)_2(Ph_2PO_2CCH_2CH_2Me)]$.

To a suspension of $[RhF(PPh_3)_3]$ (0.21g, 0.23mmol) in thf ($30cm^3$) was added a solution of $Ph_2PO_2CCH_2CH_2Me$ (0.06g, 0.23mmol) in thf ($20cm^3$). After stirring for 1h the solvent was reduced in volume, in vacuo, to $3cm^3$. Light petroleum ($50cm^3$) was added and the solution was left at -40°C for 2h, after which time a microcrystalline material was formed. This was then filtered off and dried in vacuo. Yield 0.13g (61.6%).

Reaction between $[RhF(PPh_3)_3]$ and $Ph_2PO_2CCMe=CHPh$ in $CH_2Cl_2$.

As stated in Section 3.5, in most cases the title reaction gave a mixture of products, namely $[RhCl(PPh_3)_2(Ph_2PO_2CCMe=CHPh)]$ and fluxional and non-fluxional $[RhF(PPh_3)_2(Ph_2PO_2CCMe=CHPh)]$. In other cases fluxional $[RhF(PPh_3)_2(Ph_2PO_2CCMe=CHPh)]$ was not observed, however the following synthesis is a general account of the title reaction.

To a solution of $[RhF(PPh_3)_3]$ (0.32g, 0.35mmol) in $CH_2Cl_2$ ($30cm^3$) was added a solution of $Ph_2PO_2CCMe=CHPh$ (0.12g, 0.35mmol) in $CH_2Cl_2$ ($20cm^3$). After stirring for 2h the solvent was reduced in volume, under vacuum, to $3cm^3$. Light petroleum ($50cm^3$) was added to precipitate the product mixture as an orange powder that was filtered off and dried under vacuum. $^{31}P$ and $^{1}H$ NMR showed the presence of the aforementioned product complexes.

## CHAPTER 3 REFERENCES


1 J E Huheey, "Inorganic Chemistry", 3rd ed., Harper and Row, New York, 1983, 268.

2 A Martinsen and J Songstad, J Acta Chem. Scand., A, 1977, **31**, 645.

3 R K Sharma and J L Fry, J Org. Chem., 1983, **48**, 2112.

4 L Vaska and J Peone Jr., J Chem. Soc., Chem. Comm. 1971, 418.

5 L Vaska and J Peone Jr., Inorg. Smynth., 1974, **15**, 64.

6 A A Grinberg, M M Singh and Yu S Varshavskii, Russ. J. Inorg. Chem., 1968, **13**, 1399.

7 Yu S Varshavskii, M M Singh and N A Buzina, Russ. J. Inorg. Chem., 1971, **16**, 1372.

8 M A Cairns, K R Dixon and J J McFarland, J Chem. Soc., Dalton Trans., 1975, 1159.

9 N M Doherty and N W Hoffman, Chem. Rev., 1991, **91**, 553.

10 HLM van Gaal, F L A van den Bekerom and J P J Verlaan, J Organomet., Chem., 1976, **114**, C35.

11 R R Burch, R L Harlow and S D Ittel, Organometallics, 1987, **6**, 982.

12 R Brady, B R Flynn, G L Geoffroy, H B Gray, J Peone Jr. and L Vaska, Inorg. Chem., 1976, **15**, 1485.

13

(a) G L Geoffroy, H Isci, J Litrenti and W R Mason, Inorg. Chem., 1977, **16**, 1950.

(b) G L Geoffroy, M S Wrighton, G S Hammond and H B Gray, J. Am. Chem. Soc., 1974, **96**, 3105.

14 K Goswami, M M Singh, J. Ind. Chem. Soc., 1979, **56**, 477.

15 C A McAuliffe and R J Pollock, J. Organomet. Chem., 1974, **77**, 265.

16 G Schiavon, S Zecch, G Pilloni and M Martelli, J. Inorg. Nucl. Chem., 1977, **39**, 115.

17 I J Colquhoun and W McFarlane, J Mag. Res., 1982, **46**, 525.

18 A van der Ent and A L Onderdelinden, Inorg. Synth., 1973, **14**, 92.

19 W D Jones, M G Partridge and R N Perutz, J. Chem. Soc., Chem. Commun., 1991, 264.

20 D C Cupertino and D J Cole-Hamilton, J Chem. Soc., Dalton Trans., 1987, 443.

21 A F Borowski, A Iraqi, D C Cupertino, D J Irvine and D J Cole-Hamilton, J Chem. Soc, Dalton Trans, 1990, 29.

# CHAPTER 4

# PREPARATION OF RHODIUM TRIFLUOROMETHYL COMPLEXES

## 4.1 Introduction.

As previously stated in Chapter 2, the hydrogenation of hexa-2,4-dienoic acid using catalysts of general formula $[RhCl(PPh_3)_n(Ph_2PO_2CCR=CR'R'')]$ occurs via two simultaneous mechanisms. The formation of hexanoic acid is brought about by the oxygen bound carboxylate ligand of the active species $[Rh(O_2CCR=CR'R'')(PPh_3)(Ph_2PO_2CCR=CR'R'')]$, becoming actively involved in the catalytic cycle (see Scheme 2.8.3). To prevent this from occurring, the replacement of the chloride ligand in the catalyst precursor by a ligand that cannot be substituted by a carboxylate anion must be brought about. This chapter describes attempts to prepare analogues of the catalyst precursors in which $CF_3$ replaces Cl.

## 4.2 Properties of Transition-Metal Trifluoromethyl Complexes.

Transition-metal $CF_3$ complexes exhibit properties markedly different from their alkyl counterparts. The much greater thermal stability of the $CF_3$ species is exemplified by the preparative reactions involving thermolysis at temperatures up to 210°C.[1-3] Structural studies have shown very strong metal-carbon (M-C) bonds but rather weak carbon-fluorine (C-F) bonds. The M-C bonds have been shown to

be on average 0.05Å shorter for M-$CF_3$ than for metal-alkyl species.[2,4,5] The C-F bonds however, are longer and the C-F stretching frequencies (ν(C-F)) are approximately 100$cm^{-1}$ lower than those observed for other species ($CF_3I$ or[$L_n$M-C(O)$CF_3$]) containing $sp^3$ C-F bonds.[6-9] In comparison to [$L_n$M-C(O)$CF_3$] complexes, complexes of the general formula [$L_n$M-$CF_3$] exhibit a large shift to lower field in the $^{19}F$ NMR spectrum.[10] The NMR trans influence of $CF_3$ and $CH_3$ ligands is comparable, and the structural trans influence of the $CF_3$ ligand is actually less than that of $CH_3$.[2]

4.3 · Bonding in Transition-Metal Trifluoromethyl Complexes.

The rationalization of the relatively strong M-C and weak C-F bonds of trifluoromethyl complexes, has provoked a good deal of disagreement.

An early suggestion for the apparent strength of the M-$CF_3$ bond involved the belief that the electronegative $CF_3$ group caused contraction of the metal d orbitals.[5] An even earlier proposal was a hyperconjugation argument that presented a resonance structure as illustrated in Figure 4.3.1.[6]

Figure 4.3.1

$$M\text{-}CF_3 \longleftrightarrow [M{=}CF_2]^+F^-$$

The most controversial proposal centred around the belief that if the H substituent of an alkyl group was replaced by the F of a $CF_3$ group the energy of the

antibonding C-F $\sigma^*$ orbital was sufficiently lowered that it could act as a metal $d\pi$ acceptor orbital. The resulting $\pi$ back-bonding was believed to impart some double bond character to the M-C bond and this would be consistent with the shorter M-C and longer C-F bonds.[6-8,11] This proposal, however, has been rigorously disputed. A force constant analysis on $\nu$(CO) was carried out for a large series of complexes of general formula, $[RMn(CO)_5]$, where R included $CH_3$, $CF_3$, alkyl, perfluoroalkyl, aryl, halide and main group alkyl ligands.[12] The $\sigma$ and $\pi$ effects of bonding were isolated thus allowing differentiation between electron withdrawal by inductive ($\sigma$) or back-bonding ($\pi$) mechanisms for each ligand. Both $CH_3$ and $CF_3$ ligands were found to be equally poor $\pi$-electron acceptors, suggesting that $CF_3$ is a strongly $\sigma$-withdrawing ligand but not a $\pi$-withdrawing ligand. The synergic nature of metal-ligand bonding suggests that the polarity of the M-$CF_3$ $\sigma$ bond would diminish the tendency for $\pi$ bonding of the same polarity. Further evidence against the presence of $\pi$-back-bonding was provided in the form of a qualitative electrostatic argument, also based on $\sigma$-bonding effects. The electronegativity of the $CF_3$ group will increase the s character of the C $\sigma$ orbital and will induce a higher positive charge on the metal, leading to contraction of the metal $\sigma$ orbitals. Both effects will improve overlap between the metal and carbon $\sigma$ orbitals, resulting in a stronger bond.[5,13] This proposal is supported by photoelectron spectroscopic studies on the complexes illustrated in Figure 4.3.2 in which the s character of the C-F or C-H and the Mn-C bonds was analysed.[13,14]

Figure 4.3.2

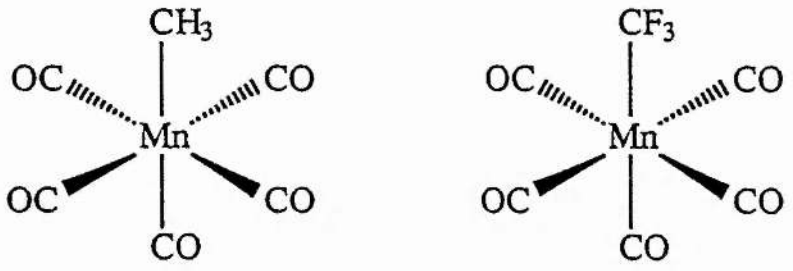


The experimental observations could be explained without invoking $\pi$-back bonding. The C-F bonds of $CF_3$ use C orbitals with more p character than do the C-H bonds of $CH_3$; thus the C orbital involved in $\sigma$ bonding to the metal has more s character for M-$CF_3$. The bonding electrons are held closer to the C atom leading to a shorter M-C bond. This also explains the longer C-F bonds since the M-C bonding orbital, which is actually anti-bonding in the C-F region, has a higher occupancy for $[Mn(CO)_5CF_3]$ than does the corresponding orbital in $ICF_3$, resulting in longer C-F bonds in the former species. A further electrostatic effect, $\sigma$-electron withdrawal by the fluorine substituents, results in a more positively charged carbon centre in $CF_3$ than in $CH_3$. This positive charge stabilizes the metal orbitals such that there is stronger bonding to all ligands in metal trifluoromethyl complexes. The only drawback with this argument is that the $[Mn(CO)_5]$ fragment is a poor choice for a study to probe the existence of $\pi$- back bonding, which would be difficult to observe in the presence of five competing carbonyl ligands. Despite this, it does seem to account better for the observed properties of transition-metal $CF_3$ complexes than do the qualitative proposals of $\pi$ back-bonding effects.

## 4.4 General Syntheses of Transition-Metal Trifluoromethyl Complexes

The synthetic methods for transition-metal trifluoromethyl complexes developed in the 1960s fall generally into two classes: decarbonylation of trifluoroacetyl complexes and oxidative addition of $CF_3I$ to suitable metal substrates. These routes were necessarily restricted to the low-valent, electron-rich late-transition-metal complexes and have been used for introducing up to two $CF_3$ groups per molecule. More recently syntheses using group 12 trifluoromethyl complexes as $CF_3$ transfer reagents and complex metal atom condensation techniques have been developed.

Decarbonylation of Trifluoroacetyl Complexes

Metal anion substitution of $CF_3COCl$, $CF_3COF$ or $(CF_3CO)_2O$ produces a metal trifluoroacetyl species, $[L_nM(COCF_3)]$, which can be thermally or in some cases photolytically decarbonylated to the trifluoromethyl complex $[L_nM(CF_3)]$.[15-17] The initial synthesis of a trifluoromethyl-substituted transition-metal compound occurred when trifluoroacetyl manganese pentacarbonyl was first formed, then thermally decarbonylated as illustrated in Figure 4.4.1.[18]

Figure 4.4.1

$$CF_3COCl + [NaMn(CO)_5] \longrightarrow \underset{(75\%)}{[(CF_3CO)Mn(CO)_5]} + NaCl$$

$$[(CF_3CO)Mn(CO)_5] \xrightarrow{110\text{-}160^\circ C} \underset{(92\%)}{[CF_3Mn(CO)_5]} + CO$$

This technique has been used to prepare a variety of $CF_3$ complexes, for metals such as Mo,Mn,Fe,Co, and Ir.[15]

In a few instances, rather than coupling of the trifluoroacetyl ligand to a metal anion, the perfluoroacyl compound has been oxidatively added to neutral Pt(O) or Ir(I) complexes with subsequent decarbonylation to give the trifluoromethyl complex.[2,19] An example of this is illustrated in Figure 4.4.2.[2]

Figure 4.4.2

$$[Pt(PMePh_2)_4] + CF_3COCl \longrightarrow [Pt(OCCF_3)Cl(PMePh_2)_2]$$

$$\xrightarrow[-\ CO]{210^\circ C} [Pt(CF_3)Cl(PMePh_2)_2]$$

The high temperatures used for the thermal decarboxylation steps demonstrate the significant thermal stability of transition-metal $CF_3$ complexes. The decarbonylation is presumed to proceed via $CF_3$ migration to the metal, followed by CO loss. The reverse migration of $CF_3$ from metal to CO has never been observed, although this process is extremely facile for the methyl analogues.[6,20]

The limitations of the decarbonylation method are:

1) The decarbonylation step is promoted by the presence of strongly electron-withdrawing ancillary ligands like CO, thus analogues with phosphine ligands may require much higher temperatures, resulting in complex decomposition.

2) Decarbonylation is difficult to achieve for second and third row transition metal complexes due to their higher M-C bond strengths. Pt and Ir are the only heavier elements for which there has been success with this method.

3) For the anion route a low-valent metal capable of forming an anion is required. Very reactive anions like $[CpFe(CO)_2]^-$ actually displace $F^-$ from $[M\text{-}COCF_3]$ species.[16]

Oxidative Addition of $CF_3I$

The displacement of iodide from RI by a anionic species, $[ML_n]^-$, is not practical for $R=CF_3$, as the more electronegative $CF_3$ group is displaced to give $[ML_nI]$ as the product. $CF_3I$ will, however, oxidatively add to coordinatively unsaturated low valent $d^8$ and $d^{10}$ metal centres,[15] as illustrated in Figure 4.4.3.[21]

Figure 4.4.3

$$[IrCl(CO)(PMePh_2)_2] + CF_3I \longrightarrow [CF_3IrCl(CO)(PMePh_2)_2I]$$

The general reaction may also proceed via oxidative addition of $CF_3I$ to metal alkyl precursors and subsequent elemination of RR or RI to give bis(trifluoromethyl) species. An example of this is illustrated in Figure 4.4.4 and it should be noted that elimination of the alkyl group is more favourable than elimination of the trifluoromethyl group.[22]

Figure 4.4.4

$$[Pt(CH_3)_2(1,5\text{-}C_8H_{12})] + 2CF_3I \longrightarrow [Pt(CF_3)_2(1,5\text{-}C_8H_{12})] + 2CH_3I$$

To date, the oxidative addition of $CF_3I$ has been limited to even-electron ($d^8$ or $d^{10}$) rather than odd-electron ($d^7$ or $d^9$) metal substrates.

Activated Metal Species with $CF_3$ Radicals

The activation of either the metal substrate or the trifluoromethyl fragment by an external energy source has led to a number of new trifluoromethyl complexes.[15] Metal atom condensation with $CF_3I$ gives the highly reactive species $CF_3MI$ (M=Ni, Pd, Ag and Zn), and ultrasound activation has been used to prepare $CF_3ZnI$. Reaction of metal halides with $CF_3$ radicals, produced by radio-frequency discharge, has produced $[M(CF_3)_2(PMe_3)_2]$ (M = Ni, Pd).

$CF_3$ Transfer from Group 12 Metals

Although trifluoromethyl mercurials were the first metal complexes containing the $CF_3$ ligand to be prepared[23] they were not utilised as a source of the $CF_3$ ligand until the 1980s. The thermally robust complex $[Hg(CF_3)_2]$ is prepared by decarboxylation of mercuric bis(trifluoroacetate) as illustrated in Figure 4.4.5., and is purified by sublimation.

Figure 4.4.5

$$HgO \xrightarrow{CF_3CO_2H} [Hg(OCOCF_3)_2] \xrightarrow[25Torr,\ 120\text{-}180^{\circ}C]{K_2CO_3} [Hg(CF_3)_2]$$

When $[Hg(CF_3)_2]$ is treated with $[CdMe_2]$ in glyme (1,2-dimethoxyethane), $[Cd(CF_3)_2]$ is formed. This highly reactive cadmium species is isolated as the glyme adduct. Facile base exchange gives adducts of the general form $[Cd(CF_3)_2.\ base]$. Stronger bases like pyridine render the cadmium species more stable but less reactive, while weaker bases like THF have the opposite effect. The glyme adduct offers the best compromise between reactivity and stability.[24-26]

There are generally two ways in which $(Hg(CF_3)_2]$ can react. Firstly, it can oxidatively add across one Hg-C bond to some low-valent metal substrates, producing novel complexes containing both $CF_3$ and $Hg(CF_3)$ ligands,[27,35] as illustrated in Figure 4.4.6.

Figure 4.4.6

$$[Pt(PPh_3)_4] + [Hg(CF_3)_2] \longrightarrow [Pt(CF_3)(HgCF_3)(PPh_3)_2]$$

Secondly, $[Hg(CF_3)_2]$ is useful for the transfer of one or more $CF_3$ groups to several main-group-metal halides. Similarly Rh(I) and Ir(I) hydride complexes react with the mercury reagent,[28] as is shown in Figure 4.4.7.

Figure 4.4.7

$$[RhH(CO)(PPh_3)_3] \xrightarrow{[Hg(CF_3)_2]} [Rh(CF_3)(CO)(PPh_3)_2]$$

The success with the rhodium(I) hydride complex $[RhH(CO)(PPh_3)_3]$ as a precursor to $[Rh(CF_3)(CO)(PPh_3)_2]$ prompted the investigation of other rhodium hydride compounds. The only other hydride complex which has been found to react satisfactorily with $[Hg(CF_3)_2]$ is $[RhHCl_2(PPh_3)_2]$.[31] The products obtained are $[RhCl(CO)(PPh_3)_2]$, $[RhCl_2(CF_2H)(PPh_3)_2]$ and $(RhCl_2(CF_3)(PPh_3)_2]$, and they have been separated by column chromatography. This reaction provides a good route to five-coordinate rhodium (III) fluorocarbon complexes.

$[Cd(CF_3)_2.glyme]$ is more reactive than $[Hg(CF_3)_2]$ and hence milder reaction conditions are required. The cadmium complex is effective for the preparation of $[CpCo(CO)_2(CF_3)]$ and $[M(CF_3)Br(PEt_3)_2]$ (M=Ni, Pd, Pt) from $[CpCo(CO)_2I]$ and $[MBr_2(PEt_3)_2]$ respectively.

## 4.5 Attempted Syntheses of $[RhCF_3(PPh_3)_3]$

The reaction of Wilkinson's catalyst with bis(trifluoromethyl) mercury has been performed by Roper et al.[31] They concluded that $[RhF(CO)(PPh_3)_2]$ was formed as the product and they presumed that this complex was generated by hydrolysis of a fluorocarbon ligand bonded to the rhodium. Their use of rigorously anhydrous conditions enabled the detection of a fluorocarbon complex by IR spectroscopy,

however they were unable to obtain a tractable product.

The reaction between $[RhCl(PPh_3)_3]$ and 0.5 mole equivalents of $[Hg(CF_3)_2]$ was performed under a dry nitrogen atmosphere and under reflux in toluene for 3 hours. A yellow microcrystalline solid was obtained from the reaction and analysis has shown the product as being $[RhCl(PF_3)(PPh_3)_2]$ which is illustrated in Figure 4.5.1.

Figure 4.5.1

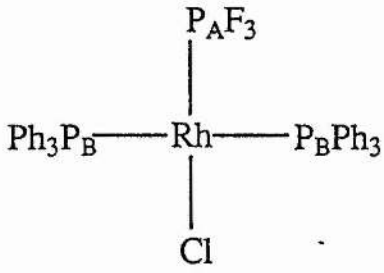


The $^{19}F$ NMR spectrum of the product (Spectrum 4.5.1) shows two widely spaced doublets of triplets ($\delta$15.9 to high field of $CCl_3F$) arising from spin - coupling with phosphorous, rhodium and the two equivalent phosphorus nuclei of the $PPh_3$ ligands, as illustrated in Figure 4.5.2.

Figure 4.5.2

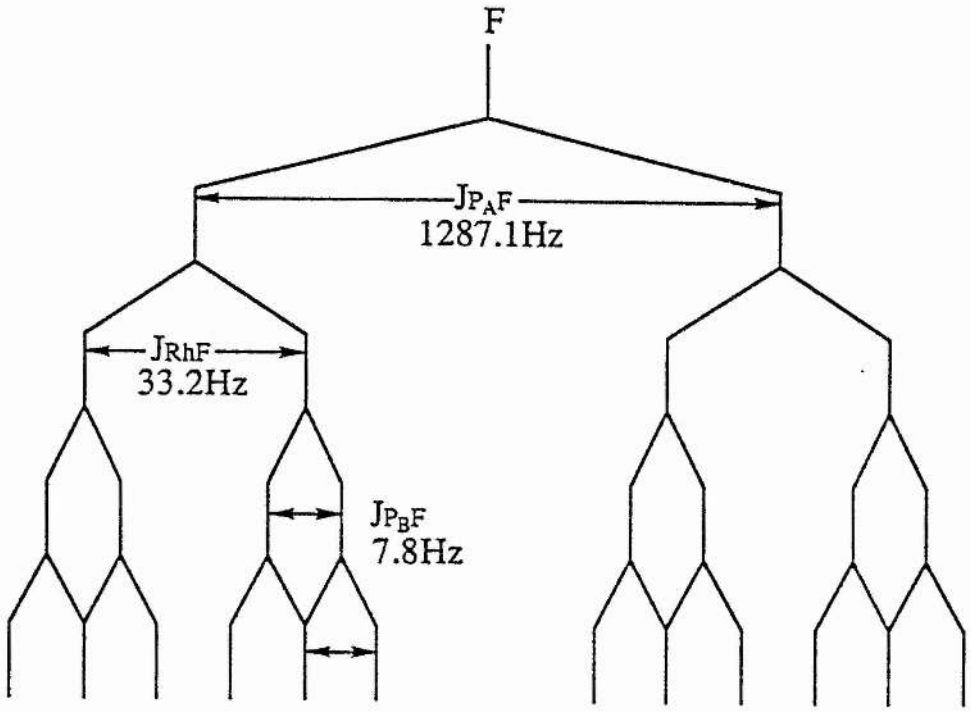


The spectrum is consistent with that reported by Nixon et al[32] who prepared $[RhCl(PF_3)(PPh_3)_2]$ in the manners shown in Figure 4.5.3.

Figure 4.5.3

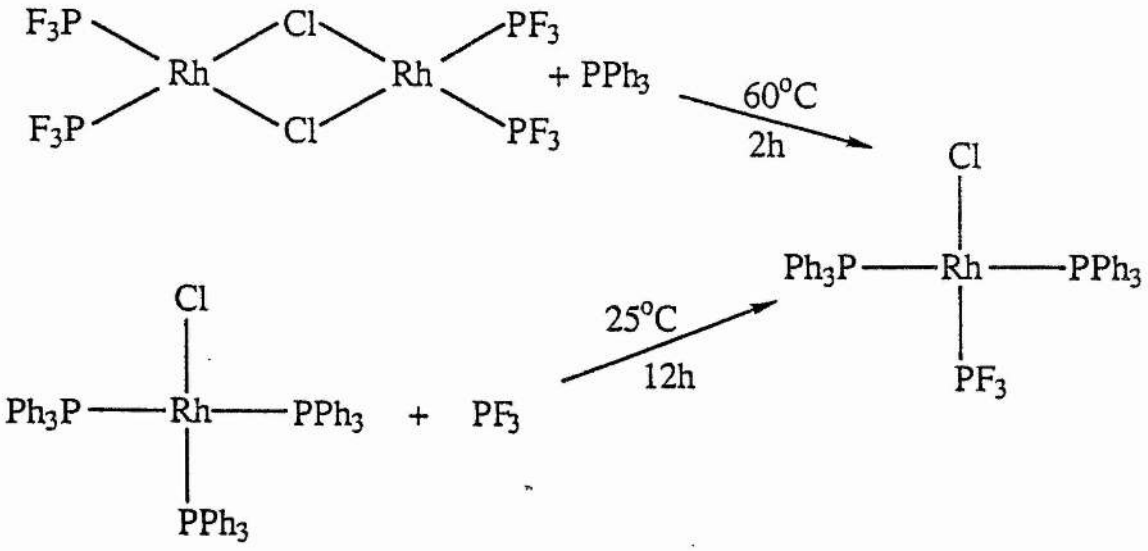

Spectrum 4.5.1 $^{19}F$ NMR of $[RhCl(PF_3)(PPh_3)_2]$

in $CD_2Cl_2$ at 298K.

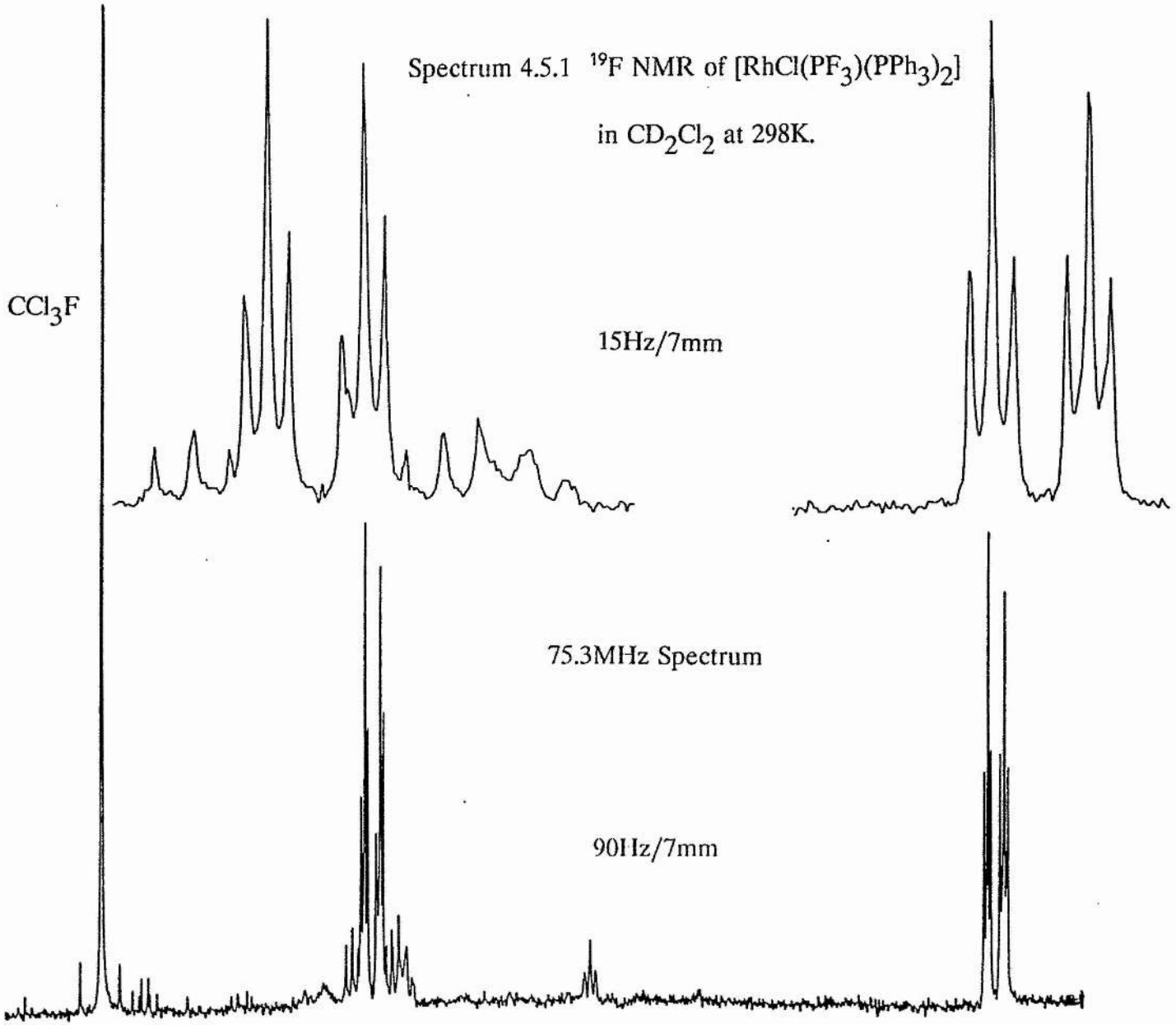

The $^{31}P$ NMR spectrum of $[RhCl(P_AF_3)(P_BPh_3)_2]$, Spectrum 4.5.2, shows the resonance of the phosphorus atom of triphenylphosphine, $P_B$, to be coupled to rhodium ($J_{RhP_B}$ 120.4Hz), to the phosphorus atom of the $PF_3$ ligand ($J_{P_AP_B}$ 55.6Hz) and to fluorine ($J_{P_BF}$ 7.8Hz). The shift of $P_B$ is at $\delta$33.1, this being normal for $PPh_3$ ligands bound to rhodium. The resonance of the phosphorus atom of the trifluorophosphine ligand ($\delta$109.4), $P_A$, is coupled to fluorine ($J_{P_AF}$ 1285.7Hz), to rhodium ($J_{RhP_A}$ 374.5Hz) and to $P_B$($J_{P_AP_B}$ 55.6Hz). The IR spectrum of $[RhCl(PF_3)(PPh_3)_2]$ shows three bands in the $\nu$(P-F) region (862cm$^{-1}$, 852cm$^{-1}$ and 837cm$^{-1}$), indicating the presence of one coordinated $PF_3$ ligand. The reaction between $[RhCl(PPh_3)_3]$ and $[Hg(CF_3)_2]$ is certainly novel and could be described in terms of a C-F bond activation. The yield of the reaction is 77% and this represents a high C-F to P-F transformation. A similar type of activation has been seen in the reaction between $[IrMe(PEt_3)_3]$ and hexafluorobenzene ($C_6F_6$)[33] as illustrated in Scheme 4.5.1. The product in this case is $[(C_6F_5)Ir(PEt_3)_2(PEt_2F)]$, and the proposed mechanism involves electron transfer, oxidative addition and reductive elimination reactions as illustrated in Scheme 4.5.1.

Scheme 4.5.1

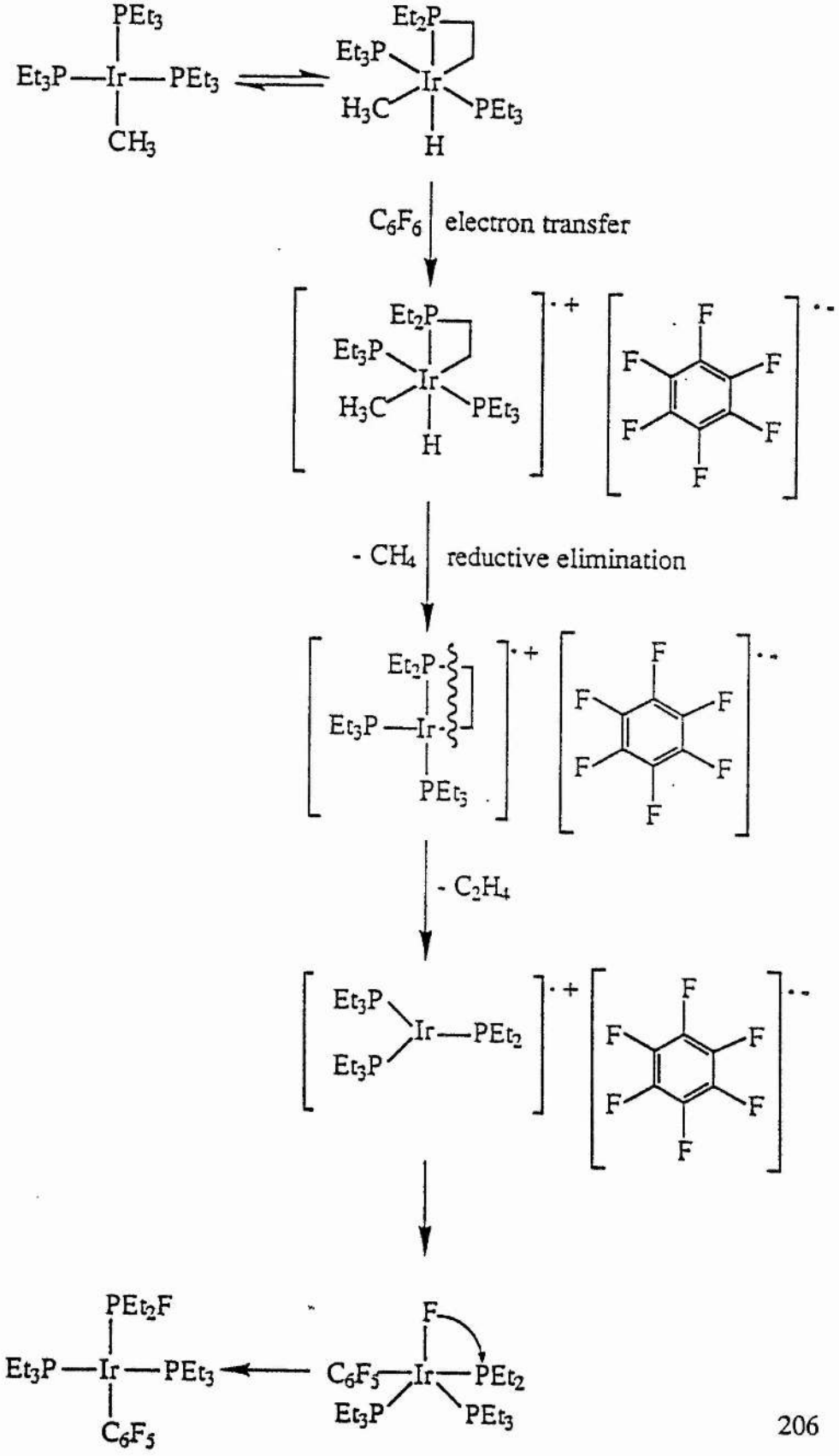
PEt3
Et3P—Ir—PEt3
CH3
Et2P
Et3P
Ir
H3C
PEt3
H
C6F6
electron transfer
- CH4
reductive elimination
- C2H4
PEt2F
C6F5
F

Spectrum 4.5.2 $^{19}P$ NMR of $[RhCl(PF_3)(PPh_3)_2]$ in $CD_2Cl_2$ at 298K.

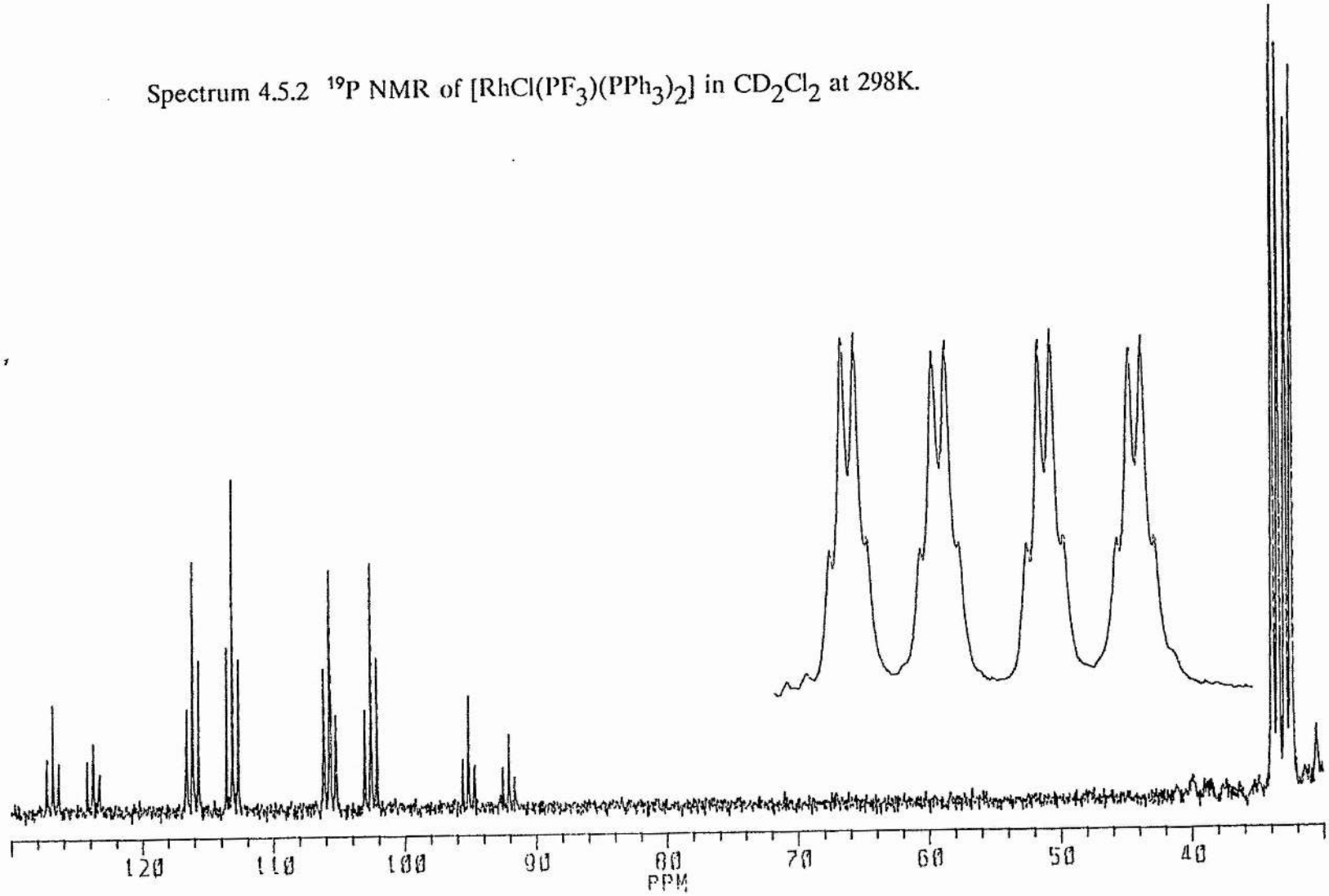

During the reaction between $[RhCl(PPh_3)_3]$ and $[Hg(CF_3)_2]$ elemental mercury is formed, however prior to this the initial deep red colouration of the reaction solution is replaced by an orange colouration which in turn becomes darker and darker. Analysis of the reaction solution at the orange colouration stage has shown that the orange form of $[RhCl(PPh_3)_3]$ is the only species present. This observation could be of significance since the orange crystalline form of $[RhCl(PPh_3)_3]$ differs structurally from the red form and is indeed less stable.[34]

Further evidence for $[RhCl(PF_3)(PPh_3)_2]$ being the product of the reaction between $[RhCl(PPh_3)_3]$ and $[Hg(CF_3)_2]$ is due to its inactivity as a hydrogenation catalyst, since when it is refluxed in THF under a hydrogen atmosphere there is no colour change. Furthermore there is no reaction between $[RhCl(PF_3)(PPh_3)_2]$ and mixed anhydrides of general formula, $Ph_2PO_2CCR=CR'R''$.

The reaction of $[RhCl(PPh_3)_3]$ and $[Hg(CF_3)_2]$ has also been carried out in the presence of excess triphenylphosphine with the aim of preventing the formation of a trifluorophosphine ligand. The Rh(III) species, $[RhCl(CF_3)_2(PPh_3)_2]$, is the product obtained from the reflux of $[RhCl(PPh_3)_3]$, 2 mole equivalents of $[Hg(CF_3)_2]$ and 4 mole equivalents of $PPh_3$ in toluene (See Figure 4.5.4).

Figure 4.5.4

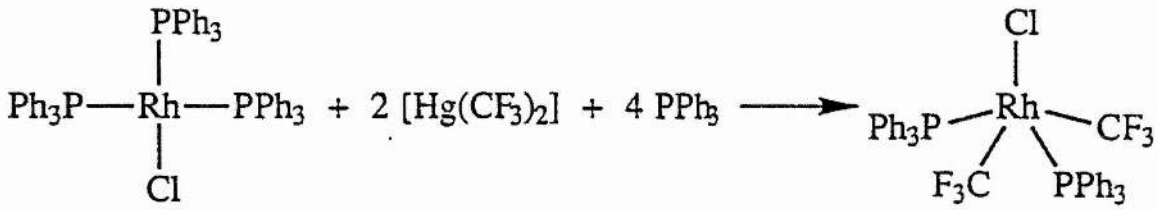


The $^{19}F$ NMR spectrum (Spectrum 4.5.3) shows that a single fluorine resonance ($\delta$1.3 to high field of $CCl_3F$) is coupled to both triphenylphosphine phosphorus atoms and to rhodium, as is illustrated in Figure 4.5.5. The value of the coupling constant $J_{PF}$ (18.2Hz) is of similar value to that seen in other such rhodium(III) trifluoromethyl complexes as illustrated in Table 4.5.1.

Figure 4.5.5

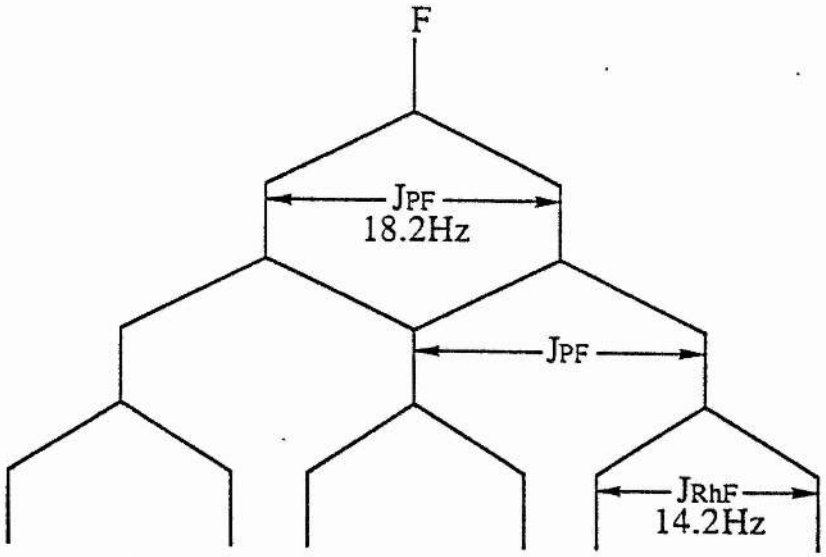

Spectrum 4.5.3 $^{19}F$ NMR of $[RhCl(CF_3)_2(PPh_3)_2]$ in $CD_2Cl_2$ at 298K.

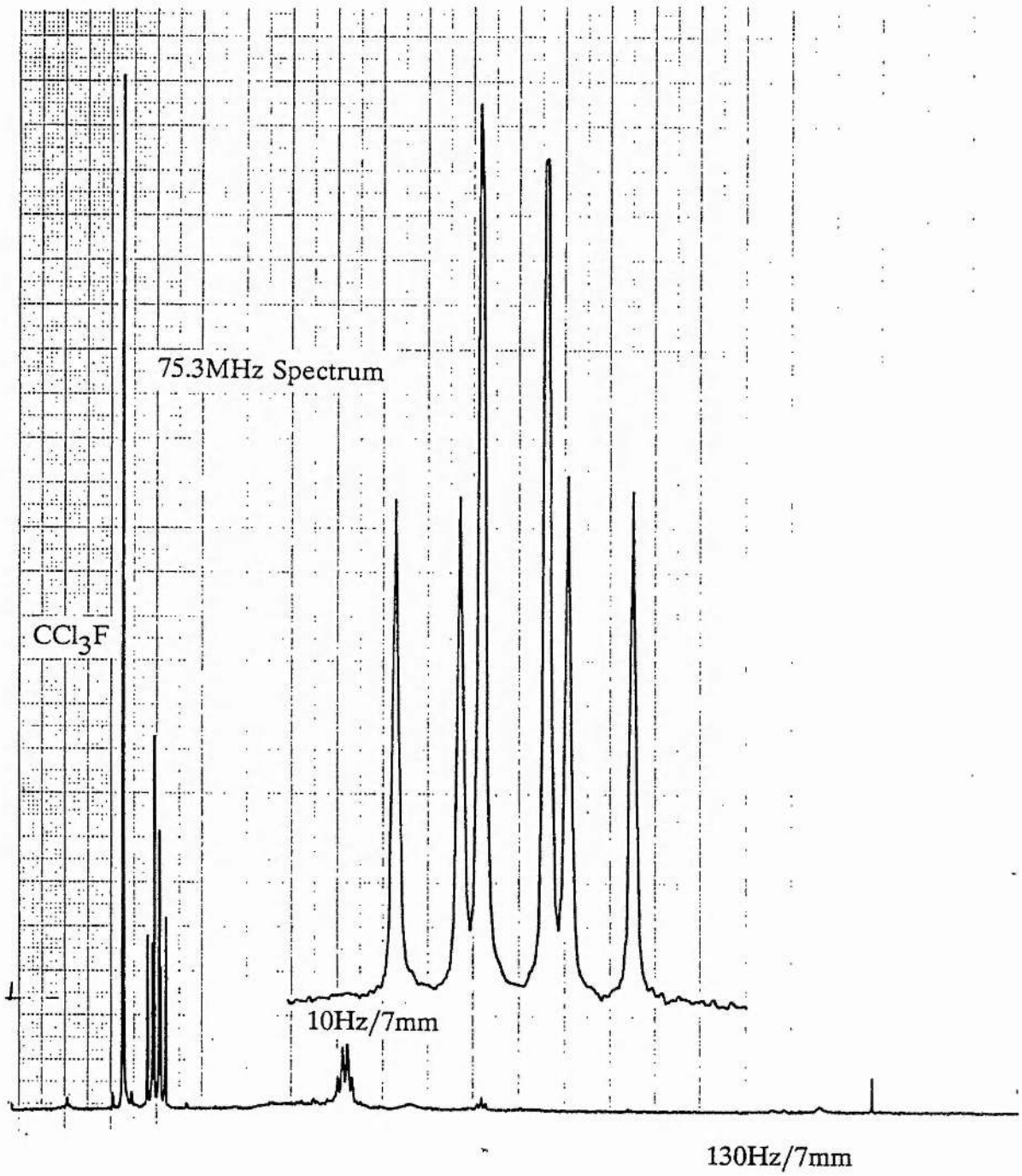

The $^{31}P$ NMR spectrum (Spectrum 4.5.4) consists of a single resonance at $\delta$29.8, since both phosphorus atoms are in equivalent environments. Each phosphorus atom is coupled to rhodium and to six fluorine atoms, giving rise to a doublet of heptets, as is illustrated in Figure 4.5.6. The coupling constant $J_{RhP}$ (116.1Hz) is of similar magnitude to the other rhodium(III) species referred to in Table 4.5.1.

Figure 4.5.6

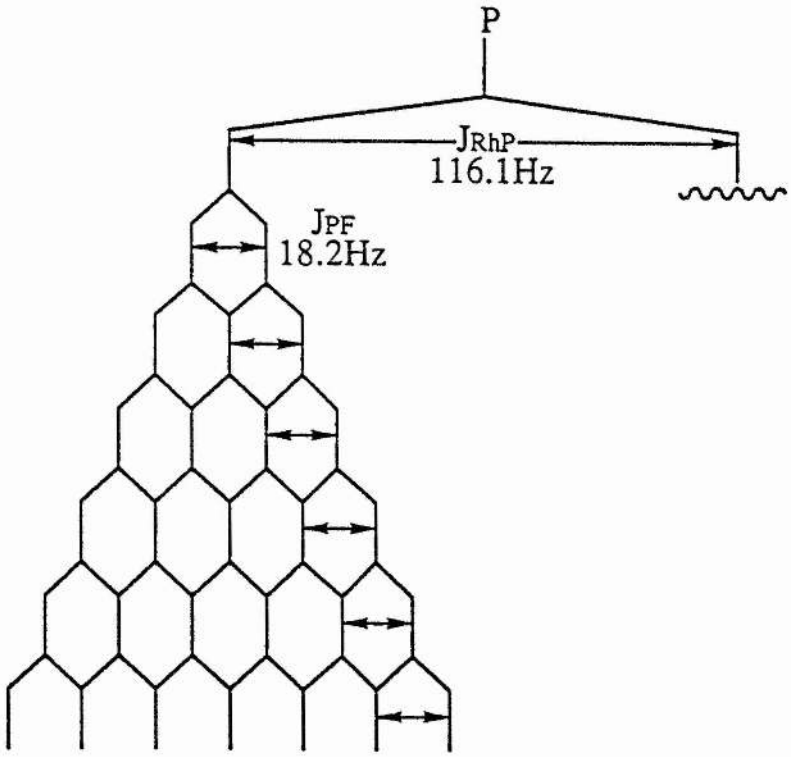

Spectrum 4.5.4 $^{19}P$ NMR of $[RhCl(CF_3)_2(PPh_3)_2]$ in $CD_2Cl_2$ at 298K.

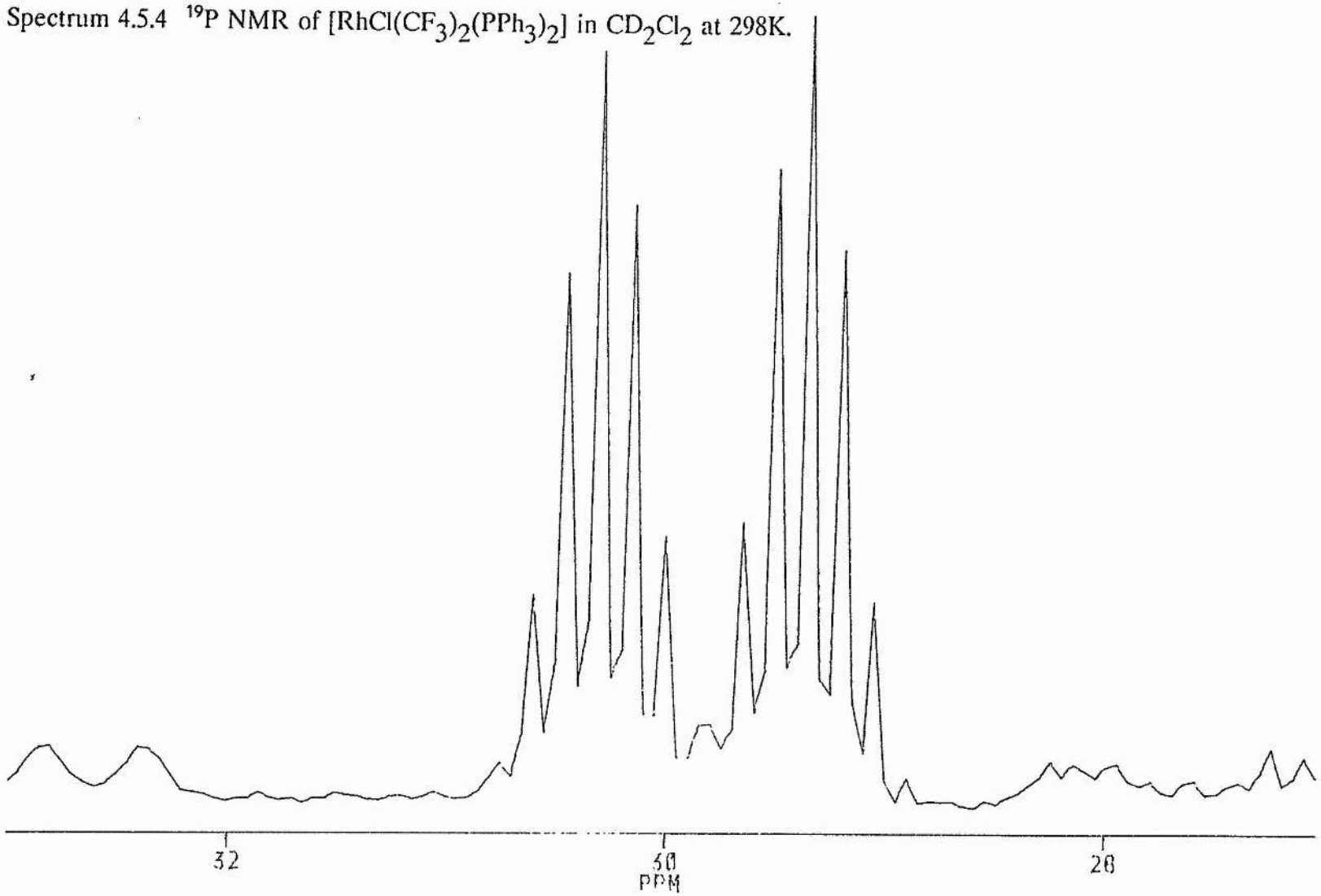

Table 4.5.1 $^{31}P$ NMR Data for Rhodium (III) Complexes

| | $\delta$(ppm) | $J_{RhP}$ (Hz) | $J_{PF}$ (Hz) |
|---|---|---|---|
| $[RhCl(CF_3)_2(PPh_3)_2]$[1] | 29.80 (dh)[2] | 116.1 | 18.2 |
| $[RhCl_2(CF_3)(CO)(PPh_3)_2]$ | 11.02 (dq) | 87.3 | 11.02 |
| $[RhHCl(CF_3)(CO)(PPh_3)_2]$ | 24.63 (dq) | 100.4 | 20.2 |
| $[RhBr_2(CF_3)(CO)(PPh_3)_2]$ | 8.40 (dq) | 88.1 | 17.1 |
| $[RhI_2(CF_3)(CO)(PPh_3)_2]$ | 5.12 (dq) | 89.3 | 16.8 |
| $[RhCl_2(CF_3)(PPh_3)_2]$ | 22.79 (dq) | 101.2 | 20.4 |

[1]NMR in $CD_2Cl_2$. [2](dh) is doublet of heptets.

The geometry of $[RhCl(CF_3)_2(PPh_3)_2]$ is square pyramidal with the chloride ligand occupying the apical position. Once again, as in the synthesis of $[RhCl(PF_3)(PPh_3)_2]$, elemental mercury is precipitated in the reaction and this is comparable with observations in the reaction of $[RhHCl_2(PPh_3)_2]$ with $[Hg(CF_3)_2]$.[31]

The IR spectrum of $[RhCl(CF_3)_2(PPh_3)_2]$ has absorption bands assignable to $\nu$(C-F) at 1113 $cm^{-1}$(s), 1068 $cm^{-1}$(s) and 1027 $cm^{-1}$(s). The band assignable to $\nu$(Rh-Cl) is at 264$cm^{-1}$(w) which is somewhat lower in value compared to 298 $cm^{-1}$

observed for ν(Rh-Cl) in $[RhCl_2(CF_3)(PPh_3)_2]$.[31] This is presumably because of a longer Rh-Cl bond length due to the apical position of the chloride ligand.

The reaction between $[RhCl(CF_3)_2(PPh_3)_2]$ and the mixed anhydride derived from 2-methyl-3-phenylpropenoic acid, $Ph_2PO_2CCMe=CHPh$, results in the formation of the six-coordinate $[RhCl(CF_3)_2(PPh_3)(Ph_2PO_2CCMe=CHPh)]$ species. The mixed anhydride is bound to rhodium by phosphorus and the carbon-carbon double bond as is illustrated in Figure 4.5.7.

Figure 4.5.7

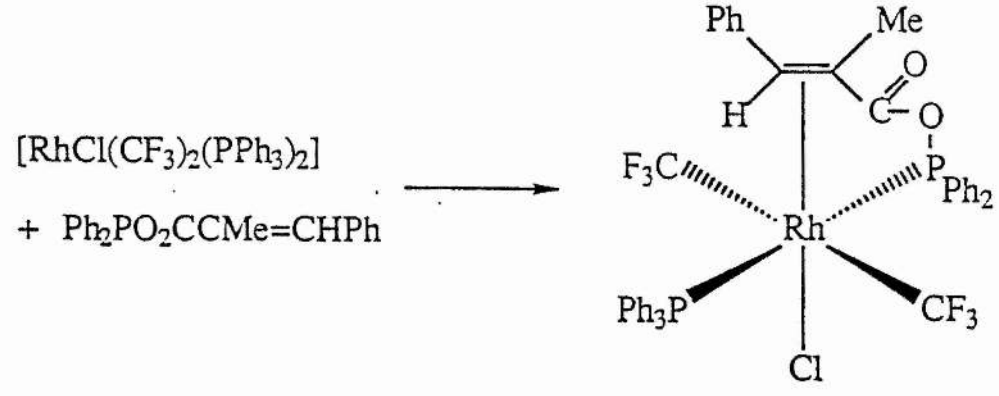


The observed room temperature $^{31}P$ NMR spectrum of $[RhCl(CF_3)_2(P_APh_3)(Ph_2P_BO_2CCMe=CHPh)]$, presented as Spectrum 4.5.5, shows that the resonance assigned to the phosphorus atom of the $PPh_3$ ligand, $P_A$, is coupled to the phosphorus atom of the mixed anhydride ligand, to rhodium and to six fluorine atoms. The shift of the resulting doublet of doublet of heptets, $\delta$24.9 and the coupling constants $J_{RhP_A}$ 114.8Hz and $J_{P_A}{}^F$ 18.2Hz are similar to those

presented for other rhodium (III) species in Table 4.5.1. The value of $J_{P_AP_B}$, 466.0Hz, is characteristic of a trans phosphorus-phosphorus coupling. The resonance assigned to the phosphorus atom of the mixed anydride, $P_B$, is also a doublet of doublet of heptets, $\delta$136.2, with the same mutual phosphorus-phosphorus coupling. The values of $J_{RhP_B}$ 124.1Hz and $J_{P_BF}$ 24.5Hz, however, are slightly greater than those of $J_{RhP_A}$ and $J_{P_AF}$.

The $^1$H NMR of the chelate bound complex shows resonances assignable to both the -$CH_3$ and the -H substituents of the carbon-carbon double bond of the mixed anhydride ligand. The shift of the resonance assigned to the -H substituent is $\delta$2.98 and this is significantly upfield from the corresponding resonance seen in [Rh($O_2$CCMe=CHPh)($PPh_3$)($Ph_2PO_2$CCMe=CHPh)], $\delta$4.70.

Spectrum 4.5.5 $^{19}P$ NMR of $[RhCl(CF_3)_2(PPh_3)(Ph_2PO_2CCMe{=}CHPh)]$ in $CD_2Cl_2$ at 298K.

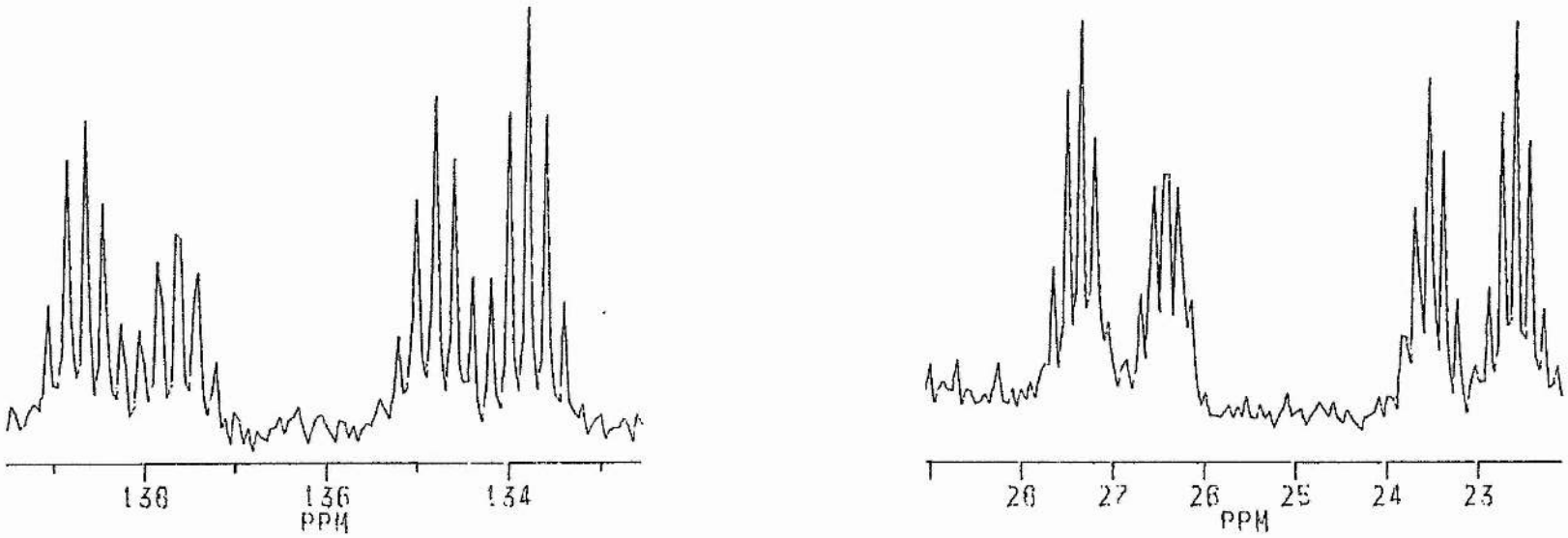

Another attempted synthesis of $[Rh(CF_3)(PPh_3)_3]$ has involved the reaction of $[RhH(PPh_3)_4]$ with bromotrifluoromethane ($CF_3Br$) in the presence of the base, triethylamine. Instead of the trifluoromethyl complex being formed, $[RhBr(PPh_3)_3]$ is formed. Its $^{31}P$ NMR spectrum at ˉ40°C is presented as Spectrum 4.5.6 and the associated shifts and coupling constants are in total agreement with literature values.[36]

Unfortunately $[Rh(CF_3)(PPh_3)_3]$ has not been synthesized, although this can perhaps be explained since if $[RhCF_3(PPh_3)_3]$ is considered to be a stable species then electron density needs to be removed from the Rh(I) metal centre to the three $PPh_3$ ligands. $[Rh(CF_3)(CO)(PPh_3)_2]$ is a stable species and therefore it must be able to remove electron density from the metal. Clearly the presence of a CO ligand in place of a $PPh_3$ ligand lends to the greater capacity to remove electron density from the metal. For a Rh(III) species there is less of a problem of electron density being on the metal centre due to the greater cationic nature of the rhodium itself.

Spectrum 4.5.6 $^{19}P$ NMR of $[RhBr(PPh_3)_3]$ in $CD_2Cl_2$ at 233K.

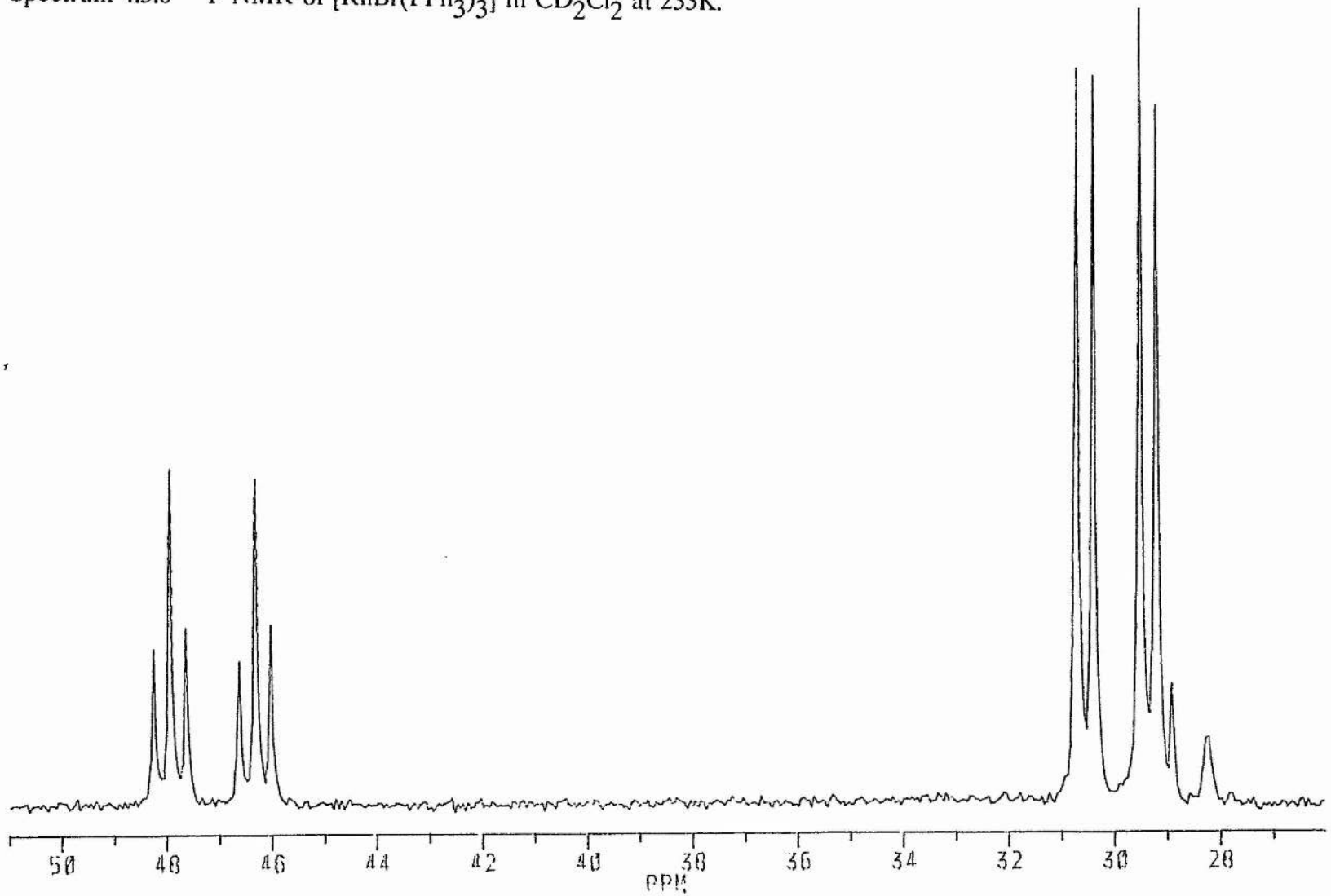

## 4.6 Experimental

All manipulations were carried out under dry oxygen-free nitrogen using standard Schlenk-line and catheter-tubing techniques. All solvents were purified by distillation from calcium hydride ($CH_2Cl_2$) or sodium diphenylketyl [toluene, light petroleum (b.p. 40 - 60°C), diethyl ether and THF.

### Preparation of $[RhCl(PF_3)(PPh_3)_2]$

Under a dry dinitrogen atmosphere $[RhCl(PPh_3)_3]$ (2.0g, 2.16mmol) and $[Hg(CF_3)_2]$ (0.37g, 1.09mmol) were refluxed in toluene ($150cm^3$) for 3 hours, after which time the reaction solution was left to cool and then filtered. The solution was reduced in vacuo to a total volume of $10cm^3$; light petroleum was added giving a brown/orange precipitate which was filtered off and dried under vacuum. Yield 1.26g (77%).

### Preparation of $[RhCl(CF_3)_2(PPh_3)_2]$

Under a dry dinitrogen atmosphere $[RhCl(PPh_3)_3]$ (0.75g, 0.81 mmol), $[Hg(CF_3)_2]$ (0.55g, 1.62 mmol) and $PPh_3$ (0.86g, 3.28 mmol) were refluxed in toluene ($150cm^3$) for 8 hours, after which time the reaction solution was left to cool and then filtered. The solution was reduced in vacuo to a total volume of 5 $cm^3$; light petroleum was added giving a brown precipitate which was filtered off and dried under vacuum. Yield 0.39g (60.2%).

The Reaction Between $[RhCl(CF_3)_2(PPh_3)_2]$ and $[Ph_2PO_2CCMe=CHPh]$

To a solution of $[RhCl(CF_3)_2(PPh_3)_2]$ (0.38g, 0.47 mmol) in THF ($25cm^3$ was added a solution of $Ph_2PO_2CCMe=CHPh$ (0.16g, 0.47mmol) in THF ($25cm^3$). The solution was stirred for 2 hours before being filtered. The solvent was then removed by evaporation to approximately $3cm^3$ and light petroleum was added to give a yellow powder and after filtration the solid was dried under vacuum. Yield 0.24g (57.7%).

Preparation of $[RhBr(PPh_3)_3]$

Under a dry dinitrogen atmosphere $[RhH(PPh_3)_4]$ (1.04g, 0.90 mmol) was dissolved in toluene ($270cm^3$) and then $CF_3Br$ was bubbled through the solution until saturation was achieved. Then $NEt_3$ (0.09g, 0.90 mmol) was added and the solution was stirred for 7 days during which time the solution turned deep red in colour. After this the solution was filtered and reduced in vacuo to a volume of $10cm^3$ during which time a brown precipitate appeared. This precipitate was then filtered off and dried under vacuum. Yield 0.64g (73.3%).

## CHAPTER 4 REFERENCES


1 M I Bruce and F G A Stone, Prep. Inorg. React., 1968, 4, 177.

P M Treichel and F G A Stone, Adv. Organomet. Chem., 1964, 1, 143.

2 M A Bennett, H K Chee and G B Robertson, Inorg. Chem., 1979, 18, 1061.

3 F Seel and R D Flaccus, J. Fluorine Chem., 1978, 12, 81.

4 M R Churchill and J P Fennessey, Inorg. Chem., 1967, 6, 1213.

5 M R Churchill, Perspect. Struct. Chem., 1970, 3, 91.

6 R B King and M B J Bisnette, J. Organomet. Chem., 1964, 2, 15.

7 F A Cotton and J A McCleverty, J. Organomet. Chem., 1965, 4, 490.

8 F A Cotton and R M Wing, J. Organomet. Chem., 1967, 9, 511.

9 M P Johnson, Inorg. Chim. Acta., 1969, 3, 232.

10 E Pitcher, A D Buckingham and F G A Stone, J. Chem. Phys., 1962, 36, 124.

11 H C Clark and J H Tsai, J. Organomet. Chem., 1967, 7, 515.

12 W A G Graham, Inorg. Chem., 1968, 7, 315.

13 M B Hall and R F Fenske, Inorg. Chem., 1972, 11, 768.

14 D L Lichtenberger and R F Fenske, Inorg. Chem., 1974, 13, 486.

15 J A Morrison, Adv. Inorg. Chem. Radiochem., 1983, 27, 295 and references therein.

16 R B King and M B Bisnette, J. Organomet. Chem., 1964, 2, 15.

17 R B King, Acc. Chem. Res., 1970, 3, 417.

18 W R McClellan, J. Am. Chem. Soc., 1961, 83, 1598.

19 D M Blake, S Shields and L Wyman, Inorg. Chem., 1974, 13, 1595.

20 K Noack, V Schaerer and F Calderazzo, J. Organomet. Chem., 1967, **8**, 517.

21 J P Collman and C T Sears, Inorg. Chem., 1968, **7**, 27.

22 H C Clark and L E Manzer, J. Organomet. Chem., 1973, **59**, 411.

23 H J Emeleus, R N Haszeldine, J. Chem. Soc., 1949, 2948.

H J Emeleus, R N Haszeldine, J. Chem. Soc., 1949, 2953.

24 R Eujen, Inorg. Synth., 1986, **24**, 52.

25 D J Burton and D M Wiemers, J. Am. Chem. Soc., 1985, **107**, 5014.

26 L J Krause and J A Morrison, J. Am. Chem. Soc., 1981, **103**, 2995.

C D Ontiveros and J A Morrison, Inorg. Synth., 1986, **24**, 55.

27 V I Sokolov, V V Bashilov and O A Reutov, J. Organomet. Chem., 1975, **97**, 299.

28 P J Brothers and W R Roper, Chem. Rev., 1988, **88**, 1293.

29 L J Krause and J A Morrison, J. Chem. Soc., Chem. Commun., 1981, 1282.

30 C D Ontiveros and J A Morrison, Organometallics, 1986, **5**, 1446.

31 A K Burnell, G R Clark, J G Jeffrey, C E F Rickard and W R Roper, J. Organomet. Chem., 1990, **388**, 391.

32 D A Clement and J F Nixon, J. Chem. Soc. Dalton Trans., 1972, 2553.

33 O Blum, F Frolow and D Milstein, J. Chem. Soc. Chem. Commun., 1991, 258.

34 M J Bennett and P B Donaldson, Inorg. Chem., 1977, **16**, 655.

35 G R Clark, S V Hoskins and W R Roper, J. Organomet. Chem., 1982, **234**, C9.

36 F H Jardine, H A Osborn and G Wilkinson, J. Chem. Soc. (A), 1967, 1574.

# CHAPTER 5

# CATALYTIC STUDIES

## 5.1 Introduction.

As stated in Chapter 2 rhodium complexes of general formula $[RhCl(PPh_3)_n(Ph_2PO_2CCR=CR'R'')]$ (n=2, R=H, R′=R″=Me; R=R′=H, R″=CH=CHMe; R=Me, R′=H, R″=Ph; n=1, R=R′=H, R″=Me or CH=CHMe) are more effective for the catalytic hydrogenation of substituted acrylic acids in the presence of added base (KOH or $Et_3N$) than is Wilkinson's catalyst. Such a difference in activity has been proven as being a result of the complexes concerned operating by different catalytic mechanisms. This suggestion has been further substantiated by the different products obtained when both catalytic precursors are used in the catalytic hydrogenation of hexa-2,4-dienoic acid. Mechanistic studies have shown that for the catalytic hydrogenation of hexa-2,4-dienoic acid using rhodium-mixed anhydride complexes two simultaneous mechanisms operate. Chapters 3 and 4 were aimed at the modification of these catalytic precursors with a view to eliminating the catalytic cycle that involved the active participation of a hexa-2,4-dienoate ligand (see Scheme 2.8.3) and as a consequence increasing the regioselectivity of the hydrogenation towards the increased production of hex-4-enoic acid. This chapter presents the results obtained when the fluoro complexes developed in Chapter 3 are used for the catalytic hydrogenation of substituted acrylic acids. Prior to this, however, this chapter covers two other ranges of experiments aimed at increasing regioselectivity towards the

production of hex-4-enoic acid.

## 5.2 The Use of Acetic Acid to Increase the Regioselectivity of the Hydrogenation of Hexa-2,4-dienoic Acid by Rhodium-Mixed Anhydride Catalyst Precursors.

In order to increase the regioselective hydrogenation of hexa-2,4-dienoic acid to hex-4-enoic acid it is necessary to prevent the active participation of an oxygen bound hexa-2,4-dienoate anion in a catalytic cycle. This section is concerned with the addition of acetic acid to catalytic reactions with the aim of preventing the hexa-2,4-dienoate substitution of the chloride ligand. It was hoped that the acetate anion would itself replace the chloride ligand and at the same time not interfere in the hydrogenation and subsequent transesterification of the hexa-2,4-dienoate anion incorporated in the chelate mixed anhydride ligand.

The choice of the acetate anion as an inhibitor was taken because it possesses no carbon-carbon double bonds that could be hydrogenated or included as part of a chelate bond to rhodium. On the other hand it is not too dissimilar from a hexa-2,4-dienoate anion in terms of the electronic effect it exerts on a rhodium metal centre. The likelihood of an acetate anion competing with a hexa-2,4-dienoate anion for incorporation into the mixed anhydride ligand is remote due to the stability offered by the chelate binding of the latter derived anhydride. The use of a rhodium-acetate species, $[Rh(O_2CMe)(PPh_3)_3]$, as a regioselective catalyst[1] further substantiates the use of the acetate anion as a plausible replacement for the hexa-2,4-dienoate anion as the species involved in the substitution of the labile

chloride ligand.

Table 5.2.1 presents the experimental results of the catalytic hydrogenation of hexa-2,4-dienoic acid using [$RhCl(PPh_3)_2(Ph_2PO_2CCMe=CHPh$] as a catalyst precursor, a triethylamine co-catalyst and an acetic acid inhibitor.

Figure 5.2.1

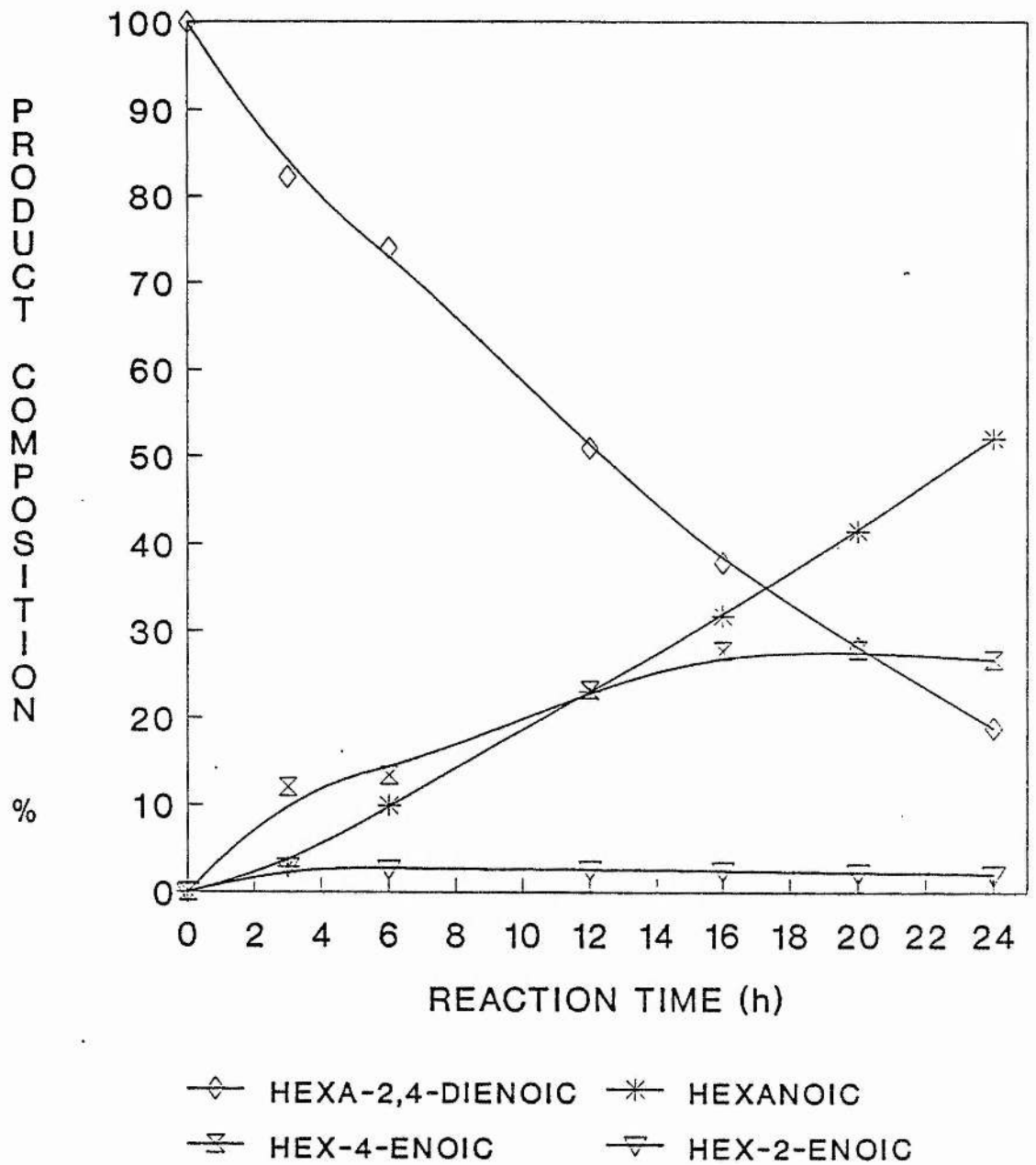
PRODUCT COMPOSITION %
100
90
80
70
60
50
40
30
20
10
0
0 2 4 6 8 10 12 14 16 18 20 22 24
REACTION TIME (h)
HEXA-2,4-DIENOIC
HEXANOIC
HEX-4-ENOIC
HEX-2-ENOIC

Table 5.2.1

| | Product Compostion (%)[a] | | | |
|---|---|---|---|---|
| Time(h) | hexa-2,4-dienoic acid | hex-4-enoic acid | hex-2-enoic acid | hexanoic acid |
| 0 | 100.0 | 0.0 | 0.0 | 0.0 |
| 3 | 82.2 | 12.0 | 2.9 | 2.9 |
| 6 | 74.0 | 13.4 | 2.7 | 9.9 |
| 12 | 51.0 | 23.3 | 2.6 | 23.1 |
| 16 | 37.9 | 27.8 | 2.5 | 31.8 |
| 20 | 28.2 | 27.9 | 2.3 | 41.6 |
| 24 | 18.9 | 26.8 | 2.1 | 52.2 |

[a]Conditions: [$RhCl(PPh_3)_2(Ph_2PO_2CCMe=CHPh)$] (0.01g,0.01mmol), $MeHC=CH-CH=CHCO_2H$ (0.022g, 0.2mmol), $CH_3CO_2H$ (0.024g, 0.4mmol), $NEt_3$(0.081g, 0.8mmol), in thf ($5cm^3$), $p(H_2)$ = 3 atm, 24 C.

Figure 5.2.1 illustrates these results in a time dependence plot for the hydrogenation of hexa-2,4-dienoic acid in the presence of $[RhCl(PPh_3)_2(Ph_2PO_2CCMe=CHPh)]$.

The aim of using acetic acid as an inhibitor is to increase the regioselectivity of the catalysis by limiting the production of hexanoic acid. When hexa-2,4-dienoic acid is hydrogenated using $[RhCl(PPh_3)_2(Ph_2PO_2CCMe=CHPh)]$ without the presence of acetic acid, 91.0% conversion to hexanoic and hex-4-enoic acids is observed after 20h.[2] In the presence of acetic acid, however, only 81.1% conversion is observed after 24h, thus the acetic acid has the effect of decreasing the overall rate of catalysis.

It should be noted that in the earlier stages of catalysis (2h), without the presence of acetic acid, the ratio of hexanoic acid to hex-4-enoic acid is 1:1. For catalysis involving acetic acid (after 3h) the aforementioned ratio is 1:4. This suggests that initially there is an increase in selectivity due to the inhibition of the mechanistic pathway involving the active participation of the oxygen bound hexa-2,4-dienoate anion. As the catalysis proceeds, however, the observed regioselectivity diminishes. Indeed after 20h in the presence of acetic acid the ratio of hexanoic acid to hex-4-enoic acid is 1.5:1, although this is proportionally greater in hex-4-enoic than the ratio of 3.5:1 observed for catalysis with no acetic acid. This decrease in observed regioselectivity as the catalysis proceeds is probably due to the reversible nature of the inhibition promoted by acetic acid. Thus if an acetate anion replaces the chloride ligand on the metal then it in turn may be replaced by a hexa-2,4-dienoate anion and as a result the acetate anions merely act as competitive inhibitors.

## 5.3 The Effect of Triphenylphosphine upon the Regioselectivity of the Hydrogenation of Hexa-2,4-dienoic Acid by Rhodium-Mixed Anhydride Catalyst Precursors.

When using $[RhCl(PPh_3)_2(Ph_2PO_2CCH=CHCH=CHMe)]$ as a catalyst precursor for the hydrogenation of but-2-enoic acid, the active species in the catalytic cycle is $[Rh(O_2CCH=CHCH=CHMe)(PPh_3)(Ph_2PO_2CCH=CHCH=CHMe)]$ with the mixed anhydride bound in a bidentate fashion. As illustrated in Scheme 2.8.2 and Figure 5.3.1 once the carbon-carbon double bond of the mixed anhydride has been hydrogenated there is a rearrangement of the anhydride. Instead of this rearrangement it is plausible that the metal bound but-2-enoate anion might itself become chelate in character thus leaving a monodentate, hydrogenated anhydride ligand which can then undergo transesterification. As a result the mechanism in Scheme 2.8.3 would be introduced and more hexanoic acid would be produced. Thus it is proposed that addition of excess triphenylphosphine to the catalytic solution might prevent the chelate binding of the rhodium bound carboxylate anion competing for the available vacant site. It might also promote the transesterification reaction if that occurs via the metal, since exchange of a metal bound carboxylate anion with a phosphorus bound carboxylate anion has only been observed in e.g. $[Rh(O_2CC_3H_7)(PPh_3)_2(Ph_2PO_2CC_3H_7)]$ which contains 2 triphenylphosphine ligands.

Figure 5.3.1

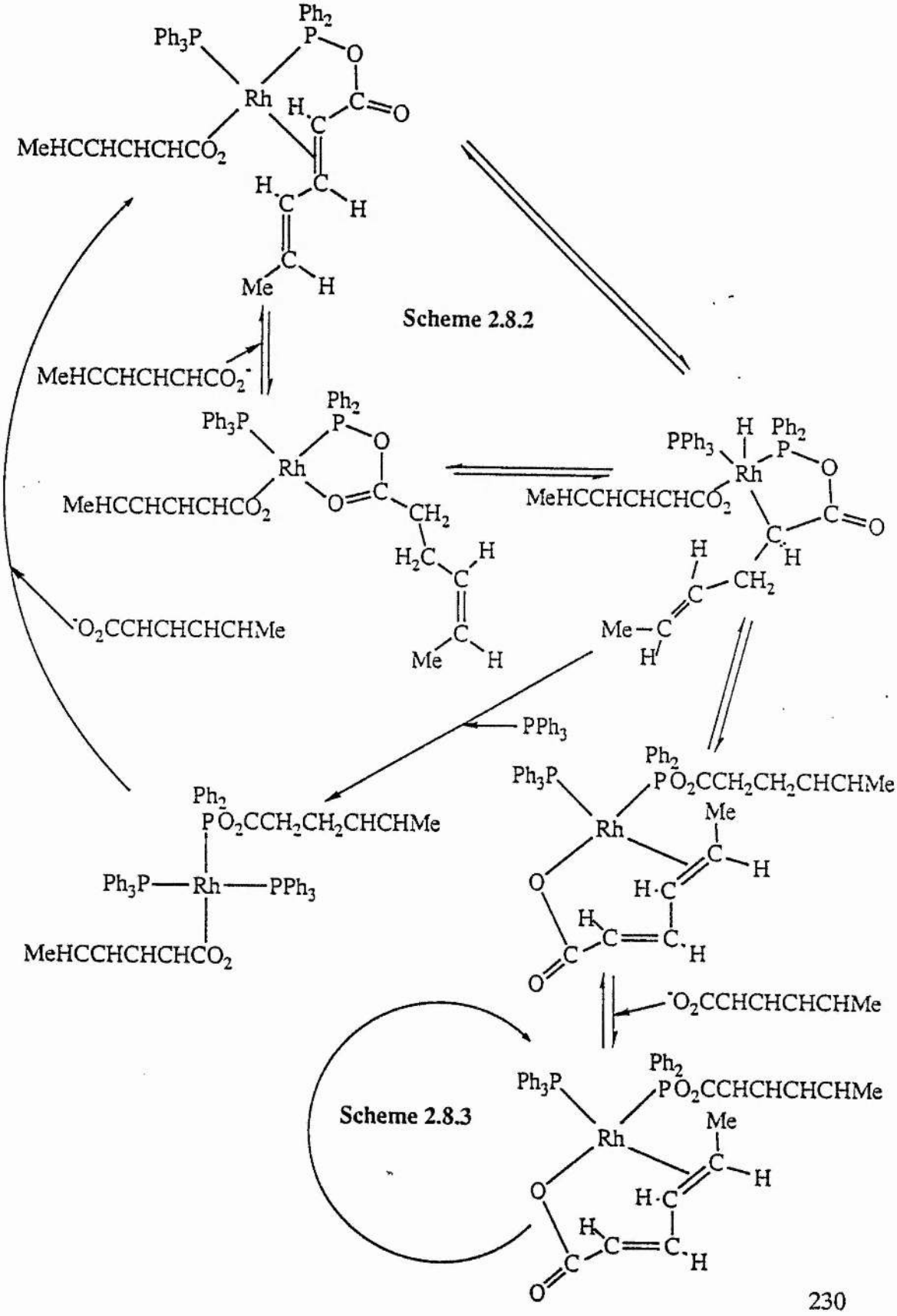


Scheme 2.8.2

Scheme 2.8.3

Catalytic hydrogenation reactions of hexa-2,4-dienoic acid using $[RhCl(PPh_3)_2(Ph_2PO_2CCMe=CHPh)]$ as the catalyst precursor, $NEt_3$ as the co-catalyst and an extra one mole equivalent of $PPh_3$ have been performed. The results of these catalyses are presented in Table 5.3.1 along with results obtained for similar catalyses performed without the presence of additional triphenylphosphine.

Table 5.3.1

| Catalyst Precursor | Time (h) | Conversion (%) | |
|---|---|---|---|
| | | a | b |
| $[RhCl(PPh_3)_2(Ph_2PO_2CCMe=CHPh)]$ | 2 | 24 | 24 |
| | 20 | 72 | 19 |
| $[RhCl(PPh_3)_2(Ph_2PO_2CCMe=CHPh)]$ | 2 | 0 | 7 |
| $+ PPh_3$ | 20 | 39 | 25 |

a Hexanoic Acid

b Hex-4-enoic Acid

It can clearly be seen that the addition of triphenylphosphine results in a decreased rate of catalysis. It is also noticeable that after two hours, in the presence of $PPh_3$, only hex-4-enoic acid is produced, whilst after 20 hours, the amount of hexanoic acid is greater than the amount of hex-4-enoic acid. Despite this, after 20 hours the relative amount of hex-4-enoic acid is greater for the catalysis performed in the presence of excess triphenylphosphine than that which is not, thus indicating that to a certain degree the addition of $PPh_3$ has had the desired effect.

## 5.4 The Use and Effects of $[RhF(PPh_3)_3]$ and $[RhF(PPh_3)_2(Ph_2PO_2CCH=CHCH=CHMe)]$ as Catalyst Precursors for the Hydrogenation of Substituted Acrylic Acids.

It has been reported that as a hydrogenation catalyst (cyclohexene in benzene, 25°C, 100cm Hg, [catalyst] $4x10^{-3}$ mol/l) $[RhF(PPh_3)_3]$ is initially slightly more active than $[RhCl(PPh_3)_3]$, but its activity falls within 25 minutes to about 15%.[3] Results for the hydrogenation of substituted acrylic acids using $[RhF(PPh_3)_3]$, are illustrated in Table 5.4.1.

Table 5.4.1

| | % Conversion[a] | |
|---|---|---|
| Substrate | $[RhCl(PPh_3)_3]$ | $[RhF(PPh_3)_3]$ |
| $Me_2C=CHCO_2H$ | 26.7 | 12.5 |
| $PhCH=CMeCO_2H$ | 14.0 | 5.1 |
| $MeCH=CHCO_2H$ | 75.8 | 64.0 |
| $MeCH=CHCH=CHCO_2H$ | 10.6[b] | 8.2[b] |

[a] Conditions: [catalyst] $=3x10^{-3}$ mol $dm^{-3}$, [substrate] $= 6x10^{-2}$ mol $dm^{-3}$, [KOH] $= 4x10^{-2}$ mol $dm^{-3}$, in acetone ($5cm^3$), 17h, 22°C, $p(H_2) = 3$ atm.

[b] Hexanoic Acid

For $[RhF(PPh_3)_3]$, as is observed for rhodium-chloro-mixed anhydride complexes,[2] catalysis involving the addition of the base, triethylamine is more efficient than

those utilising KOH due to the lower solubility of the latter. The hydrogenation of 3-methyl but-2-enoic acid in the presence of $NEt_3$ ([catalyst] = $3x10^{-3}$ mol $dm^{-3}$, [substrate] = $6 \times 10^{-2}$ mol $dm^{-3}$, [$NEt_3$] = $4x\ 10^{-2}$ mol $dm^{-3}$ in acetone ($5cm^3$), 17h, 22°C, p($H_2$)=3 atm) gives 19.1% conversion whilst in the presence of KOH, as stated previously, a 12.5% conversion is observed.

When [$RhF(PPh_3)_2(Ph_2PO_2CCH=CHCH=CHMe)$], a fluxional 5-coordinate species whose preparation was presented in Chapter 3, is used as a catalyst precursor for the hydrogenation of hexa-2,4-dienoic acid the only product formed is hexanoic acid. Catalyses over 2 hours and 24 hours (Conditions: [catalyst] = $4.25x10^{-3}$ mol $dm^{-3}$, [substrate] = $8.5x10^{-2}$ mol $dm^{-3}$, [$NEt_3$] = $12.75x10^{-2}$ mol $dm^{-3}$ in thf ($5cm^3$), 22°C, p($H_2$) = 3atm) gave 57.2% and 100% conversion respectively. The abscence of hex-4-enoic acid, especially after 2 hours, suggests that a totally different mechanism from that discussed in Chapter 2 must be operating for the 5-coordinate fluoro species, but the overall activity of the catalyst is somewhat higher than that of eg [$RhCl(PPh_3)_2(Ph_2PO_2CCMe=CHPh)$] (36% of double bonds hydrogenated in 2h under the same conditions) or of [$RhF(PPh_3)_3$] (8.2% in 17h).

## 5.5 Experimental

All hydrogenation reactions were carried out in glass vessels of ca. $100cm^3$ capacity with a valve attached for pressuring and depressurising. Ratios of catalyst:substrate:base were 1:20:30 unless otherwise stated and reactions were carried out under 3 atm of hydrogen (total pressure) at room temperature with

magnetic stirring. A typical catalytic reaction was as follows: to $[RhCl(PPh_3)_2(Ph_2PO_2CCMe=CHPh)]$ (0.028g, $3x10^{-5}$mol) was added $PhCH=CMeCO_2H$ (0.097g, $6x10^{-4}$mol) and $NEt_3$ (0.091g, $9x10^{-4}$mol) in thf ($5cm^3$). The flask was evacuated before pressuring to 3 atm total pressure with $H_2$.

At the end of the catalytic reactions involving KOH as co-catalyst, the suspension was evaporated to dryness and the resulting solid was dissolved in $D_2O$ for NMR analysis. When $NEt_3$ was used as co-catalyst, the catalytic solution was evaporated to dryness and the residue dissolved in $CH_2Cl_2$ ($15cm^3$). This solution was acidified with hydrochloric acid ($50cm^3$, 1 mol $dm^{-3}$). The organic layer was then extracted, dried over $MgSO_4$ and evaporated to dryness in vacuo to lead to the organic acids which were characterised by $^1H$ NMR spectrocopy in $CDCl_3$.

## CHAPTER 5 REFERENCES


1 A Spencer, J. Organomet. Chem., 1975, 93, 389.

2 A Iraqi, N R Fairfax, S A Preston, D C Cupertino, D J Irvine and D J Cole-Hamilton, J. Chem. Soc. Dalton Trans., 1991, 1929.

3 H L M van Gaal, F L A van den Bekerom and J P J Verlaan, J. Organomet. Chem., 1976, 114, C35.